



A University of Sussex PhD thesis

Available online via Sussex Research Online:

<http://sro.sussex.ac.uk/>

This thesis is protected by copyright which belongs to the author.

This thesis cannot be reproduced or quoted extensively from without first obtaining permission in writing from the Author

The content must not be changed in any way or sold commercially in any format or medium without the formal permission of the Author

When referring to this work, full bibliographic details including the author, title, awarding institution and date of the thesis must be given

Please visit Sussex Research Online for more information and further details

Characterizing the regulation and function of Zip1 in *Saccharomyces cerevisiae* meiosis

Dijue Sun

University of Sussex

September 2015

Acknowledgements

Firstly, I would like to thank my main supervisor Dr. Eva Hoffmann for providing me this opportunity to study in her Lab and gives appropriate advice whenever needed. I have learned a lot of things from Eva and grow stronger after training in her Lab.

Secondly and foremost, I would like to thank my parents for everything they have sacrificed for me in my entire life. I would not have and achieved what I am having today if it wasn't because of their love, support, kindness. They have always been there for me whenever I needed them and never abandoned me even when I was been unreasonable. My parents have also paid my fees and livings during my Ph.D., hence I would not achieve this degree if wasn't their support. I am ready to taking care of them and repaying back their love and support.

Thirdly, I would give massive thanks to everyone in the Hoffmann's Lab, for their support, encouragement and laughs. Particularly, I need to give an enormous thanks to Dr. Louise Newnham and Dr. Alice Copsey. I am very grateful to have them as colleagues, without their support and encouragement I would not survive during the dark times.

I would also like to acknowledge Wan Liu and Lina Chen, who are friends I have made during my Ph.D. I am very grateful that I have met them and we shares similar personalities. They made my Ph.D. life interesting and laughable. More importantly, we have supported each other whenever we are facing the horrible crisis.

Also another thanks need to give to my co-supervisor Dr. Helfrid Hochegger for his advices and supports during my Ph.D.

I would also like to thank Alison Redwood for proof reading this thesis, for her patient to spend the time to read and gives appropriate advice to make this thesis better

Finally, a very special thanks owed to my spiritual partner, my husband Haoqing Xu. I am very thankful that he has come into my life and been there for me throughout my Ph.D. I have experienced a lot of horrible times, but he has always been there to make me feel better. No matter how hard the day was, but whenever I was home he can always de-stress me. Another reason that I can keep going is because of his support. He has also sacrificed a lot for me and I am truly thankful for his unconditional love. He is the sunshine of my life.

Declaration

I hereby declare that this thesis was composed by me, and the research presented is my own, except where otherwise stated.

Dijue Sun

September 2015

University of Sussex

DPhil. Biochemistry

Characterizing the regulation and function of Zip1 in *Saccharomyces cerevisiae* meiosis

Meiosis is characterized by one round of DNA replication followed by two successive rounds of cell division, resulting in a halving of the genome. During meiotic prophase I, many events occur to allow faithful chromosome segregation. At the chromosomal level, homologs align and become closely juxtaposed along their entire lengths via a proteinaceous structure called the synaptonemal complex (SC). DNA double-strand breaks are induced during prophase I, resulting in the formation of crossover between homologs, which leads to the correct segregation during meiosis I. A well-characterized protein, termed Zip1, is the major component of the SC. Zip1 is known to involve in several different processes of meiosis. Firstly, Zip1 is involved during non-homologous centromere coupling. Secondly, Zip1 synapse homologs together. Thirdly, Zip1 promotes crossing over during prophase I as well as required for interference. The work described in this thesis has characterized the functions and regulation of several Zip1-phospho mutants during meiosis. In particular, Zip1-T114 was shown to involve partially during non-homologous centromere coupling. Zip1-S144 is a putative consensus site for Cdc5 phosphorylation and was found to have a role in SC disassembly.

Zip1 has also been known to involve in non-exchange chromosome segregation (NECS). The work described here used time lapse imaging to further study the characteristics of NECS. This study has generated another homeologous chromosome in SK1 strain background. This homeologous chromosome diploid contains one chromosome III from *Saccharomyces cerevisiae* and one chromosome III from *Saccharomyces paradoxus*. Both species share 85% homology. Using live cell imaging has revealed that the NECS is very dynamic. This dynamic movement distinguishes from exchange chromosome segregation where stable centromere pairing between homologs was observed. Therefore a model has proposed for NECS, whereby non-exchange centromeres constant been associate and dissociate from prophase until anaphase segregation during meiosis I.

Table of Contents

Chapter 1. Introduction	1
1.1 Meiosis.....	1
1.1.1 Overview of meiosis.....	1
1.1.2 Pre-meiotic S-phase in <i>S. cerevisiae</i>	2
1.1.3 Meiotic prophase in <i>S. cerevisiae</i>	10
1.1.3.1 Early meiotic prophase.....	12
1.1.3.2 Meiotic Recombination.....	17
1.2. The Synaptonemal complex	28
1.2.1 The Synaptonemal complex in budding yeast.....	28
1.2.1.1 Zip1, the transverse filament in budding yeast	29
1.2.1.2 The axial and lateral element of the Synaptonemal complex.....	33
1.2.2 The structure of the Synaptonemal complex in other organisms.....	38
1.2.2.1 Flies	38
1.2.2.2 Worms	40
1.2.2.3 Mammals	41
1.2.3 Assembly of the Synaptonemal complex	44
1.2.4 Disassembly of the Synaptonemal complex	50
1.3 Meiotic Divisions	55
1.3.1 Mono-orientation of sister chromatids at meiosis I	55
1.3.2 Protection of centromeric cohesion during meiosis I	59
1.4 Non-exchange chromosome segregation (NECS)	65
1.4.1 Discovery of NECS in yeast, flies and worms	66
1.4.1.1 Yeast	66
1.4.1.2 Flies and worms.....	67
1.4.2 NECS pathways in yeast, flies and worms	69
1.4.2.1 Yeast	69
1.4.2.2 Flies and worms.....	71
1.4.3. NECs studies in mammals.....	74
Chapter 2. Materials and methods.....	77
2.1 Materials:	77
2.1.1 Growth media	77
2.1.1.1 Bacterial media:	77
2.1.1.2 Yeast media:.....	77
2.1.2 Buffers	78
2.1.3 Enzyme.....	81
2.1.4 Drugs and antibiotics	81
2.1.6 Secondary antibody used.....	82
2.1.7 Radiations.....	83
2.1.8 Oligonucleotides	85
2.1.9 Yeast strains	87
2.1.10 Plasmids	94
2.2 Methods	95

2.2.1 Bacterial methods	95
2.2.1.1 Growth conditions	95
2.2.1.2 Yeast growth conditions	95
2.2.2 Bacterial strain construction	95
2.2.2.1 Transformation of chemically competent <i>E.coli</i> DH5α cells	95
2.2.2.2 Storage of Bacterial strains	96
2.2.3 Growth conditions of Yeast	96
2.2.3.1 Vegetative growth conditions	96
2.2.3.2 Sporulation conditions.....	96
2.2.4 Yeast strain construction.....	97
2.2.4.1 Genetic cross the strains.....	97
2.2.4.2 Transformation of Yeast cells.....	98
2.2.4.3 PCR-based gene deletion	99
2.2.4.4 PCR-based N-terminal gene tagging.....	100
2.2.4.5 Two step gene replacement method	101
2.2.4.6 Diploid isolation.....	102
2.2.4.7 Storage of yeast strains	102
2.2.4.8 Artificial chromosome transfer.....	102
2.2.5 Genetic methods.....	103
2.2.5.1 General PCR	103
2.2.5.2 Genomic DNA extraction.....	103
2.2.5.3 Phenol-chloroform DNA extraction	104
2.2.5.4 Agarose Gel electrophoresis.....	106
2.2.5.5 Making DNA plugs for pulsed-field gel electrophoresis.....	106
2.2.5.6 Pulsed-Field Gel electrophoresis	107
2.2.5.7 DNA purification (materials used from DNA QiAgen kit)	109
2.2.5.8 Restriction Digests of DNA.....	109
2.2.5.9 One-dimensional Gel (Southern).....	109
2.2.6 Protein methods.....	114
2.2.6.1 Protein extractions	114
2.2.6.1.1 Protein extractions using NaOH	114
2.2.6.1.2 Proteins extractions using Tri-Chloroacetic Acid (TCA)	115
2.2.6.2 SDS-PAGE separation of proteins	116
2.2.6.3 Western Blotting.....	116
2.2.7 Cytological methods.....	117
2.2.7.1. Assessment of nuclear divisions using DAPI.....	117
2.2.7.2 Sporulation counts	118
2.2.7.3 Visualization of GFP in tetrads and live cells.....	118
2.2.7.4 In situ immunofluorescence of fixed cells	118
2.2.7.5 Preparation and immuno-staining of chromosome spreads.....	120
2.2.7.6 Fixed Image captures	121
2.2.8 Live-capture of imaging.....	122
2.2.8.1 Preparation using Labtech chambers.....	122
2.2.8.2 Preparation using CellAsics chambers.....	122
2.2.8.3 Live cell imaging using personal Delta vision (pDV)	123
2.2.9 Computational Tools	123
2.2.9.1 Websites used	123
2.2.9.2. Software used.....	124

2.2.10 Mutagenesis	124
Chapter 3. Functional analysis of Synaptonemal complex in Zip1 point mutants	125
3.1 Introduction	125
3.2 Results	128
3.2.1 Analysis of sporulation and spore viability in Zip1 point mutants	128
3.2.2. Zip1-phospho mutants have a role in centromere coupling at pre-meiotic stage.....	134
3.2.3 Formation of Synaptonemal complex in Zip1-phosphorylation site mutants	138
3.2.4 Analysis of SC formation in <i>zip1-T114A</i> and <i>zip1-4A</i>	143
3.2.5 High levels of Zip1 protein in mutants with polycomplexes.....	147
3.2.6 A delayed SC disassembly defect observed in <i>zip1-S137A</i> and <i>zip1-S144A</i>	150
3.3 Discussion	153
Chapter 4. Cdc5-dependent phosphorylation of Zip1-S144 is important for SC disassembly	156
4.1 Introduction	156
4.2 Results	159
4.2.1 Zip1-S144 identified through a Cdc5 proteomic screen.....	159
4.2.2 Non-phosphorylatable <i>zip1-S144A</i> is defective in SC disassembly	161
4.2.2.1 SC assembly in <i>zip1-S144A</i> mutant.....	161
4.2.2.2 SC disassembly in the <i>zip1-S144A</i> mutant.....	165
4.2.3 High levels of Zip1 protein detected in <i>zip1-S144A</i>	166
4.2.4 Assessing the phosphomimetic version of Zip1-S144 (<i>zip1-S144E</i>) in SC assembly and disassembly	168
4.2.5 The <i>zip1-S144E</i> mutant does not improve SC disassembly in the absence of Cdc5	170
4.2.6 The <i>zip1-S144A</i> mutant did not show blockage of disassembly when conditionally induced by Cdc5	172
4.2.7 Non-phosphorylatable <i>zip1-S144A</i> mutant has normal sporulation efficiency and spore viability.	174
4.2.8 Zip1-S144 does not affect crossover formation	177
4.3 Discussion	184
Chapter 5. Centromere dynamics of Non Exchange Chromosomes in meiosis	186
5.1 Introduction	186
5.2 Results	190
5.2.1 Generation of a homeologous chromosome pair by using the <i>S. paradoxus</i> chromosome III.....	190
5.2.2 Dynamic association and dissociation of non-exchange centromeres throughout prophase I.....	196
5.2.3 NECs associate transiently in metaphase I prior to their segregation	199
5.2.4 Non-exchange chromosome segregation in <i>zip1-T114A</i>	202
5.2.5 Studying non-exchange chromosome segregation in two different colours.....	204

5.2.6 Examination of the phosphorylation of the <i>zip1-T114A</i> mutant in NEC pathway using red and green fluorescence.....	207
5.3 Discussion	210
Chapter 6. Discussion	213
6.1 Discussion	213
6.2 Future work.....	216
Bibliography	218
Appendix Figures.....	242

List of Figures

Figure 1.1 The overview of meiosis

Figure 1.2 The structure of cohesin complex and its proposed models

Figure 1.3 The timeline of meiotic prophase I

Figure 1.4 Centromere coupling in budding yeast

Figure 1.5 The models of DNA double strand breaks

Figure 1.6 Systemic diagram present the synaptonemal complex in different species

Figure 1.7 Categories of the ‘ZMM’ proteins and their involvement in synapsis initiation process

Figure 1.8 The orientation of centromeres

Figure 1.9 Protection of centromeric cohesion

Figure 1.10 Examples of different organisms in non-exchange chromosome segregation

Figure 2.1 PCR-based gene deletion

Figure 2.2 Tagging of cassettes by PCR

Figure 3.1 Zip1 sites identified through Zip1 IP and Cdc5 proteomic screen

Figure 3.2 Sporulation and viability characterization for Zip1-phospho mutants

Figure 3.3 Centromeric coupling in Zip1-phospho mutants

Figure 3.4 Synaptonemal complex formation analyses for Zip1-phospho mutants

Figure 3.5 Proportions of polycomplexes in some Zip1-phospho mutants.

Figure 3.6 The *zip1-8A* and *zip1-8E* mutants show defects in Synaptonemal complex assembly

Figure 3.7 Synaptonemal complex formations in *zip1-4A* and *zip1-T114A* mutants

Figure 3.8 Zip1 protein levels in the *zip1-4A* and *zip1-T114A* mutants

Figure 3.9 The *zip1-S137A* mutant shown partial delay in synaptonemal complex disassembly

Figure 4.1 Identification of Zip1-S144 through phosphor proteomic screen

Figure 4.2 The *zip1-S144A* mutant displays delayed SC disassembly

Figure 4.3 Characterization of the *zip1-S144A* mutant in synaptonemal complex assembly

Figure 4.4 Protein levels of the *zip1-S144A* mutant through meiotic progression

Figure 4.5 Phosphomimetic version of Zip1-S144 (*zip1-S144E*) forms regular synaptonemal complex and shows no sign of disassembly defect

Figure 4.6 Synaptonemal complex does not disassemble in the absence of Cdc5 at diplotene in both *zip1-S144A* & *zip1-S144E* mutants

Figure 4.7 Synaptonemal complex does not disassemble in the absence of Cdc5 at metaphase I in both *zip1-S144A* & *zip1-S144E* mutants

Figure 4.8 Disassembly of the synaptonemal complex still occurs in the *zip1-S144A* nuclei when conditionally induced by Cdc5

Figure 4.9 The *zip1-S144A* mutant displays normal sporulation and spore viability

Figure 4.10 Confirmation that the *zip1::TRP1* strain behaves the same as standard Hunter wild type

Figure 4.11 Recombination analysis of the wild type, *zip1*, and *zip1-S144A*

Figure 4.12 meiotic recombination is not affected in *zip1-S144A*

Figure 5.1 The hypothesis of centromere behaviour in non-exchange chromosome pathways

Figure 5.2 Systemic diagram showing the steps of transferring the homeologous chromosome

Figure 5.3 Verification of the successfully transferred chromosome III

Figure 5.4 Centromere pairing of the homeologous *S. paradoxus* x *S. cerevisiae* non-exchange chromosome pair is decreased compared to homologous centromere pairing in SK1 strain

Figure 5.5 Live centromere movements in the homologous wild type

Figure 5.6 Live centromere movements in homeologous wild type

Figure 5.7 Non-exchange chromosome segregation in the *zip1-T114A* mutant

Figure 5.8 Live cell imaging of the wild-type non-exchange chromosome segregation by tagging *S. cerevisiae* with mCherry and *S. paradoxus* Cen3 with lacO/LacI GFP

Figure 5.9 Live cell imaging of non-exchange chromosome centromere in the *zip1-T114A* mutant using mCherry and lacO/LacI GFP

Appendix 1 Synaptonemal complex formation in another two independent *zip1-S82A* transformants

Appendix 2 Transformation of Hunter base strain and the *zip1-S144A* Hunter transformation

Appendix 3 Southern Blot to the *zip1-4A* and *zip1-T114A* integration

Appendix 4 Southern Blot verifications on other Zip1-phospho mutants

Appendix 5 Optimisation of Rec8-Tev, Ndt80-inducible system

Appendix 6 Cleavage of Rec8-Tev leads to instability of Zip1

Appendix 7 Repeat of the *zip1-S144A* mutant in synaptonemal complex disassembly

Appendix 8 Centromere coupling is not affected in the *zip1-S144A*

Lists of Tables

Table 2.1 Amino acids used to make complete and drop out powders

Table 2.2 Buffers used in this thesis

Table 2.3 Enzymes used in this thesis

Table 2.4 Drugs and antibiotics used in this thesis

Table 2.5 Primary antibody used in this thesis

Table 2.6 Secondary antibody used in this thesis

Table 2.7 Radiations used in this thesis

Table 2.8 Oligonucleotides used in this thesis

Table 2.9 Base yeast strains used in this thesis

Table 2.10 Yeast strains used in this thesis

Table 2.11 Plasmids used in this thesis

Table 3.1 Summary of genotypes

Table 3.2 Summary of phenotypes

List of Abbreviations

APC	Anaphase Promoting Complex
ATP	Adenosine Triphosphate
AA	Axial Association
AE	Axial element
Bp	Base Pair
CAN	Canavanine
CYH	Cycloheximide
Cy5	Cyanine 5
CE	Central element
DAPI	4',6-diamidino-2-phenylindole
dHJ	Double Holliday Junction
DSB	Double strand break
DTT	Dithiothreitol
EDTA	Ethylenediaminetetraacetic acid
FITC	Fluorescein isothiocyanate
G	Gram
LE	Lateral element
Kb	Kilobase
ml	Milliliter
mM	Millimolar
mMo	Millimole
NDJ	Non-disjunction
NECS	Non-exchange chromosome segregation
ORF	Open reading frame
PBS	Phosphate Buffered Saline
PCR	Polymerase chain reaction

PSSC	Precocious sister chromatid separation
µg	Microgram
µl	Microlitre
µM	Micrometre
SC	Synaptonemal complex
SIC	Synapsis initiation complex
SEI	Single end invasion
SSC	Sister separation chromatids
<i>S.c.</i>	<i>Saccharomyces cerevisiae</i>
<i>S.p.</i>	<i>Saccharomyces paradoxus</i>
SUMO	Small Ubiquitin-like Modifier
SDS	Sodium dodecyl sulphate
w/v	Weight per unit volume
v/v	Volume per unit volume
YEPD	Yeast Extract, Peptone, Dextrose

Chapter 1. Introduction

1.1 Meiosis

1.1.1 Overview of meiosis

Meiosis is the central process for gamete production during sexual reproduction. It is characterized by one round of DNA replication followed by two successive rounds of nuclear divisions, resulting in a halving of the genome. Meiosis thus generates haploid gametes (in humans these are eggs and sperms) from diploid precursors, resulting in four genetically non-identical daughter cells (Fig. 1.1). This is in contrast to mitosis, in which a single round of DNA replication is followed by one division, resulting in two genetically identical daughter cells. The first meiotic division, where homologous chromosomes are segregated away from each other, is referred to as the 'reductional division', whereas sister chromatids are segregated from each other during meiosis II, in a manner similar to mitosis, is referred to as the 'equational division' (Fig. 1.1).

Accurate chromosome segregation at meiosis I requires several modifications (see later sections). In brief, cohesins are established between sister chromatids during DNA replication to ensure sisters stay together and eventually segregate away from each other during meiosis I (Fig. 1A, B). At meiosis prophase I, homologous chromosomes from both parents must be physically linked to each other in a bivalent to allow for the proper attachment of the chromosomes to the meiosis I spindle, and in most organisms linkage is created by reciprocal recombination with the result of forming a cytological structure called chiasma (Fig. 1.1C). Cohesion on the arms of sister chromatids is lost upon entry into anaphase I, but the centromeric cohesions are preserved by shugoshins until the second meiotic division (Fig. 1.1E). Once this is

achieved, sister kinetochores must be mono-orientated to bring about homolog segregation during meiosis I. Establishment of the bivalent results in maternal centromeres being pulled away from paternal ones, but disjunction is prevented by chiasmata. Centromeric cohesion holds sister chromatids together (Fig. 1D). Once the bivalent is resolved, a second meiotic division can take place (Fig. 1G-I). This includes the attachment of sister kinetochores to microtubules in bi-orientation, the destruction of centromeric sister chromatid cohesion leading to chromosome disjunction and segregation of chromosomes to opposite poles of the cell, which results in the formation of haploid cells containing a single chromatid of each chromosome.

1.1.2 Pre-meiotic S-phase in *S. cerevisiae*

Pre-meiotic DNA replication occurs in S-phase, which is the first step marking the beginning of the meiotic process. Pre-meiotic S-phase is distinct from DNA replication in mitotically-dividing cells (Zickler and Kleckner, 1999). For example, the duration of pre-meiotic S-phase is generally several times longer than in mitosis in *Saccharomyces cerevisiae* (SC) (Cha et al., 2000). Cells enter S-phase quicker in mitotic cells (75 minutes) compared to meiotic cells (160 minutes). Completion of mitotic S-phase is 17 minutes whereas meiotic S-phase takes 60.9 minutes to complete (Cha et al., 2000). It was thought that the reason S-phase takes longer is due to changes in chromatin structures that are required for interhomolog interactions. Spo11 is a meiosis-specific catalytic subunit of the meiotic double-strand break (DSB) transesterase and is the main topoisomerase II-like protein that is responsible for initiation of meiotic recombination (Keeney et al., 1997). Deleting *SPO11* results in shortened S-

phase, thus this might be consistent with the notion that DNA replication is being coupled to later meiotic events. To further support this idea, Borde *et al.* (2000) showed that DSB formation was abolished when deleting the S-phase cyclins *CLB5/CLB6* or when preventing DNA replication by treatment with hydroxyurea (Borde *et al.*, 2000). Another protein that has also been revealed that might be recognized during DNA replication is the meiosis-specific kleisin subunit of cohesin Rec8. Deletion of *REC8* has results in a lengthened S-phase, and it has been proposed as a positive effectors of meiotic DNA replication progression, whilst Spo11 acts as a negative regulator of DNA replication (Cha *et al.*, 2000). Therefore, these findings indicate that the assembly of DSB proteins as well as the cohesion protein may regulate the S-phase.

The involvement of Mum2 protein is another unique feature in meiotic S-phase, where this meiosis-specific protein is required for successful DNA replication. Meiotic DNA replication does not occur in the absence of *MUM2*, and meiosis proceeds with a sporulation efficiency of less than 0.1% (Engebrecht *et al.*, 1998).

Pre-meiotic S-phase is crucial as sister chromatids are generated and more importantly, sister chromatid cohesion is also established. Sister chromatids and the cohesion between them, together with inter-homolog crossover recombination and the physical manifestation chiasmata, function to ensure accurate meiosis I segregation (Klein *et al.*, 1999; Uhlmann and Nasmyth, 1998)

Cohesion proteins were first revealed by the development of the tandem repeats of bacterial *lacO* (Straight *et al.*, 1996), as well as *tetO* and *tetR*-GFP

system (Guacci et al., 1997; Michaelis et al., 1997). These studies identified the first group of cohesion proteins that are capable of holding sister chromatids together in budding yeast. This multi-subunit complex contains a core cohesin complex in the shape of a ring (Fig. 1.2A). This ring is composed of two structural maintenance of chromosome (SMC) proteins: Smc1 and Smc3 and one kleisin subunit Scc1 (Guacci et al., 1997; Michaelis et al., 1997). These components are essential for maintaining sister chromatid cohesion in post-replicative cells (Nasmyth and Haering, 2009). Meiotic cohesin is slightly different to mitotic cohesin, where a meiosis-specific kleisin named Rec8 replaces Scc1 in meiotic cells (see below). Another protein Scc3, is responsible for cohesion establishment, which completes cohesin structure (Fig 1.2A). Scc3 binds directly to the central domain of Scc1 (Rec8). So far it has only been shown that Scc3 is essential for establishment but not the maintenance of cohesion (Toth et al., 1999). Similarly, Pds5 is also required for cohesin establishment. This is an accessory protein found at similar locations on the genome as cohesin, but it binds more loosely to the cohesin complex (Panizza et al., 2000; Sutani et al., 2009). Scc2 and Scc4 proteins are involved in the association of cohesin with the chromosomes.

Smc1 and Smc3 subunits form a heterodimer at the core of the cohesin ring, which consists of globular N and C termini, joined by a large coiled-coil domain that is separated by a central hinge domain (Fig. 1.2A) (Nasmyth and Haering, 2005). Each subunit folds back on itself, forming a 50 nm long intramolecular antiparallel coiled-coil (Haering et al., 2002). Due to this unique antiparallel coiled-coil structure, half of the Smc1 N-termini with half of the Smc3 C-termini, together with Scc1 acting as a bridge, form an ATP nucleotide-binding domain

(NBD), which belongs to the ABC family (Hopfner et al., 2000; Lowe et al., 2001). Heterodimerization between the hinge domains of Smc1 and Smc3 results in a V-shaped Smc1/3 structure (Fig. 1.2A) (Haering et al., 2002). The Smc1/3 NBD is similar to other ABC-like NBD, where several helices form a rigid helical domain (HD) that is flexibly attached to a set of β -sheets containing the nucleotide-binding Walker A and B residues (Haering et al., 2004; Nasmyth and Haering, 2009). Crystallography revealed Smc1 NBD as a dimer with the slowly hydrolysable ATP analog ATPyS sandwiched in between (Gligoris et al., 2014; Haering et al., 2002).

As mentioned, Scc1 forms a bridge between the NBDs of Smc3 and Smc1. This is a remarkable feature in the structure of cohesin, as the N and C-terminal domains of Scc1 are bound tightly to the NBDs of Smc3 and Smc1, creating a tripartite ring (Haering et al., 2004). The C terminus of the Scc1 is shown in a crystal structure as a winged helix domain that binds through extensive hydrophobic interactions to the two most C-terminal β -strands of Smc1 NBD (Haering et al., 2004). Upon the interaction with Scc1, the structure of Smc1 NBD changes in a manner that is essential for ATP binding and hydrolysis.

Several models proposed how cohesin hold chromosomes together. The most favourable model with strong evidence is the “embracing” model. This model has proposed cohesin associates with chromosomes by “embracing” both sister chromatids together within the same ring (Fig. 1.2B) (Haering et al., 2002). Upon the cleavage of its Scc1 subunit by separase, it opens up the ring resulting in the liberation of the sister chromatids, which were topologically trapped together within the cohesin ring (Haering et al., 2002)

Experiment using very small (2.3 Kb) circular minichromosomes was the first strong evidence for the “embrace” model (Ivanov and Nasmyth, 2005, 2007). Cleavage of Scc1 by TEV protease converts dimeric minichromosomes into the monomeric form [reviewed by (Nasmyth and Haering, 2009)]. These studies mainly concluded that cohesin entraps sister DNAs inside its tripartite ring structure. More recently, studies have shown that by covalently sealing the cohesin ring using either the fusion proteins or by cross-linking the side chains of cohesin subunits (Farcas et al., 2011; Haering et al., 2008). The cohesin ring maintained its association with 2.3 Kb or 26 Kb circular chromosomes but not with a 42 Kb linear minichromosome after protein denaturation (Haering et al., 2008). Since both the 26 Kb circular and 42 Kb linear minichromosomes were catenated *in vivo*, Farcas *et al.* found that the persistence of catenanes after S phase is dependent on cohesin (Fig. 1.2C) (Farcas et al., 2011). Therefore, it is argued that sister chromatids are held together by cohesin preventing the resolution of catenanes, as well as through a direct topological embrace. This indicates the direct topological embrace of sister chromatids by cohesin is its critical physical property (Farcas et al., 2011). Furthermore, revealing of Scc1 N-terminal with Smc3 crystallography showed that cohesin rings entrap sister DNAs *in vivo*. A configuration of heterotrimeric ring and sister DNA are entrapped within these were shown (Gligoris et al., 2014).

In order to provide cohesion, cohesins must be loaded onto chromosomes before S-phase. This loading requires several factors, but the most important factor is the Scc2/Scc4 complex (Fig. 1.2C) (Ciosk et al., 2000). Cells lacking *scc2Δ* or *scc4Δ* contain less Smc1 and Scc1 compared to wild-type cells in chromatin extracts; this correlates with precocious sister chromatid separation

(Ciosk et al., 2000). However, the loading of cohesin is still poorly characterized. So far, it is known that the first step of loading requires Scc2/Scc4. It was originally assumed this complex prebound to DNA, but a recent study by Fernius *et al.* in 2013 has shown that association of Scc2 at the centromere requires cohesin itself (Fernius et al., 2013). Cohesin loading also requires the complete cohesin ring with ATP bound in conjunction with Scc3 together (Arumugam et al., 2006; Hu et al., 2011). This has led to the model that the assembly of the cohesin ring leads to the interaction with the Scc2/Scc4 complex, resulting in a complex composed of both the cohesin ring as well as Scc2/Scc4. This complex can then bind to the centromere and probably other loading sites too (Fernius et al., 2013).

The establishment of cohesion requires the conserved acetyl-transferase Eco1/Ctf7. This protein is not required for association of cohesin onto chromosomes but acts at the replication fork to couple DNA replication for cohesion generation (Toth et al., 1999). Tagging centromere five with GFP in mutants lacking Eco1 (*eco1-1*) leads to the observation of non-cohesed sister chromatids, but cohesin loading onto DNA still occurs (Toth et al., 1999). More recent studies have found that a pair of lysines on residue on (K112 and 113) within the NBD of Smc3's is the critical substrate for Eco1 (Rolef Ben-Shahar et al., 2008; Rowland et al., 2009; Unal et al., 2008; Zhang et al., 2008). Mutating these lysine residues or nearby residues of Eco1 leads to suppression of *eco1-1* mutant. With the possibility of cohesin loading occurring at G1, cohesin must be modified during DNA replication to facilitate cohesion between adjacent sister chromatids. Eco1 has been shown to bind to PCNA directly through its N-terminus. PCNA is a sliding clamp that travels with the replicative DNA

polymerase at the replication fork (Moldovan et al., 2006). A point mutation in Eco1 that abolishes PCNA binding results to the same defects in sister chromatid cohesion as those in the *eco1-1* mutant. This suggests that establishment of cohesion between sister chromatids is coupled to DNA replication.

1.1.3 Meiotic prophase in *S. cerevisiae*

DNA replication and establishment of cohesion is followed by a prolonged prophase I. This is a very complex stage and contains many aspects that contribute to correct chromosome segregation. Evidence of both at DNA level and at chromosomal level are temporally and spatially closely coordinated to ensure correct segregation (Fig. 1.3) (Borner, 2006). Homologous chromosomes pair and recombine during prophase and at this stage they become intimately associated through an elaborate structure called the synaptonemal complex (SC) (Sym et al., 1993).

In brief (Fig. 1.3), this lengthy prophase can be divided into five cytological sub-stages. The first stage is called leptotema, during which dynamic rearrangements of chromosomes appear; this includes telomere clustering (Bouquet), centromere clustering and centromere coupling (Fig. 1.3A) (Tsubouchi and Roeder, 2005; Zickler and Kleckner, 1998, 2015). At the DNA level, initiation of meiotic DSBs by Spo11 also begins at leptotema. The second stage is termed zygonema, which occurs when homologous chromosomes are aligned and synapsis begins. The initiation of synapsis is probably a committed step in homolog association (Fig. 1.3B) (Bhalla and Dernburg, 2008). At this time, homolog axes pair and become closely associated at sites of recombination (Shinohara et al., 2008). During zygonema, a central element of

the SC begins to polymerize to hold the two homologs together (Fig. 1.3A). In budding yeast, this process can be observed cytologically, as short stretches of Zip1, a core SC protein become apparent (Fig. 1.3A cytology image). Pachynema is the next stage where each pair of homologs is fully synapsed, and the completed SC appears as a ladder-like structure consisting of homologs closely juxtaposed via a dense array of transverse filaments (de Boer and Heyting, 2006). The chromatin is highly condensed and unresolved double Holliday Junctions (dHJs) appear (homologous chromosomes are connected via ligation of strand breaks), resulting in two four-way DNA junctions. These dHJs are precursors to crossovers (Fig. 1.3B) (Allers and Lichten, 2001; Borner et al., 2004; Hunter and Kleckner, 2001). Subset of recombination intermediates that do not form dHJs are resolved into non-crossovers (Allers and Lichten, 2001). Diplonema marks the existence of pachytene stage, during which SC disassembles with separated spindle pole bodies, and the chromatin becomes diffuse (Fig. 1.3A). The resolution of dHJs into crossovers, which results in the physical manifestation of chiasmata also occur at this stage (Allers and Lichten, 2001).

1.1.3.1 Early meiotic prophase

After DNA replication and establishment of sister chromatid cohesion, homologies are assessed between homologous chromosomes via dynamic chromosome interactions. Before homologous chromosomes paired along their entire length in a stable configuration, homologous loci paired within 400 nm and independent of meiotic recombination (Kleckner, 2006; Zickler and Kleckner, 1998). This early pairing occurs on the telomeres, which form a cluster adjacent to the spindle pole at a small region of the nuclear envelope

(NE), seen as a chromosome bouquet. Bouquet formation tends to be conserved in many organisms and is believed to be the hallmark of early prophase I (Zickler and Kleckner, 1998).

In budding yeast, this process is dependent on the Ndj1 protein (Chua and Roeder, 1997; Conrad et al., 1997). In the absence of *ndj1Δ*, bouquet formation was defective and subsequently leads to delayed homolog alignment and SC formation. Homologous non-disjunction was also increased in the *ndj1Δ* mutant (Chua and Roeder, 1997; Conrad et al., 1997). Ndj1 is not the only protein involved in bouquet formation, but functions in conjunction with the SUN domain protein Mps3 (Conrad et al., 2007). Recent work using reciprocal affinity purification has shown that Mps3 co-purifies with Ndj1 and vice versa, further confirming that Mps3 physically associates with Ndj1 (Li et al., 2015). It has been proposed that the SUN domain acts as a bridge connecting the outer nuclear envelope to the cytoskeleton. Another protein Csm4 stabilizes these interactions (Conrad et al., 2008). Recent studies have shown that the SUN-domain proteins form the inner nuclear envelope as integral membrane proteins, and these proteins bind to the KASH-domain proteins (Mps2 and Csm4) at the outer nuclear envelope (Hiraoka and Dernburg, 2009; Jaspersen et al., 2006; Koszul et al., 2008; Tapley and Starr, 2013; Wanat et al., 2008). Further to the function of Ndj1, Csm4 and Mps3 in bouquet formation, a recent study has also revealed that Ndj1 is localized to the spindle pole body (SPB) and a localization lost once the SPB separates. This localization is dependent on the N-terminus of Mps3 (Li et al., 2015).

After the formation of the bouquet, Ndj1, Csm4 and Mps3 also mediate rapid

telomere-led movements throughout meiotic prophase I, in a similar manner to bouquet formation (Conrad et al., 2008; Koszul et al., 2008; Wanat et al., 2008). Analysis of these rapid prophase movements using three-dimensional live-cell imaging showed that telomeres travel at the speed of 1 μm per second within the nucleus, and move independently of each other along common 'tracks' (Conrad et al., 2008). This movement is very rapid since the diameter of the budding yeast nucleus is only $\sim 4 \mu\text{m}$.

Fission yeast has a much more dramatic telomere movement compared to budding yeast during prophase. The entire nucleus oscillates between opposite ends of the cell in a process driven by cytoplasmic microtubules and telomeres tethering via the nuclear membrane (Chikashige et al., 1994). This movement, termed horsetail movement, can be genetically separated from earlier bouquet formation and has been believed may be involved in disrupting inappropriate recombination events. It may also been suggested to facilitate the untangling of chromosomes interlocks during recombination, reviewed in (Koszul and Kleckner, 2009).

Apart from telomere movement and subsequent bouquet formation during early meiotic prophase, another process has also been implicated in assisting homolog pairing in budding yeast. This process is termed 'centromere coupling' (Tsubouchi and Roeder, 2005; Zhang et al., 2013). This process occurs between non-homologous chromosome centromeres during leptotene, and the transverse filament Zip1 has been shown to be responsible for coupling. This process is independent of homology and telomere clustering as coupling is unaffected in bouquet mutants such as *ndj1 Δ* (Tsubouchi and Roeder, 2005).

The function of centromere coupling is unclear. One possibility is coupling assists homology search, allowing chromosomes to switch partners until they have been homologously paired. However, both telomere clustering and centromere coupling do not affect homolog alignment as mutations in both *ndj1Δ* and *zip1Δ* mutants are still observed to align their homolog alignment eventually (Chua and Roeder, 1997; Conrad et al., 1997; Tsubouchi and Roeder, 2005).

The precise mechanism of how non-homologous centromere coupling is directed towards pairing of homologous centromeres once partner chromosomes recombine is still unclear. A study by Falk et al. (2010) has shed some new light on this process. In this study, the author showed that the central element Zip1 is a phosphoprotein and it is hypophosphorylated during coupling. Upon induction of DSBs formation by Spo11, Mec1 kinase becomes activated and phosphorylates Ser75 in the N-terminus of a Zip1 (Zip1-pS75), which causes the hyperphosphorylation of Zip1. Mutation in PP4 phosphatase results in accumulation of hyper-phosphorylated Zip1 and abolishes coupling, suggesting that the hyperphosphorylated state of Zip1 or at least the pS75 is an intermediate that disrupts the protein's ability to hold two centromeres together. The requirement of the Mec1/ATR and PP4-dependent regulation is bypassed in the Zip1-S75A mutant, where S75 phosphorylation is abolished (Fig. 1.4). Since the Zip1-S75A mutant is perfectly viable, this suggests that recombination-initiated homolog pairing eventually disrupts non-homologous centromere coupling. The author proposed a model where Mec1 activation leads to phosphorylation of Zip1 at S75 residue, resulting in de-coupling of centromeres from their non-homologous partners, and eventually facilitating

homologous chromosome alignments (PP4 restored normal activity to Zip1 when homologous centromeres are paired) (Fig. 1.4) (Falk et al., 2010).

Whereas centromere coupling facilitates non-homologous interactions, other organisms have defined mechanisms. In *C. elegans*, 'pairing centres' that are chromosome-specific are responsible for homologous chromosome pairing prior to synapsis and recombination (MacQueen et al., 2005). These pairing centres are located near the ends of chromosomes, and bound to zinc finger proteins, which tether to the nuclear envelope and lead to homologous pairing initiation (Phillips and Dernburg, 2006). In mammals, non-homologous pairing was solely relied on telomeres and this phenotype is disrupted when deleting *SYCP3*, the axial element protein of the SC in mammals (Bisig et al., 2012). Moreover, in *sycp1*^{-/-} knock out mouse, dispersed telomere foci were observed at early prophase suggests telomeres are arranged in pairs or clusters (Bisig et al., 2012).

1.1.3.2 Meiotic Recombination

Meiotic homologous recombination is a faithful mechanism for the repair of DNA double-strand breaks (DSBs). This mechanism is required for accurate segregation of homologous chromosomes at meiosis I. Recombination enables strand exchange between the maternal and paternal chromosomes, ultimately generating gametes with different genetic information. Crossovers (COs) are the end products of recombination and this results in the physical linkage between homologous chromosomes, which are viewed as chiasmata. Many proteins involved in this process are widely conserved across species suggesting this is a universal programmed DSB mechanism (reviewed by de Massy B. 2013).

Initiation of meiotic recombination begins with cleavage of a pair of DNAs closely spaced on opposite strands, producing DSBs (Keeney et al., 1997). A conserved topoisomerase endonuclease, Spo11 is responsible for this process. It attacks the phosphodiester backbone of DNA and the 5' termini on both sides, creating a covalently bound DNA intermediate at the 5' phosphate group (Keeney et al., 1997). The tyrosine residue of Spo11 (Y135) is responsible for this attack.

DSB formation also depends on a number of Spo11-accessory proteins, which are termed pre-DSB recombinosome. In *S. cerevisiae*, these proteins are: Rec102; Rec104; Rec114; Mei4; Mer2; Ski8; Mre11; Rad50 and Xrs2, which form four sub-complexes to mediate Spo11-dependent DSB formation. These complexes are: Mre11-Rad50-Xrs2 (MRX); Rec102-Rec104; Rec114-Mei4-Mer2 (RMM) and Ski8-Spo11. It is believed that these complexes interact with each other (Maleki et al., 2007). However, the precise mechanisms of these proteins still remain unclear, but over past decades research has shed some light onto these proteins. Rec102, Rec104 and Ski8 have been shown to be required for Spo11 dimerization, DNA binding and efficient nuclear retention (Arora et al., 2004; Kee et al., 2004; Sasanuma et al., 2007). Spo11 binding to the DNA cleavage sites has been shown to be required by the RMM complex, and it shows partial localisation on chromatin (Li et al., 2006; Sasanuma et al., 2007). Furthermore, a more recent study using the ChIPchip method has revealed that the RMM complex strongly interacts with Red1 and Hop1, thus this interact with the axial association sites rather than DSB positions (Panizza et al., 2011). Panizza and colleagues have also shown that in the absence of *mer2Δ*, localisations of Mei4 and Rec104 were greatly reduced thus proposed

that Mer2 binds to the axial axis first and recruits its partner complexes (Panizza et al., 2011).

CDK-S (Cdc28-Clb5) and DDK (Cdc7-Dbf4) are cell cycle kinases involved in the regulation of DSB formation, they are also required for initiation of DNA replication (Hardy, 1997). Mer2 is activated by the phosphorylation of CDK-2 on serine 30, as mutation to the non-phosphorylatable version abolishes DSB formation, this indicates Mer2 in assisting in linking DSB formation to meiotic progression (Henderson et al., 2006). In situ the ChIPchip experiment has shown that Mer2 can bind to axial elements in the absence of CDK-S and is independent of its phosphorylation on serine 30 (Panizza et al., 2011). Nonetheless, there was no localisation of Rec114 and Mei4 in the *mer2-S30A* mutant, and localisation of Rec114 only had 6% of its peak compared to the wild-type in the *clb5, clb6* double mutants (Panizza et al., 2011). This finding suggests that Mer2 localisation is independent of CDK-S phosphorylation regardless of DNA replication. Yet, phosphorylation of serine 30 on Mer2 is crucial for the recruitment of its binding partners in both the presence and absence of DNA replication (Panizza et al., 2011). Mer2 is also phosphorylated by DDK on several sites, and mutations in these sites result in different degrees of DSB defects (Sasanuma et al., 2008). Particularly, the *mer2-S29A* mutation completely abolishes DSB formation (Sasanuma et al., 2008; Wan et al., 2008). However, *in vitro* kinase assays show that S29 phosphorylation by DDK only occurs when S30 is phosphorylated by CDK (Wan et al., 2008). Mutating S30 and S29 to their phosphomimetic version, which mimics the phosphorylation of S30 and S29, leads to restored DSB formation. But this only occurs in the presence of CDK-S and DDK, suggesting other independent roles of these

kinases other than promoting DSB on S30 and S29 phosphorylation. The above studies suggest that Mer2 interaction with other proteins is needed for DSBs, thereby recruiting these proteins to chromatin that requires the phosphorylation by both these kinases.

Lichten and colleagues have found that delaying replication also delays DSB formation (Borde et al., 2000), taken together with the fact that the same kinases (CDK-S and DDK) required for replication are also required for DSB formation, this suggests these two processes are closely coupled to one another (Borde et al., 2000). Indeed, a recent model has proposed that replication and DSB formation operate at least in part by recruitment of DDK to the replication machinery, and Mer2 becomes the preferential target in the replicating region for phosphorylation (Murakami and Keeney, 2014). Overexpressing DDK as well as removing the replication fork protection complex (FPC) results in elimination of replication-DSB coordination (Murakami and Keeney, 2014). Artificially tethering of DDK to the replisomes results in the FPC physically associating with DDK, and this association become dispensable for replication-DSB coordination (Murakami and Keeney, 2014). This finding further suggests that recruitment of DDK to replisomes phosphorylates Mer2 while the replication fork is active, hence synchronising replication is an early prerequisite for DSB formation.

After Spo11 attacks the DNA creating DSBs, the next step is to remove Spo11 via an endonucleolytic release, resulting in the production of short oligonucleotides bound to Spo11 proteins (Fig. 1.5A) (Neale et al., 2005). Through immunoprecipitation and radioactive labelling of Spo11 attached oligonucleotides, two discrete populations different in length were identified.

These two distinct populations tend to appear in equal abundance, suggesting asymmetrical release of Spo11 by endonuclease at the site of DSBs (Neale et al., 2005). The MRX complex and Sae2 protein are both involved in this process

The DSB repair pathway involves the resection of 5' termini ends to yield recombinogenic 3' overhangs. This involves the nuclease activity of Dna2 together with the Sgs1 helicase, as well as the 5' to 3' exonuclease activity of Exo1 (Mimitou and Symington, 2008). Eliminating *exo1* in meiosis results in a reduced level of resected DNA ends (Tsubouchi and Ogawa, 2000). A different assay examined the extent of resection by using restriction sites at regular intervals from a DSB site. This study showed that *sgs1-mn* (*sgs1*-meiotic null) single mutant showed nearly a wild-type level of resection, but resection was significantly reduced in *exo1Δ* and *dna2Δ* mutants. Double mutant *exo1 sgs1-mn* also displayed a decreased level of resection (Manfrini et al., 2010). These studies suggested that Sgs1-Dna2 act independently of Exo1 in meiotic DSB resection. Another study has shown that Mre11 is responsible for the residual resections in *exo1* and efficient DSB repair requires both exonuclease activities, and that resection occurs bidirectionally (Garcia et al., 2011). Hence a model has been proposed: Mre11 endonuclease in conjunction with Sae2 creates a nick at variable distance from the DSB end. Upon creation of this nick, resection begins bidirectionally where Exo1 is resected in the 5' to 3' direction away from the DSB, and Mre11 in the 3'-5' direction towards the DSB end (Garcia et al., 2011).

After resection, 3' overhangs are produced. These single-stranded DNA (ssDNA) become bound by bacterial RecA orthologs to form helical nucleofilaments, which are responsible for searching for intact homologous

double-stranded DNA (dsDNA). In budding yeast, RecA orthologs consist of two proteins: the ubiquitous Rad51 and the meiosis specific Dmc1 recombinase (Fig. 1.5B) (Bishop et al., 1992; Shinohara et al., 1997). Different genetic requirements in the loading of Dmc1 and Rad51 have been suggested (Shinohara et al., 1997). When both proteins work together, strand exchanges preferentially occur in homologous chromosomes rather than sister chromatids. In contrast, different phenotypes have been observed in these proteins in the absence of one or another. For example, in the absence of *rad52Δ*, accumulated DSB occurs, and in this mutant Rad51 focus formation were completely abolished but Dmc1 foci were only reduced by two-fold (Lao et al., 2008). In an opposite example, no Dmc1 foci were observed when *MEI5* and *SAE3* were absent, but Rad51 foci were not affected (Hayase et al., 2004). Furthermore, inter-sister chromatid repair became dominant when *RAD51* was deleted, and inter-homolog recombination reduced. In contrast, in a *dmc1Δ* mutant, both reduction of inter-sister and inter-homolog recombination were observed. This is due to inhibition of Rad51 by Hed1 and its effector kinase Mek1. More interestingly, recent studies have shown that Dmc1 mediates inter-homolog strand exchange, which requiring Rad51 inhibition in strand exchange activity, and this Rad51 inhibition is due to Hed1 inhibition (Lao et al., 2013; Liu et al., 2014). These studies proposed that the reason for this is because Hed1 converts the recombination enzyme Rad51 to a recombination mediator. Another study further supports this theory by showing interaction of Rad51 with DNA and formation of nucleoprotein filaments is pre-requisite for normal meiotic recombination (Cloud et al., 2012).

The 3' end/Rad51/Dmc1 complex then seeks for homologous sequence. After

this, the Rad51/Dmc1 nucleofilaments promote the formation of homologous duplex DNA (D-loops) by invading the ssDNA ends into the homologous chromatid. These D-loops have also been named as single-end invasion (SEI) (Hunter and Kleckner, 2001). The 3' end continues to extend production of the D-loop, eventually annealing with the other 3' end of the break. This annealing also requires Rad52 (Lao et al., 2008). The next stage is called a double 'Holliday Junction' (dHJ), where the second 3' end is polymerized using the D-loop as a template and ligates the two extended 3' ends to the resected 5' ends (Fig. 1.5C) (Szostak et al., 1983). Crossovers (COs) or non-crossovers (NCOs) are produced depending on how dHJs are resolved by cleavage. This situation is very complicated in meiotic recombination, and it is still unclear how decisions are made upon resolving into COs or NCOs, and several pathways are involved depending on whether the products are COs or NCOs.

The original DNA repair model by Szostak et al. (1983) proposed that cleavage of the same strand or a different strand on dHJs gives equal number of COs and NCOs. However, it has now been revealed that crossover pathways and non-crossover pathways are temporally and genetically different (Allers and Lichten, 2001). In fact, the production of non-crossover recombinants is derived from a mechanism called Synthesis-Dependent Strand Annealing (SDSA) (Fig. 1.5D) (Allers and Lichten, 2001). In this mechanism, the step of forming stable dHJs was absent and NCOs were formed after DNA synthesis by annealing of the two broken ends (Allers and Lichten, 2001; Borner et al., 2004). Molecular experiments showed that SEI and dHJs are specific precursors to the crossover pathways (Hunter and Kleckner, 2001). Furthermore, mutations in *ZMM* proteins appeared with reduced SEIs, dHJs and crossovers whereas non-

crossovers were not affected (Borner et al., 2004). Ndt80 is a meiosis-specific transcription factor. In *ndt80Δ* mutants, accumulations of dHJs occur and no COs was formed, whilst NCOs were produced normally. This further suggesting that dHJs are precursors to crossovers following exit of pachytene (Allers and Lichten, 2001). A subsequent study in Cdc5 has further supported this. In this study, conditionally induced Cdc5 in *ndt80Δ* cells leads to resolved dHJs and the formation of crossovers (Sourirajan and Lichten, 2008).

How are crossover pathways or non-crossover pathways achieved? There are two pathways involved in budding yeast to direct DSBs to be repaired by crossover pathways. The first pathway involves a group of meiosis-specific proteins named 'ZMM's (Zip1, Zip2, Zip3, Spo16, Mer3, Msh4 and Msh5) (Fig. 1.5C, Fig. 1.7A) (Borner et al., 2004; Fung et al., 2004). These proteins seem to promote stability of SEIs, formation of dHJs and ensure crossover production. In the absence of these proteins, severe defects were observed in SEI, dHJ and CO formation, whilst NCOs were largely unaffected (Borner et al., 2004). Among these proteins, Msh4 and Msh5 seem to directly stabilize early strand invasion intermediates, which is supported by *in vitro* study in human homologues of these enzymes. In this study, hMSH4 and hMSH5 form a heterodimeric complex that binds specifically to HJs (Snowden et al., 2004). 80%-95% of crossovers in *S. cerevisiae* are dependent on the ZMM pathways (Borner et al., 2004), and these crossovers are non-randomly distributed. This non-random distribution is termed 'interference'. However it is unclear how ZMM proteins monitor interference. One possible explanation by Borner was the stress-release model (Borner et al., 2004), where replication of DNA leads to condensed structure of chromatin (stress) that might eventually breaks around

some regions. It is these regions that are eligible for crossovers. However, no experimental evidence has proved this model.

Moreover, another pathway involved in budding yeast for crossover is the involvement of Mus81-Mms4 endonuclease and this pathway does not require a dHJ intermediate (Fig. 1.5E). Interference has not been observed in this pathway (Argueso et al., 2004; de los Santos et al., 2003). In *S. pombe* where there is no CO interference, this pathway is responsible for all meiotic crossovers, whereas there is only a small reduction in meiotic crossovers in *S. cerevisiae* (Argueso et al., 2004; Smith et al., 2003), suggesting this pathway as a back-up in budding yeast.

Another interesting feature that has been illuminating in recent years, are the anti-crossover proteins in *S. cerevisiae*. In budding yeast this involves the Bloom syndrome Helicase (BLM) Sgs1. In the absence of ZMM proteins, crossovers are reduced. However in the double mutants that also lack Sgs1, crossovers are restored (Jessop et al., 2006; Oh et al., 2007). Therefore it is believed that ZMM proteins antagonize the anti-crossover activity of Sgs1. Interestingly, only a modest increase in crossovers in *sgs1* mutants was expected than if all dHJs were resolved (Jessop et al., 2006; Rockmill et al., 2003). The reason for this is suggested in a recent study by (De Muyt et al., 2012). In *sgs1Δ* mutants, non-crossovers are observed when joint molecules disappear and COs appear. This phenomenon indicates that in the absence of Sgs1, dHJs are resolved into COs and NCOs, as proposed in the original model by Szostak et al. (1983). Moreover, three known Holliday junction resolvases Mus81-Mms4, Yen1 and Slx1-Slx4 also provide additional insights (Boddy et al., 2001; Fekairi et al., 2009; Ip et al., 2008). Experiments lacking these

enzymes were observed with only small reductions of crossovers and resolved majority joint molecules (De Muyt et al., 2012; Zakharyevich et al., 2012). Triple mutants lacking these enzymes were still observed with mild reduction of JM resolution and CO formation. Overall, these studies indicate that these resolvases only process a small portion of joint molecules. The majority of joint molecules are probably resolved through the ZMM pathway.

Furthermore, crossover assurance is another feature in crossover formation. This is when each chromosome pair receives at least one crossover, and an experiment in the ZMM protein Spo16 has shown that crossover insurance and interference can be genetically separated (Shinohara et al., 2008). In the absence of Spo16, crossover interference was observed. This is shown by the localization of Msh4-Msh5 foci on meiotic chromosomes. In contrast, crossover assurance was abolished in all *zmm* mutants as well as in *spo16Δ*.

1.2. The Synaptonemal complex

The appearance of SC begins with the axial element (AE), which is in association with each chromosome (pair of sisters) (Page and Hawley, 2004), forming a rod about 50 nm in diameter (Zickler and Kleckner, 1999). AE are aligned together upon the matching sequence brought from the DSB initiation. This stage occurs between early-mid leptotene (Page and Hawley, 2004). The alignment of AE can be visualised as interaxis bridges. Eventually these bridges mature into a structure known as axial association (AA), which incorporates into the SC as lateral elements (LE). LE are separated by about 100 nm throughout the length of homologous pairs (Rockmill et al., 1995). Synapsis initiation sites are believed to be nucleated from these AA and be gradually incorporated into the SC as part of the LEs (Fig. 1.6) (Rockmill et al., 1995). This initiation occurs at mid-late zygotene. Proteins known as transverse filaments expand along the LE to form the central element (CE) of the SC. Extension of the CE affects the complete synapsis of homologs. By the end of pachytene a complete SC should form as a ribbon-like tripartite protein structure. Protein components that form each element in the budding yeast SC are described below and comparisons are made to other organisms where relevant. The transverse filament is described in greater depth in section 1.2.1

1.2.1 The Synaptonemal complex in budding yeast

The transverse filament that forms the central region of the SC has been identified through several species. These are: Zip1 in *S. cerevisiae* (Sym et al., 1993); SYCP1 in mammals (Meuwissen et al., 1992); C(3)G and Corrola in *Drosophila* (Collins et al., 2014; Page and Hawley, 2001); ZYP1a and ZYP1b in plants and SYP-1 and SYP-2 in *C. elegans* (Colaiacono et al., 2003; MacQueen et al., 2002). Although they show weak conservation in their primary amino acid

sequence, they all possess an alpha-helical coiled-coil domain located in the centre of the protein, flanked by large globular domains (Fig. 1.6) (reviewed in (Page and Hawley, 2004) (see Section 1.2.2). The central region of the SC plays crucial roles not only in the formation of SC but also other functions. This thesis focuses on the characterisation of Zip1 in budding yeast therefore Zip1 is described in great depth in this section and comparisons of SC structures in different species are described in Section 1.2.2.

1.2.1.1 Zip1, the transverse filament in budding yeast

Zip1 is the central region of the SC (Sym et al., 1993) and has a coiled-coil domain flanked by C- and N-terminal globular domains, consisting of 875 amino acids (Tung and Roeder, 1998) (Fig. 1.6A). Altering the length of the coiled-coil region of *ZIP1* have shown that the width between the LE changes, furthermore this supports the theory that Zip1 is the central region of the SC. Increasing the length of the coiled-coil increases the width suggesting Zip1 lies perpendicular to the lateral elements and is the building block of the SC (Sym and Roeder, 1995). Complete knock out of *zip1Δ* results in either reduced sporulation or arrested sporulation depending on strain background (Sym and Roeder, 1994). Full length AE form with homologous pairs in *zip1Δ*, but are defective in synapsis indicating Zip1 is a central region of the SC (Sym et al., 1993). A nearly wild-type level of recombinants was observed in *zip1Δ* sporulation defective strains (Sym et al., 1993). The *zip1Δ* strains that sporulate display not only the initiation of recombination, but gene conversion and crossing over were also completed. This probably explains some viable spores in *zip1Δ* (57%) compared to the wild-type 96% (Sym and Roeder, 1994). These features in

combination with other SC proteins studied, such as *hop1Δ*, *mer1Δ* mutants, implies that recombination does not require synapsed chromosomes.

However, interference is completely abolished in *zip1Δ* mutant (Sym and Roeder, 1994). Tetrad analysis at five different intervals of *zip1Δ*, using a non parental ditype (NPD) to calculate interference has shown that in the wild type positive interference was observed (0.148 to 0.589), whereas in the *zip1Δ* mutant, interference ranged between 0.98 to 1.395 (Sym and Roeder, 1994). Ratio to 1 indicates no interference and a value small than 1 indicate positive interference (wild-type). However, a *zip1Δ* mutant displayed a ratio not significantly different to 1, suggesting interference is abolished. These data imply that crossover interference requiring SC. However, later studies revealed crossover interference does not require SC. The fact that no interference was detected in a *zip1* mutant probably is an indication that SC formation requires interference (Borner et al., 2004).

Although the crystal structure of Zip1 has not been revealed yet by crystallography, experiments using in-frame deletions based on predicted amino acids have shed light on the structure and function of Zip1 (Tung and Roeder, 1998). Deletion of the N terminus did not affect chromosome synapsis but dot linear Zip1 staining was observed in some nuclei. This implies that the N terminus is not required for synapsis but might be required for stabilizing Zip1 to chromosomes (Tung and Roeder, 1998). Two deletions were made at the C-terminus, where C1 had the first 34 amino acids deleted and C2 had the rest of C terminal deleted. Elimination of C1 resulted in full length axial element assembly and pairing between homologs (Tung and Roeder, 1998). However no SC was observed. Knocking out C2 had a more distinct defect, where it was

completely indistinguishable from the complete knock out of *zip1Δ*. Therefore this implies that the C-terminal of Zip1 plays an essential part in SC synapsis and might be the binding region with other LE. Indeed, using immune-gold labelling technique Dong and colleagues discovered the organisation of Zip1 along the chromosomes (Dong and Roeder, 2000). They found that the NH₂-terminal domain is located in the middle of the region of the SC, and the COOH-terminal domain is embedded in the lateral elements of the complex (Dong and Roeder, 2000).

As Zip1 has been assumed to form a rod-shaped homodimer flanked by globular domains (Sym et al., 1993; Sym and Roeder, 1995), Dong and colleagues have confirmed through gel filtration that two Zip1 dimers form a homotetramer. This tetramer lays head to head across the LE, where both C-terminus incorporate with LE and the N-terminus of one dimer binds with another N-terminus of the Zip1 in the middle. Space between LE is ~110 nm by electron micrograph, consistent with two Zip1 dimers, each 60 nm in length. This further confirms the configuration of Zip1 lying head to head (Dong and Roeder, 2000). How these two dimers hold together between their N terminals remains unclear.

Spore viabilities seem also to correlate with SC formation, where mutants such as the N-deletion produce wild-type-like viabilities. In contrast the C-deletion mutants behaved similarly to the null mutant. Deletion of other regions was observed as incomplete synapsis results in decreased spore viability but still higher than *zip1Δ* (Tung and Roeder, 1998). Crossover was also varied depending on the degree of spore viability; this in turn suggests that different parts of the Zip1 affect crossover to a different extent in the genome. Mutants

that displayed positive SC synapsis displayed positive interference whereas reduction in SC formation reduced interferences (Tung and Roeder, 1998). Again this further supports the fact that SC plays a role in interference.

Moreover, on chromosomal structure level, *zip1Δ* also displays aggregates of SC like material under fluorescence microscope, and has been observed in many different organisms (Sym and Roeder, 1995). This is termed polycomplexes (PCs). This feature is common among synapsis defective mutants. PCs generally appear after disassembly of the SC and tend to not associate with the nucleus. The presence of PCs has not been completely understood, and they are assumed to be aggregates of proteins that had dissociated from or were used as precursors during the SC formation (Sym and Roeder, 1995). Mutants that are defective in the SC also tend to observe with a large quantity of PCs in their nucleus, such as *zip1Δ*, *zip2Δ*, *zip3Δ*, *zip4Δ*. These PCs generally fail to associate with chromatin, as no DAPI staining was observed around the area of a PC.

Zip1 has also been found to prevent crossing over at centromeres, as crossing over occurs in high frequency when *ZIP1* is deleted (Chen et al., 2008). Why is there no crossing over around the centromere? The Roeder Lab has proposed that crossovers at centromeres would lead to precocious sister chromatid separation. Hence, Zip1 might act as crossover inhibition.

1.2.1.2 The axial and lateral element of the Synaptonemal complex

Initiation of the SC appears at the axial association (AA), and there is some evidence indicates that these AA correspond to sites where DSBs have been committed to the production of crossover (Rockmill et al., 1995). First the occurrence of AA is Spo11 dependent (Agarwal and Roeder, 2000). Secondly

RecA homologs Rad51 and Dmc1 have been indicated in establishment of AAs, in which the assembly of Rad51/Dmc1 requires the formation of DSBs (Agarwal and Roeder, 2000; Rockmill et al., 1995). Proteins required for the formation of DSBs also localise to the AA (reviewed in (Page and Hawley, 2004).

Since AA has a crucial role in synaptic initiation, it is probably interplayed with their central role in crossover maturation. Several pieces of evidence have pointed toward this notion between synapsis initiation complex (SIC) and late recombination nodules in mediating the maturation of DSBs into crossovers. SIC and late recombination nodules are both Spo11 dependent, and appearing/disappearing in parallel timing (Agarwal and Roeder, 2000). Frequency of crossing over is reduced in the absence of these SIC proteins also suggesting these proteins lie in the same epistasis group as recombination (Agarwal and Roeder, 2000; Chua and Roeder, 1998; Sym et al., 1993). Sgs1 is a RecQ family of DNA helicases and in the absence of *sgs1Δ* the number of AA and the level of crossing over is increased (Rockmill et al., 2003) further indicating the involvement of AA in crossing over.

As mentioned previously, ZMM proteins are involved in promoting crossover specific processes in DSBs and they do not inhibit the noncrossover DSB repair (Borner et al., 2004), thus indicating that DSBs are differentiated into crossover and noncrossover prior to the establishment of the SC. A model has been proposed between DSB differentiation, AA formation as well as ZMM/SIC formation (Borner et al., 2004). During early to mid leptotene, initiation of DSB creates interaxis bridges and Dmc1/Rad51 complex associates with the interaxis bridges along their length (Page and Hawley, 2004). Within these interaxis bridges, DSBs are likely to be engaged in adjacent interactions with

their partner DNA (Hunter and Kleckner, 2001). This indication has led to the proposal of this small fraction of interaxis bridges is monitored by an unknown mechanism that allow them to become future crossovers (Borner et al., 2004). However, this model does not explain the SC formation in *Drosophila* female and *C. elegans*, because SC formation is not required for DSB formation (Colaiacovo et al., 2003; Jang et al., 2003).

In budding yeast, Hop1 and Red1 are meiosis specific proteins that are constituents of the LE (Fig. 1.7A) (Hollingsworth et al., 1990; Smith and Roeder, 1997). Abnormal SC forms in the absence of *hop1Δ* and *red1Δ*. The only difference between these two proteins in SC is that fragments of AE forms in *hop1Δ* mutants whereas AE are completely abolished in *red1Δ* mutants (Loidl et al., 1994; Rockmill and Roeder, 1990). Hop1 shares similarity with protein HIM-3 in *C. elegans* (Zetka et al., 1999), and Asy1 in plants (Armstrong et al., 2002). These proteins all localise along the chromosome axes during prophase I, and they share a region of amino acids known as the HORMA domain, thus suggesting they belong to the same protein family. Hop1 seems to bind preferentially to a guanine-rich sequence at a nonspecific DNA binding site and might be mediated by a zinc finger domain, although the other two proteins lack zinc finger (Kironmai et al., 1998; Muniyappa et al., 2000). Red1 remains associated with the chromosome through pachytene and Hop1 dissociates as the chromosome synapses. It has been shown that Red1 remains bound to the chromosome in the absence of *HOP1*. However, interestingly Red1 is required for the localisation of Hop1 onto bivalent axes (Smith and Roeder, 1997). Red1 can form homo-oligomers at its C-terminus and physically interacts with Hop1.

This interaction is abolished when mutating the lysine residue on Red1 (*red1-K348*) to glutamate (Woltering et al., 2000).

Meiosis specific Rad53 homolog Mek1 is also involved in the lateral element complex. Red1 and Mek1 co-localize from zygotene through pachytene (Bailis and Roeder, 1998). Recent studies have revealed the model for Hop1/Red1/Mek1 in SC formation. Activation of Mec1 and Tel1, which are yeast homologues of mammalian ATR ATM kinases that requires Red1 in association with SUMO polymeric chains (Lin et al., 2010), as well as the 9-1-1 complex (Ddc1-Mec3-Rad17) (Eichinger and Jentsch, 2010). These kinases phosphorylate Hop1 at multiple SQ/TQ motifs within its N-terminal SCD, particularly at T318 (Carballo et al., 2008). Phosphorylation of Hop1-T318 leads to the activation of Mek1 and ultimately its recruitment to chromosomes (Carballo et al., 2008). Mek1 then phosphorylates substrates involved in DSB repair pathways (Wan et al., 2004).

Zip1 has also been shown to contain a putative SUMO binding motif in its C-terminus. It co-localizes with Smt3SUMO at the synapsed region, when the C-terminus of Zip1 is removed and SC formation is abolished (Cheng et al., 2006). In the absence of *ZIP1*, SUMO does not form linear localization, instead it localizes to foci and aggregates of polycomplexes (Hooker and Roeder, 2006). These foci tend to localize to the axial element. This indicates a link between SUMO and synapsis initiation sites. Indeed it has been found that SUMO partially localize with Zip3. An E2 enzyme (Ubc9) that is required for conjugation of SUMO to substrates shows involvement in synapsis initiation, where it requires the E3 ligase Zip3 to localize to the chromosome. Zip1 is also required for Ubc9 to localize to the chromosome, as in the absent of *zip1Δ* few foci on

the chromosome were observed. SUMO itself also requires SC since mutation of the enzyme responsible for SUMOylation is defective in SC (Hooker and Roeder, 2006). Red1 has been shown to interact with Zip1 via 'sandwiching' the polymeric Smc3SUMO (Lin et al., 2010). However, SC still assembles via SUMO in the absence of E3 ligase *ZIP3*. A small amount of SUMO is still detectable in cells that lack *zip1Δ*, although Red1 is present (Humphryes et al., 2013). Also, *smt3-allR* mutants that lack polymeric chains still form SC (Cheng et al., 2006). Therefore, the mechanism and role of SUMOylation in the SC central region still remains mysterious.

The cohesin complex is not only involved in the cohesion process during meiosis, it also forms part of the lateral elements of the SC (Fig. 1.7A). It has been found that the meiotic kleisin subunits Rec8 and Smc3 form linear stretches during pachytene, very similar to the Zip1 staining pattern. In the absence of *REC8* and *SMC3*, AE fragments are abolished, suggesting these two proteins are part of the LE complex (Klein et al., 1999). Moreover, Zip1 is aggregated into polycomplexes in a *rec8Δ* mutant, similar in a manner to other SC defective mutants. Cohesin proteins co-immunoprecipitate with Red1 which reveals a very similar profile of localization, indicating cohesin proteins are present with Red1 at the lateral element (Blat et al., 2002). A more recent study has revealed mutation of six serine residues of Rec8 (*rec8-6A*) leading to severe SC formation defects, while sister chromatid cohesion and recombination occur normally (Brar et al., 2009). This finding indicates that the function of Rec8 is clearly important for SC formation and this is independent of its other roles in meiosis. However, at the moment there is no direct evidence of Zip1 physically interacting with Rec8, possibly suggesting that Rec8 is assisting

in SC formation without directly binding to Zip1. Taken together, the SC is composed of Hop1, Red1, Smt3SUMO and cohesin, with the central element Zip1 and Ecm11-Gmc2 (see Section 1.2.3) in between.

1.2.2 The structure of the Synaptonemal complex in other organisms

The Synaptonemal complex (SC) is a conserved proteinous structure and shares similar structure homology and common functions. Most organisms that possess SC have a common structure composed of two lateral elements (LE), connected by the transverse filament (TF) (reviewed in Page and Hawley, 2004). The TFs overlap with each other forming dimers, which looks like a zipper. These TFs proteins eventually form the central element (CE) of the SC, lying at the central region between the two LE. The TFs also have a common structure consisting of a globular N-terminal domain, a coiled-coil domain and a globular C-terminal domain. The C-terminal domain connects with the LE perpendicularly and the N-terminal is located in the central region. Although the SC structures are similar in organisms they share little homology in sequence and subtle differences exist. This section describes the structural difference between organisms (Fig. 1.6).

1.2.2.1 Flies

Only female *Drosophila melanogaster* has the SC. The central region of the SC in *Drosophila* is composed of two transverse filaments: C(3)G that spans the gap between adjacent LE (Page and Hawley, 2001), and a more recently identified protein Corolla, which localizes in parallel to C(3)G (Collins et al., 2014). Furthermore, another protein Corona (CONA) has also been identified as a component of the central region, where it stabilizes the assembly of the TFs in the central region (Page et al., 2008). The CONA protein colocalises with C(3)G

in the linear form of the SC and polycomplexes (PC), and these two proteins are dependent on each other for localization (Page et al., 2008). It has been believed that CONA is required to assemble together the TFs that span across the width of the SC, allowing stabilization between the N-terminus at the central region (Page et al., 2008).

The C(3)G protein has the common predicted TF structure, where it consists of globular C- and N-terminal domains connected with a predicted coiled-coil domain (68 nm) (Page and Hawley, 2001). C(3)G has shown similar features to the budding yeast CE protein Zip1, where in-frame deletions of the coiled-coil region of C(3)G leads to elevated unsynapsed chromosomes. C(3)G only localizes to the homologously paired chromosomes at the synapsed region in female oocytes (Fig 1.6B) (Page and Hawley, 2001). Later established work using electron micrographs has revealed an identical arrangement of the position of C(3)G in the SC to yeast and mammalian TFs (Liu et al., 1996; Tung and Roeder, 1998), where the C-terminal binds to the LE and the N-terminal lies at the middle of the CE in *Drosophila* female oocytes (Anderson et al., 2005).

The most recent identified TC Corolla has shown similar features to other TFs and contains a predicted coiled-coil domain. Mutation of *corolla* were observed with elevated non-disjunction frequencies; failure to cluster centromeres during early prophase. Moreover, γ -H2AV foci were reduced indicating the requirement for normal levels of DSB formation. Corolla has also been shown to be required for processing DSBs into mature crossovers, similar to other TFs (Fig. 1.6B) (Collins et al., 2014). Using structured illumination microscopy (SIM) has revealed that Corolla localized perpendicularly between the two tracks of the

lateral edges of the C(3)G, hence running between the LE of the SC (Collins et al., 2014). Both Corolla and C(3)G are mutually dependent for localization. Direct physical interaction was determined between Corolla and CONA using yeast two-hybrid analysis (Collins et al., 2014).

There are three LE in *Drosophila* females, Ord, Solo and C(2)M (Anderson et al., 2005; Manheim and McKim, 2003; Webber et al., 2004; Yan and McKee, 2013). C(2)M is the putative cohesin klesin subunit, homolog to yeast Rec8 (Manheim and McKim, 2003). Ord protein has shown co-localization with the central element C(3)G in oocyte nuclei (Webber et al., 2004). Deletion of *ord* results in premature dissociation of C(3)G and C(2)M, and no observation of LE but some transient CE-like structures were observed using electron microscopy (Webber et al., 2004). Moreover, accumulation of C(3)G staining was observed when C(S)M was over expressed (Manheim and McKim, 2003). In addition to these proteins, another recently identified meiosis-specific cohesion protein (SOLO) has been shown as the lateral element of *Drosophila* female SC (Yan and McKee, 2013). In the absence of *solo*, both the central region of C(3)G and the LE of Smc1 have been observed to have fragmented and spotty chromosome staining, indicating instability of the LE and central regions (Yan and McKee, 2013). Overall, these studies have indicated the importance of Ord and cohesins as crucial members of the lateral elements in *Drosophila* females.

1.2.2.2 Worms

C. elegans is another organism known to form the SC. Similar to *Drosophila*, two TFs (SYP1 and SYP2) form the central region of the SC (Fig. 1.6C) (Colaiacovo et al., 2003; MacQueen et al., 2002). Both shows the common feature of the TF, where they contain coiled-coil domains and localize to the

synapsed regions but not to the unsynapsed regions of chromosomes. The width of the SC is similar (~100 nm) to other organisms. However, SYP-1 and SYP-2 are smaller than other TFs. Colaiacovo has suggested that this is probably because SYP-1 and SYP-2 both co-operate in half of the central region in *C. elegans*.

Four proteins have been found to form the LEs in *C. elegans*, consisting of HIM-3, HTP-1, HTP-2 and HTP-3. These all belong to the HIM-3 family containing a HORMA domain (Severson et al., 2009; Zetka et al., 1999). Budding yeast LE Hop1 shares the common HORMA domain indicating evolutionary conservation of the protein. Mutations in these proteins result in typical synapsis defects, where the central protein SYP-1 failed to form linear SC, instead forming poly-complexes (Goodyer et al., 2008; Severson et al., 2009). Similar to *Drosophila*, the cohesin complex also forms part of the LEs in *C. elegans*. No SC was formed when knocking down the cohesin component SCC3 or the known Kleisin subunits REC-8, COH-3 and COH-4. The LE HTP-3 and HIM-3 formed PCs (Severson et al., 2009).

1.2.2.3 Mammals

Although a similar tripartite structure has been observed in mammals, it is much more complicated than in lower eukaryotes. There are seven identified proteins so far in mammals. The central region of the SC consists of several proteins: SYCP1, SYCE1, SYCE2, SYCE3 and TEX12. The first TF discovered in mammals was SYCP1, which contains a central coiled-coil domain flanked by globular domains. This protein contains 946 amino acids (Fig 1.6D) (Meuwissen et al., 1992). Similar to its functional ortholog Zip1 in budding yeast, SYCP1 also forms dimers and is structured in the same configuration as Zip1, such that

the C-terminus connects the LEs and the N-terminus lies in the central region of the SC (Liu et al., 1996). Further to this basic central structure, another two CE, SYCE1 and SYCE2, are recruited by SYCP1 (Costa et al., 2005). Co-localization has been observed in these proteins with SYCP1 in wild-type and *sycp3*^{-/-} mice. Antibodies specific to SYCE1 and SYCE2 showed localization of these proteins to the central region under electron microscopy. Moreover, co-immunoprecipitation from testis extracts revealed interaction of SYCE1 and SYCE2 with the N-terminus of SYCP1 (Costa et al., 2005). TEX12 is another central protein identified in mammals, which showed co-localization and co-immunoprecipitation with SYCE2 only (Hamer et al., 2006). Electron microscopy revealed localization of Tex12 to the CE in mouse and rat spermatocytes (Hamer et al., 2006). Therefore the author has suggested a possible complex formed between SYCE2 and TEX12, which interacts with SYCE1. Later work has further supported this notion. Synapsis was initiated in *syce2*^{-/-} and *tex12*^{-/-} mutant mice, but failed to extend the SC from SIC (Bolcun-Filas et al., 2007; Hamer et al., 2008; Schramm et al., 2011). Normal AE formation has been observed in these mutants, but due to failure of synapsis, these axes are joined at specific sites which have SYCP1 staining (Hamer et al., 2008). In budding yeast similar axial association has been observed in mutant *zip2Δ* and *zip4Δ* that contain Zip1 staining (Chua and Roeder, 1998; Tsubouchi et al., 2006). This probably indicates that these phenotypes are analogous. In contrast, *syce1*^{-/-} mice have not been observed to show detectable central elements. Synapsis does not even initiate in the absence of SYCE1. Faint discontinuous lines of SYCP1 have been observed along the AEs in *syce1*^{-/-} mice (Bolcun-Filas et al., 2009; Schramm et al., 2011). Taking these phenotypes together,

Bolcum-Filas *et al.* have proposed a model whereby SYCE2 and TEX12 are required to promote the polymerization of SYCP1 along the axes, with the help of SYCE1 to ensure three-dimensional 'stacking' of SYCP1 (Bolcun-Filas *et al.*, 2009).

Two LE exist in mammalian SC, they are SYCP2 and SYCP3 (Dobson *et al.*, 1994; Offenberg *et al.*, 1998; Schalk *et al.*, 1998). SYCP3 is the major building block of the LE (Alsheimer *et al.*, 2010; Lammers *et al.*, 1994), and it has a similar central α -helical domain and C- and N- 85 terminal regions to the CE SYCP1 (Baier *et al.*, 2007). Furthermore, SYCP3 has been found to form a linear structure prior to the onset of synapsis, as well as after disassembly of the CE (de la Fuente *et al.*, 2007). SYCP2 has been found to share sequence homology to the yeast LE protein Red1, indicating possible evolutionary conservation in these proteins (Offenberg *et al.*, 1998). SYCP2 is the largest SC protein identified consisting of 1500 amino acids in mice (Offenberg *et al.*, 1998; Winkel *et al.*, 2009; Yang *et al.*, 2006). Both SYCP2 and SYCP3 localize to the LEs of both synapsed and unsynapsed regions (Offenberg *et al.*, 1998; Schalk *et al.*, 1998). It has been found that SYCP2 links the CE to the LE by binding to the C-terminus of SYCP1, and in turn SYCP2 interacts with SYCP3 (Winkel *et al.*, 2009).

Cohesin proteins have also been found to contribute to LE within the mammalian SC. SMC3 and STAG3 have linear staining patterns, which correspond to the synapsed chromosome axes (Prieto *et al.*, 2001; Xu *et al.*, 2005). Several meiosis-specific cohesin mutants such as *rec8Δ*, *rad21L* or *smc1-β* have been observed to show shortened AE and incomplete synapsis

(Bannister et al., 2004; Herran et al., 2011; Revenkova et al., 2004; Xu et al., 2005). In *SMC1-β* knocked out mice, chromatin loops are expanded indicating the requirement of cohesin in fixing chromatin loops onto the chromosome axes (Revenkova et al., 2004). In *rec8Δ* mice, incomplete synapsis observed between sister chromatids suggests the importance of cohesin in maintaining normal AE formation between homologous chromosomes rather than sister chromatids. However, all of these phenotypes observed in these mutants are not as severe as in STAG3 mutant mice. Recent published work using STAG3-deficient spermatocytes and oocytes has observed no AE formation and no synapse between homologous chromosomes (Winters et al., 2014). Further to this study, another study using *rec8^{-/-} rad21L^{-/-}* double mutants also observed almost complete abolition of chromosome axes (Llano et al., 2012), indicating Rec8 and Rad21 kleisins are important in axial formation. A very weak Rad21 signal was observed before pachytene in both wild-type nuclei and in the absence of *SMC1β* immunoprecipitation (Winters et al., 2014). The author has suggested that deficiency in STAG3 would affect Rad21L and Rec8, provoking a similar phenotype as the 'double-knockout' (Winters et al., 2014), therefore concluding that these two kleisins are in association with STAG3 to contribute to axial formation. However, there might be other cohesin proteins in existence as in *stag3^{KO/KO}* mutant mice which were observed to have continued presence of cohesin and impaired sister chromatid cohesion (Winters et al., 2014), whereas in *rec8^{-/-} rad21L^{-/-}* mutant mice these phenotypes were not observed (Llano et al., 2012).

1.2.3 Assembly of the Synaptonemal complex

The formation of the SC is a highly regulated event, which requires several

processes to prevent unsuitable synapsis and the coordination of synapsis with other events during meiosis. In budding yeast, synapsis requires the initiation of DSBs (Henderson and Keeney, 2005), but this is not universal as a normal SC forms when DSB initiation protein Spo11 orthologs are mutated in *Drosophila* and *C. elegans* (Dernburg et al., 1998; McKim et al., 1998). How does the SC synapse to form this elaborate structure? First, synapsis initiates at certain sites, which are believed to be both centromeres (Tsubouchi and Roeder, 2005) as well as sites responsible for crossover-designated recombination (Henderson and Keeney, 2005). This initiation results in Zip1 loading onto the chromosome and subsequently in bidirectional polymerization of Zip1 to form a mature SC (Fig. 1.7B). A complex of proteins is required in synapsis initiation and this is named the Synapsis initiation complex (SIC) (Fung et al., 2004), which consists of Zip1, Zip2, Zip3, Zip4, Spo16 and Msh4. Establishment of synapsis as well as the maturation of DSBs into crossovers are all required by this complex and thus SIC plays a critical role in the meiotic process.

The first step in the deposition of Zip1 requires Zip3, a putative SUMO E3 ligase (Cheng et al., 2006). Zip1 constantly aggregates into large PCs, which are not associated with chromatin when *zip3* is deleted (Agarwal and Roeder, 2000), suggesting Zip3 is required in the loading of Zip1 (Fig. 1.7B). Zip3 contains SUMO E3 ligase RING finger motif, and protein sequence alignment has shown that Zip3 has a conserved histidine residue within the ring that is unique to SUMO E3 ligases (Cheng et al., 2006). Tagging Zip3 with GFP allows study on the colocalisation of Zip3 with Zip1 and Zip2 in the SC (Agarwal and Roeder, 2000; Shinohara et al., 2008). Immunofluorescence has shown that Zip3 always

localizes with Zip1 and Zip2 together, most importantly in the absence of *zip2Δ*, Zip3 localizes to chromosomes normally but it precedes Zip2 localization.

In the absence of *zip3Δ*, localization of Zip2 to chromosomes is reduced, suggesting that in order for Zip2 to localize, Zip3 has to be present on chromosomes first (Chua and Roeder, 1998). In the *zip2* mutant, the AEs of the homologous chromosomes do pair and are connected by the AA bridges, but there is no localization of Zip1 to chromosomes (Fig. 1.7B). This indicates that Zip2 must be present on chromosomes before Zip1 can localize (Chua and Roeder, 1998). A later study has also shown that Zip3 recruits Zip2 as well as Zip4/Spo22, but the latter proteins do not recruit Zip3 (Tsubouchi et al., 2006). Therefore a model has been proposed on synapsis initiation where Zip3 first binds to the AA and this result in the localization of Zip2 and Zip4 onto chromosomes. Afterwards, these three proteins work together to recruit Zip1 onto the synapsis initiation site (Fig. 1.7B).

Zip1 polymerisation is the next step in SC formation. This requires Zip2, Zip4 or Spo16 (Fig. 1.7B). In the absence of these proteins, foci of Zip1 are observed to localize at AAs (Chua and Roeder, 1998; Shinohara et al., 2008; Tsubouchi et al., 2006). Furthermore, it has been proposed that these proteins 'move' at the leading edge of synapsis as they form foci on meiotic chromosomes (Chua and Roeder, 1998; Shinohara et al., 2008; Tsubouchi et al., 2006). Although the timely assembly of the SC requires these SICs, no experiments to date have shown the mechanistic requirement of Zip1 localization to chromosome axes it is interesting to see which proteins are responsible for the polymerisation of Zip1. It is also interesting to find out whether these proteins are physically interacting with each other.

Although Zip1 has been known for a while as the only protein in the central region of the SC, recent studies have revealed a few other proteins (SUMO, Ecm11, Gmc2) that might also be incorporated into the central region as substructure (Hooker and Roeder, 2006; Humphries et al., 2013; Voelkel-Meiman et al., 2013). The Ecm11-Gmc2 complex has recently been identified as functioning in the central region of the SC (Humphries et al., 2013). There is strong localization of Ecm11-Gmc2 with Zip1 in wild-type prophase, and in the absence of *Zip1* they tend to localize to the SIC rather than LE. Gmc2 localization to chromosomes is completely abolished in the absence of *ECM11*, suggesting Gmc2 localization requires Ecm11 first. In this study, several pieces of evidence have suggested that Ecm11-Gmc2 complex recruits Zip1 to the central region. First, this complex strongly co-localizes with Zip3 and without *ZIP3*, Ecm11 foci were not observed on spreads suggesting this complex comes after the localization of Zip3 to chromosomes. In fact, Ecm11 foci were not observed in *zip4Δ*, further indicating the requirement of the SIC. SUMOylation on residue K5 in Ecm11 is important for promoting the inter-chromosomal assembly of the Zip1 filament (Humphries et al., 2013), with the knowledge that Zip1 binds to SUMO further indicating the complex promotes SC formation. Taken together, Humphries and colleagues propose that this complex is involved in the facilitating of Zip1 assembly, indicating another potential regulation protein in the central region of the SC. However, whether these proteins interact with other SICs has not been studied.

How do these SIC proteins know where to start synapsis in the first place? Many evidence have pointed to sites of recombination in *S. cerevisiae*. This includes the physical interaction of Zip3 with recombination proteins Rad51,

Mre11 and Msh4-Msh5 in meiotic cell extracts and high levels of Zip3 and Zip2 foci observed to co-localise with Mre11 foci (Agarwal and Roeder, 2000; Chua and Roeder, 1998). Moreover, synapsis initiation changes in relation to changes in the number of crossovers (Henderson and Keeney, 2004). Strand invasion proteins Rad51 and Dmc1 are thought to be involved in axial association (interaxis before being incorporated into axial elements). Zip1 accumulation at axial elements occurs in mutants that fail to elongate SCs, this in turn suggests that synapsis initiation occurs at sites of recombination (Rockmill et al., 1995). The numbers of initiation sites (Zip2 and Zip3 foci) per nucleus correlates with the number of crossovers. Zip2 also show interference when they localize to the chromosome (Fung et al., 2004). In addition, deletion of *SGS2* restores crossovers in *ZMM* mutants, which is accompanied by a restoration of end-to-end synapsis (Jessop et al., 2006). Finally, crossover-designated recombination intermediates such as SEI and dHJ are affected when deleting individual *ZMM*, suggesting they are located at the same position as future crossovers (Borner et al., 2004).

It has also been proposed that synapsis initiation starts at the centromeres, where recombination is infrequent (Tsubouchi et al., 2008). This proposal is based on the observation that centromeres are often associated with short stretches of Zip1 at early stages, and *zip4Δ* mutants show axial association frequently at their centromeres whereas in *zip1Δ* mutant they did not. Also, Zip1 and Zip3 both colocalise with centromeres at zygotene (Tsubouchi et al., 2008). Therefore, it is likely that initiation begins at the centromere as well as at recombination sites. Synapsis initiation in *C. elegans* is making this theory possible, where synapsis initiates at their centromere in the absence of

recombination and chromosomal homology (Dernburg et al., 1998; McKim et al., 1998). Synapsis starts at a single site on each pair called the pairing centre, and is necessary and sufficient to trigger synapsis along the entire length of chromosomes (MacQueen et al., 2005).

How do yeast cells maintain synapsis between homologous chromosomes rather than non-homologous chromosomes if synapsis does not require homology in *C.elegans*? Several proteins have been identified as contributing to the regulation of synapsis. Zip3 is not only acting as a loading platform, but is also involved in preventing inappropriate synapsis. It has been found that Zip3 acts in parallel with the proline isomerase Fpr3 to block synapsis when the recombination initiation protein Spo11 is absent, in which case homologous chromosomes fail to pair (Macqueen and Roeder, 2009). This might also indicate the reason why Zip3 co-localizes with centromeres before the onset of recombination in wild-type meiosis (Tsubouchi et al., 2008). Hop2 functions together with Mnd1 in the repair of meiotic DSBs (Tsubouchi and Roeder, 2002). Knocking out either *HOP2* or *MND1* which results in excessive synapsis between non-homologous chromosomes, suggests these proteins are also important in maintaining homologous synapsis (Tsubouchi and Roeder, 2002).

1.2.4 Disassembly of the Synaptonemal complex

In order to exit prophase and begin meiotic division I, the SC needs to de-synapsed, thus disassemble. SC disassembly occurs during diplotene when Zip1 and other LE dissociate from the chromatin, but only remaining at chromosome ends (Newnham et al., 2010) and sites of crossovers. Diplotene is followed by diakinesis, where bivalents are individualised and only maintained at their crossovers, namely chiasmata. The presence of chiasmata is essential

for tensions between kinetochores, and hence ultimately leads to accurate segregation during meiosis I. Although less is known about disassembly compared to assembly, research in the past decade has led to some interesting ideas about this process.

Disassembly is coordinated with spindle pole body separation and resolution of dHJ into crossovers following exit from pachytene (Allers and Lichten, 2001; Newnham et al., 2010; Xu et al., 1995). The polo-like kinase Cdc5 is not only involved in regulating the resolution of dHJs, but it also drives SC disassembly. In the absence of *CDC5*, the majority of cells were arrested, leaving 10% of cell progressing towards metaphase and these 10% cells displayed mild SC disassembly phenotype (Clyne et al., 2003). This indicates that although Cdc5 is sufficient for SC disassembly it might not be the only kinase required for this event in wild-type meiosis. A more recent study has revealed that Aurora B kinase (Ipl1) is the main regulator of SC disassembly, where the SC failed to disassemble following the exit of pachytene. In the absence of *ipl1Δ*, meiotic spreads shown that Zip1 remain linear, but metaphase spindles were also formed in these nuclei (80%). This is in contrast to the wild type, where all Zip1 have disappeared upon the formation of metaphase spindles (Jordan et al., 2009). However, other cell cycle events such as SPB separation, crossover formation and entry into the meiotic divisions were unaffected in an *ipl1* mutant. Ipl1 is required in Cdc5 dependent SC disassembly, where full linear SC was observed when Cdc5 was induced in *ndt80Δ ipl1-meiotic null (ipl1-mn)* strains (Jordan et al. 2009). The mechanism of SC disassembly by Ipl1 is unclear. Mutation of several Aurora B consensus phosphorylation sites in Zip1 did not affect SC disassembly (Jordan et al., 2009), thus ruling out the possibility that

Ipl1 phosphorylates Zip1 in order to disassemble.

In budding yeast, expression of Cdc5 is regulated by the meiosis-specific Ndt80 transcription factor. This transcription factor is first expressed in late pachytene, and activates expression of more than 200 genes at mid-meiosis, including genes required for meiotic divisions such as *CLB1*, *CLB3*, and *CLB4*. It also activates spore formation (Chu and Herskowitz, 1998; Xu et al., 1995). In budding yeast, expression of CDC5 is regulated by the meiosis-specific NDT80 transcription factor. Cells lacking *Ndt80* exhibit a classic pachytene arrest, where chromosomes are fully synapsed and spindle pole bodies are duplicated, but unseparated (Xu et al., 1995). Recombination intermediates are also unresolved (Chu and Herskowitz, 1998). A study has used a strain that can artificially induce *CDC5* by placing *CDC5* under the control of *GAL* promoter (*Cdc5-IN*). The GAL4 activator was then fused to the estradiol receptor (*Gal4-ER*). This strain is also *ndt80*Δ, thus conditionally expressing *CDC5* allows the investigation of the role in pachytene exit. Upon the induction of β-estradiol, specific transcription of *CDC5* occurs, leaving the remaining genes in the Ndt80 regulon off. Surprisingly, this induction leads to HJ resolution and subsequently results in crossover formation, as well as disassembly of the SC with the disappearance of Zip1 and formation of metaphase spindles. Whereas in the kinase dead version these phenotypes were not rescued (Hollingsworth, 2008; Sourirajan and Lichten, 2008).

Other species also display disassembly but in a much different manner compared to budding yeast. For example, in *C. elegans*, due to their holocentric chromosomes, crossovers define their chromosome 'arms' rather than their

centromeres. Upon disassembly, the central element is lost asymmetrically from one 'arm' of each chromosome pair. This disassembly is controlled by the Zip3 ortholog, ZHP-3, in combination with SUMO (SMO-1), to coordinate crossover formation with asymmetric SC disassembly (Bhalla et al., 2008). This model is thought to enhance accurate chromosome segregation by assisting bivalent formation. This provides a much wider spectrum in disassembly where in yeast Zip3 couples crossover but is only required in assembly. Probably suggesting different requirements for recombination in the initiation of synapsis between these two organisms. In *Drosophila* oocytes, histone kinase NHK-1 is required for SC disassembly, as mutation in this kinase (*nhk-1^{-/-}*) leads to persistent staining of the CE C(3)G (Ivanovska et al., 2005), probably suggesting higher order chromosome dynamics are controlled by histone modifications (Ivanovska and Orr-Weaver, 2006).

SC disassembly in mice is similar to budding yeast where it requires Aurora kinase. However, subtle differences exist. *In vitro* treatment with Aurora kinase inhibitor on mouse spermatocytes shows disassembly of the central element SYCP1, but SYCP3 staining remains linear, indicating that Aurora kinase is required to remove LEs but not the CES (Sun and Handel, 2008). A recent study has also revealed that Polo-like kinase (PLK1), ortholog of yeast Cdc5 is involved in SC disassembly. An *in vivo* study has shown only PLK1 localizes to the SC but not others (PLK2-4) in spermatocytes. The CE proteins SYCP1, TEX12 and SYCE1 are phosphorylated during the G2/M1 transition *in vitro* by PLK1 (Jordan et al., 2012). Using PLK inhibitor BI2536 results in inhibiting phosphorylation of the CE proteins as well as their removal from the SC, leading to blockage of SC disassembly (Jordan et al., 2012). This interesting

finding has revealed mechanistic details of SC disassembly in mammals and with the fact that Cdc5 in yeast is also involved in SC disassembly, it suggests that this might be a conserved pathway in different species.

There are still many questions to answer, for example whether SC disassembly occurs in coordination with crossover or whether it is a separate process. With the discovery of crucial regulators in disassembly, it allows the research to be narrowed down to look for specific targets of these regulators such as Cdc5 (see Chapter 4) or Ipl1.

1.3 Meiotic Divisions

1.3.1 Mono-orientation of sister chromatids at meiosis I

In order to bring about homologous segregation during meiosis I, sister kinetochores must attach to microtubules emanating from the same spindle pole, a process known as centromere mono-orientation (Fig. 1.8). This is in contrast to meiosis II and mitosis, where sister kinetochores are required to bi-orientate. Several specific factors are involved in budding yeast mono-orientation.

Monopolin complex is involved in promoting sister kinetochore co-orientation. This complex is composed of Mam1, Lrs4, Csm1 and Hrr25 (Petronczki et al., 2006; Rabitsch et al., 2003; Toth et al., 2000). Mam1 is a meiosis I-specific protein (Toth et al., 2000). Mam1 has been found to co-localize with kinetochores throughout meiotic prophase until the onset of anaphase I. Mutation in *MAM1* results in cells failing to undergo meiosis I segregation, instead a single round of chromosome segregation is achieved in which sister kinetochores are segregated (Toth et al., 2000). The reason for this phenotype is that in the absence of *MAM1*, bipolar spindle attachment is achieved in sister kinetochores instead of mono-polar attachment. However, owing to the protection of centromeric cohesion, homologous chromosomes cannot segregate. Nonetheless, in meiosis II owing to the removal of centromeric cohesin, sister chromatids are able to segregate away from each other. Hence this results in missegregation where only two diploid daughter cells are obtained (Toth et al., 2000).

Csm1 and Lrs4 form a nucleolar protein complex in mitotic cells, and they reside in the nucleolus throughout the cell cycle where they are involved in

rDNA silencing (Rabitsch et al., 2003). But in meiotic cells, these two proteins are released from the nucleolus from late prophase until metaphase I where they associate with centromeres. These two proteins are inter-associated with each other for their release (Rabitsch et al., 2003). The same phenotype as observed in *mam1Δ* also observed in either *Csm1* or *Lrs4*, suggesting Mam1 forms a complex with Csm1 and Lrs4 (Rabitsch et al., 2003). Both suppression of sister centromere bi-orientation and the arrival of Mam1 at kinetochores is dependent on the Lrs4 protein (Rabitsch et al., 2003).

Hrr25 is a casein kinase I in *S. cerevisiae* (Petronczki et al., 2006). Mam1 binds directly to Hrr25's kinase domain and binds to Csm1/Lrs4 indirectly (Petronczki et al., 2006). Inhibiting the kinase activity of Hrr25 (using a *hrr25-as* allele) results in no mono-orientation during meiosis I, but bi-orientation in meiosis II, which is similar to the other three monopolin complexes (Petronczki et al., 2006).

Spo13 is a centromere-associated protein and is a key regulator in meiotic chromosome segregation. Spo13 is required for the localization of Mam1 during late meiotic prophase to promote sister kinetochore bi-orientation (Katis et al., 2004). In the absence of *SPO13*, cohesins are not protected around kinetochores during meiosis I but are instead lost along the entire length (Lee et al., 2004). Similarly, cells lacking PLK *CDC5* result in failed localization of Mam1 to kinetochores. Instead Mam1 was found in aggregates in association with non-centromeric chromosomal regions (Lee and Amon, 2003). Lrs4 remains localized with the Nop1 nucleolar protein in 100% of *cdc5-mn* cells with bipolar spindles at the equivalent time point (Clyne et al., 2003). Therefore Cdc5

is also responsible for the localization of Mam1 as well as the release of Lrs4, together leading to the mono-orientation during meiosis I. The phosphorylation of Lrs4 is reduced to similar extents in *cdc5-mn* and *spo13* mutants (Katis et al., 2004). Cell cycle kinase DDK assembles monopolin complex. No Mam1 foci were observed in the absence of *CDC7* activity, and it has been suggested that it is due to reduced phosphorylation of Lrs4 (Matos et al., 2008).

Chiasma also play an important role in kinetochore orientation during meiosis I. Recognition that chromosomes are properly oriented depends on the mechanical tension that results when homologs are pulled toward opposite spindle poles, and this pulling is resisted by chiasmata (Rockmill et al., 2006). Chiasmata create tension when microtubules attach to kinetochores and stabilize the kinetochore microtubule interaction (Fig. 1.8). Non-disjunction of homologous chromosomes occurs in the absence of chiasmata, it provides a vital role in preventing the bipolar attachment of sister chromatids during anaphase I (Hirose et al., 2011).

Not many orthologs of most of the monopolin proteins identified in budding yeast have been identified in other organisms. Although orthologs of Lrs4 and Csm1 exist in fission yeast (*Pcs1* and *Mde4*), their role is to prevent merotelic spindle attachments (Gegan et al., 2007). Instead, Rec8-containing cohesion enriched at the core of the centromere together with Moa-1, is required for mono-orientation in *S. pombe* (Sakuno et al., 2009; Watanabe and Nurse, 1999). However, in *S. cerevisiae* monopolin complex can sufficiently link sister kinetochores during meiosis I in the absence of cohesin (Monje-Casas et al., 2007), suggesting cohesin might not play an active role in mono-orientation in budding yeast. Nevertheless, Aurora B kinase has been either directly or

indirectly involved in both yeast species (Hauf et al., 2007; Monje-Casas et al., 2007) despite clear distinctions between their underlying mechanisms. Condensins have also recently been found to accumulate at kinetochores in budding and fission yeast (D'Ambrosio et al., 2008; Wang et al., 2004), and that condensins are required for full sister kinetochore co-orientation during meiosis I by promoting the localization of Mam1 to kinetochores (Brito et al., 2010).

Overall the above studies suggest that distinct mechanisms are in place for mono-orientation of sister kinetochores in different species. This might be due to differences in the size of the centromere and kinetochore structures between species. Budding yeast has a simple, 'point centromere' comprising a 125 bp core centromere and no flanking heterochromatin. Fission yeast has large and repetitive centromeres (40-100 kb), which comprising a central core flanked by inner- and outer-most repeats that form heterochromatin. In humans, centromeres are on average 3 Mb in size consisting of heterochromatin containing tandem alpha-satellite repeats (Brar and Amon, 2008). Moreover, kinetochores in budding yeast attach to a single microtubule (Winey et al., 1995), whereas several microtubule-binding sites exist within a single kinetochore in fission yeast and high eukaryotes (Ding et al., 1993). Therefore it might be hard to maintain a common ancestral mechanism through evolution.

1.3.2 Protection of centromeric cohesion during meiosis I

Sister chromatid cohesin holds homologous chromosomes together distal to the crossover site. Homologs align on the meiosis I spindle due to tension created by crossover (chiasmata). Cohesin along the arms must be removed for homologous chromosome segregation. However, centromeric cohesion must be protected during meiosis I to ensure accurate segregation of sister chromatids

during meiosis II. This step-wise loss of cohesin during meiosis is one of the crucial mechanisms for correct chromosome segregation.

A conserved protein named 'Shugoshin' (or Sgo1) is responsible for protection of centromeric cohesin at meiosis I (Fig. 1.9). Sgo1 was originally identified from genome-wide screens in budding yeast and fission yeast by screening through mutants that cannot maintain centromeric cohesion during first meiotic division (Kitajima et al., 2004; Marston et al., 2004). Chl4 and Iml3 were another two proteins identified from a budding yeast screen that act in the same pathway as Sgo1 (Marston et al., 2004). Cells depleted of Sgo1 were unable to retain pericentromeric Rec8 during meiosis I, subsequently leading to random chromosome segregation at meiosis II (Kitajima et al., 2004; Marston et al., 2004). The spindle-check point protein Bub1 is required for the localization of Sgo1 to kinetochores (Fig. 1.9) (Kitajima et al., 2004).

Shugoshin protects centromeric Rec8 by recruiting the phosphatase 2A (PP2A) via direct interaction with its regulatory subunit Rts1 (Kitajima et al., 2006; Riedel et al., 2006). PP2A is a multi-subunit enzymatic complex made up of regulatory and catalytic subunits. Several regulatory subunits exist in PP2A (B, B', B'', B''') (Janssens and Goris, 2001; Lechward et al., 2001). However, only the B' (Rts1) subunit has shown co-purification with Sgo1 in meiotic cells, and preferentially co-localise with Sgo1 at meiotic centromeres (Kitajima et al., 2006; Riedel et al., 2006). Deletion of the PP2A-catalytic subunit in *sgo1Δ* results in premature loss of centromeric Rec8 (Kitajima et al., 2006; Riedel et al., 2006). Interaction between PP2A-Rtf1 and Sgo1 might be highly conserved as a subsequent study has shown that the catalytic subunit of PP2A to

centromeres depends on Sgo2 in mammals (Lee et al., 2008).

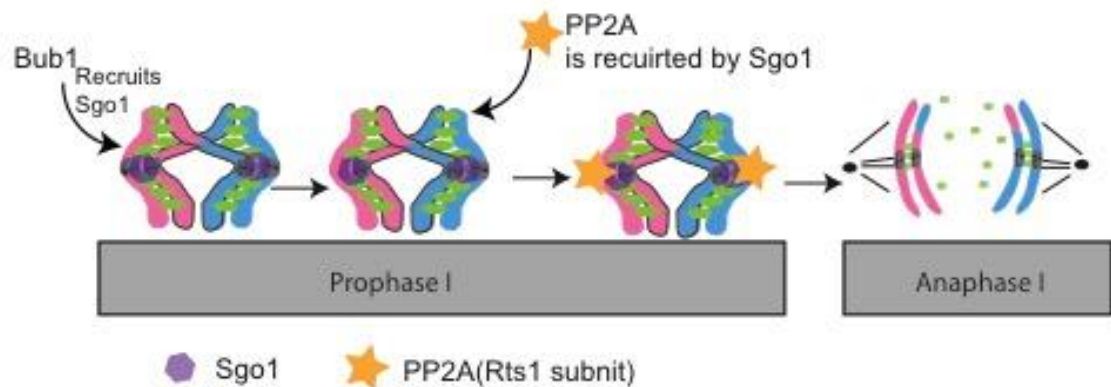


Figure 1.9 Protection of centromeric cohesion

Centromeric cohesion is protected by Shogoshin (Sgo1). The spindle check point protein Bub1 helps the recruitment of Sgo1 to centromere. Sgo1 in turns recruits PP2A phosphatase, and it is the Rts1 subunit that associate with Sgo1. This completed Sgo1-PP2A-Rts1 complex protects centromeric cohesin from cleavage of cohesins in the arm regions.

In addition to the role of recruiting PP2A by Sgo1, a subsequent study has also shown another role in inhibiting separase activity by Sgo1 (Clift et al., 2009). This work has shown that over-produced Sgo1 in mitotic cells arrest cells in metaphase with no cleavage of Scc1 (mitotic counterpart). This is due to the mitotic PP2A regulatory subunit Cdc55. Furthermore, cells depleted for *SGO1* or *CDC55* lead to cleavage of un-phosphorylated Rec8 in cells depleted for *CDC5* (Clift et al., 2009). Hence this work has shown that even when Sgo1-Cdc55 activity was inhibited, separase is able to cleave Rec8 when the 'priming' phosphorylation events were absent. Furthermore, PP2A-Rts1 complex formed in excess and increased dramatically on chromosomes when Cdc55 was absent. This action prevents Rec8 phosphorylation and cleavage (Bizzari and

Marston, 2011). Overall these studies suggest Sgo1-Cdc55 directly inhibits separase activity, which is independent of Rec8 phosphorylation.

A fundamental prerequisite for homolog segregation is the removal of distal cohesion along chromosome arms, which in turn results in chiasmata resolution. Removal of Rec8 is achieved by separase-mediated cleavage at two sites that removes cohesins from chromosome arms (Buonomo et al., 2000). Early work by Riedel and colleagues has shown that tethering of PP2A-B' subunits in *S. pombe* not only prevents loss of Rec8 on the centromeres, but also prevents Rec8 phosphorylation (Riedel et al., 2006). A subsequent study in budding yeast has also shown that efficient cleavage of Rec8 in meiosis I requires Rec8 phosphorylation (Brar et al., 2006). Nevertheless, when 17 identified sites in Rec8 are mutated to alanine to prevent its phosphorylation (*Rec8-17A*), deletion of Sgo1 led to alleviated Rec8 cleavage delay in meiosis I (Brar et al., 2006). This probably suggests that there are other sites involved in phosphorylation of Rec8 in order to cleave. It indeed, recent work by Katis and colleagues have identified more sites within Rec8, and mutation of these sites as well as the previously identified 17 sites (*rec8-24A*) have shown complete blockage of Rec8 cleavage (Katis et al., 2010). *Rec8-24A* cells depleted for *SGO1* did not show any improved cleavage and also showed resistance to cleavage by separase *in vitro* (Katis et al., 2010). Among these sites, 14 sites have been made into a phosphomimetic version (*Rec8-14D*) and have shown premature loss of centromeric Rec8 in meiosis I even when Sgo1-PP2A-Rtf1 are present at the centromere (Katis et al., 2010). These studies probably suggest that Sgo1-PP2A complex counteracts with Rec8 phosphorylation to prevent centromeric Rec8 from separase.

In budding yeast, Cdc5 has been implicated in the phosphorylation of Rec8 to promote cleavage and counteracts with PP2A-B' at the pericentromere. Cells deleted for *CDC5* have shown reduced Rec8 phosphorylation and delayed cleavage in meiosis I (Clyne et al., 2003; Lee and Amon, 2003). Furthermore, the *rec8-17A* mutant contains 11 Cdc5-dependent phosphorylation sites as well as 4 other predicted Cdc5 consensus sites showing delay in Rec8 cleavage during first meiotic division (Brar et al., 2006). Despite the above evidence, several other observations indicate that Cdc5 phosphorylation in Rec8 might not be essential for Rec8 cleavage. For example: in the absence of Sgo1, Rec8 is still cleaved in cells lacking Cdc5 (Brar et al., 2006); degradation of securin is retarded in cells depleted for Cdc5 (Clyne et al., 2003; Lee and Amon, 2003). These observations are probably comparable with the finding that Rec8 is also phosphorylated by casein kinase (Hrr25) and DDK (Cdc7-Dbf4) (Katis et al., 2010). Rec8 phosphorylation is reduced and cleavage is blocked when CK1 and DDK activities were inhibited, similar to the *rec8-24A* mutant (Katis et al., 2010). Furthermore, the phosphomimetic mutant (*rec8-14D*) partially restores Rec8 cleavage when CK1 and DDK1 were inactivated, implying that Rec8 cleavage is enhanced by CK1 and DDK1 in its phosphorylation (Katis et al., 2010). Moreover, in the absence of these two kinases, Rec8 did not cleave in cells lacking Sgo1, indicating Sgo1-PP2A counteracts with CK1 and DDK (Katis et al., 2010). This evidence shows that Rec8 phosphorylation by casein kinase and DDK is essential for its cleavage at anaphase I.

Spo13 also required for localisation of Sgo1 at centromeres (Kiburz et al., 2005). Although the precise mechanism for this is unclear, a study by Matos et al. has shown that Spo13 binds to Cdc5 during meiosis I (Matos et al., 2008),

which might indicate some correlation between Cdc5 centromeric protection with Spo13. Ipl1 has also been shown to maintain PP2A-Rts1 at the centromere, an additional role in cohesion protection (Yu and Koshland, 2007). Precise mechanisms in these factors in regulating the Sgo1-PP2A-Rts1 is unknown and it will be one of the important areas to investigate in future research.

1.4 Non-exchange chromosome segregation (NECS)

Chiasmata play important roles in ensuring accurate homologous chromosome segregation at the first meiotic division. Many organisms rely primarily on this crossover-dependent pathway. However, there are organisms that participate in achiasmatic pathway, where no crossovers occur on either all chromosome sets or in some organisms where particular chromosome partners are achiasmate. In these organisms, different mechanisms ensure high fidelity segregation of the achiasmate chromosome pairs (Fig. 1.10). However, there is now evidence (see below) that these organisms require crossover-mediated chromosome segregation to also work in conjunction with non-exchange mechanisms as 'back up' to ensure high fidelity segregation.

Human fidelity errors show high levels of NECS, hence it is crucial to understand non-exchange chromosome segregation. Roughly 40% of maternally derived cases of trisomy 21 were due to an achiasmate chromosome pair (Lamb et al., 1996). Chromosome 15, 18 and the sex chromosome were also observed to have similar frequencies of trisomy (Hassold et al., 2000). The development of cytological work using human oocytes has also shown roughly 25% of chromosome pairs did not contain any Mlh1 foci (a marker for crossovers), an indication of non-exchange (Cheng et al., 2009). In this section, NECS pathways are described in different organisms. In particular, a detailed description in yeast and *Drosophila* is made as NECs have been studied intensively in these two organisms. Comparisons to other organisms are described in Section 1.4.2

1.4.1 Discovery of NECS in yeast, flies and worms

1.4.1.1 Yeast

Although in budding yeast and fission yeast segregation of chromosomes at the first meiotic division preferentially relies on a crossover-mediated pathway, both organisms contain non-exchange segregation mechanisms as 'back up' (Davis and Smith, 2005; Dawson et al., 1986). About 30 years ago Dawson and colleagues identified NECS in budding yeast using an artificial chromosome that does not recombine (Dawson et al., 1986). Segregation fidelity in these artificial chromosomes show 90% of disjunction at meiosis I, despite a lack of crossovers (>97% of meiosis). By using a mini chromosome it was further shown that this high fidelity segregation was neither dependent on recombination nor sequence homology (Dawson et al., 1986). This experiment was done using a diploid that contains two artificial yeast chromosomes with four marker genes (*LEU2*, *TRP1*, *URA3*, *HIS3*) in a co-linear configuration. This strain also contains an ARS element and a yeast centromere embedded within a bacteriophage λ -DNA backbone. A mini-chromosome III is also contained within this diploid that shares no homology to the artificial chromosome pair. Segregation patterns of these three non-exchange chromosomes were consistent with the predicted segregation frequency (Dawson et al., 1986), hence indicating that NECS segregation is not affected by homology. Another study further confirming Dawson's finding where higher levels of DNA sequence homology (30 kb) still showed little or no crossing over between NECs (Ross et al., 1996). However, Maxfield Boumil and colleagues later suggested that too similar DNA sequence homology between NECs might affect segregation result, as certain degrees of strand invasion might bias homologous tendency to act as segregating partners (Maxfield Boumil et al., 2003).

A study using a yeast strain containing double monosomic chromosome 1 and 3 showed that non-exchange still segregates in a similar manner as artificial chromosomes (Guacci and Kaback, 1991). These univalent chromosomes showed 89% of disjunction at meiosis I in these genuine yeast chromosomes and single monosome in spore viability suggesting exchange segregation was not affected (Guacci and Kaback, 1991)

In recent years, another type of yeast strain has been constructed where in a diploid one copy of chromosome five from *S. cerevisiae* is replaced with the equivalent chromosome five from a different species (*S. calbergnesis*). This type of yeast strain is said to contain 'homeologous chromosomes' (Maxfield Boumil et al., 2003). These two species share a high level of sequence homology (roughly 70-80%) which allows them to experience high levels of meiotic DSBs, although the sequence heterology prevents crossovers (Maxfield Boumil et al., 2003). The homeologs do not recombine due to their suppression by mismatch repair proteins, which causes unwinding or rejection of heteroduplex DNA containing mismatches. A process termed antirecombination (Chambers et al., 1996). All findings from above together confirm the existence of a non-exchange system (NEC) in yeast and it has been postulated that it acts as a back up system when the crossover dependent pathway fails.

1.4.1.2 Flies and worms

The identification of achiasmate chromosome segregation was first introduced in a study on *Drosophila* females, where the X chromosomes that failed to recombine still segregated with high fidelity (Sturtevant and Beadle, 1936). Later studies on the 4th chromosome pair in *Drosophila* also observed similar

segregation fidelity (99.9%) of oocytes in the absence of recombination (Carpenter, 1973; Grell, 1964). In males, chromosome segregation is dependent on an alternative mechanism as recombination is completely absent (Fig. 1.10C) (Hawley, 2002).

Female silk worms (*Bombyx mori*) have also been found to have segregation of crossover independent segregation of chromosomes (Fig. 1.10E). In this invertebrate, chromosomes segregate normally using a modified form of the SC instead of crossing over during first meiotic division (Rasmussen, 1977). The SC tends to undergo morphological changes after pachytene exit, where the central element becomes flattened and connects to the lateral elements. These connected lateral elements gradually become dense and shorter, subsequently forming a single end-to-end structure at metaphase with the chromatin of each chromosome to either side (Rasmussen, 1977).

1.4.2 NECS pathways in yeast, flies and worms

1.4.2.1 Yeast

How is non-exchange chromosome segregation in yeast achieved? Fluorescence *In Situ* Hybridization (FISH) shows that when all chromosomes are paired and synapsed during pachytene, the monosomic chromosome 1 and 3 physically interact with each other (Loidl et al., 1994). This indicates a physical interaction between non-exchange chromosomes before their segregation at meiosis I. This hypothesis is further supported by tagging homeologous chromosomes with lacO repeats (Kemp et al., 2004). In this study, two different lacO repeats are placed on a chromosome. One places lacO repeats on the chromosome arm, about 180 Kb from the centromere. Both

homeologous and heterologous chromosomes were examined using this system. More than 80% of nuclei showed two dots, which suggests that the arms of homeologous chromosomes are no more likely to be paired than the arms of two heterologous chromosomes (Kemp et al., 2004). However, when lacO repeats were placed very close to the centromere, roughly 12 Kb, centromeres of homeologous were paired in 54% of nuclei, whereas heterologous centromeres were not paired (>80%). Importantly, by the introduction of a competitor such as a centromere-containing plasmid or an artificial chromosome, this NEC pairing fidelity decreased. However, pairing of homologous chromosomes were unaffected, indicating these competitors only interfere with NECs (Kemp et al., 2004). These findings strongly indicate that centromere pairing is crucial mechanism for NECS.

What is the mechanism of centromere pairing in non-exchange chromosomes? Recent published studies have shown that Zip1 is the key protein in holding NEC centromeres together (Gladstone et al., 2009; Newnham et al., 2010). The wild-type NEC pairs with a frequency of 56% at their centromeres during pachytene. Knocking out *zip1Δ* in the NEC results in only 14% centromere pairing and elevated missegregation from 11% to 23% (Newnham et al., 2010). These studies also show that the Zip1 dependent NEC also requires the synapsis-initiation proteins Zip2, Zip3 and Zip4 and co-localization of Zip1 with NEC centromeres is observed throughout meiotic prophase (Gladstone et al., 2009; Newnham et al., 2010). Therefore it has been postulated that Zip1 promotes tethering of NECs at their centromeres from prophase I through to segregation at anaphase I (Gladstone et al., 2009; Newnham et al., 2010).

Further to the role of Zip1 in NEC segregation, studies have also revealed a separate function of spindle checkpoint proteins Mad1, Mad2 and Mad3 in NECS (Cheslock et al., 2005; Lacefield and Murray, 2007; Newnham et al., 2010). Deletion of both *ZIP1* and *MAD3* results in elevated NECS non-disjunction (50%) (Newnham et al., 2010). Similar effects were observed when both *ZIP1* and *MAD2* were deleted (Gladstone et al., 2009). Furthermore, the segregation of NECs at the centromere were also promoted by Mad2 (Lacefield and Murray, 2007). However, precise mechanisms of spindle checkpoints in NECs still remain unclear.

A study by Davis and Smith in 2005 also revealed NEC mechanisms in *S. Pombe* (Davis and Smith, 2005). Deletion of the Spo11 ortholog *REC12* results in reduction of homologous chromosome pairing, but pairing is not completely eliminated due to the dynein heavy chain protein Dhc1 (Ding et al., 2004). Furthermore, using the lacO/LacI-GFP system to assay a non-exchange chromosome pair in meiosis segregation showed increased level of meiosis I non-disjunction. This was caused by deletion of the genes encoding the dynein heavy (*DHC1*) or light (*DLC1*) chains (Davis and Smith, 2005). Interestingly, *dch1Δ* mutation leads to elevated non-disjunction of both exchange and non-exchange chromosomes, whereas removal of the light chain *DLC1* specifically increases non-disjunction rate in non-exchange chromosomes. This finding resulted in the conclusion that the dynein light chain plays a specific role in NECS in fission yeast (Davis and Smith, 2005).

1.4.2.2 Flies and worms

In the past decade, a study using lacO/LacI-GFP to follow chromosomes in living spermatocytes has provided some insights into the behaviours of meiotic

chromosome segregation in male *Drosophila* (Vazquez et al., 2002). This study has shown that homologous chromosomes are paired at the euchromatin regions very early in spermatogenesis and the centromeres undergo dynamic clustering between non-homologous chromosomes while homologous chromosomes pair. Chromosomes are eventually sequestered to distinct territories near the nuclear envelope, and subsequently euchromatic association between both sister chromatids and homologous chromosomes are lost. However, chromosomes remain associated until the first meiotic division (Vazquez et al., 2002). Two mechanisms suggested for continued homologous association. One is suggested to be mediated by a topoisomerase-II reaction at anaphase I to resolve the chromosome entanglement, and another suggested to be mediated by heterochromatic associations that are independent of homology (Vazquez et al., 2002). Many studies have now shown that heterochromatic association is responsible for accurate achiasmate 4th chromosome segregation in females (Hawley et al., 1992; Karpen et al., 1996), hence indicating similar mechanisms may exist to segregate achiasmate chromosomes in males.

Several proteins are involved in the association between achiasmate chromosome pairs in *Drosophila* males. These include the Teflon gene, SNM (Stromalin in Meiosis) and MNM (Modifier of MDG4 in Meiosis) (Thomas et al., 2005; Tomkiel et al., 2001). In the *tef1* mutants, although the sex chromosomes are unaffected the pairing of four autosomes was all impaired. This disruption correlates with missegregation of the autosomes at meiosis I (Tomkiel et al., 2001). Increased meiosis I non-disjunction in autosomes and sex chromosomes were observed when mutating either SNM or MNM, suggesting these two

proteins are essential for the segregation of all chromosome pairs (Thomas et al., 2005). Homologous pairing is abolished and chromosomes fail to congregate into a single chromosome mass during metaphase I in these mutants. Moreover, homologs failed to be sequestered to nuclear territories, indicating the importance of these proteins in chromosome maintenance. Localisation of SNM and MNM to autosomes depends on Teflon, indicating that these proteins act together in maintaining homologous pairing (Thomas et al., 2005). However, how these proteins collaborate to ensure achiasmate chromosome association remains unclear.

In female *Drosophila*, the pathway to NECS tends to be different than in males (Fig. 1.10D). The original idea of centromere pairing involved in this process came from a study established 20 years ago. In this study, a region containing the 4th chromosome was copied and made as an artificial chromosome. This duplicated chromosome interferes with chromosome 4 normal pairing occurs, and this pairing normally carried in pericentric heterochromatin regions of chromosome 4 (Hawley et al., 1992). Therefore Hawley and colleagues proposed that correct segregation of NECs at meiosis I might be promoted by the pericentric heterochromatin regions. Cytological work using a combination of FISH and high-resolution microscopy on intact oocytes further demonstrated that large blocks of heterochromatin extending from the centromeres are the key holders to establish associations between achiasmate X and fourth chromosomes in prophase until first meiotic division (Dernburg et al., 1996). Work done by Karpen et al. using mini-chromosomes further confirmed that the centric heterochromatin is involved in high fidelity segregation of non-exchange pairs with high fidelity (Karpen et al., 1996).

Centromeres in *Drosophila* females tend to group in clusters, rather than in discrete pairs (Khetani and Bickel, 2007). The central element C(3)G and Corona, as well as cohesin proteins Smc1 and ORD (a meiosis-specific protein for cohesion in *Drosophila*) are required for this clustering. Among these, C(3)G, Corona and SMC1 remain at the clustered centromere upon SC disassembly (Takeo et al., 2011). Furthermore, recent studies have shown that homologous centromeres pair before clustering, and this clustering of centromeres tends to form into a group of one or two prior to meiotic entry (Christophorou et al., 2013; Joyce et al., 2013). How does the centromere promote correct segregation in *Drosophila* females? A recent study has proposed an 'elastic thread' model where chromatin threads connect achiasmate during the bi-orientation process (Hughes et al., 2009). Using an elegant live cell imaging technique on *Drosophila* oocytes in this study revealed that centromere pairing in *Drosophila* does not mediate pro-metaphase bi-orientation directly, instead it acts as a chromatin bridge during prophase I, providing an association to establish chromatin connections between homologous centromeres. In this study, live cell imaging has shown frequent movement of achiasmate chromosomes between the two half spindles during pro-metaphase. This movement tends to be connected by heterochromatic threads in majority-separated partners in meiotic non-exchange cells (Hughes et al., 2009).

1.4.3. NECs studies in mammals

In mammals, the sex chromosome (XY) is achiasmate and has been studied intensively in the marsupial *Thylamys elegans* and the Mongolian gerbil *Meriones unguiculatus* (de la Fuente et al., 2007; Page et al., 2006). The XY chromosome in the marsupial lacks homology regions and no continuous SC is

formed between them during prophase I. In *T. elegans* males, the XY chromosome has a structure rich in SYCP3 and SYCP1, this allows persistent joining of the chromosome pair until metaphase I (Page et al., 2006) (Fig. 1.10F). This achiasmate chromosome was first confirmed in this study by staining with the meiotic cohesin subunit STAG3. Chiasmata chromosomes contain interrupted STAG3 staining at the chiasmata. The X- and Y-chromosomes were shown opposite, where STAG3 was uninterrupted and showed no connection between the X- and Y- chromosomes. Despite this, this pair of chromosomes was still associated. This association was seen with the staining of SCP3 where there was persistent staining on XY but discontinuous for the autosomes. The central element SCP1 was also observed at this dense region during diplotene and metaphase I, but was not observed at pachytene (Page et al., 2003). The reason suggested that it was due to SCP3 forming a linear structure that connects the telomeres of the XY pair and unites two chromosomes in close proximity

Similarly, studies using the *Meriones unguiculatus* have also shown implications of the central element of the SC involved in sex chromosome achiasmate segregation (de la Fuente et al., 2007). In this study, Mlh1 foci were absent in the XY pair, which was proposed as being non-exchange chromosome pairs during late pachytene. However, no other methods have proved that the XY pair was non-exchange, thus it is unknown whether using Mlh1 focus as the only indicator is sufficient. SYCP3 showed dense staining structure during diplotene and diakinesis on the Y chromosome, but no SYCP1 was observed suggests the CE was not involved in this process. The sex chromosomes showed pairing at their chromosome ends from pachytene to metaphase I. SCYP3 still

appeared when XY chromosomes segregated during anaphase I as a 'thread', and this phenotype was proposed as a proteinaceous link between the chromosomes (de la Fuente et al., 2007). Although there are some controversial issues, which remained unclear, the argument that SYCP3 is involved in holding the XY chromosomes at their chromosome end to aid segregation remains strong. Overall, these studies imply the role of SYCP3/SCP3 in the segregation of non-exchange chromosomes in XY chromosomes. It would be interesting to see if the LE is still involved in other chromosomes when they fail to crossover.

Overall, the above studies have shown the diverse mechanisms of non-exchange chromosome segregation among different species, indicating evolutionary differences (Wolf, 1994). Despite this, common features do indeed exist across these species, such as the SC requirement for proteins, therefore probably indicating that there is more extensive function for SC proteins in meiosis.

Chapter 2. Materials and methods

2.1 Materials:

2.1.1 Growth media

2.1.1.1 Bacterial media:

Bacterial strains used in this work were grown in Luria-Bertani Broth (1% wv bacto-tryptone, 0.5% w/v yeast extract, 0.5% w/v NaCl, pH 7.0) at 37 °C. For solid media, 2% w/v agar was added before autoclaving.

STBL2 cells (Invitrogen) were used when using plasmids containing Yiplac-208. These cells were grown in SOC medium (2% w/v bacto-tryptone, 0.5% w/v yeast extract, 10 mM NaCl, 2.5 mM KCl, 10 mM MgCl₂, 10 mM MgSO₄, 20 mM glucose, pH 7.0).

2.1.1.2 Yeast media:

2.1.1.2.1 General Yeast media:

Yeast cells were generally grown in 'rich' YPD medium (1% w/v yeast extract, 2% w/v bacto-peptone, 2% w/v glucose, 500 µM adenine, pH 6.5. For solid media, 2% w/v agar was added before autoclaving. For selection of drug-resistance markers, the relevant antibiotic was added at the concentrations listed in Section 2.1.4. For enrichment of yeast cells with functional mitochondria, cells were grown in YEPEG media (1% w/v succinate, 1% w/v yeast extract, 2% w/v bacto-peptone, 2% v/v glycerol, 500 µM adenine, pH 5.5. 2% v/v ethanol added after autoclaving).

For mating tests, yeast cells were grown on minimal media, which contained 0.17% w/v yeast nitrogen base, 2% w/v D-glucose, 0.5% ammonium sulphate, pH 7.25. 'Complete' media was the same as minimal media but with 0.087% w/v of a nutrient mix containing all amino acids. Appropriate quantities of each

amino acid are given in table 1.1 where complete media contained all amino acids. ‘ Drop- out’ media was the same as complete media but with the appropriate amino acid omitted from the nutrient mix.

Table 2.1 Amino acids used to make complete and drop out powders

Amino Acids	Amount (mg)	Final concentration in media (% w/v)
Adenine (hemisulfate salt)	800	0.003
L-arginine (HCL)	800	0.003
L-aspartic acid	4000	0.016
L-histidine	800	0.003
L-leucine	800	0.003
L-lysine (mono-HCL)	1200	0.005
L-methionine	800	0.003
L-phenylalanine	2000	0.007
L-threonine	8000	0.032
L-tryptophan	800	0.003
L-tyrosine	1200	0.005
Uracil	800	0.003

For drop out powders, the appropriate amino acid is excluded from the rest. All amino acids were supplied by Sigma.

2.1.2 Buffers

Table 2.2 Buffers used in this thesis

Buffer	Composition
TAE	40 mM Tris-acetate 2 mM Na ₂ EDTA-2H ₂ O pH 8.5
TE	10 mM Tris-Cl 1 mM EDTA

	pH 8.5
PBS	137 mM NaCl 2.7 mM KCl 4.3 mM Na ₂ PO ₄ ·7H ₂ O 1.4 mM KH ₂ PO ₄
11.1 x buffer	45 mM Tris-HCl (pH 8.8) 11 mM ammonium sulphate 4.5 mM magnesium chloride 6.7 mM 2-β-mercaptoethanol 4.4 μM EDTA (pH 8.0) 1 mM adenine dNTP 1 mM cytosine dNTP 1 mM guanine dNTP 1 mM thymine dNTP 113 μg/ml BSA
10 x SDS running buffer:	250 mM Tris base 1.92 M Glycine 35 mM SDS
Semi-Dry transfer buffer	50 mM Tris base 39 mM Glycine 1.3 mM SDS
10X TBE buffer	890 mM Tris Base 890 mM Boric acid 2 mM EDTA pH8.0
Sporoblast buffer	1 M Sorbitol 50 mM KPO ₄ buffer pH 7.0

	10 mM EDTA pH 7.5 H ₂ O
1M Na-phosphate pH7.2	68.4ml 1M Na ₂ HPO ₄ 31.6ml 1M NaH ₂ PO ₄
Hybridization Buffer	0.25 M Na-phosphate pH7.2 0.25 M NaCl 1 mM EDTA 7% SDS 5% Dextran Sulphate.
20x SSC buffer	3 M NaCl 3 M trisodium citrate
Low Stringency buffer	2x SSC 0.1% SDS
High Stringency buffer	0.1x SSC 0.1% SDS
Hoechst 33258	10 mg/ml (life technologies)
Hoechst stock solution (1mg/ml)- 10X TNE	100 mM Tris Base 10 mM EDTA Na ₂ -2H ₂ O 2M NaCl pH 7.4
Hoechst working solution (50ml)	45 ml Milli-Q water 5 ml 10x TNE buffer 5 µl Hoechst stock solution
Guanidine solution	4.5 M, saturated Guanidine-HCl 0.1 M EDTA, pH 8.0 0.15 M NaCl 0.05% sodium lauryl sarkosyl

SCE solution	1 M sorbitol 1 M sodium citrate 0.05 M EDTA
--------------	---

2.1.3 Enzyme

Table 2.3 Enzymes used in this thesis

Enzyme	Supplier
Taq DNA polymerase	Thermo Scientific
Prime star HS DNA polymerase	TAKARA
Zymolyase (100T)	Seikagaku Corporations
Zymolyase (20T)	Seikagaku Corporations
RNAse	Sigma
DNAse	Sigma
Restriction enzymes:	New England Biolabs

2.1.4 Drugs and antibiotics

Table 2.4 Drugs and antibiotics used in this thesis

Drug	Concentration used	Supplier
Ampicillin	100 µg/ml	Sigma
Chloramphenicol	100 µg/ml	Sigma
Tetracyclin	100 µg/ml	Sigma
G418	400 µg/ml	Invitrogen
Hygromycin B	300 µg/ml	Invitrogen
Nourseothricin	100 µg/ml	Werner Biotech
Cycloheximide	10 µg/ml	Sigma
Canavanine	60 µg/ml	Sigma

2.1.5 Primary antibody used:

Table 2.5 Primary antibody used in this thesis

Primary antibody	Working dilution	Supplier	Catalogue number
Guinea pig anti- GFP	1:100	Roeder Lab (Tsubouchi et al., 2006)	n/a
Rat anti- tubulin	1:400	Strattech	T91504-04
Rabbit anti- ZIP1	1:400	Hoffmann Lab (Jordan et al., 2009)	n/a
Mouse anti-Myc (clone 4A6)	1:50	Millipore	05-724
Goat anti-GFP	1:100	Abcam	Ab5450-25
Mouse anti-HA (HA11)	1:100	Cambridge Bioscience	MMS-101P-200
Mouse anti-3-phosphoglycerate kinase	1:3000	Invitrogen	459250

2.1.6 Secondary antibody used

Table 2.6 Secondary antibody used in this thesis

Secondary antibody	Working dilution	Supplier	Catalogue number
Donkey anti-rabbit, FITC	1:100	Jackson ImmunoResearch	711-095-152
Donkey anti-rabbit, Texas Red	1:100	Jackson ImmunoResearch	711-075-152
Donkey anti-rabbit, Cy5	1:100	Jackson ImmunoResearch	711-175-152
Donkey anti-rat, FITC	1:100	Jackson ImmunoResearch	712-095-153
Donkey anti-rat, Texas Red	1:100	Jackson ImmunoResearch	712-075-153
Donkey anti-rat, Cy5	1:100	Jackson	712-175-153

		ImmunoResearch	
Donkey anti-mouse, FITC	1:100	Jackson ImmunoResearch	715-095-151
Donkey anti-mouse, Texas Red	1:100	Jackson ImmunoResearch	715-075-151
Donkey anti-mouse, Cy5	1:100	Jackson ImmunoResearch	715-175-151
Donkey anti-mouse, AMCA	1:100	Jackson ImmunoResearch	715-155-151
Donkey anti-mouse, Alexafluor	1:100	Invitrogen	A-21202
Donkey anti-guinea pig, FITC	1:100	Jackson ImmunoResearch	706-095-148
Donkey anti-guinea pig, Texas Red	1:100	Jackson ImmunoResearch	706-075-148
Donkey anti-guinea pig, Cy5	1:100	Jackson ImmunoResearch	706-175-148
Donkey anti-goat, FITC	1:100	Jackson ImmunoResearch	705-096-147
Donkey anti-goat, Texas Red	1:100	Jackson ImmunoResearch	705-075-147
Donkey anti-goat, Cy5	1:100	Jackson ImmunoResearch	705-175-147
Rabbit anti-rat IG, HRP	1:2000	Dako (WB)	711-095-152
Swine anti-rabbit IG, HRP	1:2000	Dako (WB)	711-075-152
Rabbit anti - mouse IG, HRP	1:2000	Dako (WB)	711-175-152

2.1.7 Radiations

Table 2.7 Radiations used in this thesis

Radiations	Catalogue number

12.5 μ l dCTP, [α - 32 P] – 6000 Ci/mmol 20 mCi/ml, 250 μ Ci	BLUO13Z250UC
25 μ l dCTP, [α - 32 P] – 6000 Ci/mmol 20 mCi/ml, 500 μ Ci	BLUO13Z500UC

2.1.8 Oligonucleotides

Table 2.8 Oligonucleotides used in this study

EH Oligo. No.	Name	Sequence (5' to 3')	Application
O7	K2	TTCAGAAACAACCTCTGGCGCA	Reverse primer 591 bp away from the ORF of KANMX4 cassette
O62	ZIP1-A1	GAAGAGCTGCTTCTTCACTTG	200 bp upstream of <i>ZIP1</i> ORF
O63	ZIP1-A4	GCAATCTAGATGACCTCTT	200 bp downstream of <i>ZIP1</i> ORF
O73	K2	TTCAGAAACAACCTCTGGCGCA	Reverse primer 592 bp into KANMX4
O108	kar1 deletion	<i>Greig et al. 2007</i>	sent from Duncan Greig
O109	kar1 deletion	<i>Greig et al. 2007</i>	sent from Duncan Greig
O224	K.I._URA3_B	CTTGACGTTTCGTTCTGACTGATGAGC	Internal primer of <i>K.lactis</i> to be used in conjunction with O221
O225	K.I._URA3_C	GAGCAATGAACCCAATAACGAAATC	Internal primer of <i>K.lactis</i> to be used in conjunction with O224
O481	ZIP1_A	TTTGTTCTAAACGGTCAAACCTTTTC	Forward primer 265 bp upstream of <i>ZIP1</i> ORF
O482	ZIP1_B	TTTTGCTACTCCTTCACTCACTTCT	Reverse primer 396 bp away from the <i>ZIP1</i> ORF
O483	ZIP1_C	GAAATCGGAGAAGCAAGATATAACA	Forward primer 553 bp towards the downstream of <i>ZIP1</i> ORF
O484	ZIP1_D	AGTCAACATAACTGACCGAAGAAAC	Reverse primer 331 bp away from the end of <i>ZIP1</i> ORF
O552	TRP1_A	AGAGACCAATCAGTAAAAATCAACG	Forward primer 306 bp upstream of <i>TRP1</i> ORF
O555	TRP1_D	GCGAAAAGACGATAAATACAAGAAA	Reverse primer 300 bp away from the downstream of <i>TRP1</i> ORF
O603	REV_ZIP1_B	AGAAGTGAGTGAAGGAGTAGCAAAA	Same as O482 but forward primer
O604	REV_ZIP1_C	TGTTATATCTTGCTTCTCCGATTTC	Same as O483 but reverse primer

Table 2.8 Oligonucleotides continued

EH Oligo. No.	Name	Sequence (5' to 3')	Application
O617	Leu2.K.L. URA3_F	ATTTCAAGCAATATATATATATATATTTCAAGGATATACCATTCTAC G ATGATGTAGTTTCTGGTT	Gene replacement of <i>LEU2</i> using <i>K.lactis</i> - <i>URA3</i> plasmid (pEH83). Bold bases anneal upstream of <i>K.lactis</i> <i>URA3</i> gene
O618	Leu2.K.L. URA3_R	CATTTATAAAGTTTATGTACAAATATCATAAAAAAAGAGAATCTTT GTGATTCTGGGTAGAAGATCG	Gene replacement of <i>LEU2</i> using <i>K.lactis</i> - <i>URA3</i> plasmid (pEH83). Bold bases anneal downstream of <i>K.lactis</i> <i>URA3</i> gene
O622	Kar1_A1	CTTTCTCTGGGGTTTTTCCC	Upstream primer checking for Kar1p
O623	Kar1_A4	ACTCATAATGCCCTTGTACC	Downstream primer checking for Kar1p
O891	Zip1_C_u p	GAATTGGAGCTTGAAGAGCAG	To check integration of cassettes made using C and D primers
O1166	Zip1_1+2 R	CTCGTCAACGTTGCAATCC	Reverse primer to check <i>ZIP1</i> intergration
O1167	Zip1_wt1_F	GGTTATTCTGATGATATGGAAATAGGTT	Forward primer checking <i>ZIP1</i> intergration, upstream of <i>ZIP1</i> ORF
O1169	Zip1_wt2_F	TGCCGCAATTGAAAATGATAC	Forward primer checking <i>ZIP1</i> intergration, upstream of <i>ZIP1</i> ORF
O1463	KIURA3_B	CACCAACGCCACGGGGTTACTGG	377 bases from <i>K.I</i> <i>URA3</i> ORF
O1464	KIURA3_C	CCCCTTGGTTCTTTGGTGACCTC	390 bases towards downstream of <i>K. I</i> <i>URA3</i> ORF

2.1.9 Yeast strains

Table 2.9 Base yeast strains used in this study

EH Strain No.	Strain background	Ploidy	Genotype
Y712	S288C	2N	<i>S. carlbergensis</i> chr. V (<i>ilv1-Kpn</i> , <i>PAC2::[pD174::LEU2 lacO array]</i> , <i>RAD3</i> , <i>TRP2</i> , <i>Mata/α</i>
Y867	SK1	1N	<i>leu2::LEU2</i> , <i>tetR-GFP-tetO-HIS3</i> , <i>his3::hisG</i> , <i>leu2::hisG</i> , <i>trp1::hisG</i> , <i>lys2,ura3</i> , <i>ho::LYS2</i> , <i>Mata</i>
Y957	SK1	1N	<i>his3::hisG</i> , <i>leu2::hisG</i> , <i>trp1::hisG</i> , <i>lys2,ura3</i> , <i>ho::LYS2</i> , <i>Mata</i>
Y958	SK1	1N	<i>his3::hisG</i> , <i>leu2::hisG</i> , <i>trp1::hisG</i> , <i>lys2</i> , <i>ura3</i> , <i>ho::LYS2</i> , <i>Mata</i>
Y965	SK1	1N	<i>ura3::pGPD1-GAL4(848).ER::URA3</i> , <i>proGAL1-NDT80 (TRP1)</i> , <i>his3::hisG</i> , <i>leu2::hisG</i> , <i>trp1::hisG</i> , <i>lys2</i> , <i>ho::LYS2</i> , <i>Mata</i>
Y966	SK1	1N	<i>ura3::pGPD1-GAL4(848).ER::URA3</i> , <i>proGAL1-NDT80 (TRP1)</i> , <i>his3::hisG</i> , <i>leu2::hisG</i> , <i>trp1::hisG</i> , <i>lys2</i> , <i>ho::LYS2</i> , <i>Mata</i>
Y1176	SK1	1N	<i>leu2::hisG</i> , <i>ura3(Sma-Pst)</i> , <i>ho::hisG HIS4::LEU2-(BamHI; +ori)</i> , <i>Mata</i>
Y1177	SK1	1N	<i>his4-X::LEU2-(NgoMIV; +ori)::URA3</i> , <i>leu2::hisG</i> , <i>ura3(Sma-Pst)</i> , <i>ho::his</i> , <i>Mata</i>
Y1323	S.P.	1n	<i>S.paradoxus N17</i> , <i>ura3</i> , <i>Mata</i>
Y1528	SK1	1N	<i>ZIP1::KI-URA3</i> , <i>his3::hisG</i> , <i>leu2::hisG</i> , <i>trp1::hisG</i> , <i>lys2</i> , <i>ura3</i> , <i>ho::LYS2,Mata</i>
Y1529	SK1	1N	<i>ZIP1::KI-URA3</i> , <i>his3::hisG</i> , <i>leu2::hisG</i> , <i>trp1::hisG</i> , <i>lys2</i> , <i>ura3</i> , <i>ho::LYS2,Mata</i>
Y1530	SK1	2N	Diploid of Y1528 and Y1529
Y1665	SK1	1N	<i>CTF19-13MYC (KANMX6)</i> , <i>his3::hisG</i> , <i>leu2::hisG</i> , <i>trp1::hisG</i> , <i>lys2</i> , <i>ura3</i> , <i>ho::LYS2</i> , <i>Mata</i>
Y1666	SK1	1N	<i>CTF19-13MYC (KANMX6)</i> , <i>his3::hisG</i> , <i>leu2::hisG</i> , <i>trp1::hisG</i> , <i>lys2</i> , <i>ura3</i> , <i>ho::LYS2</i> , <i>Mata</i>
Y2149	SK1	1N	<i>CDC5::pCLB2-CDC5::KANMX6</i> , <i>his3::hisG</i> , <i>leu2::hisG</i> , <i>trp1::hisG</i> , <i>lys2</i> , <i>ura3</i> <i>ho::LYS2</i> , <i>Mata</i>
Y2150	SK1	1N	<i>CDC5::pCLB2-CDC5::KANMX6</i> , <i>his3::hisG</i> , <i>leu2::hisG</i> , <i>trp1::hisG</i> , <i>lys2</i> , <i>ura3</i> <i>ho::LYS2</i> , <i>Mata</i>
Y2159	SK1	1N	<i>NDT80::HYG (HPH)</i> , <i>his3::hisG</i> , <i>leu2::hisG</i> , <i>trp1::hisG</i> , <i>lys2</i> , <i>ura3</i> <i>ho::LYS2</i> , <i>Mata</i>
Y2160	SK1	1N	<i>NDT80::HYG (HPH)</i> , <i>his3::hisG</i> , <i>leu2::hisG</i> , <i>trp1::hisG</i> , <i>lys2</i> , <i>ura3</i> <i>ho::LYS2</i> , <i>Mata</i>
Y2229	SK1	1N	<i>NDT80::KANMX</i> , <i>pCDC5-CDC5-pFA6a-HPHMX4-pGAL1-CDC5</i> , <i>ura3::pGPD1-GAL4(848).ER::URA3</i> , <i>leu2-R::URA3-tel-ARG4</i> , <i>lys2</i> , <i>arg4D(eco47III-hpa1)</i> , <i>ho::LYS2</i>
Y2332	SK1	1N	<i>spo11-Y135F-HA-URA3</i> , <i>his3::hisG</i> , <i>leu2::hisG</i> , <i>trp1::hisG</i> , <i>lys2</i> , <i>ura3</i> , <i>ho::LYS2</i> , <i>Mata</i>
Y2333	SK1	1N	<i>spo11-Y135F-HA-URA3</i> , <i>his3::hisG</i> , <i>leu2::hisG</i> , <i>trp1::hisG</i> , <i>lys2</i> , <i>ura3</i> , <i>ho::LYS2</i> , <i>Mata</i>
Y2620	SK1	1N	<i>PDS1-tdTomato-KITRP1</i> , <i>his3::hisG</i> , <i>leu2::hisG</i> , <i>trp1::hisG</i> , <i>lys2</i> , <i>ura3</i> , <i>ho::LYS2</i> , <i>Mata</i>

Table 2.9 Base yeast strains used continued

EH Strain No.	Strain background	Ploidy	Genotype
Y2621	SK1	1N	<i>PDS1-tdTomato-KITRP1, his3::hisG, leu2::hisG, trp1::hisG, lys2, ura3, ho::LYS2, Mata</i>
Y2622	SK1	1N	<i>CNM67-3mCherry-NATMX4, his3::hisG, leu2::hisG, trp1::hisG, lys2, ura3, ho::LYS2, Mata</i>
Y2623	SK1	1N	<i>CNM67-3mCherry-NATMX4, his3::hisG, leu2::hisG, trp1::hisG, lys2, ura3, ho::LYS2, Mata</i>
Y2629	SK1	1N	<i>PDS1-tdTomato-KITRP1, CNM67-3mCherry-NATMX4, his3::hisG, leu2::hisG, trp1::hisG, lys2, ura3, ho::LYS2, Mata</i>
Y3974	SK1	1N	<i>KAR1Δ13, his3::hisG, leu2::his, trp1::hisG, lys2, ura3, ho::LYS2, Mata</i>
Y3975	SK1	1N	same as Y3974, but <i>canR</i> , <i>Mata</i>
Y3976	SK1	1N	same as Y3976, but <i>canR</i> , <i>cyhR</i> , <i>Mata</i>
Y4158	SK1	1N	<i>ZIP1::URA3, his3::hisG, leu2::hisG, trp1::hisG, lys2, ura3, ho::LYS2, Mata</i>
Y4159	SK1	1N	<i>trp1::ZIP1::TRP1, ZIP1::URA3, his3::hisG, leu2::hisG, trp1::hisG, lys2, ura3, ho::LYS2, Mata</i>
Y4160	SK1	1N	<i>ZIP1::URA3, his3::hisG, leu2::hisG, trp1::hisG, lys2, ura3, ho::LYS2, Mata</i>
Y4161	SK1	1N	<i>ZIP1::URA3, trp1::ZIP1::TRP1, his3::hisG, leu2::hisG, trp1::hisG, lys2, ura3, ho::LYS2, Mata</i>
Y4164	SK1	1N	<i>ZIP1::URA3, trp1::ZIP1-S75E::TRP1, his3::hisG, leu2::hisG, trp1::hisG, lys2, ura3, ho::LYS2, Mata</i>
Y4165	SK1	1N	<i>ZIP1::URA3, trp1::ZIP1-S75E::TRP1, his3::hisG, leu2::hisG, trp1::hisG, lys2, ura3, ho::LYS2, Mata</i>
Y4382	S288C	1N	<i>kar1-Δ13, S. paradoxus chromo III, Mata</i>
Y5224	SK1	1N	<i>CTF19-13MYC (KANMX6), spo11-Y135F-HA-URA3, Mata</i>
Y5225	SK1	1N	<i>CTF19-13MYC (KANMX6), spo11-Y135F-HA-URA3, Mata</i>

Table 2.10 Yeast strains used in this study

EH Strain No.	Strain background	Ploidy	Genotype
Y4355	SK1	1N	Same as Y3976, but <i>thr4::KIURA3</i>
Y4356	SK1	1N	Same as Y3976, but <i>ade1::KIURA3</i>
Y4357	SK1	1N	Same as Y3976, but <i>met8::KIURA3</i>
Y4505	SK1	2N	Same Y4813, but <i>trp1::ZIP1-4A::TRP1/trp1::ZIP1-4A::TRP1</i>
Y4534	SK1	2N	Same as Y1666, but <i>trp1::ZIP1-4A::TRP1/trp1::ZIP1-4A::TRP1, Mata/α</i>
Y4535	SK1	1N	Same as Y3976, but <i>leu2::KIURA3</i>
Y4706	SK1	2N	Same as Y1665, but <i>trp1::ZIP1::TRP1/trp1::ZIP1::TRP1</i>
Y4731	SK1	2N	Same as Y4706, but <i>spo11-Y135F-HA-URA3</i>
Y4734	SK1	2N	Same as Y5224, but <i>zip1::URA3/zip1::URA3, trp1::ZIP1-4A::TRP1/ trp1::ZIP1-4A::TRP1</i>
Y4756	SK1	1N	Same as Y4535, but <i>S.paradoxus ChrIII, Mata</i>
Y4757	SK1	1N	Same as Y4535, but <i>S.paradoxus ChrIII, Mata</i>
Y4760	SK1	2N	Same as Y2160, but <i>zip1::URA3/ zip1::URA3, trp1::ZIP1::TRP1/trp1::ZIP1::TRP1</i>
Y4763	SK1	2N	Same as Y2160, but <i>ZIP 1::URA3/ ZIP1::URA3, trp1::ZIP1-4A::TRP1/trp1::ZIP1-4A::TRP1</i>
Y4771	SK1	2N	Same as Y5224, but <i>zip1::URA3/zip1::URA3</i>
Y4794	SK1	2N	Same as Y2160, but <i>zip1::URA3/zip1::URA3, trp1::ZIP1-S75A::TRP1/trp1::ZIP1-S75A::TRP1</i>
Y4797	SK1	1N	Same as Y2160, but <i>zip1::URA3/zip1::URA3, trp1::ZIP1-S75E::TRP1/trp1::ZIP1-S75E::TRP1</i>
Y4800	SK1	2N	Same as Y1665, but <i>zip1::URA3/zip1::URA3, trp1::ZIP1-S75A::TRP1/trp1::ZIP1-S75A::TRP1</i>
Y4803	SK1	2N	Same as Y1665, but <i>zip1::URA3/zip1::URA3, trp1::ZIP1-S75E::TRP1/trp1::ZIP1-S75E::TRP1</i>
Y4806	SK1	2N	Same as Y5224, but <i>zip1::URA3/zip1::URA3, trp1::ZIP1-S75A::TRP1/trp1::ZIP1-S75A::TRP1</i>
Y4809	SK1	2N	Same as Y5224, but <i>zip1::URA3/zip1::URA3, trp1::ZIP1-S75E::TRP1/trp1::ZIP1-S75E::TRP1</i>
Y4813	SK1	2N	Same as Y4159, but <i>zip1::URA3/zip1::URA3, trp1::ZIP1::TRP1/trp1::ZIP1::TRP1</i>
Y4834	SK1	2N	Same as Y4813, but <i>zip1::URA3/zip1::URA3, trp1::ZIP1-T114A::TRP1/rp1::ZIP1-T114A::TRP1</i>

Table 2.10 Yeast strains used continued

EH Strain No.	Strain background	Ploidy	Genotype
Y4851	SK1	2N	Same as Y4813, but <i>zip1::URA3/zip1::URA3, trp1::ZIP1-T127A::TRP1/rp1::ZIP1-T127A::TRP1</i>
Y4854	SK1	2N	Same as Y4813, but <i>zip1::URA3/zip1::URA3, trp1::ZIP1-7A::TRP1/rp1::ZIP1-7A::TRP1</i>
Y4857	SK1	2N	Same as Y958, but <i>leu2::LEU2-tetR-GFP tetO-HIS3(linked to S.c Leu2 locus)</i>
Y4860	SK1	2N	Same as Y1665, but <i>zip1::URA3/zip1::URA3, trp1::ZIP1-T114A::TRP1/trp1::ZIP1-T114A::TRP1</i>
Y4863	SK1	2N	Same as Y5224, but <i>zip1::URA3/zip1::URA3, trp1::ZIP1-T114A::TRP1/ trp1::ZIP1-T114A::TRP1</i>
Y4869	SK1	1N	Same as Y4756, but <i>leu2::NAT</i> , independent colony 3
Y4885	SK1	1N	Same as Y4869, but <i>LacI-GFP(URA3)</i> , colony 1
Y4891	SK1	1N	Same as Y4885, but <i>LacI-GFP(URA3);LacO(Leu2-S.p CEN3)</i>
Y4900	SK1	2N	Same as Y966, but <i>zip1::URA3/ zip1::URA3, trp1::ZIP1-T114A::TRP1/trp1::ZIP1-T114A::TRP1</i>
Y4903	SK1	2N	Same as Y867, but <i>PDS1-tdTomato-KITRP1/PDS1-tdTomato-KITRP1, CNM67-3mCherry-NATMX4/ CNM67-3mCherry-NATMX4</i>
Y4904	SK1	1N	Same as Y4891, but <i>PDS1-tdTomato-KITRP1</i>
Y4905	SK1	1N	Same as Y4904, but <i>CNM67-3mCherry-NATMX4</i>
Y4938	SK1	1N	Same as Y4903, but <i>zip1::URA3, trp::ZIP1::TRP1</i>
Y4947	SK1	1N	Same as Y4903, but <i>zip1::URA3, trp::ZIP1-T114A::TRP1</i>
Y4949	SK1	1N	<i>leu2::LEU2-tetR-GFP tetO-HIS3(linked to S.c Leu2 locus), CNM67-3mCherry-NATMX4, zip1::URA3,</i>
Y4950	SK1	1N	<i>leu2::LEU2-tetR-GFP tetO-HIS3(linked to S.c Leu2 locus), CNM67-3mCherry-NATMX4, zip1::URA3,</i>
Y4955	SK1	1N	Same as Y4891, but <i>zip1::URA3/zip1::URA3, trp::ZIP1::TRP1/trp::ZIP1::TRP1</i>
Y4956	SK1	1N	Same as Y2629, but <i>zip1::URA3, trp::ZIP1::TRP1,</i>
Y4961	SK1	1N	Same as Y4891, but <i>zip1::URA, trp::ZIP1-T114A::TRP1</i>
Y4962	SK1	1N	Same as Y4891, but <i>PDS1-tdTomato-KITRP1, CNM67-3mCherry-NATMX4</i>
Y4963	SK1	1N	Same as Y4891, but <i>zip1::URA3</i>
Y4964	SK1	1N	Same as Y4963, but <i>PDS1-tdTomato-KITRP1, CNM67-3mCherry-NATMX4</i>

Table 2.10 Yeast strain continued

EH Strain No.	Strain background	Ploidy	Genotype
Y4965	SK1	2N	Diploid of Y4938 and Y4956
Y4968	SK1	2N	Diploid of Y4947 and Y4962
Y4992	SK1	2N	Same as Y5224, but <i>zip1::URA3/zip1::URA3, trp1::ZIP1-ddkA::TRP1/trp1::ZIP1-ddkA::TRP1</i>
Y4995	SK1	2N	Same as Y5224, but <i>zip1::URA3/zip1::URA3, trp1::ZIP1-ddkE::TRP1/trp1::ZIP1-ddkE::TRP1</i>
Y4996	SK1	1N	<i>zip1::URA3, trp1::zip1-S144E::TRP1</i>
Y4997	SK1	1N	<i>zip1::URA3, trp1::zip1-S144E::TRP1</i>
Y4998	SK1	2N	Same as Y4831, but <i>trp1::ZIP1-S144E::TRP1/trp1::ZIP1-S144E::TRP1</i>
Y5001	SK1	2N	Same as Y4998, but <i>cdc5::pCLB2-CDC5::kanMX6</i>
Y5002	SK1	1N	<i>zip1::URA3, trp1::zip1-3A::TRP1(first colony)</i>
Y5003	SK1	1N	<i>zip1::URA3, trp1::zip1-3A::TRP1(first colony)</i>
Y5004	SK1	2N	Same as Y4831, but <i>trp1::ZIP1-3A::TRP1/trp1::ZIP1-3A::TRP1 (first colony)</i>
Y5014	SK1	2N	Same as Y5224, but <i>zip1::URA3/zip1::URA3, trp1::ZIP1-7A::TRP1/trp1::ZIP1-7A::TRP1</i>
Y5017	SK1	2N	Same as Y5224, but <i>zip1::URA3/zip1::URA3, trp1::ZIP1-3A::TRP1/trp1::ZIP1-3A::TRP1</i>
Y5019	SK1	1N	Same as Y1176, but <i>zip1::HYG, trp1::hisG, Mata</i>
Y5020	SK1	1N	Same as Y1176, but <i>zip1::HYG, trp1::hisG, Mata</i>
Y5021	SK1	1N	Same as Y1177, but <i>zip1::HYG, trp1::hisG, Mata</i>
Y5022	SK1	1N	Same as Y1177, but <i>zip1::HYG, trp1::hisG, Mata</i>
Y5023	SK1	1N	Same as Y5021, but <i>zip1::HYG, trp1::ZIP1::TRP1, Mata</i>
Y5024	SK1	1N	Same as Y5020, but <i>zip1::HYG, trp1::ZIP1::TRP1, Mata</i>
Y5025	SK1	2N	Diploid of Y5023 and Y5024
Y5026	SK1	1N	Same as Y5021, but <i>zip1::HYG, trp1::ZIP1-S144A::TRP1, Mata</i>
Y5027	SK1	1N	Same as Y5020, but <i>zip1::HYG, trp1::ZIP1-S144A::TRP1, Mata</i>
Y5029	SK1	2N	Diploid of Y5026 and Y5027
Y5032	SK1	2N	Same as Y4813, but <i>ndt80::HYG (HPH)/ndt80::HYG (HPH)</i>
Y5033	SK1	1N	Same as Y5021, but <i>zip1::HYG, trp1::ZIP1-S81A::TRP1, Mata</i>
Y5034	SK1	1N	Same as Y5020, but <i>zip1::HYG, trp1::ZIP1-S82A::TRP1, Mata</i>

Table 2.10 Yeast strains used continued

EH Strain No.	Strain background	Ploidy	Genotype
Y5035	SK1	1N	Diploid of Y5033 and Y5034
Y5036	SK1	1N	Same as Y5020, but <i>zip1::HYG</i> , <i>trp1::ZIP1-S127A::TRP1</i> , <i>Mata</i>
Y5037	SK1	1N	Same as Y5021, but <i>zip1::HYG</i> , <i>trp1::ZIP1-S127A::TRP1</i> , <i>Mata</i>
Y5038	SK1	1N	Diploid of Y5036 and Y5037
Y5040	SK1	1N	Same as Y4158, but <i>CEN3-TetO::HIS3</i> , <i>ade2</i> , <i>TetR-GFP::KAN</i> , <i>TetR-mCherry::ADE2</i>
Y5041	SK1	2N	Diploid of Y5040 and Y4963
Y5057	SK1	2N	Same as Y4834, but <i>ndt80::HYG (HPH)</i>
Y5070	SK1	1N	Same as Y5020, but <i>zip1::HYG</i> , <i>trp1::ZIP1-T114A::TRP1</i> , <i>Mata</i>
Y5071	SK1	1N	Same as Y5021, but <i>zip1::HYG</i> , <i>trp1::ZIP1-T114A::TRP1</i> , <i>Mata</i>
Y5072	SK1	1N	Same as Y5022, but <i>zip1::HYG</i> , <i>trp1::ZIP1-T114A::TRP1</i> , <i>Mata</i>
Y5075	SK1	2N	Diploid of Y5019 and Y5022
Y5077	SK1	1N	Same as Y4159, but <i>CEN3-TetO::HIS3</i> , <i>ade2</i> , <i>TetR-GFP::KAN</i> , <i>TetR-mCherry::ADE2</i>
Y5082	SK1	1N	Same as Y4852, but <i>CEN3-TetO::HIS3</i> , <i>ade2</i> , <i>TetR-GFP::KAN</i> , <i>TetR-mCherry::ADE2</i>
Y5084	SK1	2N	Diploid of Y5082 and Y4961
Y5085	SK1	2N	Diploid of Y5077 and Y4955
Y5105	SK1	2N	Same as Y4813, but <i>trp1::ZIP1-S82A::TRP1/trp1::ZIP1-S82A::TRP1</i>
Y5108	SK1	2N	Same as Y4813, but <i>trp1::ZIP1-S95A::TRP1/trp1::ZIP1-S95A::TRP1</i>
Y5111	SK1	2N	Same as Y4813, but <i>trp1::ZIP1-S137A::TRP1/trp1::ZIP1-S137A::TRP1</i>
Y5114	SK1	2N	Same as Y4813, but <i>trp1::ZIP1-S144A::TRP1/trp1::ZIP1-S144A::TRP1</i>
Y5117	SK1	2N	Same as Y4813, but <i>trp1::ZIP1-T114E::TRP1/trp1::ZIP1-T114E::TRP1</i>
Y5120	SK1	2N	Same as Y4813, but <i>NDT80::KanMX/NDT80::KanMX</i> , <i>pCDC5-CDC5-pFA6a-HPHMX4-pGAL1-CDC5/pCDC5-CDC5-pFA6a-HPHMX4-pGAL1-CDC5</i> , <i>ura3::pGPD1-GAL4(848).ER::URA3/pCDC5-CDC5-pFA6a-HPHMX4-pGAL1-CDC5</i>
Y5133	SK1	1N	<i>zip1::URA3</i> , <i>trp1::zip1-S82A::TRP1(second colony)</i>
Y5134	SK1	1N	<i>zip1::URA3</i> , <i>trp1::zip1-S82A::TRP1(second colony)</i>
Y5135	SK1	2N	Same as Y5105, but second independent colony
Y5168	SK1	2N	Same as Y4813, but <i>trp1::ZIP1-8A::TRP1/trp1::ZIP1-8A::TRP1</i>

Table 2.10 Yeast strains used continued

EH Strain No.	Strain background	Ploidy	Genotype
Y5170	SK1	2N	Same as Y4813, but <i>trp1::ZIP1-8E::TRP1/trp1::ZIP1-8E::TRP1</i>
Y5228	SK1	2N	Same as Y5114, but second independent colony
Y5284	SK1	2N	Same as Y5114, but <i>cdc5::pCLB2-CDC5::kanMX6/cdc5::pCLB2-CDC5::kanMX6</i>
Y5328	SK1	2N	Same as Y2229
Y5331	SK1	2N	Same as Y5328, but <i>zip1::URA3/ zip1::URA3, trp1::ZIP1-S144A::TRP1/trp1::ZIP1-S144A::TRP1</i>
Y5362	SK1	1N	<i>CEN3-TetO::HIS3, ade2, TetR-GFP::KAN, TetR-mCherry::ADE2, Mata</i>
Y5480	SK1	2N	Same as Y2149, but diploid
Y5483	SK1	2N	Same as Y966, but <i>zip1::URA3/ zip1::URA3, trp1::ZIP1-S144A::TRP1/trp1::ZIP1-S144A::TRP1</i>
Y5486	SK1	2N	Same as Y5328, but <i>zip1::URA3/ zip1::URA3, trp1::ZIP1-S144E::TRP1/trp1::ZIP1-S144E::TRP1</i>
Y5487	SK1	1N	<i>CEN3-TetO::HIS3, ade2, TetR-GFP::KAN, TetR-mCherry::ADE2, Mata</i>
Y5488	SK1	1N	<i>CEN3-TetO::HIS3, ade2, TetR-GFP::KAN, TetR-mCherry::ADE2, Mata</i>
Y5489	SK1	1N	<i>CEN3-TetO::HIS3, ade2, TetR-GFP::KAN, TetR-mCherry::ADE2, Mata</i>
Y5552	SK1	2N	Same as Y5224, but <i>zip1::URA3/zip1::URA3, trp1::zip1-S144A::TRP1/ trp1::zip1-S144A::TRP1</i>
Y5555	SK1	2N	Same as Y5224, but <i>zip1::URA3/zip1::URA3, trp1::zip1-S144E::TRP1/ trp1::zip1-S144E::TRP1</i>
Y5637	SK1	2N	Same as Y5105, but third independent colony
Y5640	SK1	2N	Same as Y5105, but fourth independent colony

2.1.10 Plasmids

Table 2.11 Plasmids used in this study

pEH plasmid No.	Other name	Description	Source
pEH83	pRED376	pWJ716 <i>KIURA3</i>	Rothstein
pEH89	pAG25	For amplification of <i>NATMX4</i> cassette	Yeast 15: 1541-1553
pEH90	pAG32	For amplification of <i>HPHMX4</i> cassette	Yeast 15: 1541-1553
pEH724	Yiplac204- <i>ZIP1-4A</i>	Integrate at <i>TRP1</i> locus	Hoffmann's Lab
pEH754	Yiplac204- <i>ZIP1-T114A</i>	Integrate at <i>TRP1</i> locus	Genscript
pEH778	Yiplac204- <i>ZIP1-S127A</i>	Integrate at <i>TRP1</i> locus	Genscript
pEH779	Yiplac204- <i>ZIP1-7A</i>	Integrate at <i>TRP1</i> locus	Genscript
pEH790	Yiplac204- <i>ZIP1-S82A</i>	Integrate at <i>TRP1</i> locus	Genscript
pEH791	Yiplac204- <i>ZIP1-137A</i>	Integrate at <i>TRP1</i> locus	Genscript
pEH792	Yiplac204- <i>ZIP1-S95A</i>	Integrate at <i>TRP1</i> locus	Genscript
pEH793	Yiplac204- <i>ZIP1-S144A</i>	Integrate at <i>TRP1</i> locus	Genscript
pEH796	Yiplac204- <i>ZIP1-T114E</i>	Integrate at <i>TRP1</i> locus	Genscript
pEH805	Yiplac204- <i>ZIP1-S89A+S763A+S783A</i>	Integrate at <i>TRP1</i> locus	Genscript
pEH811	Yiplac204- <i>ZIP1-S144E</i>	Integrate at <i>TRP1</i> locus	Genscript

2.2 Methods

2.2.1 Bacterial methods

2.2.1.1 Growth conditions

Cells were grown at 37°C in LB (2.1.1.1). For liquid cultures cells were taken up from -80°C into 5 ml of LB and grown overnight at 37°C shaking at 180 r.p.m.

Plasmids were extracted using a QIAprep Spin Miniprep kit as described in the manufacturer's instructions.

2.2.1.2 Yeast growth conditions

2.2.1.2.1 Vegetative growth conditions

2.2.1.2.1.1 Liquid media

A single colony was inoculated into 5 ml YPD for growth in a shaking 30°C incubator until cells had reached the appropriate OD₆₀₀.

2.2.1.2.1.2 Solid media

Cells were streaked onto the YPD agar media and incubated at 30°C overnight. For growth of single colonies/spore germination, plates were left in the incubator for 2 days.

2.2.2 Bacterial strain construction

2.2.2.1 Transformation of chemically competent *E.coli* DH5α cells

Aliquots of chemically competent DH5α cells were thawed on ice in the cold room. Once thawed, a 100 µl of cell suspension was transferred to a pre-chilled polypropylene tube for each transformation reaction. 10 ng (in around 10-30 µl volume) of plasmid DNA was added to the cell suspension, gently mixed with a pipette tip and left on ice for 20 minutes in the cold room. The cells were then

placed in a 42°C water bath for 45 seconds and then placed on ice for a further 2 minutes. 500 µl of LB medium (minus drug) was added to the cell suspension and incubated at 37°C for 1 hour. Cells were spread on a LB agar plate containing ampicillin drug so that plasmids that give resistance grow. Plates were incubated overnight at 37°C.

2.2.2.2 Storage of Bacterial strains

Cells were grown overnight in 5 ml LB. The following day, cells were spun down, resuspended in 1 ml 30% glycerol and transferred to a 1.5 ml screw-top tube. Tubes were then frozen and stored at -80°C.

2.2.3 Growth conditions of Yeast

2.2.3.1 Vegetative growth conditions

2.2.3.1.1 Liquid media growth

A single colony was inoculated into 5 ml of YPD for growth in a shaking 30°C incubator until cells had reached the appropriate OD₆₀₀.

2.2.3.1.2 Solid media growth

Cells were streaked onto the appropriate agar media and incubated at 30°C overnight. For growth of single colonies/spore germination, plates were left in the incubator for 2 days.

2.2.3.2 Sporulation conditions

Diploid cells were streaked onto YEPEG medium (Section 2.2.3.1.2). A single colony was inoculated into 5 ml YEPD medium and incubated overnight in a 30°C shaking incubator at 200 R.P.M. Cells were added to pre-sporulation media (SPS) next day when growth in YEPD reached saturation. Starting OD₆₀₀ in pre-sporulation media was ~ 0.2. For S288C strains, the pre-sporulation

media used was YPA (1% yeast extract, 2% bacto-peptone, 2% potassium acetate pH 7.0), for SK1 and Y55 strains, SPS media (0.5% yeast extract, 1% peptone, 0.17% yeast nitrogen base, 1% potassium acetate, 0.5% ammonium sulfate, 0.05M potassium hydrogen phthalate, pH 5.5) was used. The next morning when cultures reached a density of $4-5 \times 10^7$ cells/ml, cells were spun down at 3500 R.P.M and washed in pre-warmed sporulation media (S288C: 2% KAc, 0.02% raffinose, 0.01% Antifoam 204 (Sigma), pH 7.0, and 1% KAc, 0.02% raffinose, 0.01% Antifoam 204 (Sigma), pH 7.0 for SK1 and Y55 strains). Finally, cells were inoculated into the same volume of pre-warmed sporulation media as the pre-sporulation media in which they were grown, and incubated in a shaking (250 rpm) incubator at the appropriate temperature. For sporulation on solid media, cells were replica-plated directly from a YEPD plate to a KAc-COM plate and incubated at 30°C. Tetrads were formed after 2 days of incubation.

2.2.4 Yeast strain construction

2.2.4.1 Genetic cross the strains

Genetic crosses were performed by thoroughly mixing two haploid strains on a YPD plate using a wooden dowel. Cells were left to mate overnight or for at least 5 hours in a 30°C incubator. Cells were then replica-plated onto KAc-COM (2% KAc and 0.0875% w/v COM powder, pH 7.0) and incubated at 30°C for 3 days. Afterwards, sporulation was assessed by taking a small amount of cells from the sporulation plate and looking for tetrad formation under the light microscope. When sporulation was complete cells were taken from the plate using a wooden dowel and placed in a 1.5 ml Eppendorf tube containing 100 µl PBS with 5 µl of 10 mg/ml zymolyase (20T). Cells were incubated at 37°C for

30 minutes and then 400 µl of dissection buffer was added. Samples were then streaked onto a dissection plate (a YPD plate but with a much thinner and flatter surface) and a Nikon Eclipse 500I microscope and micromanipulator was used to separate each ascospore form within a tetrad. Spores were incubated at 30°C to germinate for 3 days and then replica-plated onto the appropriate media for selection of markers.

2.2.4.2 Transformation of Yeast cells

Yeast cells were transformed using the lithium acetate procedure. Cells to be transformed were grown overnight in 5 ml YPD medium at 30°C in a shaking incubator and then diluted 25-fold into fresh YPD the following morning. The fresh cultures were grown for 3-4 hours and then harvested by centrifugation at 2000 R.P.M for 3 minutes. Cell pellets were then washed twice in 10ml of 100 mM LiAc and the final cell pellet was re-suspended in 1 ml 100 mM LiAc and transferred to a sterile 1.5 ml Eppendorf tube. Cells were centrifuged for 30 seconds in a benchtop centrifuge (Eppendorf 5415D) set to 13,000 R.P.M and cell pellets were re-suspended in 250 µl LiAc. 50 µl of this cell suspension was aliquoted into separate sterile 1.5 ml Eppendorf tubes for each transformation reaction. These tubes were centrifuged for 30 seconds in a benchtop centrifuge (Eppendorf 5415D) set to 13,000 R.P.M and the supernatant was removed. The following reagents were layered onto the cell pellets in the following order 250 µl 50% (w/v) PEG-3500, 36 µl 1M LiAc, 50 µl boiled salmon sperm DNA and ~1 µg DNA in a volume of ~50µl (or 50 µl sterile dH₂O for the negative control). Cells were then gently mixed with the layered reagents using a pipette tip and left at 30°C for 30 minutes. Following this, the tubes containing the

cells/transformation mix were transferred to a 42°C water bath for 20 minutes (SK1), 30 minutes (S288C, BR) or 40 minutes (Y55) after which 1 ml of sterile distilled H₂O was added to the tubes and the cells were centrifuged at 4000 RPM in a benchtop centrifuge (Eppendorf 5415D). When selecting for prototrophy, cell pellets were re-suspended in 500 µl dH₂O and 250µl selected for drug resistance. The cell pellets were re-suspended in YPD (minus drugs) and left in a shaking 30°C incubator for 3 hours. Cells were then centrifuged at 4000 R.P.M for 1 minute and re-suspended in 500 µl dH₂O and 250 µl was plated onto YPD plates containing the appropriate drug selection. Plates were incubated at 30°C for 3 days for growth of transformants.

2.2.4.3 PCR-based gene deletion

Gene deletion cassettes were made by PCR-based amplification of drug resistance genes from a plasmid vector with flanking regions of ~45 base pairs homology to the intended site of integration (Longine *et al* 1998). This is achieved through designing primers to include the 45 bp flanking regions of homology. Correct integration of the gene-deletion cassette was checked by performing PCR using primers that flank the junction between upstream/downstream sequences and the gene-deletion cassette (Fig. 2.1).

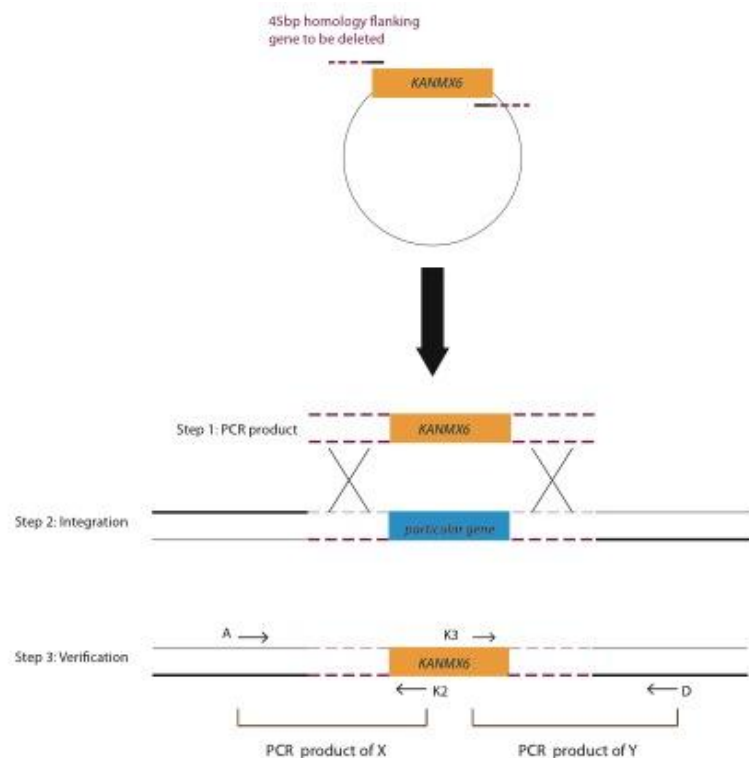


Figure 2.1 PCR-based gene deletion

A gene deletion cassette is amplified by PCR using primers that anneal upstream and downstream of the selectable marker (orange box). These primers have 45 base pair (bp) 'tails' homologous to the desired site of cassette integration (red dotted lines). Integration of the cassette was achieved through homologous recombination. Correct integration of the deletion cassette was assessed by PCR using primers flanking the integration sites and recovery of a DNA fragment of the correct size. The blue box denotes gene to be deleted.

2.2.4.4 PCR-based N-terminal gene tagging

C-terminal tagging cassettes were made by PCR-based amplification of the desired C-terminal tag together with a drug resistance gene from a plasmid vector (see Table 2.11 for different vectors) with flanking regions of ~45 bp homology to the intended site of integration. Primers were designed so that the site of cassette integration was immediately upstream of the stop codon of the gene. Correct integration of the C-terminal gene tagging cassette was checked by performing PCR using primers that flank the junction between the cassette and downstream sequences [Fig. 2.2 and (Longtine et al., 1998)] and by

Western blotting of the tagged protein.

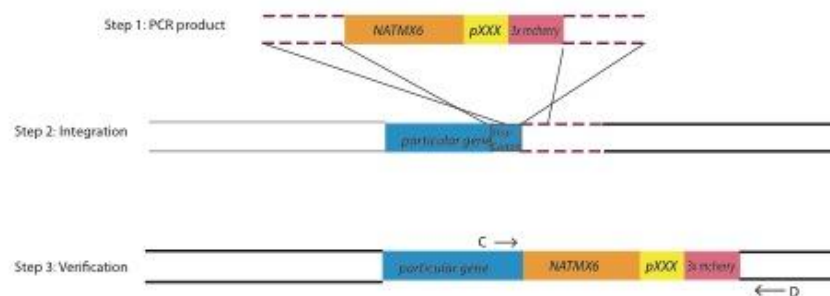


Figure 2.2 Tagging of cassettes by PCR

An N- terminal gene tagging cassette comprises a N-terminal protein tag (pink box), an ADH1 terminator sequence (yellow box) and a selectable marker (orange box). A cassette is amplified by PCR using primers that anneal upstream of the tag sequence and downstream of the selectable marker. These primers have 45 bp ‘tails’ homologous to the desired site of cassette integration (red dotted lines). Integration of the cassette is achieved through homologous recombination. Correct integration of the tagging cassette is assessed by PCR using primers flanking the integration sites and recovery of a DNA fragment of the correct size.

2.2.4.5 Two step gene replacement method

Plasmids are linearized first by restriction enzyme (see Section 2.2.5.8); this allows the plasmid to loop into the genome. Recombination of the plasmid with wild-type genome occurs to allow loop out of the wild-type gene. The selection of mutated gene was grown on *URA3* drop out medium. Once obtained, colonies were replicated to 5'FOA to kill off any chromosomes that marked with *URA3*. Then standard PCR was applied to verify the mutated gene.

2.2.4.6 Diploid isolation

Diploids were obtained by thorough mixing of two haploid strains on a YEPD plate and incubation for at least 5 hours at 30°C. For SK1 strains, mated strains were streaked onto a fresh YEPD plate for single colonies and incubated at 30°C for two days. The SK1 haploid colony has the appearance of a rough surface, whereas a diploid of SK1 had the appearance of a smooth surface. Smooth colonies were picked for screening. For S288c, Y55 strains, zygotes were picked using a micromanipulator microscope. Diploid candidates were screened by replica plating to sporulation plates or mating tester strains. Failure of the candidate to mate with either tester strain indicated that the candidate was diploid.

2.2.4.7 Storage of yeast strains

For long-term storage of yeast strains, cells were grown overnight on YPD agar media and transferred using a wooden dowel into a 1.5 ml screw-top tube containing 1 ml 30% glycerol. Tubes were then frozen and stored at -80°C. For short term storage, cells were kept on agar plates at 4°C.

2.2.4.8 Artificial chromosome transfer

Two strains of different mating types were grown to late log phase in YEPED. An equal number of cells were mixed and incubated for 30 minutes at room temperature, and thereafter centrifuged. The pellets were further incubated for four hours. Afterwards the pellets were washed in water and resuspended in 1 ml water. 0.1 ml, 0.3 ml and 0.5 ml of cells were plated onto YEPED and grown for two days. Cells were then replica to drop out medium supplemented with canavanine and cycloheximide, then incubated further for 4-6 days.

2.2.5 Genetic methods

2.2.5.1 General PCR

PCR based DNA amplification was used for the amplification of cassettes for gene tagging/gene deletion and for verification of cassette integration. For PCR reactions not requiring a stringent proof-reading activity, 1 unit of Taq polymerase (Abergene) was used per 20 µl PCR reaction. The accompanying buffer contained 45 mM Tris-HCl pH 8.8, 11 mM ammonium sulphate, 4.5 mM MgCl₂, 6.7 mM β-mercaptoethanol, 4.4 µM EDTA, 113 µg/ml BSA and 1 mM of each dNTP. This buffer was used in an 11.1x dilution. Primers were diluted 100-fold to a final concentration of 1 µM. 50-250 ng of template DNA was used in a volume of 1 µl per 20 µl reactions. Volumes were made up to 20 µl with dH₂O. All PCR reactions were performed using an Eppendorf Mastercycler RP-Gradient with the following standard program:

Step1: 95°C for 3 minutes

Step2: 35 cycles of:

95°C for 30 seconds

50-60°C (subject to the T_m of each primer pair)

72°C for 1 minute/KB

Step3: 72°C for 10 minutes

Step 4: hold at 14°C

2.2.5.2 Genomic DNA extraction

Cells were grown overnight in 15 ml polypropylene tubes containing 5 ml YPD and were centrifuged at 3500 R.P.M for 3 minutes. Cell pellets were resuspended in 1ml sterile dH₂O and were transferred to 1.5 ml Eppendorf tubes. Tubes were centrifuged for 1 minute at 13,000 R.P.M in a benchtop

centrifuge, the supernatant was discarded and the cell pellets were resuspended in 500 μ l 1M sorbitol. 15 μ l of 1 M DTT and 8 μ l of Zymolyase (100T, 10 mg/ml) was added to the cell suspension and plated in a shaking incubator set to 37°C for 1 hour. After this, 200 μ l TE and 70 μ l 10% SDS were added to each tube and incubated in a 65°C water bath for 10 minutes. 320 μ l 5 M KAc was added to each tube, inverted six times and left on ice for 30 minutes. Tubes were then spun at 13000 R.P.M in a benchtop centrifuge for 6 minutes and 650 μ l of the resulting supernatant was added to a fresh 2 ml Eppendorf tube containing 1 ml isopropanol and 200 μ l 5 M ammonium acetate and inverted 6 times. Each 2 ml tube was then spun down in a benchtop centrifuge at 4000 R.P.M for 1 minute, the supernatant was discarded and the pellets were dried in a vacuum. 300 μ l TE was added to the pellets with 10 μ l of 10 mg/ml RNase and tubes were placed in a 37°C water bath for 30 minutes. The DNA was then quantified and used in the appropriate dilution for PCR reactions.

2.2.5.3 Phenol-chloroform DNA extraction

For vegetative DNA extraction, cells were inoculated into 50 ml of YPD overnight. For meiotic DNA extraction, 10% NaN₃ was added to each 30 ml sample. Samples were spun for 4 minutes at 3000 R.P.M and drained well on paper towels. The pellets were resuspended into 0.9 ml spheroplasting buffer, and 0.4 mg of 100T Zymolyase and 1% β -mercaptoethanol were added to the resuspended samples. Samples were incubated at 37°C for 15 minutes, and then shaken every five minutes. Spheroplasted samples were then centrifuged for four minutes at 3000 R.P.M. Supernatants were discarded and the pellets

kept. 2.5 ml guanidine solution was added to the pellet and stringy pellets were resuspended by finger vortexing. Samples were placed at 65°C waterbath for 20 minutes and finger vortexed several times during this incubation to completely lyse and resuspend cells. After the guanidine treatment, sample tubes were cooled on ice. 2.5 ml cold EtOH was added to the cooled samples and mixed well by inverting the tubes, and then left in the freezer for more than one hour. The pellets were then centrifuged for 15 minutes at 4000 R.P.M in a benchtop centrifuge. Supernatants were discarded and re-centrifuged briefly again to remove remaining traces of supernatant. 0.7 ml RNase solution was added to the pellets and dispersed pellets using blue tips. Samples were agitated on the roller drum in a 37°C room for one hour to facilitate dispersal of the pellet. 25 µl proteinase-K solution was added to samples after RNase treatment and incubated at 65°C for 1 hour. Samples were transferred to a 1.5 ml Eppendorf tube and extracted with 0.7 ml phenol/chloroform/isoamyl alcohol. Samples were shaken and inverted several times to ensure complete extraction. They were left to stand for 3 minutes, then shaken again and spun at 13000 R.P.M for 10 minutes. Two layers formed after centrifugation. Top layer supernatants were carefully removed and kept. Phenol/chloroform extraction was repeated again on the kept supernatants. After extraction, the top layer supernatants were transferred into a 2 ml Eppendorf tube. DNA was precipitated by adding 35 µl 4M NaOAc and 2 ml of EtOH. Samples were inverted several times and left to stand for 20 minutes. The DNA was spun for 5 minutes at full speed and supernatants were discarded. The DNA was rinsed with 1.5 ml of 70% EtOH through centrifugation. The supernatants were removed and air-dried at 30°C in an incubator for 10 minutes. Pellet DNA was

resuspended in 100 µl TE. The DNA was left to hydrate in the fridge overnight. It was then stored at 20°C for long-term use.

2.2.5.4 Agarose Gel electrophoresis

Agarose gel electrophoresis was used to separate DNA fragments by size. The gel was roughly 150 mm x 150 mm, and contained 1% agarose (made of 1xTAE and 10 µl ethidium bromide (10 mg/ml)) in general. However higher or lower percentage gels were made for separation of especially small or large DNA samples. Agarose powder was added into a 150 ml TAE buffer solution. The mixture was heated up in the microwave until all powder was dissolved. The trays were sealed with tapes and the combs positioned. The solution bottle was cooled down with water to body temperature, and then 10 µl of ethidium bromide was added to the solution and mixed well. Then the solution was poured into the tray to cool for 30 minutes. DNA was loaded into the gel lanes with 1x loading buffer (1 part loading dye, 5 parts 30% glycerol) usually in a volume of ~15 µl. 250 ng of 1 KB or 100 BP ladder (New England Biolabs) was also loaded. Gels were run by applying a charge difference of ~120Vs for 30 minutes. Photographs of the gels were taken under UV light using a SYNGENE INGenius BIO imager.

2.2.5.5 Making DNA plugs for pulsed-field gel electrophoresis

Yeast cultures were inoculated into 5 ml YEPD liquid medium and harvested overnight to saturation. Entire cell cultures were spun down in a centrifuge for 5 minutes at 10°C for 2,500 R.P.M. Supernatants were removed and the pellets were resuspended in 1 ml 50 mM cold EDTA. Samples were spun again as previously, and pellets were resuspended in 200 µl of 50 mM cold EDTA.

SCE/zymolyase/ β ME solution was prepared before proceeding to the next step. Each sample required 100 μ l of SCE/zymolyase/ β ME solution [1 ml stock contained 1 ml SCE, 50 μ l β ME and 3 mg zymolyase (20T)]. 1% low melting agarose was made up in 0.125 M EDTA, which was also prepared by boiling in the microwave. 0.5 ml of malted agarose was needed per sample. Boiled agarose was kept in warm water at approximately 40-45°C. The plug molds were taped with autoclave tape and labelled to correspond to the samples. After preparation, 100 μ l of SCE/zymolyase/ β ME solution was added to each sample and boiled at 55°C for 10 seconds. 0.5 ml of agarose was added straight away to samples and pipetted a few times until resuspended. Afterwards cells were loaded into plug molds. The plugs were left to set in the 4°C fridge. Once they were set, each plug was added to a clean Eppendorf tube and overlay with 0.5 ml 0.45M EDTA, 0.1 M Tris (pH 8.0) and 50 μ l β ME per ml. Two plugs per sample were placed in an Eppendorf tube. Inoculated samples were placed in a 37°C roller drum for at least 4 hours. Before proceeding to the next stage, a stock solution containing 1% Sarkosyl, 1 mg/ml proteinase K, 0.1 mg/ml RNase and 0.4 M EDTA was prepared. The incubated plugs were washed with 50mM EDTA three times. Afterwards 0.5 ml of the stock solution was added. The cultures were incubated overnight at 37°C. The next day rinse the plugs were rinsed with cold 0.5 M EDTA, and stored in a storage buffer, containing 0.45 M EDTA, 0.1 M Tris and 50% glycerol in a -20°C freezer. The plugs were washed in TE buffer before being loaded onto the gel.

2.2.5.6 Pulsed-Field Gel electrophoresis

One litre of 0.5x TBE was prepared and stored at 4°C. 1.5l cold TBE buffer was placed into the running tank one hour prior to running the gel, which was

equilibrated to 14°C. The pump speed was at 80 with no air bubbles through the pipes. 1% agarose gel was boiled in 0.5x TBE. 5ml of aliquot from the boiled agarose was kept in a heat block at 55°C. The remaining agarose gel was placed in a 55°C water bath. Each plug (Section 2.2.5.5) was cut into half with a clean scalpel and added to 1.5 ml 0.5x TBE in a 2ml Eppendorf tube. Samples were washed for 15 minutes on a rotating wheel. The gel casting stand and comb were assembled, with the teeth positioned flat on the plate. The comb was laid horizontally on top. The plugs were removed from the washing solution using a small spatula, and dried briefly with tissue. The plugs were then laid on the comb. Each sample was sealed to the comb using molten agarose and left to set for five minutes. The comb was placed in the casting stand and the agarose was slowly poured from the waterbath into the stand. The gel was left to set for 30 minutes. The drop of agarose was cut above the gel on each tooth and the comb was slowly removed. The wells of the gel were filled with the remainder of the agarose, and left to set for 5 minutes. The gel was dismantled from the casting and placed in the gel tank, with the frame to hold it in place, and allowed to be equilibrated for 10 minutes. Electrophoresis for separating the entire chromosome was done under the following conditions:

Block 1: 6 V/cm, 15 hours, 70s initial switch, 70s final switch

Block 2: 6 V/cm, 11 hours, 120s initial switch, 120s final switch

After electrophoresis, the gel was stained in 0.5 µg/ml EtBR for 20 minutes.

Rinsed in water for 5 minutes and imaged the gel on the UV box.

2.2.5.7 DNA purification (materials used from DNA QiAgen kit)

5 volumes of buffer PB to 1 volume of the PCR sample were mixed and loaded onto a QiAgen mini column and centrifuged at full speed for 30 seconds to allow the DNA to bind to the column. Fluids were discarded and 0.75 ml of Buffer PE was added to the column, this was then centrifuged for 30 seconds. Afterwards the flow was discarded and centrifuged for 1 minute further. DNA was then eluted by adding 50 µl of water to the column and centrifuged for 1 minute. Concentration of the DNA was determined by spectrophotometry.

2.2.5.8 Restriction Digests of DNA

Restriction digests of plasmid DNA were carried out in 50 µl reaction volumes using ~10 Units (or 1 µl) of the relevant restriction enzyme (New England Biolabs) and 1 µg of DNA. The appropriate NEB Buffer is used in a 10-fold dilution and BSA is added to a final concentration of 100 µg/ml. Tubes containing all reagents were placed in a 37°C water bath for 2 hours and 2 µl of this was run on an agarose gel alongside un-digested plasmid DNA.

2.2.5.9 One-dimensional Gel (Southern)

2.2.5.9.1 Measuring of DNA concentration using Fluorometer

198µl of Hoechst working solution was placed into the relevant wells of a 96 well plate. Standard DNA concentrations (0.1-09 mg/ml) were added to the top row, mixed with 198 µl of Hoechst solution. Following this, 2 µl of DNA was added to each well, and then mixed well using a 200 µl pipette. This stage was particularly important as accurate volume measurement was essential. The plate was covered with tin foil, and loaded onto the 96 plate reader. The UV filter (purple) was inserted into the plate reader. The program named Hoechst 33258 protocol was selected. Hoechst solution excitation wavelength =352 nm and emission wavelength =461 nm. The wells containing DNA were selected on

the software, which started reading the concentrations. The final concentration was calculated to the required amount in Section 2.2.5.9.1

2.2.5.9.2 Southern gel electrophoresis

DNA was extracted using the method in Section 2.2.5.3. Afterwards DNA was digested following the method in Section 2.2.5.8. 2 µg of DNA was digested in the 80 µl final volume with 20-fold excess of restriction enzyme (5 µl restriction enzyme; 8 µl digestion buffer). Samples were digested for 2 hours in a water bath at 37°C. While waiting for the DNA to digest, 2.1 g SeaKem LE agarose was added to 350 ml 1XTBE (0.6%, *without* ethidium bromide). The agarose was dissolved completely by heating in the microwave and boiling steadily for 30 seconds. Afterwards the solution was cooled to 50°C and poured into a clean, level gel tray in the cold room. It was left to harden for at least 30 minutes. The DNA was precipitated following digestion. This was done by adding 5 µl 3 M NaOAc pH5.2 and 190 µl EtOH (200 proof). The samples were mixed well by inversion and left to stand for 20 minutes. The DNA was spun at full speed in an Eppendorf centrifuge for 10 minutes and the supernatant was poured off. Any remaining supernatant was dried using a rack. The pellets were then rinsed with 100 µl 70% EtOH. Samples were spun for 5 minutes at full speed. Ethanol supernatants were removed completely using 200 µl tip, and left to air dry for ~10 minutes. 15 µl of 1X TE was added to the dried DNA pellets and the tube flicked to resuspend. The pellets were left to stand for 10 minutes to dissolve in TE and were gently flicked again to resuspend. 5 µl of special loading buffer was added to the dissolved DNA (100 µl 6X loading dye with 60 µl 10X NEB3). This special loading buffer contained extra salt, which prevents the sample from diffusing out of well. The samples were loaded onto the gel

with the markers required. For a Southern integration gel, a normal 1 KB DNA ladder was used (BioLabs). For the recombination assay, a lambda HindIII digest was used as a ladder (BioLabs). Approximately 2 litres of 1X TBE (*without* EtBr) was poured into the tank. The current was set at: 70V (~2 V/cm between the electrodes) for 24 hours at room temperature. After gel electrophoresis, The DNA gel was stained with 1 litre of dH₂O with EtBr (0.5 µg/ml final conc.) (50 µl of 10 mg/ml stock to 1 litre volume) in a clean Pyrex dish with gentle shaking for 30 minutes. The gel was viewed on a UV box to check the quality of the DNA.

2.2.5.9.3 Blotting of Southern gel

All steps used one litre volumes of solution. The gel was soaked in dH₂O for 10 minutes. Meanwhile, 0.25 M HCl and 0.4 M NaOH solutions were prepared. 2 litres of 0.4 M NaOH solutions were required to soak the gel as well as to transfer. The gel was flipped in water so that flat side was face up. Large gels were gently sandwiched between two gel trays and flipped quickly. Once flipped, the gel was soaked in 0.25 M HCl for 20 minutes. This step deurinates the DNA causing nicking which assists transfer of larger fragments. The HCl solution was poured off and the gel rinsed with dH₂O briefly. The gel was then transferred into 0.4 M NaOH and shaken for 30 minutes. This step denatures the DNA so the single strands can bind the membrane. During this time 4 pieces of Whatman blotting paper that were the same size as the gel were prepared; one piece of Whatman blotting paper suitable for a wick was cut and one piece of Zeta Probe (BioRad) nylon membrane the same size as the gel was also prepared. The wick was folded evenly across a clean glass plate and placed across a clean Pyrex dish. The surface of the wick was wet with NaOH

and flattened by rolling with a 25 ml pipette. More NaOH was added to the dish to create a reservoir. Two gel-size pieces of Whatman blotting paper were placed on top of the wick in the centre, and subsequently wet with NaOH and rolled flat. After soaking the gel in NaOH, it was placed on top of the wick. Trapped air bubbles were gently pushed out. The membrane in the dH₂O was wet and carefully placed on top of the gel. The remaining two pieces of Whatman blotting paper were soaked in dH₂O and placed on top of the membrane. A 25 ml pipette was used to carefully, but firmly, roll out any bubbles, working from the centre outwards. A piece of Saran Wrap was placed across the whole construction and cut around the gel with a sharp razor blade. A pack of paper towels were unfolded and laid flat on top of the Whatman blotting paper. Then a glass plate and a small weight (a bottle or similar) was added on top to provide some pressure. The gel was blotted overnight. Next day, the blot was neutralized in 1 litre of 50 mM Na-phosphate pH7.2 by shaking for five minutes. Washing was repeated twice. Excess buffer was drained from the blot and carefully wrapped in Saran Wrap. It was stored at 4°C or -20 °C or proceeded directly to hybridisation (Section 2.2.5.9.3).

2.2.5.9.4 Radioactivity for Southern Gel

Hybridisation Solution was pre-warmed to 65°C and mixed well. A hybridisation bottle(s) was also rinsed and pre-warmed to 65°C. 20 ml of hybridisation solution was added per bottle once it was warmed. Salmon sperm DNA (10 mg/ml, Boehringer) was denatured through heating in a 95°C dry block for 5 minutes. It was immediately quenched on ice/water and then stored on ice. The membrane was wet in a 50 mM Na-phosphate buffer before hybridised. Making sure it was DNA-side up, the membrane was carefully rolled-up with the DNA

side on the inside. It was then placed into the hybridisation bottle and slowly unrolled by turning the bottle, keeping the opening face wet with hybridisation solution. Bubbles were avoided. 0.3 ml of denatured Salmon sperm DNA was added once the membrane was spread out inside the tube. The blot was left and it was removed to hybridise overnight or at least 10 hours. Next day, the radioactive label from the freezer was removed and left to thaw. A probe was prepared using a Random Priming Kit (Agilent). 40.5 μ l of ddH₂O was added to the 0.2 ml PCR tube with dried reaction mix. 25ng probe (1 μ l) and 0.5 μ l of 0.25 ng/ μ l BstEII λ digest was also added to the tube, making up a total of 42 μ l solution. This mixture was transferred to a 1.5 ml tube and denatured in a 95°C heating block for 5 minutes, then quenched immediately on ice for another 5 minutes. Afterwards the probe mix was centrifuged for 30 seconds at maximum speed. 3 μ l magenta polymerase was then added and mixed well. 5 μ l ³²P-dCTP radioactivity using a filter tip was added quickly into the probe tube and incubated at 37°C for 1 hour. The probe was separated from the unincorporated label using an Amersham Probe-Quant G-50 Micro Column. The cap of the column was loosened, turned ¼ and snapped at the bottom. The column was centrifuged at 3000 R.P.M for 1 minute. The column was placed into a fresh 1.5 ml Eppendorf tube. The labelled radioactive probe was added to the column using a filter tip and spun at 3000 R.P.M for 2 min. The probe was denatured at 95°C using a heating block for 2 minutes. It was quenched on ice for 1 minute and centrifuged for another 30 seconds at maximum speed. The denatured probe was quickly added to the hybridisation bottle and promptly returned to the oven. The membrane was left to hybridise overnight. One litre of low stringency wash buffer and high stringency sash buffer was pre-warmed in the 65°C oven

overnight. On the third day, the radioactive hybridisation mix was carefully poured off into the radioactive sink. The (Techne) hybridising tube was filled with 100-150 ml pre-heated low stringency buffer for 10 minutes. The solution was poured off afterwards and this step was repeated once more. Following this, the membrane was washed with high stringency solution for 20 minutes with gentle shaking. This step was repeated 3 times. Radioactivity was monitored on the blot after the wash. The edges of the membrane had to be essentially free of counts (~2X background). If there was significant background, washing in a high-stringency solution needed to be done again. The membrane was quickly and carefully removed from the tube with long-nosed forceps. Excess wash was drained off onto a wad of paper towels. Afterwards the blot was carefully wrapped in Saran Wrap and placed into a Phosphoimager plate overnight. The phosphoimager plate was scanned the next day.

2.2.6 Protein methods

2.2.6.1 Protein extractions

2.2.6.1.1 Protein extractions using NaOH

5 ml of cell culture was harvested, placed in 14 ml polypropylene tubes and centrifuged at 3500 R.P.M for 3 minutes. Cell pellets were resuspended in 100 µl sterile dH₂O and transferred to a 1.5 ml Eppendorf tube. To this, 100 µl of 0.2 M NaOH was added, left at room temperature for 5 minutes and then tubes were spun at 13,000 R.P.M at 4°C in an Eppendorf benchtop cooling centrifuge. The supernatant was discarded and the pellets were thoroughly resuspended in 100 µl 1xLaemmli sample buffer (2% SDS, 10% glycerol, 0.002% bromophenol blue, 0.06 M Tris HCl, pH 8.5, with 40 µl β-mercaptoethanol per ml sample

buffer added before use) and boiled at 100°C for 5 minutes. Tubes were centrifuged at max-speed in a cooling benchtop centrifuge and the supernatant was collected and kept.

2.2.6.1.2 Proteins extractions using Tri-Chloroacetic Acid (TCA)

2ml of meiotic time cultures ($\sim 4.5 \times 10^7$ cells/ml) were transferred to Ribolyser tubes, resuspended in 200 μ l of 20% TCA and snap-frozen in liquid nitrogen for processing at a later date. A small scoop of 425 – 600 μ m acid-washed glass beads (Sigma) were added to samples in 20% TCA. These were ribolysered five times in an MP Biomedicals FastPrep®-24 Ribolyser set to 6.5 m/s with an intervening 5 minute resting of the tubes on ice. Cells were checked for complete and uniform lysis under the light microscope and once fully lysed the supernatant was collected from the beads (taking care not to withdraw any beads into the pipette tip) and placed into a fresh 2 ml Eppendorf tube. The beads were washed once using 200 μ l of cold 10% TCA and a further two times with 400 μ l cold 10% TCA, vortexing thoroughly during each wash and pooling the supernatants from each wash into the corresponding 2 ml tube. The beads were discarded and the 10% TCA wash solution was centrifuged at 5000 R.P.M for 10 minutes in a benchtop cooling centrifuge set at 4°C. The cell pellet was thoroughly resuspended in 100-200 μ l 4x sample buffer (0.25 M Tris-HCl pH 6.8, 8% SDS, 10% β -mercaptoethanol, 30% glycerol, 0.02% bromophenol blue) and 35 μ l of 1.5 M Tris-HCl pH 8.8 to neutralize the acidity. Samples were boiled at 100 °C for 3 minutes and immediately centrifuged at max-speed in a benchtop cooling centrifuge for 2 minutes. The supernatant was collected and kept.

2.2.6.2 SDS-PAGE separation of proteins

One-dimensional separation of proteins on the basis of protein size was achieved by SDS-PAGE. Generally this was done with 100 mm x 70 mm mini-gels, but for better resolution of bands (e.g. Smt3 IP), larger format 180 mm x 160 mm gels were run. A typical 5 ml 10% resolving gel consisted of 2 ml H₂O, 2 ml of 30% Bis-acrylamide, 1.3 ml 1.5 M Tris pH 8.8, 50 µl 10% SDS, 50 µl 10% APS and 2 µl TEMED. Amounts were adjusted appropriately for gels of different percentages. H₂O-saturated butanol was applied to the top of the resolving gel to ensure even polymerisation at the top of the gel. After the resolving gel had set, the butanol was removed and 2ml of stacking gel was applied to the top of the gel with the desired gel comb. 1 ml of stacking gel consisted of 680µl of H₂O, 170 µl of 30% Bis- acrylamide, 130 µl of 1M Tris pH 6.8, 10 µl of 10% SDS, 10 µl of 10% APS and 1 µl TEMED. Small and large format gels were run in a Mini-PROTEAN® Tetra Cell (BIORAD) and an SE 600 Ruby dual cooled gel electrophoresis unit (Amersham Biosciences), respectively, with 1XSDS running buffer (Section 2.1.2). Small gels were run at 200 volts for ~30 minutes or until the dye front ran off the gel and large-format gels were run at 25 mA for ~5 hours at 4°C. Full range RAINBOW™ protein markers (GE Healthcare) were used to determine protein size (15 µl per lane).

2.2.6.3 Western Blotting

After SDS-PAGE, proteins were transferred to nitrocellulose membrane for immuno-blotting. Nitrocellulose membranes (WHATMAN Protran™ 0.45 µm pore size) were cut slightly larger than the gel and two pieces of filter paper (BIORAD extra-thick filter paper) were cut to the same size as the gel. The filter paper and nitrocellulose membrane were soaked in a semi-dry transfer buffer

(Section 2.1.2) for 5 minutes. The nitrocellulose membrane was placed on top of the filter paper and the gel was placed on top of the membrane. The other piece of filter paper was placed on top of the gel and the 'sandwich' was rolled with a glass tube to remove air bubbles. The membrane/gel sandwich was placed onto a pre-wetted semi-dry transfer chamber and transferred at 15 volts for 1 hour (or more for larger gels). When transfer was complete the membrane was carefully removed, rinsed with Ponceau (1g Ponceau, 15 g TCA, 50 ml dH₂O), followed by dH₂O to visualise protein bands. Membranes were then incubated in 5% milk (Marvel milk powder made up in PBS) at room temperature for 30 minutes and washed 3 times in PBS- Tween (1 ml TWEEN in 1000 ml PBS). Primary antibodies were then added to the membrane at the appropriate dilution in 5% milk and were incubated overnight at 4°C. The following day, the membrane was washed 3 times in PBS-Tween and the secondary antibodies diluted in 5% milk were added to the membrane. The membrane was incubated with the secondary antibodies (conjugated to horseradish peroxidase) for one hour at room temperature and then washed 3 times with PBS-Tween. Pierce® ECL Western Blotting Substrate was used for chemiluminescent detection of secondary antibodies and blots were exposed to chemiluminescent film (18 x 24 cm Hyperfilm ECL, GE Healthcare) in the dark room, following which films were developed.

2.2.7 Cytological methods

2.2.7.1. Assessment of nuclear divisions using DAPI

500µl samples were harvested from sporulation cultures at the appropriate time points and placed in sterile 1.5 ml Eppendorf tubes. Samples were centrifuged in a benchtop centrifuge (Eppendorf 5415D) at 4000 R.P.M and cell pellets

were resuspended in 100% ethanol. Samples were stored at 4°C until ready to be processed. Samples were processed by centrifugation in a benchtop centrifuge at 4000 R.P.M, the supernatant was removed and 20 µl DAPI-mount solution was added (1 mg/ml p-phenylenediamine in 10% v/v PBS and 90% v/v glycerol and DAPI 1 µg/ml). 5 µl of DAPI-stained cells were applied to a glass slide and a 22 x 22 mm² cover slip was added. Nuclei were visualized using the DAPI filter on the Nikon Eclipse 50i microscope.

2.2.7.2 Sporulation counts

Sporulation counts were carried out by taking 10 µl sporulation media after an appropriate time for sporulation to have occurred, they were applied to a glass slide and covered with a 22 x 222 mm cover slip. Cells were visualized using a light microscope and the proportion of total cells that had formed tetrads were counted. >100 cells were counted to obtain a sporulation frequency.

2.2.7.3 Visualization of GFP in tetrads and live cells

For visualization of GFP in live cells or tetrads 500 µl of sporulation culture was harvested and placed in a sterile 1.5 ml Eppendorf tube. Samples were centrifuged at 4000x g in a benchtop centrifuge (Eppendorf 5415D) for 1 minute and the supernatant was discarded. Cell pellets were resuspended in 20 µl PBS and 5 µl of cell suspension was applied to a glass slide and covered by a 22 x 222 mm cover slip. Cells were visualized using the transmitted light on a Nikon Eclipse 50i microscope and GFP was visualized using the fluorescent FITC filters.

2.2.7.4 In situ immunofluorescence of fixed cells

8 ml of sporulation culture was harvested at the appropriate time point and placed into a 14 ml round-bottomed polypropylene tube (Falcon). Formaldehyde

was added to a final concentration of 4% and cells were left for up to 1 hour at room temperature. 2 ml of SKP solution (1.2 M sorbitol, 50 mM KPO₄ pH 7.0) was added and cells were centrifuged at 3500 R.P.M for 3 minutes. This was repeated twice to ensure removal of all of the formaldehyde. Following the third spin, the cell pellets were resuspended in 100 µl SKP and transferred to a 1.5 ml Eppendorf tube. To this, 2 µl of 1 M DTT and 10 µl of 10 mg/ml Zymolyase (100T) were added and tubes were incubated at 37°C until spheroplasting was complete. Spheroplasting was assessed by mixing 2 µl of cell suspension with 2 µl distilled H₂O on a glass slide and observing the cells under a light microscope.

Spheroplasting is complete when cells lose their dark 'halo' and some cells burst. 100 µl of PBS was added to the spheroplast solution and tubes were centrifuged for 1 minute at 4000 r.p.m in a benchtop centrifuge (Eppendorf 5415D). Cell pellets were then gently resuspended in 67 µl PBS + 0.1% NP40 and left at room temperature for 30 minutes. 33 µl fetal bovine serum (FBS) was added followed by the appropriate dilutions of primary antibodies (section 2.1.5). Cells were incubated with the primary antibodies overnight at 4°C. The following day, cells were washed gently three times in 100 µl PBS and after the last wash, cell pellets were gently resuspended in 100 µl PBS + 4% BSA with the appropriate dilutions of secondary antibodies (Section 2.1.5). Cells were incubated in the dark at room temperature for 2 hours and then washed three times in PBS. 50 µl of DAPI mount solution (1 mg/ml p-phenylenediamine in 10% v/v PBS and 90% v/v glycerol) containing DAPI (1 µg/ml mount), was used to resuspend the cells and ~20 µl was dispensed onto a 22 x 50 cover slip (Menzel-Glaser) balanced on an Eppendorf rack. A Superfrost® microscope

slide (Thermo Scientific) pre-cleaned in ethanol was added face down to the cover slip and immediately rotated 180°. The cover slip was sealed to the slide with clear nail varnish.

2.2.7.5 Preparation and immuno-staining of chromosome spreads

8 ml of sporulation culture was harvested at the appropriate time point and placed into a 14 ml round-bottomed polypropylene tube. Cells were centrifuged at 4000 rpm for 5 minutes and cell pellets were resuspended in 500 µl KAc-Sorbitol (2% KAc, 1 M Sorbitol, pH 7.0) to which 5 µl 1 M DTT were added as well as 12 µl zymolyase (100T, 10 mg/ml). Cells were incubated in a roller drum incubator at 30°C for 30 min (BR, S288C & Y55 strains) or 10-15 minutes (SK1 strains). Tubes were then placed on ice while spheroplasting was assessed (see Section 2.2.4.4). Once spheroplasting was complete, 2ml of cold (4 °C) MES-Sorbitol (0.1 M MES, 1 mM EDTA, 0.5 mM MgCl₂, 1M sorbitol) was added and the spheroplasts were centrifuged at 1100 R.P.M (271 x g). The supernatant was carefully decanted and the tube was drained by briefly upturning it on a piece of tissue. 50 µl chilled MES solution (0.1 M MES, 1 mM EDTA, 0.5 mM MgCl₂, pH 6.4) was added to the side of the tube and then flicked gently to mix with the spheroplasts in the pellet. The tube was flicked for no longer than 10 seconds after which 100 µl of chilled 4% para-formaldehyde (pH 8.5) was added and gently pipetted up and down 8 times. 50 µl of cell suspension was dispensed onto a 22 x 50 mm cover slip (Menzel-Glaser) balanced on an Eppendorf rack. An upturned Superfrost® Slide (Thermo Scientific) that had been pre-cleaned in ethanol was added to the cover slip and immediately rotated 180°. Slides were left for 1 hour at room temperature and then cover slips were washed off using 0.4% Photo-Flo 200 (KODAK) solution

(made up in PBS). Slides were left to air-dry for at least an hour. Primary antibodies were applied to a fresh 22 x 50 mm cover slip diluted in 50 µl of 1 part FBS: 2 parts PBS-4% BSA to which the air-dried slides were placed face-down and again rotated 180°. Slides were kept in a 'humidity chamber' overnight at 4°C and the following day, the cover slips were removed and the slides were washed for 5 minutes in PBS. This was repeated 3 times in total. Secondary antibodies were applied to a fresh 22 x 50 mm cover slip diluted in 50 µl of PBS-4% BSA to which the slides were placed face down and rotated 180°. Slides were placed in a humidity chamber and incubated for 2 hours in the dark, at room temperature. Cover slips were then removed and the slides were washed for 5 minutes in PBS as before. The slides were then mounted with DAPI-Mount solution (1 mg/ml p-phenylenediamine in 10% v/v PBS and 90% v/v glycerol) and DAPI (1 µg/ml mount), a fresh cover slip was added and the edges sealed with nail varnish.

2.2.7.6 Fixed Image captures

Images were captured using a Deltavision IX70 system (Applied Precision) using the accompanying softWoRx software, and an Olympus Plan Apo 100 1.4 numerical aperture objective lens. Emission and excitation filters for DAPI (DAPI- 5060B, FF01-387/11-25 and FF409-Em02-25), FITC (FITC-3540B, FF506-Ex04- 25 and FF506-Em02-25), Texas Red (TXRED-4040B, FF593-Ex03-25 and FF593- Em02-25), and Cy5 (Cy5-4040A, FF660-Ex03-25 and FF660-Em02-25) were obtained from Semrock. The ranges of excitation wavelengths for each filter set are, DAPI (350 nm to 410 nm), FITC (465 nm to 500 nm), Texas Red (542 nm to 582 nm) and Cy5 (608 nm to 648 nm). Images were captured by a 12-bit CoolSnap HQ CCD camera (Roper Scientific) and

deconvolved using the proprietary constrained iterative deconvolution algorithm until the standard residual, r , was <0.02 . The exposure times of the camera were optimised for each channel to allow detection of $\sim 3000 - 3600$ counts on the 12-bit CoolSnap HQ CCD camera (Roper Scientific). The softWoRx software was used to take Z-stack images (set at $0.2\ \mu\text{m}$ increments) and to do 2D-projections of such images.

2.2.8 Live-capture of imaging

2.2.8.1 Preparation using Labtech chambers

One well of the Labtech chamber was loaded with $30\ \mu\text{l}$ of ConA and spread across the bottom of the well, then left to dry in a microbial hood for 20 minutes. $80\ \mu\text{l}$ of cells at the appropriate time point from the harvested meiotic cell culture were added to the Labtech. Cells were evenly spreaded out at the bottom of the well. Cells in the Labtech were then left to stick to the plate in 30°C incubator for 30 minutes. Excess cells were removed after 30 minutes incubation and replaced with $500\ \mu\text{l}$ of 1% KAc. The Labtech was placed onto the personal Deltavision (pDV) and imaging was started using SoftWoRx or Micromanager.

2.2.8.2 Preparation using CellAsics chambers

Antibiotic solutions in the inlets of the microfluidic plate were removed and washed three times with distilled water. The first 6 wells from the left were filled with $300\ \mu\text{l}$ of warm 1% KAc. The first well from the right was filled with $50\ \mu\text{l}$ of the sample with $50\ \mu\text{l}$ of warm 1% KAc. The CellAsics plate was then sealed to the F84 manifold. The entire plate was placed onto the personal Deltavision microscope for imaging. Cells were loaded into the wells by using the attached computer program. KAc liquid was set to load into cell chambers every three

hours. The microscope was focused on the area of imaging and start imaging was started using SoftWorKx or Micromanager.

2.2.8.3 Live cell imaging using personal Delta vision (pDV)

Plates were placed onto the pDV and cells were focused. The olympus Plan Apo 1.4 NA 100x oil objective was used for imaging samples. Two filters were used: GFP (excitation filter 470/40 nm and emission filter 520/40 nm); mCherry (excitation filter 572/35 nm and emission filter 630/60 nm). The camera used was a photometrics EMCCD. The temperature around the microscope was controlled at 30°C.

2.2.8.3.1 Conditions using SoftWoRx software:

Z-stacks were set at 10 optical sections for deconvolution. Centromeres tagged with GFP were imaged using the following conditions: 0.08 exposure, 100% transmittance, 7 z-sections with 0.3 optical spacing, gain 240 using fast/aggressive imaging. Cnm67 was tagged with mCherry and Pds1-tdTomato used the following conditions:

2.2.8.3.2 Conditions using Micromanager software:

Top of Z stacks: 4 µM; bottom of Z stacks -4 µM; Z section is 1 optical spacing. Exposure to GFP channel is 30, mCherry Channel (Tricy) 30. Transmission for GFP is 10 and transmission for mCherry is 10.

2.2.9 Computational Tools

2.2.9.1 Websites used

Saccharomyces Cereviase Genome Database:

<http://www.yeastgenome.org/>

Reverse Complement:

http://www.bioinformatics.org/sms/rev_comp.html

BLAST:

<http://www.ncbi.nlm.nih.gov/>

2.2.9.2. Software used

Adobe Photoshop, Adobe Illustrator version CS5.1

SoftWoRx Deltavision software

Micromanager software

Ayida for recombination quantification

Prism

2.2.10 Mutagenesis

Mutagenesis used Genescript service

Chapter 3. Functional analysis of Synaptonemal complex in Zip1 point mutants

3.1 Introduction

The synaptonemal complex is a proteinaceous structure that is implicated in meiotic chromosome dynamics, but its function and regulation are still poorly understood (see introduction). One of the early functions of Zip1 is to promote the association of any two centromeres (non-homologous centromere coupling). This occurs prior to the onset of recombination and synapsis of homologous chromosomes. The significance of non-homologous centromere coupling is unclear. Tsubouchi and Roeder (2005) proposed that coupling facilitates rough chromosome alignment by holding any two chromosomes together in a semi stable configuration while homology along chromosome arms is being assessed. However, it is not known whether homolog pairing is delayed in the absence of centromere coupling. Throughout this chapter, 'coupling' is used when non-homologous centromeres are within close proximity to each other, whereas 'pairing' refers to closely association of homologous centromeres juxtaposed to each other (Sym and Roeder, 1995).

Non-homologous centromere coupling has to be replaced by homologous centromere pairing. How is this process regulated and coordinated with recombination-based chromosome pairing? A study by Falk *et al.* (2010) has revealed apposing of activity of Mec1/ATR kinase and Pph3/PP4 phosphatase in phosphorylating and de-phosphorylating of Zip1, which allows the switch from centromere coupling to homologous centromere pairing. Upon induction of DSBs by Spo11, Mec1/ATR is activated. Activated Mec1/ATR phosphorylates

Zip1 on S75 resulting in de-coupling of centromeres. This phosphorylation causes further phosphorylation of Zip1 at sites that are currently unknown (Falk et al., 2010). In *pph3Δ* mutants, a hyper-phosphorylated form of Zip1 accumulates and pairing of homologous centromeres as well as synapsis is impaired.

Since non-homologous centromere coupling is unaffected by the loss of Pph3, this suggests that Pph3 is important in restoring centromere pairing. Consistent with this, homologous centromere pairing is restored in *pph3Δ* mutants when Mec1/ATR activity is suppressed, i.e. the *mec1-1 pph3Δ* double mutants had normal pairing of homologous centromeres. Secondly, mutating Zip1-S75 to alanine (*zip1-S75A*) restores centromere pairing in the absence of Pph3. Taken together, these observations suggest that the homologous centromere pairing defect in *pph3Δ* mutants is due to checkpoint dependent phosphorylation of Zip1-S75 by Mec1/ATR. Pph3 in turn causes de-phosphorylation of Zip1, thereby restoring pairing between homologous centromeres.

In addition to functioning prior to recombination, Zip1 is also essential during prophase I. Zip1 specifically localizes to the synapsed regions of SC but not to un-synapsed regions. In *zip1Δ* mutants, homologous chromosomes are paired but not synapsed further indicating the importance of Zip1 in synapsis (Rockmill et al., 1995; Sym et al., 1993). There is some heterogeneity in meiotic progression in *zip1Δ* mutants depending upon strain background. However, all *zip1Δ* mutants have two-to three-fold reduction in crossing over and Holliday Junctions persist longer than in the wild-type (Borner et al., 2004). In *zip1Δ* mutants, crossover designation and patterning of crossover are unperturbed.

The pattern of genetic crossovers (interference) however, is abrogated in *zip1* Δ mutants (Borner et al., 2004; Sym and Roeder, 1994). This suggests that Zip1 is important in the implementation of crossover after their early destination.

Finally, Zip1 persists at centromeres, including between non-exchange chromosomes where it promotes their association at the onset of metaphase I (Gladstone et al., 2009; Newnham et al., 2010). This is important for accurate chromosome segregation (see Chapter 5).

Taken together, Zip1 clearly is important in many aspects of meiosis, such as synaptonemal complex dynamics, recombination, and chromosome segregation. Following the identification of several Zip1 phosphorylation sites through mass spectrometry, the functionality and regulation of these sites have been characterized to look at whether mutation of phosphorylation would cause any defects in chromosome segregation. By detailed studying of these Zip1 point mutants, this chapter has shown a fine-tuning of Zip1 functions by multiple putative kinases throughout meiotic prophase. Specifically, SC dynamics may occur independently of crossover formation and perturbation of the SC does not cause meiotic arrest.

3.2 Results

3.2.1 Analysis of sporulation and spore viability in Zip1 point mutants

Several studies have shown that Zip1 is a phosphoprotein and that different phosphorylation sites changes throughout meiosis (Falk et al., 2010; Zhu et al., 2010). To identify the phosphorylation sites in Zip1, Dr. Alice Copsey (Hoffmann Lab) immunoprecipitated Zip1 or analysed peptides by mass spectrometry (MS). These approaches identified 10 sites (Fig. 3.1A). The Hochwagen's Lab used similar approaches in *pph3Δ* mutants and identified some overlapping sites as well as phosphorylated S75 (Fig. 3.1E). 8 out of 10 sites identified by Dr. Alice Copsey were selected for further characterization. These included three of the four putative CDK1 sites (S89, S763, S828) (Fig. 3.1C), four CK2 and DDK sites (S82; S127; T114; S144), a CK2 only site (Zip1-S137) (Fig. 3.1B). Zip1-S144 is described further in Chapter 4. A multiple Zip1 phosphomutant is also made (*zip1-7A*) (Fig. 3.1D). The summaries of the genotypes are shown in Table 3.1.

To understand the functions of these phosphorylation sites in meiosis, a non-phosphorylatable version of each site was made by changing serine/threonine to alanine (Fig. 3.1C,D). Phosphomimetic version was also created by changing the serine/threonine to glutamic acid and aspartic acid. The *YipLac204-ZIP1-TRP1* plasmid was used as backbone to generate mutations and integrated at the *TRP1* locus. All plasmids used are listed in Table 2.11. Wild-type *ZIP1* (*trp1::ZIP1-TRP1/trp1::ZIP1-TRP1*) integrated at *TRP1* but expressed under its native promoter has normal SC assembly, crossing over, and viability (Falk et al., 2010)(Fig. 3.2A). Diploid strains were introduced to sporulation media and

samples were collected after 24 hours to determine sporulation efficiency and spore viability. As expected the wild-type strain showed 98% sporulation efficiency, whereas this was reduced to 78% of the total sporulation in *zip1* Δ (Fig. 3.2A). The majority of mutants observed to have sporulation efficiency similar to that in the wild-type. The only mutant with sporulation defect is the *zip1-S127DE* mutant. This might be due to disruption of the local structure of Zip1 by insertion of two charged amino acids. This hypothesis might be supported with the fact that changing the serine to glutamic acid (*zip1-S127E*) did not cause any sporulation defects (Fig. 3.2A). Therefore at this stage it is hard to distinguish between whether this defect in sporulation is due to alteration of phosphorylation status or disruption of Zip1 structure. In conclusion, there are no major sporulation defects in meiotic progress in the majority of mutants.

To assess spore viability, tetrads were dissected onto a rich medium to allow germination, and subsequent growth of haploid gametes was assessed (Fig. 3.2B). In the wild-type, 99% spore viability was observed, whereas in *zip1* Δ this was reduced to 48%. The majority of strains displayed wild-type-like viabilities. However, the original transformant *zip1-S82A* (*zip1-S82A-O*) showed decreased viability (16% with 4 viable spores). This was much lower than the *zip1* Δ (31% with four viable spores). It is known that transformation can generate mutations. Although the *ZIP1* gene was sequenced and the insertion

was checked by Southern Blot analysis (Appendix 2-4), independent mutation elsewhere in the genome could have caused severe loss of viability. Therefore, to clarify further the viability loss in the *zip1-S82A-O* mutant, three further independent diploids were generated from three separate transformants. All of these diploids displayed wild-type viability (Fig. 3.2B). These observations suggest that S82 mutation does not affect spore viability and that the original S82-O phenotype is most likely due to secondary mutation elsewhere in the genome.

Mutating multiple phosphorylation sites in the N-terminal of Zip1 also resulted in lowered spore viability, in particular with the *zip1-8A* and *zip1-8E* mutants (Fig. 3.2B). These viability reductions in the multiple point mutants could be due to change of protein structure or due to changing the phosphorylation status. Overall, the above data together indicate that individual mutation in these amino acids do not trigger any obvious spore viability defects. However, multiple mutants may affect the functions of the protein, consistent with the hyperphosphorylation observed when centromere coupling is aggregated (Fig. 3.3). However, at this stage we cannot rule out the hypothesis that mutating multiple sites does not disrupt the structure of the protein.

Table 3.1 Summary of genotypes

Strain No.	Genotype	Abbreviation
Y4813	<i>trp1::ZIP1-TRP1/trp1::ZIP1-TRP1</i>	ZIP1
Y1530	<i>zip1::URA3/zip1::URA3</i>	<i>zip1</i>
Y5105	<i>trp1::ZIP1-S82A-TRP1/trp1::ZIP1-S82A-TRP1</i>	<i>zip1-S82A-O</i>
Y5135	<i>trp1::ZIP1-S82A-TRP1/trp1::ZIP1-S82A-TRP1</i>	<i>zip1-S82A-1</i>
Y5637	<i>trp1::ZIP1-S82A-TRP1/trp1::ZIP1-S82A-TRP1</i>	<i>zip1-S82A-2</i>
Y5640	<i>trp1::ZIP1-S82A-TRP1/trp1::ZIP1-S82A-TRP1</i>	<i>zip1-S82A-3</i>
Y5108	<i>trp1::ZIP1-S95A-TRP1/trp1::ZIP1-S95A-TRP1</i>	<i>zip1-S95A</i>
Y4851	<i>trp1::ZIP1-S127A-TRP1/trp1::ZIP1-S127A-TRP1</i>	<i>zip1-S127A</i>
Y5111	<i>trp1::ZIP1-S137A-TRP1/trp1::ZIP1-S137A-TRP1</i>	<i>zip1-S137A</i>
Y4843	<i>trp1::ZIP1-T114A-TRP1/trp1::ZIP1-T114A-TRP1</i>	<i>zip1-T114A</i>
Y5117	<i>trp1::ZIP1-T114E-TRP1/trp1::ZIP1-T114E-TRP1</i>	<i>zip1-T114E</i>
Y4505	<i>trp1::ZIP1-4A-TRP1/trp1::ZIP1-4A-TRP1</i>	<i>zip1-4A</i>
Y4854	<i>trp1::ZIP1-7A-TRP1/trp1::ZIP1-7A-TRP1</i>	<i>zip1-7A</i>
Y5168	<i>trp1::ZIP1-8A-TRP1/trp1::ZIP1-8A-TRP1</i>	<i>zip1-8A</i>
Y5170	<i>trp1::ZIP1-8DE-TRP1/trp1::ZIP1-8DE-TRP1</i>	<i>zip1-8E</i>

Table 3.2 Summary of phenotypes

Mutants	Sporulation	Viability	SCA	PC	SCD	Coupling
ZIP1	0.97	0.97	Normal	No	Normal	Normal
<i>zip1</i>	0.5	0.31	NA	N/A	N/A	Abnormal
<i>zip1-S82A-O</i>	0.91	0.16	Normal	YES	Normal	N/A
<i>zip1-S82A-1</i>	0.97	0.86	Normal	NO	Normal	N/A
<i>zip1-S82A-2</i>	0.96	0.91	Normal	NO	Normal	N/A
<i>zip1-S82A-3</i>	0.96	0.91	Normal	NO	Normal	N/A
<i>zip1-S95A</i>	0.91	1	Normal	NO	Normal	N/A
<i>zip1-S127A</i>	0.81	0.9	Normal	NO	Normal	N/A
<i>zip1-S137A</i>	0.96	1	Normal	YES	Abnormal	N/A
<i>zip1-T114A</i>	0.96	0.95	Normal	YES	Normal	Abnormal
<i>zip1-T114E</i>	0.94	1	Normal	NO	Normal	Normal
<i>zip1-4A</i>	0.95	0.9	Normal	YES	Normal	Abnormal
<i>zip1-7A</i>	0.85	0.85	Normal	NO	Normal	Abnormal
<i>zip1-8A</i>	0.97	0.87	Abnormal	YES	Abnormal	Abnormal
<i>zip1-8E</i>	0.98	0.75	Abnormal	YES	Abnormal	Abnormal

SCA: Synaptonemal complex assembly. SCD: Synaptonemal complex disassembly. NA: not assessed. Yes: polycomplexes observed; No: no polycomplexes observed.

3.2.2. Zip1-phospho mutants have a role in centromere coupling at pre-meiotic stage

Although Zip1 is the building block of the SC, it begins to function in meiosis much earlier, during which it holds the non-homologous centromere together, a process termed ‘centromere coupling’ (Tsubouchi and Roeder, 2005). During wild-type meiosis, approximate ~16 centromere foci are observed under a fluorescence microscope (Fig. 3.3A). In the absence of *zip1* Δ , non-homologous centromeres are not coupled, resulting in ~32 foci observed (Fig. 3.3C). Previous study has also shown that mutation of four putative CDK consensus sites (S89, S763, S783, and S828, named *zip1-4SA* in the paper) had normal viability and SC formation when mutated to their non-phosphorylatable state. A slight delay in SC disassembly in *zip1-4SA* was observed (Zhu et al., 2010). This delay is consistent with the observation of a one-hour delay of nuclear

division delay is consistent with the observation of a one-hour delay of nuclear division in *zip1-4SA* at the onset of MI. Therefore suggesting a slight defect in prophase I. This study concluded that putative regulation by CDK had little role in SC dynamics (Zhu et al., 2010).

Three CDK sites (S763, S783, and S828) as well as another CK2/DDK site (T114) were identified by the Hoffmann Lab. Coupling was not studied in the previous study by Zhu et al. so it would be interesting to see whether these CDK sites as well as Zip1-T114 involves in centromere coupling. Hence, T114, S763, S783 and S828 together are mutated to alanine, termed *zip1-4A* mutant (Fig. 3.3I). Moreover, *zip1-T114A* was picked alone to study for centromeric coupling (Fig. 3.3E). As well as these, three combination mutants (*zip1-7A*; *zip1-8A*; *zip1-8E*) were also studied (Fig. 3.3M,O,Q). Centromere coupling is independent of Spo11, whereas centromere pairing is dependent on Spo11 (Tsubouchi and Roeder, 2005). Hence to eliminate the possibility of homologous centromere pairings, all experiments were performed in *Spo11-Y135F* background, which is a catalytic subunit of Spo11. This mutant does not form DSB, but it does not affect meiotic progression, SC and spore formation neither.

Meiotic spreads were taken at 3 hours for all mutants analysed. This is the time when Zip1 becomes apparent on chromatin and sister chromatids are finding their partner to pair up with. Samples were surface spread and immune-stained with α -Ctf19, which is a kinetochore protein marking the centromere. Magenta showed α -Zip1 staining. Interestingly, a partial coupling phenotype was observed in the *zip1-T114A* mutant, where averages of 22-25 foci were seen (Fig. 3.3E). This partial coupling suggests that coupling is not totally disrupted,

but it is also not wild-type-like. Hence, the *zip1-4A* mutant was also analyzed. The *zip1-4A* mutant was observed to have the same partial coupling phenotype (Fig. 3.3I) as with the *zip1-T114A* mutant. This suggests that Zip1-T114 is the only site involved in coupling. To further confirm this, it was hypothesized that the *zip1-3A* mutant should show wild-type-like coupling. Indeed, after separate *zip1-4A* into *zip1-3A*, ~16 centromeres were observed; indicating these three sites are not involved in coupling (Fig. 3.3K). In conclusion, these data suggest that phosphorylated Zip1-T114 is partly required to couple non-homologous centromeres. A phosphomimetic mutant was made (*zip1-T114E*) to verify this hypothesis (Fig. 3.3G). Changing threonine to glutamic acid would mimic the environment of T114, and if indeed this site is required to phosphorylate when the centromere couples sister chromatids, then changing T114 to its phosphomimetic version would restore coupling. Results in Figure 3.3G have proved this theory. A shift more towards the left of the scale in *zip1-T114E* was been observed. ~17-21 foci were observed rather than ~16. This difference suggests that the *zip1-T114E* mutant improves coupling relative to the *zip1-T114A* mutant. But remain deficient relative to the wild-type. The reason that the average of 16 foci was not detected might due to the phosphomimetic mutation not sufficient enough to act as wild-type. But overall the peak in *zip1-T114E* shifted more towards the left on the scale. Hence it can be concluded that *zip1-T114E* can rescue coupling. Subsequently, these data propose that coupling requires the phosphorylation of Zip1-T114. The meaning of coupling is still unclear. This process has been proposed to provide stability for sister chromatids before they enter meiosis I. Lack of phosphorylation in *zip1-T114A* probably unstable coupling, results in partial pairing between sister chromatids.

In conclusion, the above data indicate that Zip1-T114 is probably important in centromere coupling. Moreover, the *zip1-S144A* mutant (chapter 4) that is involved in SC disassembly showed wild-type-like centromere coupling (Appendix 8), whereas *zip1-T114A* mutant is not involved in SC disassembly but required for coupling, probably suggests separate functions between these two sites.

Changing seven sites (*zip1-7A*) results in abolishing centromere coupling completely (Fig. 3.3M), similar to the complete knockout of *zip1Δ* (Fig. 3.3C). This was also observed for *zip1-8A* and *zip1-8E* mutants. The *zip1-7A* mutant could suggest that phosphorylation of these sites in combination is required to couple non-homologous centromeres. However, the phosphomimetic version of *zip1-8E* mutant did not retain non-homologous coupling. This might be due to disruption of the stability of the Zip1 structure and therefore acts like a *zip1Δ*. SC assembly defects observed in *zip1-8E* mutant also supports this theory (see below).

3.2.3 Formation of Synaptonemal complex in Zip1-phosphorylation site mutants

The above data indicate that Zip1 is highly dynamic in its phosphorylation. To determine how phosphorylation requires SC formation, mutants were harvested in sporulation media and selective time points were taken. SC formation normally begins around 4 hours in the SK1 strain background and hence every half hour time point samples were mixed for 3 hours (Fig. 3.4). For example,

four hours sample mixed with four and a half hours; five hours sample mixed with five and a half hours and so on. α -Zip1 antibody stains the CE of the SC, which is shown in green. α -Tubulin stains tubulin, which marks the stage of meiosis, whilst the timing each mutant formed linear Zip1 varies significantly, eventually all of them form linear SC (Fig. 3.4). Among these, *zip1-S137A* (Fig. 3.5E) was observed with PCs in all nuclei counted, *zip1-S127A* was observed with some PCs at onset of prophase (Fig. 3.5D). The diploid that had viability defects in *zip1-S82A* also showed PCs (Fig. 3.5B). Nevertheless, no PCs were observed in diploids that had normal viability in *zip1-S82A* (Fig. 3.5C) (Appendix 1). As mentioned previously, the viability defect seen in *zip1-S82A-O* might due to a secondary mutation in the genome. This is consistent with observing PCs in this mutant. In contrast, in *zip1-S82A-1* with normal spore viability, no PCs were formed. In conclusion, formation of PCs in *zip1-S82A-O* might due to secondary mutation and hence cannot be counted as a phenotype. In another word, *zip1-S82A* forms normal SC. Mutants that also had high levels of PCs were *zip1-4A* and *zip1-T114A* mutants where synapsis is normal but a build-up of aggregates (Zip1) remains in the nucleus (Fig. 3.7). *Zip1-S95A* (Fig. 3.4D) and *zip1-S127A* (Fig. 3.4E) behaved very wild-type-like, as seen with linear Zip1, and no PCs. Taking the fact that *zip1-S95A* and *zip1-S127A* have normal sporulation and spore viabilities, this indicates mutation of phosphorylation in these two sites on their own does not trigger any meiosis defects. Surprisingly, *zip1-7A* (Fig. 3.4H) was not observed to have any SC formation defects. SC formation observed in *zip1-7A* is unexpected, because both *zip1-S137A* and *zip1-T114A* mutants have polycomplexes. Furthermore, *zip1-7A* had total disruption of centromere coupling. Why is coupling affected but not the SC? One suggestion to explain

this is that mutation for all sites results in changing the structure of Zip1, which destabilizes coupling. However, this instability somehow did not affect SC, perhaps due to cancellation of different phosphorylation events during prophase I. To conclude, in the absence of phosphorylation in these sites neither alone nor in combination affects the synapsis of SC formation. Following the identification of all Zip1-point mutants, Dr Andreas Hochwagen also identified different Zip1 phosphorylation sites through mass spectrometry. These are named as *zip1-8A* and *zip1-8E*. These mutants contain similar sites identified by the Hoffmann Lab, which are S82, T114, S127, S144. How does SC behave in *zip1-8A* and *zip1-8E*? Do they behave the same as other mutants already characterized? To investigate this question further, similar experiments were conducted. Sporulation was shown to be wild-type-like in both mutants (Fig. 3.2A), but a slight reduction in viability was observed (Fig. 3.2B). The *zip1-7A* mutant exhibited normal SC with no PCs and it is assumed that maybe the *zip1-8A* and *zip1-8E* mutants would behave the same. Surprisingly, SC defects were observed in both mutants. The *zip1-8A* mutant was observed to have dot linear Zip1 when DNA was fully condensed (Fig. 3.6A), suggesting cells do not form linear Zip1 in pachynema. However, the majority of nuclei were examined were dotty, suggesting a defect in SC formation. Nevertheless, normal progression of nuclei division in the *zip1-8A* and *zip1-8E* mutants was observed (Fig. 3.6E,F), hence indicating normal cell cycle progression. The *zip1-8E* mutant appears to have even more severe defects, where only dotty Zip1 was observed with diffused DNA (Fig. 3.6B). This might indicate delay of pachytene nuclei, but disassembly of SC was observed from 5 hours onwards, suggesting sufficient exit of pachytene. The phosphomimetic version in theory should improve the

phenotype, but in this case opposite results are shown. This leads to the hypothesis that mutation to the phosphomimetic version might disrupt the Zip1 structure and hence no proper SC is formed in *zip1-8E*. This could also explain why centromeric coupling was abnormal in *zip1-8E*. Yet, this disruption of structure does not affect the overall progression of meiosis hence cells divide normally in the *zip1-8E* mutant. In conclusion, although no proper SC formed in both mutants, they are sufficient to exit after pachytene and segregate in a wild-type manner.

3.2.4 Analysis of SC formation in *zip1-T114A* and *zip1-4A*

The above results suggest that phosphorylation on Zip1-T114 might be important for centromere coupling during early meiosis. Therefore to test whether phosphorylation of the putative CK2/DDK site T114 is important for Zip1 activity, threonine residue on Zip1-T114 was mutated to alanine (*zip1-T114A*) alone or in combination with the three CDK1 sites that were found to be phosphorylated in Zip1 (*T114A, S89A, S763A, S783A- zip1-4A*).

Wild-type diploids, *zip1-4A* and *zip1-T114A* were added to sporulation media and samples were taken at appropriate times for assessment of meiotic nuclear spreads and immune stained with α -Zip1 and α -Tubulin (Fig. 3.7A-C). The meiotic time course for these three strains was performed in parallel. Nuclei with different Zip1 pattern were categorized into three different groups as 'Dotty', when the Zip1 staining pattern was mainly punctate (foci) with diffuse DNA. This represents leptotene (Fig 3.7A). As meiosis proceeds, short stretches of Zip1 with some dots are formed and termed as dot-linear. The DNA is partially condensed. This dot-linear staining presents zygotene (Fig. 3.7A). Once SC is

fully synapsed at pachytene (Fig 3.7A), full linear Zip1 is seen on immunostaining spreads with condensed DNA. In the wild-type cells, 12% of nuclei have formed linear Zip1 by four hours. Nuclei stained with DAPI also show consistency with SC dynamics (Fig. 3.7J), where the wild-type begins MII at five hours. No SC formation delay was observed in *zip1-T114A* (Fig. 3.7F), but the *zip1-4A* mutant showed an appearance of Zip1 one hour later compared to the wild-type (Fig. 3.7E). Yet, despite the Zip1 appearance in meiotic spread, the *zip1-4A* and *zip1-T114A* nuclear divisions started around 6 hours (Fig. 3.7K, L). The *zip1-T114A* mutant showed a slight difference between the timing of SC formation (4 hours) and the timing of nuclear division (6 hours) compared to the wild-type (Fig. 3.7L). In comparison, full linear SC was observed from 5 hours in the *zip1-4A* mutant whereas the wild-type began at 4 hours, hence the *zip1-4A* mutant was observed to have a consistent delay in both SC and nuclear divisions (Fig. 3.7K). Different timings might suggest an asynchronous time course. The major peak of pachytene nuclei was observed between 5 to 6 hours in the wild-type cells (55%), which declined 2 hours later, from around 7 to 8 hours after transfer to a sporulation medium. A similar case for pachytene peak was observed in both *zip1-4A* and *zip1-T114A* mutants, where the majority of nuclei had gone into pachytene between 5 and 6 hours. Nevertheless, the *zip1-T114A* mutant seems to have more pachytene at 7 and 8 hours compared to the wild-type. At 7 hours, pachytene nuclei observed in the *zip1-T114A* mutant were 5% whereas the wild-type was 2%. At 8 hours there was 13% of pachytene nuclei in the *zip1-T114A* mutant compared to 4% in the wild-type. Higher portions of pachytene at late hours in the *zip1-T114A* mutant could suggest a defect in SC disassembly. However, no SC disassembly

defects were observed in *zip1-T114A*, this is probably because of an asynchronous time course and might explain why different timings between SC formation and nuclei were observed. Nevertheless, aggregates of Zip1 were observed in 100% nuclei examined for both *zip1-4A* and *zip1-T114A* mutants. Often mutants that are defective in SC formation such as SIC mutants appear with this phenotype. This PC phenotype is particularly obvious in the *zip1-T114A* in comparison to the *zip1-4A*, where a much brighter and larger PC was observed in *zip1-T114A* (Fig 3.7C). Despite this, linear SC does form in both mutants, indicating synapsis does occur in these mutants. Why do *zip1-T114A* and *zip1-4A* mutants have PCs in all nuclei regardless of their ability to form SC? This appearance of PCs probably indicates some correlation with their phosphorylation. Mutating these sites might alter the steady state of Zip1 turnover. Therefore, Zip1 was constitutively produced in the nuclei, resulting in build up of Zip1 that cannot get elongated. These PCs do not trigger meiosis defects such as SC formation (Fig. 3.7), sporulation and spore viability (Fig. 3.2). Overall, the above data indicate that phosphorylation at these CDK/DDK consensus sites does not affect synapses of the SC as well as disassembly of the SC. But Zip1 proteins tend to aggregate in these mutants.

3.2.5 High levels of Zip1 protein in mutants with polycomplexes

Meiotic spreads in *zip1-4A* and *zip1-T114A* showed large and bright PCs. This is a common phenotype in the *zmm* mutants and other recombination mutants (Lynn et al., 2007). Aggregates of Zip1, and other components and regulators of the SC, suggests altered dynamics of SC formation, although Zip1 association with meiotic chromosomes appears more or less normal. Thus, to understand whether these mutants are associated with altered protein levels, Western blot

analyses of meiotic protein extracts from *zip1-4A* and *zip1-T114A* mutants were conducted in parallel with wild-type controls. After transfer to a sporulation medium, samples were taken every hour and protein was extracted using TCA. A higher level of Zip1 was observed in the *zip1-4A* mutant (5 & 6 hours) compared to the wild-type (Fig. 3.8B), suggesting a correlation between higher levels of Zip1 proteins when PCs are present. Zip1 proteins in the *zip1-4A* mutant persist for longer relatively to the wild-type. Zip1 band was still present from 6 hours onwards in the *zip1-4A*, whereas in the wild-type Zip1 had already disappeared. In addition to Zip1 protein levels in these mutants, several markers are also used to stage different events during meiosis. Meiotic progression seems normal in the *zip1-4A* mutant shown by γ -H2A levels. But DSBs in the *zip1-4A* mutant seem to remain in a longer timeframe, as shown by Hop1-T318 (Fig. 3.8A). With the observation of a one-hour delay in the *zip1-4A* mutant (Fig. 3.8A), this might suggest insufficiency in recombination. However, given the fact that spore viability is normal, this probably indicates a delay in recombination due to high levels of Zip1 protein. Much higher levels of Zip1 protein are detected in the *zip1-T114A* mutant, about 7-fold higher compared to the *zip1-4A* mutant. A high level of Zip1 protein in the *zip1-T114A* is consistent with more PCs observed in the meiotic spread (Fig. 3.8C). Zip1 degradation in the *zip1-T114A* mutant is similar to the *zip1-4A* mutant. Overall protein levels indeed increased in the mutants compared to wild-type cells, and probably explain the phenotype of PCs.

To understand more precisely about the higher levels of Zip1 in *zip1-4A* and *zip1-T114A* mutants, 50 μ m phos-tag gels were used to increase the resolution of phosphorylated species of Zip1 (Fig. 3.8E&F). These gels contain

binding sites that bind to the negative charges on the phosphate and preferentially retard phosphoproteins, which will give an additional band on the Western blot. If multiple phosphorylation sites occur in *zip1-4A* and *zip1-T114A* mutants, then extra bands would appear. The *zip1-4A* mutant migrated faster compared to the wild-type (Fig. 3.8E), thus indicating its under-phosphorylation. Zip1-T114A seems to have been under-phosphorylated as a high mobility band was observed in *zip1-T114A* extracts compared to the wild-type extracts. However, both mutants still show multiple bands, and these band patterns could represent reduction in phosphorylation due to knocking out of phosphor sites, but it is hard to be certain, and several modified bands remain which are likely to represent other phosphorylation sites (Fig. 3.8F). These mutants appeared to be different from another published mutant (*zip1-S75A*) (Falk et al., 2010), where additional phosphorylation was prevented when mutated to alanine. Overall, this finding suggests that steady-state levels of Zip1 protein are higher than normal in these mutants and that their phosphorylation patterns are different.

3.2.6 A delayed SC disassembly defect observed in *zip1-S137A* and *zip1-S144A*

After examining the formation of SC in all mutants, SC disassembly was assessed next. This was achieved through a meiotic spread to assess tubulin formation. In wild-type meiosis, two dots of tubulin present when Zip1 disassembles from the SC. Tubulin formation gradually elongates during metaphase, with a short stretch of tubulin observed. Zip1 completely disassembles from the SC. DNA also becomes very diffuse. The *zip1-S82A*; *Zip1-S95A*; *Zip1-S127A* and *zip1-7A* mutants were not observed to have any delayed disassembly in SC. This probably indicates that these sites are not

important for the regulation of the timely disassembly of the SC. However, a slight SC disassembly delay in the *zip1-S137A* mutant was observed (Fig. 3.9). This delay is unlike the SC disassembly defect in the *zip1-S144A* mutant (see Chapter 4 for details), only a portion of nuclei showed delayed disassembly (Fig. 3.9E). Approximately 30% of nuclei showed dotted Zip1 during diplotene (Fig. 3.9A) and 30% of dotted Zip1 during metaphase I (Fig. 3.9B). The remaining 70% disassembled as normal. Polycomplexes were observed in the *zip1-S137A* mutant, which is similar to the *zip1-S144A* mutant. Taken together, these data suggest that Zip1-S137 might be required for the timely disassembly of the SC.

3.3 Discussion

This chapter provides further insight into the role of phosphorylation of Zip1 in meiosis. Zip1 is known as a phosphor-protein with its globular head domains connected by coiled-coil bridges. The majority of the mutants in this study lie within the N-terminus. A previous study used in-frame deletion to study precise functions of Zip1 in different regions. Tung and colleagues deleted the N-terminal (aa21-163), the coiled-coil regions as well as the C-terminal. Their result showed that the N-terminal is not required for SC synapsis and crossover formation, it is in fact the C-terminal that is involved in these functions (Tung and Roeder, 1998). This is probably a sign indicating that the sites in this study might not lead to disruption of the SC or crossovers. However, some of these sites such as S82, S137, T114, S144 (see Chapter 4), lie adjacent to the coiled-coil region that mediates bridging interactions. Tung et al. (2000) have proposed that the N-terminal might be required for Zip1 stability. Therefore with polycomplexes seen in some of the mutants (S82, T114, S137) this suggests that maybe phosphorylation of these sites is required for stability or loading of Zip1 onto chromatin. However, the overall formation of synapsis is not affected suggesting these sites alone might not be strong enough to cause a synapsis defect.

Zip1-S75 has been revealed to have a function in centromeric coupling and it has been proposed that coupling is there to allow the recognition for homologous pairing (Falk et al., 2010). In this study it has been revealed that another Zip1 site (T114) is partially involved in centromere coupling. Zip1-T114 phosphorylation is not absolutely defective in coupling but indeed without Zip1-T114 some sister chromatids cannot be paired. The mechanism of how this

happens remains elusive. A mass spectrometry study by Dr. Alice Copsey has shown that Zip1-T114 is a consensus site for CK2 or DDK phosphorylation. These two kinases are the future work to follow. However, there are some complications in testing these two kinases. CK2 is constitutively active throughout meiosis and its involvement is very broad. It is very hard to test this kinase in relation to coupling because of the changing of CK2 would affect other pathways. Dr. Copsey has done a CK2-pull down kinase assay and shown that Zip1 is phosphorylated by CK2 *in vivo*. However, whether T114 is partially phosphorylated remains unknown. It is known that S75 is a direct target of Mec1 and requires phosphorylation in order to de-couple (Falk *et al.*, 2010). Hence it would be intriguing to reveal the purpose of T114 in the future.

Mutation of all seven sites identified leads to total disruption of centromere coupling, similar to *zip1Δ*. This is very interesting and probably suggests that phosphorylation of these seven sites in Zip1 influences centromere coupling, action of the pathway remains unclear. Questions such as whether CK2 or DDK is required to phosphorylate Zip1 in order for centromere coupling to proceed, or whether centromere coupling is independent of the Mec1-Zip1-S75 phosphorylation pathway remains unsolved.

Another intriguing phenotype found is the partial SC disassembly in the *zip1-S137A* mutant. This mutant behaves similarly to the *zip1-S144A* mutant (Chapter 4) in terms of SC assembly, but it also has shown a partial delay in SC disassembly. This is very interesting, probably indicating that maybe blocking the phosphorylation on S137 leads to instability of the SC, and hence PCs are formed, as well as some defects in disassembly of the SC. Yet again, what kinases are phosphorylating this site remains to be determined. It is worth

noting that, S137 is the only site that has shown consensus for CK2 only (Fig 3.1). S144 has been shown to be the consensus site for either CK2 or DDK, although the degree of delayed SC disassembly varies between *zip1-S137A* and *zip1-S144A*, both S137 and S144 have the potential to be CK2 consensus sites, which may indicate that CK2 is another kinase involved in SC disassembly. These questions remain to be answered in the future.

With the identification of all these Zip1 phospho-sites and different aspects of their function in meiosis, this indicates that Zip1 is a highly dynamic phosphor protein. It is highly regulated by different kinases to ensure correct phosphorylation to occur. It is intriguing to further investigate the precise mechanism of these sites in meiosis.

Chapter 4. Cdc5-dependent phosphorylation of Zip1-S144 is important for SC disassembly

4.1 Introduction

Disassembly of the tripartite SC marks a crucial step in meiotic prophase I exits. Entry into meiotic I division requires de-synapsis of the SC. This event occurs at the diplotene stage, where decondensation of DNA and removal of central elements of Zip1 along chromosome arms occurs, but Zip1 remains at the centromere. As a result, homologous chromosomes individualize only connected at the site of crossover, which is the physical manifestation of chiasmata. Following exit from pachytene, disassembly of the SC is coordinated with spindle pole body separation, and resolution of dHJ into crossovers or non-crossovers (Allers and Lichten, 2001; Newnham et al., 2010; Xu et al., 1995).

How are these processes coupled and regulated to ensure the accurate exit of pachytene? It has been found that *S. cerevisiae* Plk Cdc5 is the master regulator in pachytene exit. It ensures accurate recombination events; cohesion removal, sister kinetochore mono-orientation; as well as SC disassembly (Attner et al., 2013; Clyne et al., 2003; Lee and Amon, 2003; Sourirajan and Lichten, 2008). Budding yeast Plk (Cdc5) is similar to all other Plks, as it contains an amino-terminal kinase domain as well as a carboxy-terminal Polo box domain (PBD) that is similar to other Plks, which bind to the phosphorylated motifs in target proteins (Archambault and Glover, 2009).

Cdc5 also regulates Mus81-Mms4^{Eme1} endonuclease activity (Matos et al., 2011), which is one of the pathways that resolves dHJ (Sourirajan and Lichten,

2008). Normal chromosome metabolism requires the temporal regulation of Mus81-Mms4^{Eme1} by Cdc5, as phosphomimetic of Mus81-Mms4^{Eme1} in mitotic S-phase causes genome instability (Szakal and Branzei, 2013). Multiple mechanisms suppress Plk activity during prophase I arrest to prevent genomic instability in meiosis (Archambault et al., 2007; Chu and Herskowitz, 1998; Gilliland et al., 2009; Von Stetina et al., 2008; Xiang et al., 2007). In budding yeast, Cdc5 expression is regulated by Ndt80. Induction of CDC5 (*CDC5-IN*) in *ndt80Δ* cells, which arrests at pachytene, results in dHJ resolution occurring, and subsequently results in crossover formation, as well as disassembly of SC and formation of metaphase spindles (Hollingsworth, 2008; Sourirajan and Lichten, 2008). However, Zip1 protein is not degraded, indicating removal of Zip1 from the SC (Hollingsworth, 2008; Sourirajan and Lichten, 2008).

Cdc5 might not be the only kinase required for SC disassembly in wild-type meiosis. A recent study has revealed that Aurora B kinase (Ipl1) is the main regulator of SC disassembly. Following the exit of pachytene, SC remain assembled in the *ipl1Δ* mutants. Furthermore, inducing Cdc5 to cells at pachytene arrest in *ipl1Δ* mutants also leads to linear form of SC. This suggests that Ipl1 disassembly is Cdc5 dependent (Jordan et al., 2009). The mechanism of SC disassembly by Ipl1 is unclear. Mutation of several Aurora B consensus phosphorylation sites in Zip1 did not influence SC disassembly (Jordan et al., 2009), which might suggest that Ipl1 is phosphorylating somewhere else.

However, it is still unclear whether Cdc5 controls SC disassembly and whether SC disassembly is a prerequisite for crossover formation. More importantly, it is still unknown whether these processes independently regulated by Cdc5. To address these unanswered questions, a proteome-wide screen for targets that

is dependent on Cdc5 was carried out by a member of the Hoffmann Lab. This screen identified many candidates such as known and new potential targets are the ZMM network; cohesin; the FEAR network (Cdc14 early anaphase release), which ensures transition from metaphase to anaphase in both mitotic and meiotic cells. Components of the spindle pole body (SPB), the microtubule organizing centre in yeast, as well as several transcription factors. Several sites were identified in the transverse filament protein Zip1. One of the sites identified, Serine 144, is consensus for Cdc5. Hence characterization of this site was carried out to understand the role of Zip1 in SC disassembly and crossover formation by Cdc5.

4.2 Results

4.2.1 Zip1-S144 identified through a Cdc5 proteomic screen

Dr. Alice Copsey (Hoffmann Lab, unpublished) carried out a phosphoproteomic wide screen for targets, whose phosphorylation is dependent upon Cdc5 (Fig4.1). In this method, *CDC5* was placed under the regulation of the P_{CLB2} promoter that can only be repressed during meiosis (P_{CLB2} -3HA-*CDC5*, referred to as *cdc5*) (Sourirajan and Lichten, 2008). The *NDT80* promoter is replaced with the $P_{GAL1/10}$, which only expresses when Gal4 binds to an estrogens receptor. Induction of *NDT80* leads to synchronous release of arrested cells in pachynema in the absence or presence of Cdc5 (Sourirajan and Lichten, 2008). After pachytene release, the wild-type progressed into metaphase I at around 60-75 minutes (Fig. 4.1A). In contrast, cells depleted for *CDC5* showed delayed SC disassembly as well as spindle formation. Meiotic progression is also delayed and arrests at anaphase I, similar to previous findings (Jordan et al., 2009; Sourirajan and Lichten, 2008).

Proteins from both wild-type cells and *cdc5Δ* at pachytene arrest (T=0) and one hour after release (T=1) were extracted and digested with trypsin. Phosphopeptides were identified via either isotope labeling or label-free methods for relative quantification of protein levels (data not shown). Wild-type cells were labelled with formaldehyde as the light epitope, *cdc5Δ* was labelled with deuterated formaldehyde as the heavy epitope during stable isotope dimethyl labelling of peptides. Afterward, peptide samples were mixed and analyzed via mass spectrometry to phosphopeptides (log2 ratio of *cdc5Δ*: WT) at both time points.

Several phospho-peptides were identified for Zip1 (Fig. 4.1B), some had also been identified from immunoprecipitation of the Zip1 protein previously (Chapter 3). Only one site among these identified peptides in Zip1 was decreased in the Cdc5-depleted mutant (Fig. 4.1C). Zip1-S144 showed a ratio of 0.8 at pachytene arrest (T=0) and decreased to 0.2 one hour after release from pachynema (T=1) (Fig. 4.1C T=0). This reduction in ratio of phosphorylated S144 specifically after pachytene release suggests that Zip1-S144 is a putative phosphorylation target of Cdc5.

4.2.2 Non-phosphorylatable *zip1-S144A* is defective in SC disassembly

4.2.2.1 SC assembly in *zip1-S144A* mutant

To assess the role of Zip1-S144 phosphorylation during meiosis, S144 is mutated to alanine (*zip1-S144A*), which abolishes the potential phosphorylation of this residue. Full meiotic time course is performed to look at both SC assembly (Fig. 4.2) and SC disassembly (Fig. 4.3). Since Zip1-S144 is a putative consensus site for Cdc5, this hypothesize that *zip1-S144A* might be defective in SC disassembly but not in SC assembly.

Firstly to begin with SC assembly, the *zip1-S144A* mutant was sampled from a meiotic time course every hour from 4 hours to 8 hours; this is the period when SC synapsis initiates and elongates into the full tripartite structure. Meiotic chromosomes were surface spread and immune-stained with α -Zip1 to follow SC assembly and α -tubulin to assess meiotic stage. Chromatin was stained with DAPI (Fig. 4.2).

In wild-type meiosis, linear Zip1 (pachytene) is shown between 4 hours and 7 hours. Most linear nuclei observed at 6 hours indicate the stage of pachytene. Linear Zip1 eventually disappears in the wild-type (after 7 hours), and this is an indication of pachytene exit. Compared to the *zip1-S144A* mutant, the appearance of linear Zip1 is still observed from 4 hours onward (Fig. 4.2D). This suggests that SC can synapse normally in the *zip1-S144A* mutant (Fig. 4.2B). There is no delay in SC formation in the *zip1-S144A* mutant, because both strains start forming linear SC in a similar time (4T) (Fig. 4.2C&D). Taken together, it can be concluded that synapsis can occur with normal timing to form SC. However, the *zip1-S144A* mutant still shows some proportions of SC assembly at 8 hours, whereas wild type cells had almost no dotted or dot linear nuclei at 8 hours. This longer period of assembly might propose a defect in disassembly of the *zip1-S144A* mutant.

Although SC synapsis assembles in Zip1-S144, the appearance of PCs found in all nuclei cannot be ignored (Fig. 4.2F). These PCs in the *zip1-S144A* mutant are even appearing during initiation of the SC (e.g, PCs observed at early hours: 3 hours). In many organisms, aggregates of SC tend to be observed in post-pachytene nuclei [reviewed by (Zickler and Kleckner, 1999)]. In SK1 wild-type, 20 to 30 per cent of PC are observed (Fig. 4.2E), and this appearance of PCs only occurs more at the exit of pachytene, consistent with previous findings (see review Zickler and Kleckner 1999). In budding yeast, PCs also appear in many mutants that are defective in SC, such as SIC proteins *zip1Δ*, *zip2Δ*, *zip3Δ*, *zip4Δ*, *spo16Δ*. Nevertheless, the biological relevance of PCs still remains unclear. Taking this into consideration, it can be proposed that the

formation of SC in Zip1-S144 is not affected. Yet, changing its phosphorylation status may influence the conformation of Zip1, resulting in elevated proportion of Zip1 in the nucleus, which cannot get polymerized along the chromosomes. Subsequently Zip1 forms aggregates within the nucleus, and are not associated with the chromatin.

4.2.2.2 SC disassembly in the zip1-S144A mutant

In wild-type meiosis, SC disassembly has two distinct phases. First, central element Zip1 dissociates during diplotene, as SPB separate (two foci of tubulin) (Fig. 4.3A). SC disassembly is normally completed at the onset of metaphase I, where the meiosis I spindle has been formed (elongated tubulin) (Fig. 4.3A). In the *zip1-S144A* mutant, 40% of nuclei had linear Zip1 with PC when tubulin separates, another 40% had dot linear with PC at diplotene (Fig. 4.3B). Only a small fraction of cells (20%) showed dotty Zip1 that were similar to the wild-type (Fig. 4.3G). Upon entry into metaphase I, tubulin elongates and a short stretch of tubulin (2-4 μ m) is observed in the wild-type. Previous studies have shown that Zip1 around arm regions are removed, but the centromere region remains bound with Zip1 (Newnham et al., 2010). However, due to the SK1 strain background, localization of Zip1 at the centromere was not observed on spreads shown in Figure 4.3. Wild-type cells show 100% nuclei with no Zip1 in metaphase I cells (Fig. 4.2E). In contrast, the majority of nuclei in the *zip1-S144A* mutant (80%) were observed with dotty Zip1 and higher PC signals (Fig. 4.2G&H). The observed disassembly phenomenon in the *zip1-S144A* mutant is similar to the *cdc5-mn* cells, where cells appear to have dotty Zip1 when tubulin elongates (Jordan et al., 2009). However, this is not as severe as in the *ilp1-mn*, where 80% of cells had full SC during metaphase I (Jordan et al., 2009). This

lower percentage in the *zip1-S144A* mutant probably implies that Zip1-S144 is required for SC disassembly.

To ensure this apparent failure to disassemble was not due to a general cell cycle delay, DAPI staining of nuclei were scored (Fig. 4.2G-H). Both the wild-type and *zip1-S144A* started to divide from 5 hours and completed their meiosis II division by 12 hours. The protein level in Figure 4.4 is also consistent with the nuclear division data, where γ -H2A appeared at the same time. Therefore, in all likelihood this delay was not a gross meiotic progression, but a defect in SC disassembly. However, SC does eventually disassemble in the *zip1-S144A* mutant, suggesting that Zip1-S144 might not be the only site that is required for SC disassembly. To further clarify the phenotype, another *zip1-S144A* colony was selected and analyzed (Appendix 7). The same kinetics in SC disassembly was observed in both colonies. Therefore above data further proving the role of S144 in disassembly.

4.2.3 High levels of Zip1 protein detected in *zip1-S144A*

Because all nuclei in the *zip1-S144A* mutant contained significant PCs, and Zip1 is a phosphoprotein, this probably suggests that PC phenotype is due to higher level of Zip1 that cannot get degraded during synapsis. To check the level of Zip1, a Western blot was performed. Zip1 generally starts to appear when initiation of DSB starts and builds up as cells progress towards pachytene. Zip1 then begins to degrade as SC disassembles and eventually disappears when cells enter metaphase I. Wild-type Zip1 begin to appear at 3 hours compared to *zip1-S144A* at 2 hours, this is probably due to asynchronous time course. Zip1 level reach its maximum at 5 hours (Fig. 4.4B), similar to cytological observations (Fig. 4.2C). After Zip1 reaches its maximum, it begins

to degrade gradually indicating pachytene exit and meiotic division. In comparison, the *zip1-S144A* mutant has shown very high amounts of Zip1 between 4-6 hours (Fig. 4.4B). A high protein level supports the cytological data that all nuclei in the *zip1-S144A* mutant appeared with PCs. Therefore this implies that the disruption of Zip1 phosphorylation results in this defects. Errors in elongation ultimately lead to Zip1 to build up as aggregates. Furthermore, Zip1 level stayed high until 12 hours in the *zip1-S144A* mutant, whereas in the wild-type this had already disappeared, which further backs up the SC disassembly defect.

4.2.4 Assessing the phosphomimetic version of Zip1-S144 (*zip1-S144E*) in SC assembly and disassembly

The previous findings indicate that S144 phosphorylation is required to trigger SC disassembly. To further investigate this, a phosphomimetic version of Zip1-S144 (*zip1-S144E*) was created. The S144 was substituted for a glutamic acid (E), as the side group of the glutamic acid negatively charged like a phosphate group, which 'mimics' phosphorylation. If phosphorylation on S144 is truly required to proceed to SC disassembly, then mimicking this phosphorylation could result in normal SC disassembly in *cdc5-mn* mutants. Moreover, no elevated Zip1 would be observed and this probably leads to the absence of PCs. It is worth noting that sometimes when making a phosphomimetic version in these point mutants, the amino acid before S144 is also mutated to aspartic acid (D) to mimic the phosphorylation as similarly as possible. Sometimes one glutamic acid might not be negative enough to trigger any defects. Interestingly, the amino acid before S144 is aspartic acid itself. Thus, it would be interesting to examine the *zip1-S144E* phenotype.

The wild-type and the *zip1-S144E* strains were harvested and put under sporulation media; appropriate time points were taken for meiotic nuclei spreads as well as nuclear division analysis (Fig. 4.5). As expected, PCs could not be detected in the *zip1-S144E* mutant and full linear SC was observed (Fig. 4.5B). Due to the asynchronous time course (Fig. 4.5G&H), the wild-type had a delay in forming SC and was still under division around 10 hours (Fig. 4.5C). During the period of tubulin elongation, Zip1 normally become absent in the wild-type cells (Fig. 4.3). This disappearance of Zip1 indicates SC disassembly. In the *zip1-S144E* mutant, Zip1 was not observed when tubulin elongates. This could suggest SC disassembly is normal in the phosphomimetic mutant. However, due to higher proportion of pachytene nuclei in the *zip1-S144E* mutant at T6.5 compared to the wild-type (Fig. 4.5D), it might indicate a delay in SC disassembly. Further experiments are required to repeat this with later time points in order to verify SC disassembly seen in the *zip1-S144E* mutant.

4.2.5 The *zip1-S144E* mutant does not improve SC disassembly in the absence of Cdc5

Preliminary data showed that mimicking phosphorylation S144 might results in the restoring of SC disassembly. In order to further confirm this, a strain that is depleted for Cdc5 is used to study (i.e. *zip1-S144E* bypasses the Cdc5 phosphorylation pathway leading to disassembly). To test this, the meiotic specific *cdc5-meiotic null* (*cdc5-mn*) allele was made. Only minor portions of nuclei (10%) in *cdc5-mn* proceeds into metaphase I, thus making assessing disassembly difficult. Hence, using the *NDT80*-inducible system where the promoter of *NDT80* replaces the $P_{GAL1/10}$. Upon β -estradiol activation, pachytene cumulated cells can be artificially exited into metaphase where they arrest due to lack of Cdc5 (*cdc5-mn*, *NDT80*-inducible; hereafter referred as

cdc5-mn). *NDT80* was introduced to cells at five and half hours, and samples were assessed every half hour after pachytene with published data (Sourirajan and Lichten, 2008), the *cdc5-mn ZIP1* cells did not disassemble in the absence of Cdc5 (Fig. 4.6A; Fig.4.7A). The *zip1-S144A* mutant was not observed to have any disassembly in the absence of Cdc5 (Fig. 4.6B & Fig. 4.7B), similar to the wild-type (*cdc5mn, ZIP1⁺*).

An improvement of disassembly in the *zip1-S144E* mutant can be hypothesized as if Zip1-S144 was the only site required for SC disassembly by Cdc5. Phosphomimetic version would acquire a similar activity as phosphorylated S144, resulting in disassembling of the SC in the absence of Cdc5. However, the *zip1-S144E* mutant appears to be very similar to the *cdc5-mn ZIP1* during both diplotene (Fig. 4.6C) and metaphase I (Fig. 4.7C). At diplotene, similar portions of linear Zip1 were observed in comparison to both the *cdc5-mn ZIP1⁺* and *cdc5-mn zip1-S144A* (Fig. 4.6D). At metaphase I a similar Zip1 staining pattern is seen in the *zip1-S144E* mutant observed in comparison to the other two strains (Fig. 4.7D). This result shows that the *zip1-S144E* mutant does not rescue the disassembly defect in the absence of Cdc5, possibly indicating that Zip1-S144 is not the only site required in the Cdc5 disassembly pathway. There might be other sites required by Cdc5 to cause disassembly.

4.2.6 The *zip1-S144A* mutant did not show blockage of disassembly when conditionally induced by Cdc5

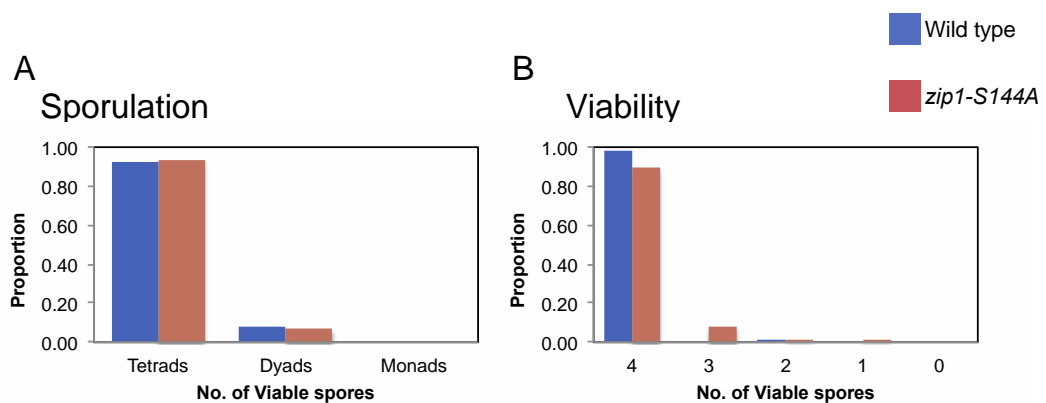
Although the *zip1-S144E* mutant did not bypass disassembly defects in the absence of Cdc5, whether Cdc5 phosphorylates Zip1-S144 directly to cause SC disassembly remains unknown. To address this issue, Cdc5 was conditionally induced in pachytene arrest cells. In wild-type meiosis, conditionally induced

Cdc5 results in SC disassembly, whereas uninduced cells lead to no disassembly. It can be hypothesized that mutation of S144 to its non-phosphorylatable state would give rise to no disassembly because Cdc5 cannot phosphorylate this site, thus indicating the specification of disassembly by S144. Cells were induced at 6 hours for both the wild-type (*ZIP1 ndt80Δ*) and *zip1-S144A ndt80Δ*. Samples were collected for spread every half hour after induction (Fig. 4.8H). Linear Zip1 was observed in the pachytene arrested wild-type that lack *ndt80Δ* and *cdc5-mn* (Fig. 4.8I). Upon artificial activation of Cdc5, SC disassembly occurs in the wild-type. The consequence of this is the disappearance of Zip1 (Fig. 4.8J). Turning on *CDC5* in the *zip1-S144A* mutant still leads to disassembled SC, similar in a manner to the wild-type (Fig. 4.8K&L). Taking both *zip1-S144A* and *zip1-S144E* mutants results together, it is most likely that other sites are probably involved in the Cdc5-dependent SC disassembly.

4.2.7 Non-phosphorylatable *zip1-S144A* mutant has normal sporulation efficiency and spore viability.

To further assess the role of Zip1-S144 in meiosis, sporulation and spore viability were checked. In a *zip1Δ*-SK1 strain, sporulation is similar to the wild-type and the viability is reduced two- to three-fold (57%) (Sym and Roeder, 1994). This is due to reduction in crossing over and a loss of the Zip1-mediated segregation mechanism (Newnham et al., 2013). To assess whether the *zip1-S144A* mutant was affected in sporulation and spore viability, samples from sporulating cultures were taken after 24 hours to count sporulation (Fig. 4.9A). In the wild-type 90% of cells formed tetrads, 10% dyads and no monads were observed. As expected, the *zip1Δ* showed half reduction of the wild-type (50%).

The sporulation frequency in the *zip1-S144A* mutant was similar to the wild-type, with 92% forming tetrads and 8% dyads (Fig. 4.9C). These observations suggest that the mutation and potential phosphorylation of Zip1-S144 does not affect meiotic progression and sporulation in budding yeast meiosis. In conclusion, these observations of the *Zip1-S144A* protein support normal progression and sporulation through meiosis. To understand whether gamete



viability was reduced in the *zip1-S144A*, 100 tetrads were dissected, and individual spores were allowed to germinate and form colonies on rich medium. The wild-type strain displayed 98% overall viable spores (classes 4:0 98%; classes 3:0 2%), the *zip1 Δ* mutant showed expected viable spores (31%). A slight reduction of viable spores (90% overall) in the *zip1-S144A* mutant was observed compared to the wild-type (classes 4:0 90%; 3:0 8%; 1:0 2%). This reduction might indicate a slight defect in spore viability. Nevertheless, a G-test for homogeneity was used to calculate the significant difference between the wild type and the *zip1-S144A* mutant and the results has shown that the *zip1-S144A* mutant is not significantly different than the wild-type ($P > 0.05$). Therefore suggests normal spore viability in the *zip1-S144A* mutant. Collectively, neither completion of meiosis nor viability was affected in the *zip1-*

S144A mutant. Previously, in-frame deletion of amino acids (21-163) at the N-terminus of Zip1 showed no sporulation or spore viability defects (Tung and Roeder, 1998). Zip1-S144 lies within the N globular domain thus it is not surprising that no sporulation or spore viability defects were observed.

4.2.8 Zip1-S144 does not affect crossover formation

Cdc5 promotes resolution of dHJ and subsequently leads to crossover formation. Whether dHJ resolution occurs before SC disassembly, and whether these two processes are independent of each other is unclear. Although Zip1-S144 has a role in SC disassembly and mutation to alanine does not affect spore viability, it is still unknown whether changing of phosphorylation state would cause any reduction in crossovers. To test crossovers, a *zip1-S144A* plasmid was incorporated into Hunter strains (see methods) for recombination analysis using the Southern blot (Hunter and Kleckner, 2001) (Fig. 4.10A).

Before analysing crossover formation in a *zip1-S144A* mutant, wild-type strains were checked by the Southern blot (Fig. 4.10B). This testing is to make sure the exogenous wild-type behave the same as endogenous. The Hunter strain was particularly modified to contain the *HIS4LEU2* locus and this is a hotspot for DSB. A DSB site was inserted between *NFST* and *RRP7* sites. To ensure every single cell that enters meiosis has a single DSB at this site (Hunter and Kleckner, 2001). Meiotic recombination is monitored over time in cultures undergoing synchronous meiosis. Samples were collected at correct time points, and DNA extracted (see method). After extraction, DNA was then digested using *XhoI* restriction enzyme and species of interest were resolved by gel electrophoresis. Southern hybridization was used to detect DNA of interest, using a probe that binds to the right of DSB site I (Fig. 4.10A). Cells lacking Zip1

proceed with regular DSB but have reduced crossovers due to defects forming SEIs and subsequent dHJs (Borner et al., 2004). Early recombination products such as JM and dHJ are not shown on this gel, as the interest is in crossover formation. To check the *ZIP1-TRP1* wild-type system, normal wild-type samples (Hunter_WT) extracted by member of Hoffmann Lab (Jacob Kirk). The *ZIP1-TRP1* time course was done at the same time as in Figure 4.11. After treatment with radiation, both the wild types were detected on the gel. They all appeared to have a similar trend (Fig. 4.10B). DSB accumulated most between 4 hours and 5 hours, and exited from 6 hours. The *ZIP1-TRP1* wild type had accumulated less DSB compared to Hunter_WT (Fig. 4.10C). At 4 hours, *ZIP1-TRP1* had 4% and 5% DSB respectively. In contrast, the Hunter_WT had 5% and 8% respectively. Crossover products in the *ZIP1-TRP1* were at very similar levels to Hunter-WT (Fig. 4.10D). These small variations might be due to strain differences or time course changes, yet the overall kinetics are the same. Therefore, experiments can be done in the *ZIP1-TRP1* Hunter strain background.

After verification of *ZIP1-TRP1* in Hunter background, the *zip1-S144A* mutant was analyzed via a Southern blot (Fig. 4.11). As previous findings have shown, *zip1* Δ results in normal progression of DSBs regardless of higher or lower temperature, but the degree of forming COs varies. At a higher temperature COs only form ~15% of the wild-type. There is an enormous delay in forming COs at a lower temperature (COs appear to increase after 12 hours, whereas the wild-type begins to form COs after 8 hours) (Borner et al., 2004).

Where does *zip1-S144A* lie on the scale between the wild-type and *zip1Δ*? To find out the answer, the wild-type; *zip1Δ*; *zip1-S144A* were put under sporulation and hourly samples were taken up to 13 hours (Fig. 4.11A). All experiments were performed at 30°C. Quantification between each candidate was analyzed via Aiyda. However, one of the samples in *zip1-S144A* (T=7) revealed a very high concentration of DNA, probably due to experiment error during DNA dilution. This error might result in bias quantification for the *zip1-S144A* mutant. Nevertheless, this gel still provides a rough estimate between these three strains. In the wild-type, COs start to accumulate from 6 hours, whereas in the *zip1Δ* mutants, COs begin to gather from 11 hours (Fig. 4.11C). This delay is synchronous with meiotic progression where *zip1Δ* starts to divide from 11 hours (data not shown). COs in the *zip1Δ* mutant compared to the wild-type are similar to previous findings. The level of DSBs formed in the *zip1Δ* mutant is similar to the wild-type, although the fact that DSBs were delayed in the *zip1Δ* (Fig. 4.11B). This delay in DSBs might be due to experiment procedure in knocking out *zip1Δ* in Hunter strains (*zip1::HYG*). In contrast to *zip1-S144A*, the timing of DSBs formation was similar to the wild-type (Fig. 4.11B). Probably suggests that the *ZIP1-TRP1* strain is usable in this system. At this stage, no conclusion can be made for the phenotype seen for *zip1Δ*, this requires further examination. Regardless of the correct timing in forming DSBs in the *zip1-S144A* mutant, the amount of DSBs in the *zip1-S144A* was reduced about twofold (Fig. 4.11B). Crossovers seem to have accumulated at the same time as to the wild-type, and no reduction was observed (Fig. 4.11C). However, due to a high concentration at 7 hours in the *zip1-S144A* mutant, this result

might not reflect reality. To make an accurate conclusion, samples for the wild-type and the *zip1-S144A* were repeated are shown in Figure 4.12.

After repeating the samples, the *zip1-S144A* mutant appeared to have wild-type level of DSBs (Fig 4.12D). However, the timing of entering DSB formation was delayed for about two hours but exited at the same time as the wild-type. Despite this delay, the nuclear division has shown a synchronous time course for both strains (Fig. 4.12B, C). Crossover formation is almost wild-type-like and has shown no sign of delaying (Fig. 4.12E). Overall, the above findings imply that phosphorylation of S144 is dispensable for crossover formation, suggesting ZMM-dependent crossover maturation may be independent of SC disassembly.

4.3 Discussion

The work here outlines the analysis of a Zip1-point mutant on SC disassembly. Zip1-S144 was initially identified via proteomic screen for Cdc5 target sites and showed a higher level of epitope change compared to other sites. This suggests that S144 could be a direct target of Cdc5. Cdc5 has many roles in mitosis and marks the central regulator of Meiosis I. In the absence of Cdc5, SC disassembly is delayed but this delay is not as severe as in the *lpl1-mn* mutant, suggesting that other kinases are also involved in SC disassembly. Mutating the site (Zip1-S144) identified from the screen to alanine, SC disassembly defects were found. But no SC disassembly defects were observed with the other zip-phosphor mutants identified (Chapter 3). This indicates that Zip1-S144 is specific to SC disassembly and might have a direct relationship with Cdc5. To prove this, a phosphomimetic version *zip1-S144E* was examined in the absence of Cdc5. However, this mutant did not show rescue of SC disassembly defects. Rather it was shown to be similar to the wild-type. Therefore, suggesting that either, Cdc5 does not directly phosphorylate S144 or Cdc5 phosphorylates more than one site to cause SC disassembly. The non-phosphorylatable version, *zip1-S144A* was conditionally induced with Cdc5 in pachytene-arrested cells, resulting in SC disassembly similar to the wild-type. This again indicates that this site is not the only site Cdc5 phosphorylates to cause disassembly.

Disassembly observed in the *zip1-S144A* mutant was only shown at an early stage of metaphase I, where tubulin shown under fluorescence microscopy as a short stretch (~5 μ M). When tubulin elongated, an indication of late metaphase or anaphase, Zip1 disappeared in the *zip1-S144A* mutant. This implies that disassembly does eventually happen. This disappearance is probably

consistent with the normal sporulation and spore viabilities. In-frame deletions by Tung and colleagues have shown that the N-terminal globular domain is not required for SC assembly, sporulation and spore viability. Therefore, it is not surprising to see normal viability and sporulation in a *zip1-S144A* mutant. Zip1 is such an abundant protein and probably changing one amino acid might only show small defects. But, on the whole, its effects are too small to trigger the entire disassembly. Moreover, cleavage of Rec8 in pachytene arrest cells leads to disassembly of Zip1 and results in SC disassembly (Appendices 5&6).

What causes this delay of disassembly in a *zip1-S144A* mutant? Perhaps it is because removing the phosphorylation on S144 results in hypophosphorylation of Zip1 and this leads to blockage of Zip1 loading on to chromatin, thus much brighter and bigger PCs were observed in all nuclei (Fig 4.3). Also the Western blot showed that Zip1 levels remained higher compared to the wild-type (Fig 4.4). This will ultimately lead cells to slow down when they are required to disassemble because Zip1 is in its hypophosphorylated state. Thus a delay in SC disassembly is observed. However, Zip1 may slowly turn over and eventually disassemble without affecting meiotic progression. When S144 phosphorylation was mimicked in the *zip1-S144E* mutant, all nuclei behaved like the wild-type (full linear SC, no PCs). This means that no elevated Zip1 was required, due to normal phosphorylation. As a result, regular SC disassembly happens. But whether Cdc5 phosphorylates this directly still remains unclear. It is hoped that identification of more targets from the Cdc5 screen will provide more hits to be characterized and maybe in the near future a site could be found that is involved in SC disassembly and acts together with Zip1-S144 to trigger Cdc5-dependent disassembly.

Chapter 5. Centromere dynamics of Non Exchange Chromosomes in meiosis

5.1 Introduction

After the discovery of the chiasma by Janssens's (reviewed in (Koszul et al., 2012)), it was thought that chiasma-mediated segregation was the major mechanism of segregating chromosomes in meiosis. However, subsequent studies revealed that many organisms are capable of segregating homologous chromosomes correctly in the absence of crossovers. The best-characterized mechanism that mediates non-exchange chromosome (NEC) segregation is in *Drosophila* females. In this organism, the female uses a recombination-dependent system for the meiotic segregation in three of four of their chromosomes and a recombination independent system for their shortest fourth chromosomes (Grell, 1962; Sturtevant, 1951).

Yeast has also been identified as being capable of non-exchange chromosome (NEC) segregation (Dawson et al., 1986). Testing segregation fidelity between two non-homologous artificial chromosomes, this study found that in 90% of meioses, the two non-homologous chromosomes were segregated away from each other despite a lack of crossover. Using a minichromosome further supported this, and also it was concluded that this high fidelity segregation depended on neither recombination nor sequence homology (Dawson et al., 1986).

Later on, other studies appeared to show similar results to Dawson, where different systems of yeast NEC were examined. For example, the use of two monosomic chromosomes (Loidl et al., 1994); the minichromosomes (Ross et al., 1996) and the use of homeologous chromosomes (Maxfield Boumil et al.,

2003). Homeologs are pairs of chromosomes that are derived from two different types of yeast species. Although they share a high level of sequence homology (roughly 70-80%), the sequence heterology prevents crossovers, due to the activity of mismatch repair proteins, which cause unwinding or rejection of heteroduplex DNA containing mismatches. This process is termed anti-recombination (Chambers et al., 1996). All of these studies found that segregation was far better than random segregation (50%). Taken all together, this led the belief that a non-exchange system (NEC) in yeast does exist and the existence of this might be a backup system when crossover dependent pathway failed.

The mediation of NECs was shown to be dependent on centromeres (Kemp et al., 2004). This was shown by tagging particular chromosomal locations with lacO repeats where LacI-GFP binds to. The NEC were observed to be paired prior to their segregation when tagging fluorescence near the centromeres rather than the arm region (Kemp et al., 2004). How are centromeres being paired in NECs? Recently published studies have shown that Zip1 is the key protein in holding NEC centromeres together (Gladstone et al., 2009; Newnham et al., 2010). Wild-type NEC homeologs showed a frequency of 56% at their centromeres during pachytene (Newnham et al., 2010). Knocking out *zip1Δ* in NEC results in only 14% (or 20% in Gladstone et al.) paired and elevated missegregation from 11% to 23% (Gladstone et al., 2009; Newnham et al., 2010). Therefore, it has been postulated that Zip1 promotes tethering of NECs at their centromeres from prophase I until segregation at anaphase I (Gladstone et al., 2009; Newnham et al., 2010).

However, what is fascinating in these studies is the observation of minor

tethering in *zip1Δ* (14% in Newnham et al. and 20% in Gladstone et al.). It was surprising that such low pairing frequency gave rise to higher segregation efficiency (25%) in *zip1*. The above studies used fixed meiotic spreads for characterising non-exchange chromosome segregation; it might not reflect the whole process in NECs, as only a certain time frame was captured on fixed cells. In wild-type NECs, 50% showed paired and 50% showed unpaired centromeres. How do these 50% unpaired centromeres segregate with high fidelity (Fig. 5.1)? To understand NEC segregation more clearly, live cell imaging has been used. With the establishment of live cell techniques, dynamics of centromere pairing can be assessed throughout prophase I to anaphase I.

This chapter focus on the interesting dynamics of NECs in yeast segregation (Fig. 5.1). Non-exchange chromosomes tend to behave through a series of dynamic association and dissociation until anaphase I. Some are paired just before anaphase I, and segregate away at the entry point of anaphase I. However, there are a minority of cells paired at the beginning of anaphase, and these bounce to opposite spindle poles 5 to 10 minutes later. These observed dynamics in NECs probably suggest multiple mechanisms that exist to ensure these unpaired NECs segregate with high fidelity. Centromere behaviours have also been studied in *zip1Δ* and *zip1-T114A* mutants as a comparison to the wild-type.

5.2 Results

5.2.1 Generation of a homeologous chromosome pair by using the *S. paradoxus* chromosome III

Homeologous chromosomes in previous studies were all studied in the S288c strain, which unfortunately do not sporulate as synchronously nor as efficiently as SK1. Therefore SK1 strain background has used for all the live cell imaging developed in this study. Synchrony is very important for time-lapse imaging of live cells in limiting photo toxicity

To generate a homeologous chromosome pair in SK1, a karyogamy defective mutant was used, a method that was used successfully previously (Chambers et al., 1996; Greig, 2007). This method takes advantage of the karyogamy mutant, *kar1-13*, which was found to be defective in nuclear fusion (Dutcher, 1981; Vallen et al., 1992). During natural mating, diploids are formed by a process that first involves cytoplasmic fusion and subsequently in nuclear fusion of the two haploid cells (Fig. 5.2 B). Nuclear fusion fails when only one parent contains the *kar1-13* mutation and leads to heterokaryons. A heterokaryon is referred to as a zygote containing two unfused parental nuclei (Spencer et al., 1994), where one chromosomal set is transferred into the daughter bud (cytoductant). This cytoductant contains parental genotypes but with a mixture cytoplasmic origin (Spencer et al., 1994). Sometimes, by chance one chromosome from one parent is transferred to the other parental nucleus, keeping the genotype of the recipient the same. This is referred as YACductant and occurs with a 0.1% frequency (Fig. 5.2 B). By using markers to tag the chromosome of interest followed by subsequent selection on appropriate media, desired karyotypes can be generated. *S. paradoxus* has been selected as this is the closest known relative to *S. cerevisiae*. These two species have co-

linear gene arrangements, but have 15% sequence divergence (Fig. 5.3A), which is sufficient to prevent meiotic recombination between their chromosomes (Greig and Leu, 2009). The majority of *S. paradoxus* chromosomes confer viability when replacing their *S. cerevisiae* counterpart. This method has also been used by Chambers group, where they studied the homeologous chromosome III containing one *S. cerevisiae* homolog and one *S. paradoxus* homolog in meiosis (Chambers et al., 1996).

The original idea in this study was to replace a range of different *S. paradoxus* chromosomes with its recipient SK1 chromosomes. Unfortunately after many attempts only chromosome III was successfully transferred (Fig. 5.3 B). As the data shows in Figure 5.3 A, both species contained the similar size of chromosome III, although *S. paradoxus* is slightly smaller than *S. cerevisiae* (316.62 Kb in *S.c* and 312.371 Kb in *S.p*) (Fig. 5.3B). After the recipient SK1 had successfully taken up the chromosome from the donor, a disomy of chromosome III (two bands) is seen on pulsed-field gel electrophoresis (PFGE) (Fig. 5.3B, IIItra). This disomy yeast was subsequently grown on 5'FOA to remove *S. cerevisiae* Chr.III that is tagged with *URA3*⁺, as FOA is toxic to cells that contain *URA3*⁺. A positive candidate was obtained shown in Figure 5.3B (IIIrep). This candidate showed similar bands to the control strain where *S. paradoxus* chromosome III is in S288c background (Fig. 5.3B IIIcon). However, due to the resolution on PFGE, this cannot accurately confirm that no other chromosome had transferred. Therefore, the best way to confirm this was by using PCR on all chromosome arms in both species (64 in total), as well as the whole genome sequencing. However, since there is 85% homology shared between *S. paradoxus* and *S. cerevisiae*, a lot of PCRs showed double binding

to both species. Other parallel approaches were used to confirm that only one chromosome was transferred to this candidate. First, a previous study showed transferred *S. paradoxus* chromosome III into Y55 background lowered spore viability from 95% to 67.7% (Chambers et al., 1996). To assess whether this was the case for the candidate generated in Figure 5.3, 100 tetrads were dissected from the candidate strain and the spore viability compared to that of a pure SK1. Whereas the pure SK1 had a spore viability of 91%, the candidate containing the homeologous *S. paradoxus* x *S. cerevisiae* Chr.III showed decreased viability of 74% (Fig. 5.3C). This dissection result preliminarily suggests that the candidate was correct. Moreover, if more additional chromosomes had been transferred, diploids would not have sporulated. However, normal sporulation was observed, suggesting only 16 chromosomes are in this genome.

The next verification was to check centromere pairing in this homeologous strain. Chromosome III in *S. paradoxus* was tagged very closely to *CEN3* at its *LEU2* locus (18 KB), and disjunction under a fluorescence microscope confirmed positive tagging on *CEN3* in *S. paradoxus* (Fig. 5.4A)(NDJ frequency was confirmed as 13%). This is similar to S288c homeologous chromosomes (11% in Newnham et al.), further confirming the accuracy of this homeologous chromosome. Using published homeologous wild-type strain as a control (Newnham et al., 2010), a pairing frequency of 48% was observed (Fig. 5.4I). This proportion is lower than published data (56%), and is probably due to different spreading techniques used by the two authors. Moreover, Newnham has categorized anything that is less than 0.7 μm as paired, whereas, in this

study, centromeres that showed a distance of less than 0.5 μm were counted as paired. Collectively, these observations suggest that the candidate strain (haploid) contains the *S. cerevisiae* karyotype with chromosome III replaced by that from *S. paradoxus*.

5.2.2 Dynamic association and dissociation of non-exchange centromeres throughout prophase I

Previous studies used fixed meiotic spreads showing only 50% of centromeres paired in wild-type homeologous chromosomes during pachytene, but 90% segregates with high fidelity (Gladstone et al., 2009; Newnham et al., 2010). With the result of 11% non-disjunction (NDJ) in wild-type cells, it suggests that the remaining 40% that unpaired can also segregate normally. To understand the centromere interactions, time lapse imaging is used to follow the exchange pair and non-exchange pair movement.

Centromeres of exchange chromosomes are paired in prophase I and metaphase I. It is separated on the onset of anaphase I. Before studying NECs centromere behaviour, exchange chromosomes are studied. They are probably less dynamic and more stable than NECs due to the presence of crossovers. Indeed, live cell tagging of both centromeres 3 in *S.cerevaise* shows a much simpler pattern (Fig. 5.5). Centromeres were paired from prophase I to metaphase I in all nuclei examined (Fig. 5.5D). Upon entry into anaphase I, centromeres were separated and segregated away from each other. An example of a particular cell is shown in Figure 5.5F, where blue represents *CEN3* and a 0 μm distance was observed from prophase I to metaphase I. *Cnm67* was also stable in prophase I and showed dynamic movement when two spindle pole bodies formed during metaphase I; perhaps some tension was

generated to get ready before anaphase I.

Do the NECs behave the same? To investigate, meiosis in diploid cells were harvested containing the homeologous chromosome pair, which are tagged with lacO/LacI-GFP as well as Cnm67 and Pds1 that allowed us to follow the spindle pole bodies (Cnm67) (Schaerer et al., 2001), and the behaviour of Securin (Pds1) (Matos et al., 2008). The spindle pole bodies separate at the onset of diplotene and reach a 2 μm distance at metaphase I (Fig. 5.6). Pds1 is degraded at onset of anaphase (Fig. 5.6). These two cellular markers can be used to stage meiotic events with high precision (Fig. 5.1A). Imaging conditions were optimized to limit photo toxicity (Fig. 5.4A was taken after live cell imaging), such that meiotic cells completed both divisions and sporulated (Copsey et al., 2013). Cells were imaged in the green and red channel every 5 minutes, using 30 z-sections, with 0.3 μm spacing. Cells that only went through to anaphase I were selected for analysis. A total of 32 cells were analysed. A 100% of examined nuclei were observed with dynamic movements of centromeres and SPBs. The associations between centromeres on average were about 5 minutes. This dynamic is observed all the way through until the beginning of metaphase I (Fig. 5.6A), completely different than the homologous chromosome (Fig. 5.5). Centromeres tend to be paired and unpaired in the wild-type throughout prophase to metaphase I in all cells analysed (Fig 5.6D). Interestingly, the spindle pole body (Cnm67) also tends to be very dynamic (Fig 5.6E), and it also shows a very similar patterns to centromere movements. This probably suggests some connections between spindle pole body and centromeres. Centromeres seem to dissociate and associate in 100% nuclei

examined from prophase despite the fate of their segregation (i.e. disjunction or non-disjunction). In conclusion, homeologous chromosome segregation is much more dynamic and they do not stay tethered all the time, unlike the homologous centromeres.

5.2.3 NECs associate transiently in metaphase I prior to their segregation

Dynamic centromere association and dissociation continue throughout metaphase I. In the 28 cells that showed correct segregation, 71% of cells showed tethering of the centromeres 10 minutes before anaphase I and dissociated 5 minutes before anaphase I (Fig. 5.6A). Upon degradation of Pds1, the two centromeres dissociated from each other within 5 minutes of the onset of anaphase I and segregated to opposite SPBs (Fig. 5.5D). These results suggest that NECs associate transiently prior to their segregation in anaphase I. In a minority of correct segregated cells (29%), the two centromeres of the NEC pair were not paired 10 minutes prior to anaphase I. The same dynamic observed in prophase I and metaphase I, but the centromeres just happen to be dissociated 10 minutes before and gradually moved further away from each other.

Moreover, in these 28 normal segregated cells, 10 out of 28 cells (35%) showed interesting features compared to the rest of cells (Fig. 5.6B). The centromeres in these cells tended to remain paired even after Pds1 degradation and associate at one spindle pole body. As anaphase I proceeds, Cnm67 moves further away, one might expect these cells segregate as non-disjunction. However, interestingly after 5 or 10 minutes entering into anaphase I, one

centromere suddenly 'bounced' back to the opposite pole and started to segregate normally (Fig. 5.6B). Overall, these patterns suggest dynamic non-exchange chromosome segregation. The meaning of constant dissociation/association remains unknown. This dynamic observed before anaphase I might suggest that the NEC give rise to altered spindle dynamics. However, NEC wild-type cells tended to behave the same with exchange chromosome during anaphase I where centromeres are gradually moved further apart from each other to opposite pole. In conclusion, different scenarios were observed between exchange chromosomes and NECs during prophase I and metaphase I. This probably indicates different mechanisms exist to ensure both crossover dependent chromosomes and non-crossover dependent chromosomes segregate accurately.

Although high efficiency of segregation is observed in NEC, four cells (13%) were observed with non-disjunction (Fig. 5.5B). These cells also showed dynamic movements in their centromeres from prophase to metaphase, indistinguishable from normally segregated cells (Fig. 5.6C). They tended to be paired before anaphase I entry and segregate to one spindle pole when anaphase I begin (Fig 5.6C). However, interestingly centromeres tended to dissociate and become attached to opposite spindle poles, in a manner similar to normal segregation. But after 5 minutes this centromere somehow had been pulled back from the opposite pole and remained with its partner centromere at one end (Fig 5.6C). It almost looked opposite to normal segregated cells in Figure 5.6B. This interesting behaviour might suggest some tensions in centromere pairing when there is a lack of crossovers. The reason they paired

and unpaired most of the time might be because centromeres paired in a very unstable manner in the absence of crossovers. Nevertheless, Zip1 is held in place with some tension to ensure centromeres are not segregating randomly.

5.2.4 Non-exchange chromosome segregation in *zip1-T114A*

Zip1-T114 phosphorylation is required during centromere coupling but it is not involved in SC formation, sporulation and spore viability (Chapter 3). It has also been shown that Zip1 is required for centromere coupling as well as centromere pairing in non-exchange chromosome segregation. Therefore, this leads to the question whether the same phosphorylation involved in coupling is also required in non-exchange chromosome segregation.

The *trp1::ZIP1-T114A::TRP1* allele was introduced into the strain carrying the homeologous pair. Meiotic spreads using fixed cells were first examined in the *zip1-T114A* NEC mutant (Fig 5.7A). Zip1 is stained with anti-Zip1 shown in orange, *CEN3* is stained with GFP shown in green, and tubulin was stained in red. 17% of nuclei had paired centromeres and 54% had unpaired centromeres during prophase I. 28% of nuclei showed potential premature separation of sister chromatid (PSSC). This low percentage of pairing is almost similar to a *zip1* Δ mutant, where 14% showed paired centromeres (Fig. 5.4). Among the unpaired centromeres, there were increased levels of PSSC in the *zip1-T114A* mutant. Overall, this suggests that Zip1-mediated centromere tethering during prophase I requires the phosphorylation of the *zip1-T114A* mutant. However, this data cannot be certain, as *S. paradoxus CEN3* was tagged with lacO/LacI, which can sometimes be lost during spreading. This is also due to the use of a

commercial GFP antibody in the *zip1-T114A* mutant, which give rise to a higher background compared to the Roeder Lab GFP antibody used in the wild type spread (Fig. 5.4C). Therefore this data might be biased.

To understand how this reduced centromere pairing in prophase I behave during live movements, time-lapse imaging was used to follow the tagged homeologs (Fig. 5.7). Similar dynamic movement of centromere was observed in the *zip1-T114A* mutant in comparison to the wild-type (Fig. 5.7E), suggesting this dynamic is a common phenomenon in the NEC system. However, an increased level of non-disjunction was observed in the *zip1-T114A* live cells (Fig. 5.7F&G). The above data suggests either T114 is involved in NEC segregation, or the lacO/LacI signals are lost during the experiment. Due to methodology reasons, it is hard to cross the *zip1-T114A* mutant into other *S. crevissiae* homeologous chromosomes for comparison.

5.2.5 Studying non-exchange chromosome segregation in two different colours

S. paradoxus chromosome III was tagged with lacO/LacI, and this was not a stable GFP signal compared to the tetO/TetR. Signals sometimes can get lost during an experiment. Previous data showed that the *zip1-T114A* mutant had a high percentage of non-disjunction as well as precocious sister chromatid separation (Fig. 5.7G). However, it could indicate loss of lacO/LacI signals. Therefore, to further confirm whether Zip1-T114 was truly involved in NEC, *S. cerevisiae* chromosome three was tagged with mCherry. In this way, the two homeologous chromosomes were tagged with different colours so it can be distinguished during time-lapse imaging. However, Pds1-tdTomato marking

anaphase I entry cannot be used because it shares the same wavelength as mCherry. Hence they both are in the same Channel and no distinguishment can be made. Therefore, the way to distinguish anaphase I entry is to measure the distance between the LacI-GFP. In this study, $> 4 \mu\text{m}$ in length is categorized as metaphase I entry. Moreover, due to development of the software, no distance was measured between two centromeres; only the segregation pattern was assessed.

Similar patterns were observed in the wild type NEC with the green system (Fig. 5.8), where dynamic of *CEN3* was observed from early stage. Dynamic cycles of association and dissociation were observed in all nuclei inspected ($n=111$). In agreement with previous observations in Figure 5.5, the two homeologous centromeres only became juxtaposed 5-10 minutes prior to the onset of anaphase I. Only 1% of cells were observed with MI NDJ (Fig. 5.8B), and this percentage was much lower than the green system (Fig. 5.7). This probably suggests loss of signals when both centromeres were tagged with the green colour. However, despite low proportion of MI NDJ was observed, the similar pattern of NDJ movement was observed in comparison to the green system. Homeologous centromeres tended to be unpaired at the entry of anaphase I (Fig. 5.8B), and presumably each homolog would stayed at each spindle pole body. However, as anaphase I began, they became paired again and tethered at one spindle pole body. Both centromeres only started separating from anaphase II (Fig 5.8B). This pattern was observed when using the green system. Both systems probably suggests that the mechanisms that ensure accurate segregation somehow failed at the onset of anaphase I and centromeres were unable to stay at the opposite pole during segregation, hence

one centromere was pulled back with its partner centromere. Another suggestion for this could be that the spindle did not cluster unattached/untensioned centromeres in the centre or that the univalent were at the centre because they were constantly turned over and attaching/reattaching to MTs from opposing spindle poles. An increased level of precocious sister chromatid separation was observed in NEC (4%) (Fig. 5.8C). These cells tended to lose their sister cohesions at the onset of anaphase I or at metaphase I. Three centromere dots were observed with random segregation during anaphase I. This probably indicates a role of cohesins in the NEC pathway. Overall, using this red/green system further showed the dynamic of non-exchange chromosome segregation with an increased level of PSSC. In the green/red system, the result that no PSSC was observed is probably because when sister centromeres separated, the GFP signal became weaker, thus it was not detected.

5.2.6 Examination of the phosphorylation of the *zip1-T114A* mutant in NEC pathway using red and green fluorescence

It was demonstrated that Zip1-T114 had a potential role in the phosphorylation of non-exchange chromosome centromere pairing. In order to eliminate the possibility that lacO/LacI signal was not lost during imaging, tagging the homeologous chromosomes with one in mCherry and one in lacO/LacI are used to study (Fig. 5.9).

Normal segregation was observed in a *zip1-T114A* mutant where centromeres were paired prior to anaphase I, but they showed dynamic association from prophase I to metaphase I (Fig. 5.9A). PSSC was also observed to a similar level to the wild-type (Fig. 5.9B), where one of sister centromeres were

separated during either metaphase I or anaphase I. It is hard to tell the stage without any marker. Nevertheless, from the distance of centromere separating, it could suggest sister cohesions were lost during anaphase I. Meiosis I NDJ was also observed in a *zip1-T114A* mutant (4%) (Fig. 5.9C). The proportion of normal segregation using the red/green system was elevated to 88%, whereas in the green/green system only 14% correct segregation was observed. This probably suggests the loss of lacO/LacI signals biased the result. However, the segregation using red/green system revealed 95% accurate segregation in the wild type, whereas only 88% was showed in *zip1-T114A*. Using T-test showed that $P=0.0045$ (calculated using Prism), suggesting the difference between the wild-type and the *zip1-T114A* mutant was insignificant. Therefore, it indicates a similar segregation in both the wild-type and the *zip1-T114A* mutant. Meiosis I non-disjunction was increased from 1% in the wild-type to 4% in the *zip1-T114A* mutant, proportion of PSSC was also increased by two-fold in the *zip1-T114A* mutant (4% to 8%). Overall, this indicates that phosphorylation of Zip1-T114 was not involved in holding centromeres of NEC together. There are probably more sites required to hold NEC centromeres together.

5.3 Discussion

This chapter has revealed an interesting phenomenon in non-exchange chromosome segregation by using live cell imaging. Previous published studies on NEC have showed that centromere pairing is indeed required to ensure accurate segregation in NEC. The SC protein Zip1 ensures the accurate segregation. However, using live cell has now revealed the reason why only 50% of pairing was observed in previous studies using fixed cell spread. This is because centromeres tend to behave very dynamically during NEC system, where they are not paired all the time. Instead a dissociation/association pattern was observed in NEC wild-type from prophase I to anaphase I. Moreover, despite such dynamics, the majority of centromeres tend to be paired just before entry into anaphase I, which suggests a mechanism that ensures homeologous chromosomes lie on the central plate, ready for microtubules attachment in a similar manner to exchange chromosomes. Nonetheless, minority cells with paired centromere were observed even at the onset of anaphase I. One centromere tended to move to the opposite pole 5 to 10 minutes later, perhaps after some checkpoint mechanisms they were assigned to the opposite pole for accurate segregation. These observations probably suggest multiple mechanisms exist in NEC to ensure accurate segregation. One mechanism is monitored by SC central element protein Zip1, but there are other mechanisms that also control this. Since the result that 14% of centromeres were paired in the *zip1Δ* mutant probably indicates other existent mechanisms.

Zip1-T114 was showed to get involved in centromere coupling (Chapter 3), and a partial-coupling defect was observed when Zip1-T114 was under-phosphorylated. Deletion of *ZIP1* also results in total loss of centromere

coupling. Furthermore, knocking out of Zip1 also leads to elevated NEC non-disjunction. In this chapter, the *zip1-T114A* mutant has shown reduction of segregation in NEC, which perhaps suggests a linkage between coupling and NEC segregation. Perhaps the same mechanisms are involved in holding non-homologous centromeres together, as well as non-exchange chromosomes together. Zip1-T114 is hyper-phosphorylated during coupling and reduction in NEC, which suggests this hyper-phosphorylation, is probably also required for sufficient NEC tethering. An increased level of PSSC was observed in the *zip1-T114A* mutant, which probably indicates the phosphorylation of this site is sufficient for maintaining sister chromatid separation in the NEC pathway.

With the development of live cell imaging, it allows precise study of non-exchange chromosome segregation. In this chapter only one ZIP1-point mutant was studied, and it would be interesting to see how other characterized *ZIP1*-point mutant behaves. For example: *zip1-7A*; *zip1-8A*; *zip1-8E* mutants showed complete loss of centromere coupling when phosphorylation of multiple sites was eliminated. If the hypothesis of same pathway is involved in both coupling and NEC pairing, then it would be expected a reduction of NEC segregation in these mutants as well. Perhaps *zip1-7A*; *zip1-8A*; *zip1-8E* mutants would act in a similar manner as *zip1Δ* mutant in NECS. Moreover, Falk *et al.* established a role of PP4 complex in meiosis (Falk et al., 2010). They have found that prior to homologous centromere pairing, non-homologous are centromere coupled and PP4 complex plays a role in regulating this coupling. Upon initiation of double strand breaks by Spo11, Mec1 phosphorylate Zip1-S75 result in de coupling of centromere. PP4 complex activated results in de-phosphorylation of Zip1 and leads to homologous centromere paring. However, the behaviour of PP4 has

only been examined up to this stage. Anything further than prophase I still remain unclear. More importantly, creating a phosphomimic mutant of *zip1-S75E*, hyper-phosphorylation of Zip1 was observed and coupling was blocked. It indicates that Zip1-S75 is required for decoupling of non-homologous. It is interesting to investigate the possible role of Pph3 (part of PP4 complex) and Zip1-S75 in NEC pathway. Perhaps this will provide further clearance of non-exchange chromosomes segregation.

Chapter 6. Discussion

6.1 Discussion

This thesis has characterized the functions of specific Zip1 amino acids in meiosis through the analysis of point mutants. In recent years, Zip1 has been shown as a phosphor-protein and though much work has revealed some roles of Zip1, it is still unclear how phosphorylation of Zip1 contributes to each stage of meiosis. With the development of mass spectrometry, several Zip1 sites have been identified through a Cdc5 screen and these sites have been picked to characterize (Chapter 3). Among these sites, Zip1-S144 has been identified with a role in SC disassembly, and Zip1-S144 is a putative consensus site for Cdc5 (Chapter 4). Moreover, another role of Zip1 has been discovered in the non-exchange chromosome segregation (NECS) (Gladstone et al., 2009; Newnham et al., 2010), in this thesis, the behaviour of NECS has been studied using live-cell imaging (Chapter 5).

The work outlined in this thesis has shown fine-tuning phosphorylation events of Zip1 during meiosis. Phosphorylation is not controlled by a single event, instead it is highly regulated. For example: previously work by *Falk et al.* showed a mechanism involving the phosphorylation of Zip1-S75 during early prophase I. However, the work outlined in this thesis also showed another phosphorylation of Zip1 amino acid that is involved during early prophase I (Zip1-T114). Yet, Zip1-T114 is not functioning in the same pathway as Zip1-S75. Moreover, this thesis has demonstrated that Zip1-S144 is involved in SC disassembly, but it is not the only site that is involved during this process. Since Zip1-S144 is a putative consensus site of Cdc5, the results obtained from this thesis probably

suggests that SC disassembly by Cdc5 requires more than one phosphorylation sites, further demonstrating the fine-tuning process of Zip1 phosphorylation.

Why is it important to study Zip1? The transverse filament Zip1 is a structurally conserved protein and is very important in several stages in meiotic prophase. Firstly, it is the building block of the SC as it forms the central region. It is involved in the synapsis of homologous chromosomes as well as the coupling of non-homologous centromeres. Zip1 is also involved in crossover regulation. In the absence of Zip1, severe defects observed leads to chromosome missegregation. As this protein is conserved, mutation in orthologs of other species also results in meiotic arrest and/or errors in chromosome segregation. More importantly, experiments in mammals have shown that mutations in its ortholog SYCP1 result in infertility or reduce fertility due to meiotic arrest (Bolcun-Filas et al., 2007; Bolcun-Filas et al., 2009; de Vries et al., 2005; Hamer et al., 2008). Budding yeast is a good model organism to study meiosis, and studying meiosis in humans is extremely difficult for many reasons. This includes the paucity of material and the absence of cell lines. As Zip1 has been shown to be a phosphoprotein, it would also suggest its ortholog in human can also undergo phosphorylation. However, it would be hard to study the phosphorylation of human SYCP1.

Previous work on NECS in budding yeast has revealed a novel role for Zip1, as it holds the non-exchange chromosome centromeres together from prophase I to anaphase I. However, there are still many unanswered questions. The development of live cell imaging techniques has provide a tool to more closely examine this mechanism. Why is it so important to study NECS? This is because aneuploidy in humans derives from erroneous chromosome

segregation at meiosis I or II. More than 90% of aneuploidy in the resulting foetus are due to chromosome segregation errors in the human oocytes. There are two main causes implicated in this, which are the increased age of the mother and the recombination pattern of the mis-segregated chromosomes. Trisomy 21 needs to be particularly noted. This aneuploidy is mainly due to two chromosomes being transmitted from the mother and these have often failed to crossover (30%) (Nagaoka et al., 2012). Moreover, another study has suggested ~25% of all chromosomes lack crossover in human oocytes (Cheng et al., 2009). These works together suggest a link between increased ages of a woman with less efficient non-exchange chromosome segregation. It is impossible to study the live movement of an oocyte, hence using yeast as a model in live cell imaging would provide more insight on how human aneuploidy occurs. It could also provide some ideas on how non-crossover chromosomes in oocytes are achieved.

Overall, the work demonstrated in this thesis has revealed further functions of Zip1 during meiosis. Taken these work with other published literatures on Zip1, it is clear that Zip1 plays a very important role during meiosis. Firstly, Zip1 is required for non-homologous centromere coupling during early stage of meiosis. Secondly, Zip1 is involved in the regulation of determining the fate of crossover formation and it is required for crossover interference. Thirdly, Zip1 is the main building block of the SC. Fourthly, Zip1 has an important role during NEC pathway, where it holds centromere together. However, how these fine-tuning of phosphorylation is regulated still remain unclear and it is still unknown which kinases are contributed in these processes. Hoping these issues will be addressed in the future research.

6.2 Future work

There are still many unanswered questions involving completion of this work. For example, it is still unclear which kinases trigger these phosphorylation events in Zip1. Several sites such as Zip1-T114, Zip1-S144 are consensus sites for CK2 or DDK. Dr. Alice Copsey used kinase pull-down to show that Zip1 is phosphorylated by CK2 *in vitro*. However, since CK2 is an active kinase through meiosis and it is involved in many pathways, knocking out CK2 is difficult. Therefore at this stage it is hard to prove that these Zip1 sites are phosphorylated by CK2 *in vivo*. Moreover, the meaning of centromere coupling still remains unknown. This work has shown that Zip1-T114 has a role in centromere coupling, but Zip1-T114 does not affect other stages in meiosis. It would be interesting to find out whether this site, or other unidentified sites, function together in meiosis. It is also unknown how mutation of seven sites (*zip1-7A*) would restore normal SC formation, whereas the single mutation such as *zip1-S137A*, *zip1-S82A*, *zip1-S144A* and *zip1-T114A* mutants would result in high proportions of polycomplexes. In contrast, *zip1-8A* and *zip1-8E* mutants result in defects in SC formation as well as centromere coupling. But it is unclear whether this defect was due to disrupting of the Zip1 structure or whether these mutants do indeed affect meiosis. Therefore, with the hope of revealing the crystallography structure of Zip1 in the future, these questions can be answered.

The role of Zip1-S144 is also unclear, as it has shown that Zip1-S144 has a role in SC disassembly. This phenotype is consistent with the fact that Zip1-S144 is a putative consensus site for Cdc5, and Cdc5 is required for SC disassembly. However, experiments in Cdc5-inducible have shown that the *zip1-S144A*

mutant is still disassembled similar to the wild-type. Moreover, in the absence of Cdc5, the *zip1-S144E* mutant did not restore SC disassembly. Taken together, do these findings suggest that Zip1-S144 is not required by Cdc5? Or does it imply that more sites are involved to require Cdc5 to disassemble the SC? These questions are remained to be answered with the hope of identifying more sites in the future.

Furthermore, though a step forward of making SK1 homeologous chromosome allows easy access of live cell imaging, it is still unsure how *zip1* knock out behaves in NEC under time-lapse imaging. Previous work has shown 14% tethering of centromeres in *zip1Δ*, it would be interesting to see how this 14% tethering arise using live cell imaging. Zip1-T114 was the only site picked to study in NEC, and it would also be interesting to see whether other Zip1 phospho sites would result in the tethering of non-exchange chromosomes. The wild-type NEC has indeed shown very dynamic pattern in centromeres as well as spindle pole body. But it is unknown why such dynamic exists. Hence, with the hoping of future research in identifying more unknown proteins, this question would be answered.

Bibliography

- Agarwal, S., and Roeder, G.S. (2000). Zip3 provides a link between recombination enzymes and synaptonemal complex proteins. *Cell* 102, 245-255.
- Allers, T., and Lichten, M. (2001). Intermediates of yeast meiotic recombination contain heteroduplex DNA. *Molecular cell* 8, 225-231.
- Alsheimer, M., Baier, A., Schramm, S., Schutz, W., and Benavente, R. (2010). Synaptonemal complex protein SYCP3 exists in two isoforms showing different conservation in mammalian evolution. *Cytogenetic and genome research* 128, 162-168.
- Anderson, L.K., Royer, S.M., Page, S.L., McKim, K.S., Lai, A., Lilly, M.A., and Hawley, R.S. (2005). Juxtaposition of C(2)M and the transverse filament protein C(3)G within the central region of *Drosophila* synaptonemal complex. *Proceedings of the National Academy of Sciences of the United States of America* 102, 4482-4487.
- Archambault, V., and Glover, D.M. (2009). Polo-like kinases: conservation and divergence in their functions and regulation. *Nature reviews Molecular cell biology* 10, 265-275.
- Archambault, V., Zhao, X., White-Cooper, H., Carpenter, A.T., and Glover, D.M. (2007). Mutations in *Drosophila* Greatwall/Scant reveal its roles in mitosis and meiosis and interdependence with Polo kinase. *PLoS genetics* 3, e200.
- Argueso, J.L., Wanat, J., Gemici, Z., and Alani, E. (2004). Competing crossover pathways act during meiosis in *Saccharomyces cerevisiae*. *Genetics* 168, 1805-1816.
- Armstrong, S.J., Caryl, A.P., Jones, G.H., and Franklin, F.C. (2002). Asy1, a protein required for meiotic chromosome synapsis, localizes to axis-associated chromatin in *Arabidopsis* and *Brassica*. *Journal of cell science* 115, 3645-3655.
- Arora, C., Kee, K., Maleki, S., and Keeney, S. (2004). Antiviral protein Ski8 is a direct partner of Spo11 in meiotic DNA break formation, independent of its cytoplasmic role in RNA metabolism. *Molecular cell* 13, 549-559.
- Arumugam, P., Nishino, T., Haering, C.H., Gruber, S., and Nasmyth, K. (2006). Cohesin's ATPase activity is stimulated by the C-terminal Winged-Helix domain of its kleisin subunit. *Current biology : CB* 16, 1998-2008.
- Attner, M.A., Miller, M.P., Ee, L.S., Elkin, S.K., and Amon, A. (2013). Polo kinase Cdc5 is a central regulator of meiosis I. *Proceedings of the National Academy of Sciences of the United States of America*.

Baier, A., Alsheimer, M., Volff, J.N., and Benavente, R. (2007). Synaptonemal complex protein SYCP3 of the rat: evolutionarily conserved domains and the assembly of higher order structures. *Sex Dev* 1, 161-168.

Bailis, J.M., and Roeder, G.S. (1998). Synaptonemal complex morphogenesis and sister-chromatid cohesion require Mek1-dependent phosphorylation of a meiotic chromosomal protein. *Genes & development* 12, 3551-3563.

Bannister, L.A., Reinholdt, L.G., Munroe, R.J., and Schimenti, J.C. (2004). Positional cloning and characterization of mouse mei8, a disrupted allele of the meiotic cohesin Rec8. *Genesis* 40, 184-194.

Bhalla, N., and Dernburg, A.F. (2008). Prelude to a division. *Annual review of cell and developmental biology* 24, 397-424.

Bhalla, N., Wynne, D.J., Jantsch, V., and Dernburg, A.F. (2008). ZHP-3 acts at crossovers to couple meiotic recombination with synaptonemal complex disassembly and bivalent formation in *C. elegans*. *PLoS genetics* 4, e1000235.

Bishop, D.K., Park, D., Xu, L., and Kleckner, N. (1992). DMC1: a meiosis-specific yeast homolog of *E. coli* recA required for recombination, synaptonemal complex formation, and cell cycle progression. *Cell* 69, 439-456.

Bisig, C.G., Guiraldelli, M.F., Kouznetsova, A., Scherthan, H., Hoog, C., Dawson, D.S., and Pezza, R.J. (2012). Synaptonemal complex components persist at centromeres and are required for homologous centromere pairing in mouse spermatocytes. *PLoS genetics* 8, e1002701.

Bizzari, F., and Marston, A.L. (2011). Cdc55 coordinates spindle assembly and chromosome disjunction during meiosis. *The Journal of cell biology* 193, 1213-1228.

Blat, Y., Protacio, R.U., Hunter, N., and Kleckner, N. (2002). Physical and functional interactions among basic chromosome organizational features govern early steps of meiotic chiasma formation. *Cell* 111, 791-802.

Boddy, M.N., Gaillard, P.H., McDonald, W.H., Shanahan, P., Yates, J.R., 3rd, and Russell, P. (2001). Mus81-Eme1 are essential components of a Holliday junction resolvase. *Cell* 107, 537-548.

Bolcun-Filas, E., Costa, Y., Speed, R., Taggart, M., Benavente, R., De Rooij, D.G., and Cooke, H.J. (2007). SYCE2 is required for synaptonemal complex assembly, double strand break repair, and homologous recombination. *The Journal of cell biology* 176, 741-747.

Bolcun-Filas, E., Hall, E., Speed, R., Taggart, M., Grey, C., de Massy, B., Benavente, R., and Cooke, H.J. (2009). Mutation of the mouse Syce1 gene disrupts synapsis and suggests a link between synaptonemal complex structural components and DNA repair. *PLoS genetics* 5, e1000393.

Borde, V., Goldman, A.S., and Lichten, M. (2000). Direct coupling between meiotic DNA replication and recombination initiation. *Science* 290, 806-809.

Borner, G.V. (2006). Balancing the checks: surveillance of chromosomal exchange during meiosis. *Biochemical Society transactions* 34, 554-556.

Borner, G.V., Kleckner, N., and Hunter, N. (2004). Crossover/noncrossover differentiation, synaptonemal complex formation, and regulatory surveillance at the leptotene/zygotene transition of meiosis. *Cell* 117, 29-45.

Brar, G.A., and Amon, A. (2008). Emerging roles for centromeres in meiosis I chromosome segregation. *Nature reviews Genetics* 9, 899-910.

Brar, G.A., Hochwagen, A., Ee, L.S., and Amon, A. (2009). The multiple roles of cohesin in meiotic chromosome morphogenesis and pairing. *Molecular biology of the cell* 20, 1030-1047.

Brar, G.A., Kiburz, B.M., Zhang, Y., Kim, J.E., White, F., and Amon, A. (2006). Rec8 phosphorylation and recombination promote the step-wise loss of cohesins in meiosis. *Nature* 441, 532-536.

Brito, I.L., Yu, H.G., and Amon, A. (2010). Condensins promote coorientation of sister chromatids during meiosis I in budding yeast. *Genetics* 185, 55-64.

Buonomo, S.B., Clyne, R.K., Fuchs, J., Loidl, J., Uhlmann, F., and Nasmyth, K. (2000). Disjunction of homologous chromosomes in meiosis I depends on proteolytic cleavage of the meiotic cohesin Rec8 by separin. *Cell* 103, 387-398.

Carballo, J.A., Johnson, A.L., Sedgwick, S.G., and Cha, R.S. (2008). Phosphorylation of the axial element protein Hop1 by Mec1/Tel1 ensures meiotic interhomolog recombination. *Cell* 132, 758-770.

Carpenter, A.T. (1973). A meiotic mutant defective in distributive disjunction in *Drosophila melanogaster*. *Genetics* 73, 393-428.

Cha, R.S., Weiner, B.M., Keeney, S., Dekker, J., and Kleckner, N. (2000). Progression of meiotic DNA replication is modulated by interchromosomal interaction proteins, negatively by Spo11p and positively by Rec8p. *Genes & development* 14, 493-503.

Chambers, S.R., Hunter, N., Louis, E.J., and Borts, R.H. (1996). The mismatch repair system reduces meiotic homeologous recombination and stimulates recombination-dependent chromosome loss. *Molecular and cellular biology* 16, 6110-6120.

Chen, S.Y., Tsubouchi, T., Rockmill, B., Sandler, J.S., Richards, D.R., Vader, G., Hochwagen, A., Roeder, G.S., and Fung, J.C. (2008). Global analysis of the meiotic crossover landscape. *Developmental cell* 15, 401-415.

Cheng, C.H., Lo, Y.H., Liang, S.S., Ti, S.C., Lin, F.M., Yeh, C.H., Huang, H.Y., and Wang, T.F. (2006). SUMO modifications control assembly of synaptonemal

complex and polycomplex in meiosis of *Saccharomyces cerevisiae*. *Genes & development* 20, 2067-2081.

Cheng, E.Y., Hunt, P.A., Nalwai-Cecchini, T.A., Fligner, C.L., Fujimoto, V.Y., Pasternack, T.L., Schwartz, J.M., Steinauer, J.E., Woodruff, T.J., Cherry, S.M., *et al.* (2009). Meiotic recombination in human oocytes. *PLoS genetics* 5, e1000661.

Cheslock, P.S., Kemp, B.J., Boumil, R.M., and Dawson, D.S. (2005). The roles of MAD1, MAD2 and MAD3 in meiotic progression and the segregation of nonexchange chromosomes. *Nature genetics* 37, 756-760.

Chikashige, Y., Ding, D.Q., Funabiki, H., Haraguchi, T., Mashiko, S., Yanagida, M., and Hiraoka, Y. (1994). Telomere-led premeiotic chromosome movement in fission yeast. *Science* 264, 270-273.

Christophorou, N., Rubin, T., and Huynh, J.R. (2013). Synaptonemal Complex Components Promote Centromere Pairing in Pre-meiotic Germ Cells. *PLoS genetics* 9, e1004012.

Chu, S., and Herskowitz, I. (1998). Gametogenesis in yeast is regulated by a transcriptional cascade dependent on Ndt80. *Molecular cell* 1, 685-696.

Chua, P.R., and Roeder, G.S. (1997). Tam1, a telomere-associated meiotic protein, functions in chromosome synapsis and crossover interference. *Genes & development* 11, 1786-1800.

Chua, P.R., and Roeder, G.S. (1998). Zip2, a meiosis-specific protein required for the initiation of chromosome synapsis. *Cell* 93, 349-359.

Ciosk, R., Shirayama, M., Shevchenko, A., Tanaka, T., Toth, A., Shevchenko, A., and Nasmyth, K. (2000). Cohesin's binding to chromosomes depends on a separate complex consisting of Scc2 and Scc4 proteins. *Molecular cell* 5, 243-254.

Ciosk, R., Zachariae, W., Michaelis, C., Shevchenko, A., Mann, M., and Nasmyth, K. (1998). An ESP1/PDS1 complex regulates loss of sister chromatid cohesion at the metaphase to anaphase transition in yeast. *Cell* 93, 1067-1076.

Clift, D., Bizzari, F., and Marston, A.L. (2009). Shugoshin prevents cohesin cleavage by PP2A(Cdc55)-dependent inhibition of separase. *Genes & development* 23, 766-780.

Cloud, V., Chan, Y.L., Grubb, J., Budke, B., and Bishop, D.K. (2012). Rad51 is an accessory factor for Dmc1-mediated joint molecule formation during meiosis. *Science* 337, 1222-1225.

Clyne, R.K., Katis, V.L., Jessop, L., Benjamin, K.R., Herskowitz, I., Lichten, M., and Nasmyth, K. (2003). Polo-like kinase Cdc5 promotes chiasmata formation

and cosegregation of sister centromeres at meiosis I. *Nature cell biology* 5, 480-485.

Colaiacono, M.P., MacQueen, A.J., Martinez-Perez, E., McDonald, K., Adamo, A., La Volpe, A., and Villeneuve, A.M. (2003). Synaptonemal complex assembly in *C. elegans* is dispensable for loading strand-exchange proteins but critical for proper completion of recombination. *Developmental cell* 5, 463-474.

Collins, K.A., Unruh, J.R., Slaughter, B.D., Yu, Z., Lake, C.M., Nielsen, R.J., Box, K.S., Miller, D.E., Blumenstiel, J.P., Perera, A.G., *et al.* (2014). Corolla is a novel protein that contributes to the architecture of the synaptonemal complex of *Drosophila*. *Genetics* 198, 219-228.

Conrad, M.N., Dominguez, A.M., and Dresser, M.E. (1997). Ndj1p, a meiotic telomere protein required for normal chromosome synapsis and segregation in yeast. *Science* 276, 1252-1255.

Conrad, M.N., Lee, C.Y., Chao, G., Shinohara, M., Kosaka, H., Shinohara, A., Conchello, J.A., and Dresser, M.E. (2008). Rapid telomere movement in meiotic prophase is promoted by NDJ1, MPS3, and CSM4 and is modulated by recombination. *Cell* 133, 1175-1187.

Conrad, M.N., Lee, C.Y., Wilkerson, J.L., and Dresser, M.E. (2007). MPS3 mediates meiotic bouquet formation in *Saccharomyces cerevisiae*. *Proceedings of the National Academy of Sciences of the United States of America* 104, 8863-8868.

Copsey, A., Tang, S., Jordan, P.W., Blitzblau, H.G., Newcombe, S., Chan, A.C., Newnham, L., Li, Z., Gray, S., Herbert, A.D., *et al.* (2013). Smc5/6 coordinates formation and resolution of joint molecules with chromosome morphology to ensure meiotic divisions. *PLoS genetics* 9, e1004071.

Costa, Y., Speed, R., Ollinger, R., Alsheimer, M., Semple, C.A., Gautier, P., Maratou, K., Novak, I., Hoog, C., Benavente, R., *et al.* (2005). Two novel proteins recruited by synaptonemal complex protein 1 (SYCP1) are at the centre of meiosis. *Journal of cell science* 118, 2755-2762.

D'Ambrosio, C., Schmidt, C.K., Katou, Y., Kelly, G., Itoh, T., Shirahige, K., and Uhlmann, F. (2008). Identification of cis-acting sites for condensin loading onto budding yeast chromosomes. *Genes & development* 22, 2215-2227.

Davis, L., and Smith, G.R. (2005). Dynein promotes achiasmate segregation in *Schizosaccharomyces pombe*. *Genetics* 170, 581-590.

Dawson, D.S., Murray, A.W., and Szostak, J.W. (1986). An alternative pathway for meiotic chromosome segregation in yeast. *Science* 234, 713-717.

de Boer, E., and Heyting, C. (2006). The diverse roles of transverse filaments of synaptonemal complexes in meiosis. *Chromosoma* 115, 220-234.

de la Fuente, R., Parra, M.T., Viera, A., Calvente, A., Gomez, R., Suja, J.A., Rufas, J.S., and Page, J. (2007). Meiotic pairing and segregation of achiasmate sex chromosomes in eutherian mammals: the role of SYCP3 protein. *PLoS genetics* 3, e198.

de los Santos, T., Hunter, N., Lee, C., Larkin, B., Loidl, J., and Hollingsworth, N.M. (2003). The Mus81/Mms4 endonuclease acts independently of double-Holliday junction resolution to promote a distinct subset of crossovers during meiosis in budding yeast. *Genetics* 164, 81-94.

De Muyt, A., Jessop, L., Kolar, E., Sourirajan, A., Chen, J., Dayani, Y., and Lichten, M. (2012). BLM Helicase Ortholog Sgs1 Is a Central Regulator of Meiotic Recombination Intermediate Metabolism. *Molecular cell* 46, 43-53.

de Vries, F.A., de Boer, E., van den Bosch, M., Baarends, W.M., Ooms, M., Yuan, L., Liu, J.G., van Zeeland, A.A., Heyting, C., and Pastink, A. (2005). Mouse Sycp1 functions in synaptonemal complex assembly, meiotic recombination, and XY body formation. *Genes & development* 19, 1376-1389.

Dernburg, A.F., McDonald, K., Moulder, G., Barstead, R., Dresser, M., and Villeneuve, A.M. (1998). Meiotic recombination in *C. elegans* initiates by a conserved mechanism and is dispensable for homologous chromosome synapsis. *Cell* 94, 387-398.

Dernburg, A.F., Sedat, J.W., and Hawley, R.S. (1996). Direct evidence of a role for heterochromatin in meiotic chromosome segregation. *Cell* 86, 135-146.

Ding, D.Q., Yamamoto, A., Haraguchi, T., and Hiraoka, Y. (2004). Dynamics of homologous chromosome pairing during meiotic prophase in fission yeast. *Developmental cell* 6, 329-341.

Ding, R., McDonald, K.L., and McIntosh, J.R. (1993). Three-dimensional reconstruction and analysis of mitotic spindles from the yeast, *Schizosaccharomyces pombe*. *The Journal of cell biology* 120, 141-151.

Dobson, M.J., Pearlman, R.E., Karauskakis, A., Spyropoulos, B., and Moens, P.B. (1994). Synaptonemal complex proteins: occurrence, epitope mapping and chromosome disjunction. *Journal of cell science* 107 (Pt 10), 2749-2760.

Dong, H., and Roeder, G.S. (2000). Organization of the yeast Zip1 protein within the central region of the synaptonemal complex. *The Journal of cell biology* 148, 417-426.

Dutcher, S.K. (1981). Internuclear transfer of genetic information in *kar1-1/KAR1* heterokaryons in *Saccharomyces cerevisiae*. *Molecular and cellular biology* 1, 245-253.

Eichinger, C.S., and Jentsch, S. (2010). Synaptonemal complex formation and meiotic checkpoint signaling are linked to the lateral element protein Red1.

Proceedings of the National Academy of Sciences of the United States of America *107*, 11370-11375.

Engbrecht, J., Masse, S., Davis, L., Rose, K., and Kessel, T. (1998). Yeast meiotic mutants proficient for the induction of ectopic recombination. *Genetics* *148*, 581-598.

Falk, J.E., Chan, A.C., Hoffmann, E., and Hochwagen, A. (2010). A Mec1- and PP4-dependent checkpoint couples centromere pairing to meiotic recombination. *Developmental cell* *19*, 599-611.

Farcas, A.M., Uluocak, P., Helmhart, W., and Nasmyth, K. (2011). Cohesin's concatenation of sister DNAs maintains their intertwining. *Molecular cell* *44*, 97-107.

Fekairi, S., Scaglione, S., Chahwan, C., Taylor, E.R., Tissier, A., Coulon, S., Dong, M.Q., Ruse, C., Yates, J.R., 3rd, Russell, P., *et al.* (2009). Human SLX4 is a Holliday junction resolvase subunit that binds multiple DNA repair/recombination endonucleases. *Cell* *138*, 78-89.

Fernius, J., Nerusheva, O.O., Galander, S., Alves, F.D., Rappsilber, J., and Marston, A.L. (2013). Cohesin-Dependent Association of Scc2/4 with the Centromere Initiates Pericentromeric Cohesion Establishment. *Current biology : CB*.

Fung, J.C., Rockmill, B., Odell, M., and Roeder, G.S. (2004). Imposition of crossover interference through the nonrandom distribution of synapsis initiation complexes. *Cell* *116*, 795-802.

Garcia, V., Phelps, S.E., Gray, S., and Neale, M.J. (2011). Bidirectional resection of DNA double-strand breaks by Mre11 and Exo1. *Nature* *479*, 241-244.

Gilliland, W.D., Hughes, S.F., Vietti, D.R., and Hawley, R.S. (2009). Congression of achiasmate chromosomes to the metaphase plate in *Drosophila melanogaster* oocytes. *Developmental biology* *325*, 122-128.

Gladstone, M.N., Obeso, D., Chuong, H., and Dawson, D.S. (2009). The synaptonemal complex protein Zip1 promotes bi-orientation of centromeres at meiosis I. *PLoS genetics* *5*, e1000771.

Gligoris, T.G., Scheinost, J.C., Burmann, F., Petela, N., Chan, K.L., Uluocak, P., Beckouet, F., Gruber, S., Nasmyth, K., and Lowe, J. (2014). Closing the cohesin ring: structure and function of its Smc3-kleisin interface. *Science* *346*, 963-967.

Goodyer, W., Kaitna, S., Couteau, F., Ward, J.D., Boulton, S.J., and Zetka, M. (2008). HTP-3 links DSB formation with homolog pairing and crossing over during *C. elegans* meiosis. *Developmental cell* *14*, 263-274.

Gregan, J., Riedel, C.G., Pidoux, A.L., Katou, Y., Rumpf, C., Schleiffer, A., Kearsy, S.E., Shirahige, K., Allshire, R.C., and Nasmyth, K. (2007). The kinetochore proteins Pcs1 and Mde4 and heterochromatin are required to prevent merotelic orientation. *Current biology : CB* 17, 1190-1200.

Greig, D. (2007). A screen for recessive speciation genes expressed in the gametes of F1 hybrid yeast. *PLoS genetics* 3, e21.

Greig, D., and Leu, J.Y. (2009). Natural history of budding yeast. *Current biology : CB* 19, R886-890.

Grell, R.F. (1962). A new model for secondary nondisjunction: the role of distributive pairing. *Genetics* 47, 1737-1754.

Grell, R.F. (1964). Distributive Pairing: The Size-Dependent Mechanism for Regular Segregation of the Fourth Chromosomes in *Drosophila Melanogaster*. *Proceedings of the National Academy of Sciences of the United States of America* 52, 226-232.

Guacci, V., and Kaback, D.B. (1991). Distributive disjunction of authentic chromosomes in *Saccharomyces cerevisiae*. *Genetics* 127, 475-488.

Guacci, V., Koshland, D., and Strunnikov, A. (1997). A direct link between sister chromatid cohesion and chromosome condensation revealed through the analysis of MCD1 in *S. cerevisiae*. *Cell* 91, 47-57.

Haering, C.H., Farcas, A.M., Arumugam, P., Metson, J., and Nasmyth, K. (2008). The cohesin ring concatenates sister DNA molecules. *Nature* 454, 297-301.

Haering, C.H., Lowe, J., Hochwagen, A., and Nasmyth, K. (2002). Molecular architecture of SMC proteins and the yeast cohesin complex. *Molecular cell* 9, 773-788.

Haering, C.H., Schoffnegger, D., Nishino, T., Helmhart, W., Nasmyth, K., and Lowe, J. (2004). Structure and stability of cohesin's Smc1-kleisin interaction. *Molecular cell* 15, 951-964.

Hamer, G., Gell, K., Kouznetsova, A., Novak, I., Benavente, R., and Hoog, C. (2006). Characterization of a novel meiosis-specific protein within the central element of the synaptonemal complex. *Journal of cell science* 119, 4025-4032.

Hamer, G., Wang, H., Bolcun-Filas, E., Cooke, H.J., Benavente, R., and Hoog, C. (2008). Progression of meiotic recombination requires structural maturation of the central element of the synaptonemal complex. *Journal of cell science* 121, 2445-2451.

Hardy, C.F. (1997). Identification of Cdc45p, an essential factor required for DNA replication. *Gene* 187, 239-246.

Hassold, T., Sherman, S., and Hunt, P. (2000). Counting cross-overs: characterizing meiotic recombination in mammals. *Human molecular genetics* 9, 2409-2419.

Hauf, S., Biswas, A., Langeegger, M., Kawashima, S.A., Tsukahara, T., and Watanabe, Y. (2007). Aurora controls sister kinetochore mono-orientation and homolog bi-orientation in meiosis-I. *The EMBO journal* 26, 4475-4486.

Hawley, R.S. (2002). Meiosis: how male flies do meiosis. *Current biology : CB* 12, R660-662.

Hawley, R.S., Irick, H., Zitron, A.E., Haddox, D.A., Lohe, A., New, C., Whitley, M.D., Arbel, T., Jang, J., McKim, K., *et al.* (1992). There are two mechanisms of achiasmate segregation in *Drosophila* females, one of which requires heterochromatic homology. *Dev Genet* 13, 440-467.

Hayase, A., Takagi, M., Miyazaki, T., Oshiumi, H., Shinohara, M., and Shinohara, A. (2004). A protein complex containing Mei5 and Sae3 promotes the assembly of the meiosis-specific RecA homolog Dmc1. *Cell* 119, 927-940.

Henderson, K.A., Kee, K., Maleki, S., Santini, P.A., and Keeney, S. (2006). Cyclin-dependent kinase directly regulates initiation of meiotic recombination. *Cell* 125, 1321-1332.

Henderson, K.A., and Keeney, S. (2004). Tying synaptonemal complex initiation to the formation and programmed repair of DNA double-strand breaks. *Proceedings of the National Academy of Sciences of the United States of America* 101, 4519-4524.

Henderson, K.A., and Keeney, S. (2005). Synaptonemal complex formation: where does it start? *BioEssays : news and reviews in molecular, cellular and developmental biology* 27, 995-998.

Herran, Y., Gutierrez-Caballero, C., Sanchez-Martin, M., Hernandez, T., Viera, A., Barbero, J.L., de Alava, E., de Rooij, D.G., Suja, J.A., Llano, E., *et al.* (2011). The cohesin subunit RAD21L functions in meiotic synapsis and exhibits sexual dimorphism in fertility. *The EMBO journal* 30, 3091-3105.

Hiraoka, Y., and Dernburg, A.F. (2009). The SUN rises on meiotic chromosome dynamics. *Developmental cell* 17, 598-605.

Hirose, Y., Suzuki, R., Ohba, T., Hinohara, Y., Matsuhara, H., Yoshida, M., Itabashi, Y., Murakami, H., and Yamamoto, A. (2011). Chiasmata promote monopolar attachment of sister chromatids and their co-segregation toward the proper pole during meiosis I. *PLoS genetics* 7, e1001329.

Hollingsworth, N.M. (2008). Deconstructing meiosis one kinase at a time: polo pushes past pachytene. *Genes & development* 22, 2596-2600.

Hollingsworth, N.M., Goetsch, L., and Byers, B. (1990). The HOP1 gene encodes a meiosis-specific component of yeast chromosomes. *Cell* 61, 73-84.

Hooker, G.W., and Roeder, G.S. (2006). A Role for SUMO in meiotic chromosome synapsis. *Current biology : CB* 16, 1238-1243.

Hopfner, K.P., Karcher, A., Shin, D.S., Craig, L., Arthur, L.M., Carney, J.P., and Tainer, J.A. (2000). Structural biology of Rad50 ATPase: ATP-driven conformational control in DNA double-strand break repair and the ABC-ATPase superfamily. *Cell* 101, 789-800.

Hu, B., Itoh, T., Mishra, A., Katoh, Y., Chan, K.L., Upcher, W., Godlee, C., Roig, M.B., Shirahige, K., and Nasmyth, K. (2011). ATP hydrolysis is required for relocating cohesin from sites occupied by its Scc2/4 loading complex. *Current biology : CB* 21, 12-24.

Hughes, S.E., Gilliland, W.D., Cotitta, J.L., Takeo, S., Collins, K.A., and Hawley, R.S. (2009). Heterochromatic threads connect oscillating chromosomes during prometaphase I in *Drosophila* oocytes. *PLoS genetics* 5, e1000348.

Humphries, N., Leung, W.K., Argunhan, B., Terentyev, Y., Dvorackova, M., and Tsubouchi, H. (2013). The Ecm11-Gmc2 Complex Promotes Synaptonemal Complex Formation through Assembly of Transverse Filaments in Budding Yeast. *PLoS genetics* 9, e1003194.

Hunter, N., and Kleckner, N. (2001). The single-end invasion: an asymmetric intermediate at the double-strand break to double-holliday junction transition of meiotic recombination. *Cell* 106, 59-70.

Ip, S.C., Rass, U., Blanco, M.G., Flynn, H.R., Skehel, J.M., and West, S.C. (2008). Identification of Holliday junction resolvases from humans and yeast. *Nature* 456, 357-361.

Ivanov, D., and Nasmyth, K. (2005). A topological interaction between cohesin rings and a circular minichromosome. *Cell* 122, 849-860.

Ivanov, D., and Nasmyth, K. (2007). A physical assay for sister chromatid cohesion in vitro. *Molecular cell* 27, 300-310.

Ivanovska, I., Khandan, T., Ito, T., and Orr-Weaver, T.L. (2005). A histone code in meiosis: the histone kinase, NHK-1, is required for proper chromosomal architecture in *Drosophila* oocytes. *Genes & development* 19, 2571-2582.

Ivanovska, I., and Orr-Weaver, T.L. (2006). Histone modifications and the chromatin scaffold for meiotic chromosome architecture. *Cell Cycle* 5, 2064-2071.

Jang, J.K., Sherizen, D.E., Bhagat, R., Manheim, E.A., and McKim, K.S. (2003). Relationship of DNA double-strand breaks to synapsis in *Drosophila*. *Journal of cell science* 116, 3069-3077.

Janssens, V., and Goris, J. (2001). Protein phosphatase 2A: a highly regulated family of serine/threonine phosphatases implicated in cell growth and signalling. *Biochem J* 353, 417-439.

Jaspersen, S.L., Martin, A.E., Glazko, G., Giddings, T.H., Jr., Morgan, G., Mushegian, A., and Winey, M. (2006). The Sad1-UNC-84 homology domain in Mps3 interacts with Mps2 to connect the spindle pole body with the nuclear envelope. *The Journal of cell biology* 174, 665-675.

Jessop, L., Rockmill, B., Roeder, G.S., and Lichten, M. (2006). Meiotic chromosome synapsis-promoting proteins antagonize the anti-crossover activity of Sgs1. *PLoS genetics* 2, 1402-1412.

Jordan, P., Copsey, A., Newnham, L., Kolar, E., Lichten, M., and Hoffmann, E. (2009). Ipl1/Aurora B kinase coordinates synaptonemal complex disassembly with cell cycle progression and crossover formation in budding yeast meiosis. *Genes & development* 23, 2237-2251.

Jordan, P., Karppinen, J., and Handel, M. (2012). Polo-like kinase is required for synaptonemal complex disassembly and phosphorylation in mouse spermatocytes. *Journal of cell science*.

Joyce, E.F., Apostolopoulos, N., Beliveau, B.J., and Wu, C.T. (2013). Germline progenitors escape the widespread phenomenon of homolog pairing during *Drosophila* development. *PLoS genetics* 9, e1004013.

Karpen, G.H., Le, M.H., and Le, H. (1996). Centric heterochromatin and the efficiency of achiasmate disjunction in *Drosophila* female meiosis. *Science* 273, 118-122.

Katis, V.L., Lipp, J.J., Imre, R., Bogdanova, A., Okaz, E., Habermann, B., Mechtler, K., Nasmyth, K., and Zachariae, W. (2010). Rec8 phosphorylation by casein kinase 1 and Cdc7-Dbf4 kinase regulates cohesin cleavage by separase during meiosis. *Developmental cell* 18, 397-409.

Katis, V.L., Matos, J., Mori, S., Shirahige, K., Zachariae, W., and Nasmyth, K. (2004). Spo13 facilitates monopolin recruitment to kinetochores and regulates maintenance of centromeric cohesion during yeast meiosis. *Current biology : CB* 14, 2183-2196.

Kee, K., Protacio, R.U., Arora, C., and Keeney, S. (2004). Spatial organization and dynamics of the association of Rec102 and Rec104 with meiotic chromosomes. *The EMBO journal* 23, 1815-1824.

Keeney, S., Giroux, C.N., and Kleckner, N. (1997). Meiosis-specific DNA double-strand breaks are catalyzed by Spo11, a member of a widely conserved protein family. *Cell* 88, 375-384.

- Kemp, B., Boumil, R.M., Stewart, M.N., and Dawson, D.S. (2004). A role for centromere pairing in meiotic chromosome segregation. *Genes & development* **18**, 1946-1951.
- Khetani, R.S., and Bickel, S.E. (2007). Regulation of meiotic cohesion and chromosome core morphogenesis during pachytene in *Drosophila* oocytes. *Journal of cell science* **120**, 3123-3137.
- Kiburz, B.M., Reynolds, D.B., Megee, P.C., Marston, A.L., Lee, B.H., Lee, T.I., Levine, S.S., Young, R.A., and Amon, A. (2005). The core centromere and Sgo1 establish a 50-kb cohesin-protected domain around centromeres during meiosis I. *Genes & development* **19**, 3017-3030.
- Kironmai, K.M., Muniyappa, K., Friedman, D.B., Hollingsworth, N.M., and Byers, B. (1998). DNA-binding activities of Hop1 protein, a synaptonemal complex component from *Saccharomyces cerevisiae*. *Molecular and cellular biology* **18**, 1424-1435.
- Kitajima, T.S., Kawashima, S.A., and Watanabe, Y. (2004). The conserved kinetochore protein shugoshin protects centromeric cohesion during meiosis. *Nature* **427**, 510-517.
- Kitajima, T.S., Sakuno, T., Ishiguro, K., Iemura, S., Natsume, T., Kawashima, S.A., and Watanabe, Y. (2006). Shugoshin collaborates with protein phosphatase 2A to protect cohesin. *Nature* **441**, 46-52.
- Kleckner, N. (2006). Chiasma formation: chromatin/axis interplay and the role(s) of the synaptonemal complex. *Chromosoma* **115**, 175-194.
- Klein, F., Mahr, P., Galova, M., Buonomo, S.B., Michaelis, C., Nairz, K., and Nasmyth, K. (1999). A central role for cohesins in sister chromatid cohesion, formation of axial elements, and recombination during yeast meiosis. *Cell* **98**, 91-103.
- Koszul, R., Kim, K.P., Prentiss, M., Kleckner, N., and Kameoka, S. (2008). Meiotic chromosomes move by linkage to dynamic actin cables with transduction of force through the nuclear envelope. *Cell* **133**, 1188-1201.
- Koszul, R., and Kleckner, N. (2009). Dynamic chromosome movements during meiosis: a way to eliminate unwanted connections? *Trends in cell biology* **19**, 716-724.
- Koszul, R., Meselson, M., Van Doninck, K., Vandenhaute, J., and Zickler, D. (2012). The Centenary of Janssens's Chiasmatype Theory. *Genetics* **191**, 309-317.
- Lacefield, S., and Murray, A.W. (2007). The spindle checkpoint rescues the meiotic segregation of chromosomes whose crossovers are far from the centromere. *Nature genetics* **39**, 1273-1277.

Lamb, N.E., Freeman, S.B., Savage-Austin, A., Pettay, D., Taft, L., Hersey, J., Gu, Y., Shen, J., Saker, D., May, K.M., *et al.* (1996). Susceptible chiasmate configurations of chromosome 21 predispose to non-disjunction in both maternal meiosis I and meiosis II. *Nature genetics* 14, 400-405.

Lammers, J.H., Offenberger, H.H., van Aalderen, M., Vink, A.C., Dietrich, A.J., and Heyting, C. (1994). The gene encoding a major component of the lateral elements of synaptonemal complexes of the rat is related to X-linked lymphocyte-regulated genes. *Molecular and cellular biology* 14, 1137-1146.

Lao, J.P., Cloud, V., Huang, C.C., Grubb, J., Thacker, D., Lee, C.Y., Dresser, M.E., Hunter, N., and Bishop, D.K. (2013). Meiotic crossover control by concerted action of rad51-dmc1 in homolog template bias and robust homeostatic regulation. *PLoS genetics* 9, e1003978.

Lao, J.P., Oh, S.D., Shinohara, M., Shinohara, A., and Hunter, N. (2008). Rad52 promotes postinvasion steps of meiotic double-strand-break repair. *Molecular cell* 29, 517-524.

Lechward, K., Awotunde, O.S., Swiatek, W., and Muszynska, G. (2001). Protein phosphatase 2A: variety of forms and diversity of functions. *Acta Biochim Pol* 48, 921-933.

Lee, B.H., and Amon, A. (2003). Role of Polo-like kinase CDC5 in programming meiosis I chromosome segregation. *Science* 300, 482-486.

Lee, B.H., Kiburz, B.M., and Amon, A. (2004). Spo13 maintains centromeric cohesion and kinetochore coorientation during meiosis I. *Current biology : CB* 14, 2168-2182.

Lee, H.Y., Chou, J.Y., Cheong, L., Chang, N.H., Yang, S.Y., and Leu, J.Y. (2008). Incompatibility of nuclear and mitochondrial genomes causes hybrid sterility between two yeast species. *Cell* 135, 1065-1073.

Li, J., Hooker, G.W., and Roeder, G.S. (2006). *Saccharomyces cerevisiae* Mer2, Mei4 and Rec114 form a complex required for meiotic double-strand break formation. *Genetics* 173, 1969-1981.

Li, P., Shao, Y., Jin, H., and Yu, H.G. (2015). Ndj1, a telomere-associated protein, regulates centrosome separation in budding yeast meiosis. *The Journal of cell biology* 209, 247-259.

Lin, F.M., Lai, Y.J., Shen, H.J., Cheng, Y.H., and Wang, T.F. (2010). Yeast axial-element protein, Red1, binds SUMO chains to promote meiotic interhomologue recombination and chromosome synapsis. *The EMBO journal* 29, 586-596.

Liu, J.G., Yuan, L., Brundell, E., Bjorkroth, B., Daneholt, B., and Hoog, C. (1996). Localization of the N-terminus of SCP1 to the central element of the synaptonemal complex and evidence for direct interactions between the N-

termini of SCP1 molecules organized head-to-head. *Experimental cell research* 226, 11-19.

Liu, Y., Gaines, W.A., Callender, T., Busygina, V., Oke, A., Sung, P., Fung, J.C., and Hollingsworth, N.M. (2014). Down-Regulation of Rad51 Activity during Meiosis in Yeast Prevents Competition with Dmc1 for Repair of Double-Strand Breaks. *PLoS genetics* 10, e1004005.

Llano, E., Herran, Y., Garcia-Tunon, I., Gutierrez-Caballero, C., de Alava, E., Barbero, J.L., Schimenti, J., de Rooij, D.G., Sanchez-Martin, M., and Pendas, A.M. (2012). Meiotic cohesin complexes are essential for the formation of the axial element in mice. *The Journal of cell biology* 197, 877-885.

Loidl, J., Scherthan, H., and Kaback, D.B. (1994). Physical association between nonhomologous chromosomes precedes distributive disjunction in yeast. *Proceedings of the National Academy of Sciences of the United States of America* 91, 331-334.

Longtine, M.S., McKenzie, A., 3rd, Demarini, D.J., Shah, N.G., Wach, A., Brachat, A., Philippsen, P., and Pringle, J.R. (1998). Additional modules for versatile and economical PCR-based gene deletion and modification in *Saccharomyces cerevisiae*. *Yeast* 14, 953-961.

Lowe, J., Cordell, S.C., and van den Ent, F. (2001). Crystal structure of the SMC head domain: an ABC ATPase with 900 residues antiparallel coiled-coil inserted. *J Mol Biol* 306, 25-35.

MacQueen, A.J., Colaiacovo, M.P., McDonald, K., and Villeneuve, A.M. (2002). Synapsis-dependent and -independent mechanisms stabilize homolog pairing during meiotic prophase in *C. elegans*. *Genes & development* 16, 2428-2442.

MacQueen, A.J., Phillips, C.M., Bhalla, N., Weiser, P., Villeneuve, A.M., and Dernburg, A.F. (2005). Chromosome sites play dual roles to establish homologous synapsis during meiosis in *C. elegans*. *Cell* 123, 1037-1050.

Macqueen, A.J., and Roeder, G.S. (2009). Fpr3 and Zip3 ensure that initiation of meiotic recombination precedes chromosome synapsis in budding yeast. *Current biology : CB* 19, 1519-1526.

Maleki, S., Neale, M.J., Arora, C., Henderson, K.A., and Keeney, S. (2007). Interactions between Mei4, Rec114, and other proteins required for meiotic DNA double-strand break formation in *Saccharomyces cerevisiae*. *Chromosoma* 116, 471-486.

Manfrini, N., Guerini, I., Citterio, A., Lucchini, G., and Longhese, M.P. (2010). Processing of meiotic DNA double strand breaks requires cyclin-dependent kinase and multiple nucleases. *The Journal of biological chemistry* 285, 11628-11637.

- Manheim, E.A., and McKim, K.S. (2003). The Synaptonemal complex component C(2)M regulates meiotic crossing over in *Drosophila*. *Current biology : CB* 13, 276-285.
- Marston, A.L. (2014). Chromosome segregation in budding yeast: sister chromatid cohesion and related mechanisms. *Genetics* 196, 31-63.
- Marston, A.L., Tham, W.H., Shah, H., and Amon, A. (2004). A genome-wide screen identifies genes required for centromeric cohesion. *Science* 303, 1367-1370.
- Matos, J., Blanco, M.G., Maslen, S., Skehel, J.M., and West, S.C. (2011). Regulatory control of the resolution of DNA recombination intermediates during meiosis and mitosis. *Cell* 147, 158-172.
- Matos, J., Lipp, J.J., Bogdanova, A., Guillot, S., Okaz, E., Junqueira, M., Shevchenko, A., and Zachariae, W. (2008). Dbf4-dependent CDC7 kinase links DNA replication to the segregation of homologous chromosomes in meiosis I. *Cell* 135, 662-678.
- Maxfield Boumil, R., Kemp, B., Angelichio, M., Nilsson-Tillgren, T., and Dawson, D.S. (2003). Meiotic segregation of a homeologous chromosome pair. *Mol Genet Genomics* 268, 750-760.
- McKim, K.S., Green-Marroquin, B.L., Sekelsky, J.J., Chin, G., Steinberg, C., Khodosh, R., and Hawley, R.S. (1998). Meiotic synapsis in the absence of recombination. *Science* 279, 876-878.
- Meuwissen, R.L., Offenberg, H.H., Dietrich, A.J., Riesewijk, A., van Iersel, M., and Heyting, C. (1992). A coiled-coil related protein specific for synapsed regions of meiotic prophase chromosomes. *The EMBO journal* 11, 5091-5100.
- Michaelis, C., Ciosk, R., and Nasmyth, K. (1997). Cohesins: chromosomal proteins that prevent premature separation of sister chromatids. *Cell* 91, 35-45.
- Mimitou, E.P., and Symington, L.S. (2008). Sae2, Exo1 and Sgs1 collaborate in DNA double-strand break processing. *Nature* 455, 770-774.
- Moldovan, G.L., Pfander, B., and Jentsch, S. (2006). PCNA controls establishment of sister chromatid cohesion during S phase. *Molecular cell* 23, 723-732.
- Monje-Casas, F., Prabhu, V.R., Lee, B.H., Boselli, M., and Amon, A. (2007). Kinetochore orientation during meiosis is controlled by Aurora B and the monopolin complex. *Cell* 128, 477-490.
- Muniyappa, K., Anuradha, S., and Byers, B. (2000). Yeast meiosis-specific protein Hop1 binds to G4 DNA and promotes its formation. *Molecular and cellular biology* 20, 1361-1369.

- Murakami, H., and Keeney, S. (2014). Temporospatial coordination of meiotic DNA replication and recombination via DDK recruitment to replisomes. *Cell* 158, 861-873.
- Nagaoka, S.I., Hassold, T.J., and Hunt, P.A. (2012). Human aneuploidy: mechanisms and new insights into an age-old problem. *Nature reviews Genetics* 13, 493-504.
- Nasmyth, K., and Haering, C.H. (2005). The structure and function of SMC and kleisin complexes. *Annu Rev Biochem* 74, 595-648.
- Nasmyth, K., and Haering, C.H. (2009). Cohesin: its roles and mechanisms. *Annual review of genetics* 43, 525-558.
- Nasmyth, K., Peters, J.M., and Uhlmann, F. (2000). Splitting the chromosome: cutting the ties that bind sister chromatids. *Science* 288, 1379-1385.
- Neale, M.J., Pan, J., and Keeney, S. (2005). Endonucleolytic processing of covalent protein-linked DNA double-strand breaks. *Nature* 436, 1053-1057.
- Newnham, L., Jordan, P., Rockmill, B., Roeder, G.S., and Hoffmann, E. (2010). The synaptonemal complex protein, Zip1, promotes the segregation of nonexchange chromosomes at meiosis I. *Proceedings of the National Academy of Sciences of the United States of America* 107, 781-785.
- Newnham, L., Jordan, P.W., Carballo, J.A., Newcombe, S., and Hoffmann, E. (2013). Ipl1/Aurora Kinase Suppresses S-CDK-Driven Spindle Formation during Prophase I to Ensure Chromosome Integrity during Meiosis. *PLoS one* 8, e83982.
- Offenberg, H.H., Schalk, J.A., Meuwissen, R.L., van Aalderen, M., Kester, H.A., Dietrich, A.J., and Heyting, C. (1998). SCP2: a major protein component of the axial elements of synaptonemal complexes of the rat. *Nucleic acids research* 26, 2572-2579.
- Oh, S.D., Lao, J.P., Hwang, P.Y., Taylor, A.F., Smith, G.R., and Hunter, N. (2007). BLM ortholog, Sgs1, prevents aberrant crossing-over by suppressing formation of multichromatid joint molecules. *Cell* 130, 259-272.
- Page, J., Berrios, S., Rufas, J.S., Parra, M.T., Suja, J.A., Heyting, C., and Fernandez-Donoso, R. (2003). The pairing of X and Y chromosomes during meiotic prophase in the marsupial species *Thylamys elegans* is maintained by a dense plate developed from their axial elements. *Journal of cell science* 116, 551-560.
- Page, J., Viera, A., Parra, M.T., de la Fuente, R., Suja, J.A., Prieto, I., Barbero, J.L., Rufas, J.S., Berrios, S., and Fernandez-Donoso, R. (2006). Involvement of synaptonemal complex proteins in sex chromosome segregation during marsupial male meiosis. *PLoS genetics* 2, e136.

Page, S.L., and Hawley, R.S. (2001). c(3)G encodes a *Drosophila* synaptonemal complex protein. *Genes & development* 15, 3130-3143.

Page, S.L., and Hawley, R.S. (2004). The genetics and molecular biology of the synaptonemal complex. *Annual review of cell and developmental biology* 20, 525-558.

Page, S.L., Khetani, R.S., Lake, C.M., Nielsen, R.J., Jeffress, J.K., Warren, W.D., Bickel, S.E., and Hawley, R.S. (2008). Corona is required for higher-order assembly of transverse filaments into full-length synaptonemal complex in *Drosophila* oocytes. *PLoS genetics* 4, e1000194.

Panizza, S., Mendoza, M.A., Berlinger, M., Huang, L.Z., Nicolas, A., Shirahige, K., and Klein, F. (2011). Spo11-Accessory Proteins Link Double-Strand Break Sites to the Chromosome Axis in Early Meiotic Recombination. *Cell* 146, 372-383.

Panizza, S., Tanaka, T., Hochwagen, A., Eisenhaber, F., and Nasmyth, K. (2000). Pds5 cooperates with cohesin in maintaining sister chromatid cohesion. *Current biology : CB* 10, 1557-1564.

Petronczki, M., Matos, J., Mori, S., Gregan, J., Bogdanova, A., Schwickart, M., Mechtler, K., Shirahige, K., Zachariae, W., and Nasmyth, K. (2006). Monopolar attachment of sister kinetochores at meiosis I requires casein kinase 1. *Cell* 126, 1049-1064.

Phillips, C.M., and Dernburg, A.F. (2006). A family of zinc-finger proteins is required for chromosome-specific pairing and synapsis during meiosis in *C. elegans*. *Developmental cell* 11, 817-829.

Prieto, I., Suja, J.A., Pezzi, N., Kremer, L., Martinez, A.C., Rufas, J.S., and Barbero, J.L. (2001). Mammalian STAG3 is a cohesin specific to sister chromatid arms in meiosis I. *Nature cell biology* 3, 761-766.

Rabitsch, K.P., Petronczki, M., Javerzat, J.P., Genier, S., Chwalla, B., Schleiffer, A., Tanaka, T.U., and Nasmyth, K. (2003). Kinetochores recruitment of two nucleolar proteins is required for homolog segregation in meiosis I. *Developmental cell* 4, 535-548.

Rasmussen, S.W. (1977). The transformation of the Synaptonemal Complex into the 'elimination chromatin' in *Bombyx mori* oocytes. *Chromosoma* 60, 205-221.

Revenkova, E., Eijpe, M., Heyting, C., Hodges, C.A., Hunt, P.A., Liebe, B., Scherthan, H., and Jessberger, R. (2004). Cohesin SMC1 beta is required for meiotic chromosome dynamics, sister chromatid cohesion and DNA recombination. *Nature cell biology* 6, 555-562.

Riedel, C.G., Katis, V.L., Katou, Y., Mori, S., Itoh, T., Helmhart, W., Galova, M., Petronczki, M., Gregan, J., Cetin, B., *et al.* (2006). Protein phosphatase 2A

protects centromeric sister chromatid cohesion during meiosis I. *Nature* **441**, 53-61.

Rockmill, B., Fung, J.C., Branda, S.S., and Roeder, G.S. (2003). The Sgs1 helicase regulates chromosome synapsis and meiotic crossing over. *Current biology : CB* **13**, 1954-1962.

Rockmill, B., and Roeder, G.S. (1990). Meiosis in asynaptic yeast. *Genetics* **126**, 563-574.

Rockmill, B., Sym, M., Scherthan, H., and Roeder, G.S. (1995). Roles for two RecA homologs in promoting meiotic chromosome synapsis. *Genes & development* **9**, 2684-2695.

Rockmill, B., Voelkel-Meiman, K., and Roeder, G.S. (2006). Centromere-proximal crossovers are associated with precocious separation of sister chromatids during meiosis in *Saccharomyces cerevisiae*. *Genetics* **174**, 1745-1754.

Rolef Ben-Shahar, T., Heeger, S., Lehane, C., East, P., Flynn, H., Skehel, M., and Uhlmann, F. (2008). Eco1-dependent cohesin acetylation during establishment of sister chromatid cohesion. *Science* **321**, 563-566.

Ross, L.O., Rankin, S., Shuster, M.F., and Dawson, D.S. (1996). Effects of homology, size and exchange on the meiotic segregation of model chromosomes in *Saccharomyces cerevisiae*. *Genetics* **142**, 79-89.

Rowland, B.D., Roig, M.B., Nishino, T., Kurze, A., Uluocak, P., Mishra, A., Beckouet, F., Underwood, P., Metson, J., Imre, R., *et al.* (2009). Building sister chromatid cohesion: smc3 acetylation counteracts an antiestablishment activity. *Molecular cell* **33**, 763-774.

Sakuno, T., Tada, K., and Watanabe, Y. (2009). Kinetochore geometry defined by cohesion within the centromere. *Nature* **458**, 852-858.

Sasanuma, H., Hirota, K., Fukuda, T., Kakusho, N., Kugou, K., Kawasaki, Y., Shibata, T., Masai, H., and Ohta, K. (2008). Cdc7-dependent phosphorylation of Mer2 facilitates initiation of yeast meiotic recombination. *Genes & development* **22**, 398-410.

Sasanuma, H., Murakami, H., Fukuda, T., Shibata, T., Nicolas, A., and Ohta, K. (2007). Meiotic association between Spo11 regulated by Rec102, Rec104 and Rec114. *Nucleic acids research* **35**, 1119-1133.

Schaerer, F., Morgan, G., Winey, M., and Philippsen, P. (2001). Cnm67p is a spacer protein of the *Saccharomyces cerevisiae* spindle pole body outer plaque. *Molecular biology of the cell* **12**, 2519-2533.

Schalk, J.A., Dietrich, A.J., Vink, A.C., Offenberger, H.H., van Aalderen, M., and Heyting, C. (1998). Localization of SCP2 and SCP3 protein molecules within synaptonemal complexes of the rat. *Chromosoma* 107, 540-548.

Schramm, S., Fraune, J., Naumann, R., Hernandez-Hernandez, A., Hoog, C., Cooke, H.J., Alsheimer, M., and Benavente, R. (2011). A novel mouse synaptonemal complex protein is essential for loading of central element proteins, recombination, and fertility. *PLoS genetics* 7, e1002088.

Severson, A.F., Ling, L., van Zuylen, V., and Meyer, B.J. (2009). The axial element protein HTP-3 promotes cohesin loading and meiotic axis assembly in *C. elegans* to implement the meiotic program of chromosome segregation. *Genes & development* 23, 1763-1778.

Shinohara, A., Gasior, S., Ogawa, T., Kleckner, N., and Bishop, D.K. (1997). *Saccharomyces cerevisiae* recA homologues RAD51 and DMC1 have both distinct and overlapping roles in meiotic recombination. *Genes to cells : devoted to molecular & cellular mechanisms* 2, 615-629.

Shinohara, M., Oh, S.D., Hunter, N., and Shinohara, A. (2008). Crossover assurance and crossover interference are distinctly regulated by the ZMM proteins during yeast meiosis. *Nature genetics* 40, 299-309.

Smith, A.V., and Roeder, G.S. (1997). The yeast Red1 protein localizes to the cores of meiotic chromosomes. *The Journal of cell biology* 136, 957-967.

Smith, G.R., Boddy, M.N., Shanahan, P., and Russell, P. (2003). Fission yeast Mus81.Eme1 Holliday junction resolvase is required for meiotic crossing over but not for gene conversion. *Genetics* 165, 2289-2293.

Snowden, T., Acharya, S., Butz, C., Berardini, M., and Fishel, R. (2004). hMSH4-hMSH5 recognizes Holliday Junctions and forms a meiosis-specific sliding clamp that embraces homologous chromosomes. *Molecular cell* 15, 437-451.

Sourirajan, A., and Lichten, M. (2008). Polo-like kinase Cdc5 drives exit from pachytene during budding yeast meiosis. *Genes & development* 22, 2627-2632.

Spencer, F., Hugerat, Y., Simchen, G., Hurko, O., Connelly, C., and Hieter, P. (1994). Yeast kar1 mutants provide an effective method for YAC transfer to new hosts. *Genomics* 22, 118-126.

Straight, A.F., Belmont, A.S., Robinett, C.C., and Murray, A.W. (1996). GFP tagging of budding yeast chromosomes reveals that protein-protein interactions can mediate sister chromatid cohesion. *Current biology : CB* 6, 1599-1608.

Sturtevant, A.H. (1951). A map of the fourth chromosome of *Drosophila melanogaster*, based on crossing over in triploid females. *Proceedings of the National Academy of Sciences of the United States of America* 37, 405-407.

Sturtevant, A.H., and Beadle, G.W. (1936). The Relations of Inversions in the X Chromosome of *Drosophila Melanogaster* to Crossing over and Disjunction. *Genetics* 21, 554-604.

Sun, F., and Handel, M.A. (2008). Regulation of the meiotic prophase I to metaphase I transition in mouse spermatocytes. *Chromosoma* 117, 471-485.

Sutani, T., Kawaguchi, T., Kanno, R., Itoh, T., and Shirahige, K. (2009). Budding yeast Wpl1(Rad61)-Pds5 complex counteracts sister chromatid cohesion-establishing reaction. *Current biology : CB* 19, 492-497.

Sym, M., Engebrecht, J.A., and Roeder, G.S. (1993). ZIP1 is a synaptonemal complex protein required for meiotic chromosome synapsis. *Cell* 72, 365-378.

Sym, M., and Roeder, G.S. (1994). Crossover interference is abolished in the absence of a synaptonemal complex protein. *Cell* 79, 283-292.

Sym, M., and Roeder, G.S. (1995). Zip1-induced changes in synaptonemal complex structure and polycomplex assembly. *The Journal of cell biology* 128, 455-466.

Szakai, B., and Branzei, D. (2013). Premature Cdk1/Cdc5/Mus81 pathway activation induces aberrant replication and deleterious crossover. *The EMBO journal* 32, 1155-1167.

Szostak, J.W., Orrweaver, T.L., Rothstein, R.J., and Stahl, F.W. (1983). The Double-Strand-Break Repair Model for Recombination. *Cell* 33, 25-35.

Takeo, S., Lake, C.M., Morais-de-Sa, E., Sunkel, C.E., and Hawley, R.S. (2011). Synaptonemal complex-dependent centromeric clustering and the initiation of synapsis in *Drosophila* oocytes. *Current biology : CB* 21, 1845-1851.

Tapley, E.C., and Starr, D.A. (2013). Connecting the nucleus to the cytoskeleton by SUN-KASH bridges across the nuclear envelope. *Current opinion in cell biology* 25, 57-62.

Thomas, S.E., Soltani-Bejnood, M., Roth, P., Dorn, R., Logsdon, J.M., Jr., and McKee, B.D. (2005). Identification of two proteins required for conjunction and regular segregation of achiasmate homologs in *Drosophila* male meiosis. *Cell* 123, 555-568.

Tomkiel, J.E., Wakimoto, B.T., and Briscoe, A., Jr. (2001). The teflon gene is required for maintenance of autosomal homolog pairing at meiosis I in male *Drosophila melanogaster*. *Genetics* 157, 273-281.

Toth, A., Ciosk, R., Uhlmann, F., Galova, M., Schleiffer, A., and Nasmyth, K. (1999). Yeast cohesin complex requires a conserved protein, Eco1p(Ctf7), to establish cohesion between sister chromatids during DNA replication. *Genes & development* 13, 320-333.

- Toth, A., Rabitsch, K.P., Galova, M., Schleiffer, A., Buonomo, S.B., and Nasmyth, K. (2000). Functional genomics identifies monopolin: a kinetochore protein required for segregation of homologs during meiosis I. *Cell* 103, 1155-1168.
- Tsubouchi, H., and Ogawa, H. (2000). Exo1 roles for repair of DNA double-strand breaks and meiotic crossing over in *Saccharomyces cerevisiae*. *Molecular biology of the cell* 11, 2221-2233.
- Tsubouchi, H., and Roeder, G.S. (2002). The Mnd1 protein forms a complex with hop2 to promote homologous chromosome pairing and meiotic double-strand break repair. *Molecular and cellular biology* 22, 3078-3088.
- Tsubouchi, T., Macqueen, A.J., and Roeder, G.S. (2008). Initiation of meiotic chromosome synapsis at centromeres in budding yeast. *Genes & development* 22, 3217-3226.
- Tsubouchi, T., and Roeder, G.S. (2005). A synaptonemal complex protein promotes homology-independent centromere coupling. *Science* 308, 870-873.
- Tsubouchi, T., Zhao, H., and Roeder, G.S. (2006). The meiosis-specific zip4 protein regulates crossover distribution by promoting synaptonemal complex formation together with zip2. *Developmental cell* 10, 809-819.
- Tung, K.S., and Roeder, G.S. (1998). Meiotic chromosome morphology and behavior in zip1 mutants of *Saccharomyces cerevisiae*. *Genetics* 149, 817-832.
- Uhlmann, F., Lottspeich, F., and Nasmyth, K. (1999). Sister-chromatid separation at anaphase onset is promoted by cleavage of the cohesin subunit Scc1. *Nature* 400, 37-42.
- Uhlmann, F., and Nasmyth, K. (1998). Cohesion between sister chromatids must be established during DNA replication. *Current Biology* 8, 1095-1101.
- Unal, E., Heidinger-Pauli, J.M., Kim, W., Guacci, V., Onn, I., Gygi, S.P., and Koshland, D.E. (2008). A molecular determinant for the establishment of sister chromatid cohesion. *Science* 321, 566-569.
- Vallen, E.A., Hiller, M.A., Scherson, T.Y., and Rose, M.D. (1992). Separate domains of KAR1 mediate distinct functions in mitosis and nuclear fusion. *The Journal of cell biology* 117, 1277-1287.
- Vazquez, J., Belmont, A.S., and Sedat, J.W. (2002). The dynamics of homologous chromosome pairing during male *Drosophila* meiosis. *Current biology : CB* 12, 1473-1483.
- Voelkel-Meiman, K., Taylor, L.F., Mukherjee, P., Humphries, N., Tsubouchi, H., and Macqueen, A.J. (2013). SUMO Localizes to the Central Element of Synaptonemal Complex and Is Required for the Full Synapsis of Meiotic Chromosomes in Budding Yeast. *PLoS genetics* 9, e1003837.

Von Stetina, J.R., Tranguch, S., Dey, S.K., Lee, L.A., Cha, B., and Drummond-Barbosa, D. (2008). alpha-Endosulfine is a conserved protein required for oocyte meiotic maturation in *Drosophila*. *Development* 135, 3697-3706.

Wan, L., de los Santos, T., Zhang, C., Shokat, K., and Hollingsworth, N.M. (2004). Mek1 kinase activity functions downstream of RED1 in the regulation of meiotic double strand break repair in budding yeast. *Molecular biology of the cell* 15, 11-23.

Wan, L., Niu, H., Futcher, B., Zhang, C., Shokat, K.M., Boulton, S.J., and Hollingsworth, N.M. (2008). Cdc28-Clb5 (CDK-S) and Cdc7-Dbf4 (DDK) collaborate to initiate meiotic recombination in yeast. *Genes & development* 22, 386-397.

Wanat, J.J., Kim, K.P., Koszul, R., Zanders, S., Weiner, B., Kleckner, N., and Alani, E. (2008). Csm4, in collaboration with Ndj1, mediates telomere-led chromosome dynamics and recombination during yeast meiosis. *PLoS genetics* 4, e1000188.

Wang, B.D., Yong-Gonzalez, V., and Strunnikov, A.V. (2004). Cdc14p/FEAR pathway controls segregation of nucleolus in *S. cerevisiae* by facilitating condensin targeting to rDNA chromatin in anaphase. *Cell Cycle* 3, 960-967.

Watanabe, Y., and Nurse, P. (1999). Cohesin Rec8 is required for reductional chromosome segregation at meiosis. *Nature* 400, 461-464.

Webber, H.A., Howard, L., and Bickel, S.E. (2004). The cohesion protein ORD is required for homologue bias during meiotic recombination. *The Journal of cell biology* 164, 819-829.

Winey, M., Mamay, C.L., O'Toole, E.T., Mastronarde, D.N., Giddings, T.H., Jr., McDonald, K.L., and McIntosh, J.R. (1995). Three-dimensional ultrastructural analysis of the *Saccharomyces cerevisiae* mitotic spindle. *The Journal of cell biology* 129, 1601-1615.

Winkel, K., Alsheimer, M., Ollinger, R., and Benavente, R. (2009). Protein SYCP2 provides a link between transverse filaments and lateral elements of mammalian synaptonemal complexes. *Chromosoma* 118, 259-267.

Winters, T., McNicoll, F., and Jessberger, R. (2014). Meiotic cohesin STAG3 is required for chromosome axis formation and sister chromatid cohesion. *The EMBO journal* 33, 1256-1270.

Wolf, K.W. (1994). How meiotic cells deal with non-exchange chromosomes. *BioEssays : news and reviews in molecular, cellular and developmental biology* 16, 107-114.

Woltering, D., Baumgartner, B., Bagchi, S., Larkin, B., Loidl, J., de los Santos, T., and Hollingsworth, N.M. (2000). Meiotic segregation, synapsis, and

recombination checkpoint functions require physical interaction between the chromosomal proteins Red1p and Hop1p. *Molecular and cellular biology* 20, 6646-6658.

Xiang, Y., Takeo, S., Florens, L., Hughes, S.E., Huo, L.J., Gilliland, W.D., Swanson, S.K., Teeter, K., Schwartz, J.W., Washburn, M.P., *et al.* (2007). The inhibition of polo kinase by matrimony maintains G2 arrest in the meiotic cell cycle. *PLoS Biol* 5, e323.

Xu, H., Beasley, M.D., Warren, W.D., van der Horst, G.T., and McKay, M.J. (2005). Absence of mouse REC8 cohesin promotes synapsis of sister chromatids in meiosis. *Developmental cell* 8, 949-961.

Xu, L., Ajimura, M., Padmore, R., Klein, C., and Kleckner, N. (1995). NDT80, a meiosis-specific gene required for exit from pachytene in *Saccharomyces cerevisiae*. *Molecular and cellular biology* 15, 6572-6581.

Yan, R., and McKee, B.D. (2013). The cohesion protein SOLO associates with SMC1 and is required for synapsis, recombination, homolog bias and cohesion and pairing of centromeres in *Drosophila* Meiosis. *PLoS genetics* 9, e1003637.

Yang, F., De La Fuente, R., Leu, N.A., Baumann, C., McLaughlin, K.J., and Wang, P.J. (2006). Mouse SYCP2 is required for synaptonemal complex assembly and chromosomal synapsis during male meiosis. *The Journal of cell biology* 173, 497-507.

Yu, H.G., and Koshland, D. (2007). The Aurora kinase Ipl1 maintains the centromeric localization of PP2A to protect cohesin during meiosis. *The Journal of cell biology* 176, 911-918.

Zakharyevich, K., Tang, S., Ma, Y., and Hunter, N. (2012). Delineation of joint molecule resolution pathways in meiosis identifies a crossover-specific resolvase. *Cell* 149, 334-347.

Zetka, M.C., Kawasaki, I., Strome, S., and Muller, F. (1999). Synapsis and chiasma formation in *Caenorhabditis elegans* require HIM-3, a meiotic chromosome core component that functions in chromosome segregation. *Genes & development* 13, 2258-2270.

Zhang, J., Pawlowski, W.P., and Han, F. (2013). Centromere pairing in early meiotic prophase requires active centromeres and precedes installation of the synaptonemal complex in maize. *Plant Cell* 25, 3900-3909.

Zhang, J., Shi, X., Li, Y., Kim, B.J., Jia, J., Huang, Z., Yang, T., Fu, X., Jung, S.Y., Wang, Y., *et al.* (2008). Acetylation of Smc3 by Eco1 is required for S phase sister chromatid cohesion in both human and yeast. *Molecular cell* 31, 143-151.

Zhu, Z., Mori, S., Oshiumi, H., Matsuzaki, K., Shinohara, M., and Shinohara, A. (2010). Cyclin-dependent kinase promotes formation of the synaptonemal

complex in yeast meiosis. *Genes to cells : devoted to molecular & cellular mechanisms* 15, 1036-1050.

Zickler, D., and Kleckner, N. (1998). The leptotene-zygotene transition of meiosis. *Annual review of genetics* 32, 619-697.

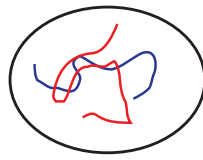
Zickler, D., and Kleckner, N. (1999). Meiotic chromosomes: integrating structure and function. *Annual review of genetics* 33, 603-754.

Zickler, D., and Kleckner, N. (2015). Recombination, Pairing, and Synapsis of Homologs during Meiosis. *Cold Spring Harbor perspectives in biology*

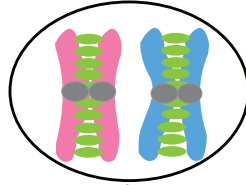
Figure 1.1 The overview of meiosis

Green dots indicate cohesins, homologue is coloured in blue and homologue is coloured in red. Black lines and dots indicate spindle pole bodies. Meiosis starts with the replication of chromosomes at S-phase (A) and the establishment of cohesins, which holds sister chromatids together (B). At prophase I, non-sister chromatids crossing with each other are created by DNA double-strand breaks (not shown). This eventually leads to the formation of chiasmata and a bivalent. (C) The bivalents line up in the centre and attach to the spindle via kinetochores. Sister kinetochores are mono-orientated and resisted by chiasmata (arrows indicate the direction of orientation) (D) This results in chromatids being pulled apart in anaphase I (E) At telophase I, the occurrence of cytokinesis leads to formation of two cells. Each cell contains a set of chromatids (F) Meiosis II is similar to mitosis where sister chromatids line up in the centre in metaphase II and sister kinetochores bi-orientate (directions are shown by the arrows (G) This ultimately results in sister chromatids been pulled over by spindle poles to opposite sides (H) At the very end of meiosis, four cells each with different genotype have been produced (I).

a) pre-meiotic S phase

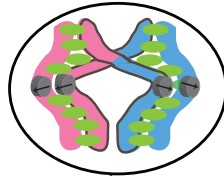


b) DNA replication and cohesion establishment

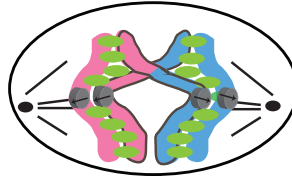


Meiosis I

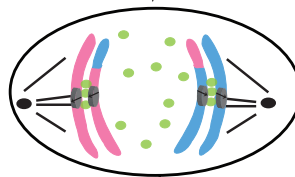
c) Prophase I



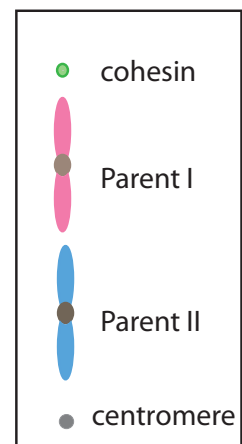
d) Metaphase I



e) Anaphase I



f) Telophase I

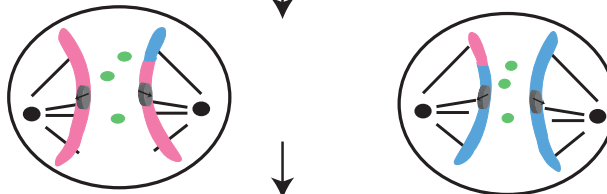


Meiosis II

g) Metaphase II



h) Anaphase II



i) Telophase II

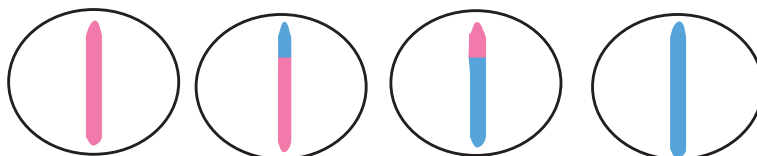


Figure 1.2 The structure of cohesin complex and its proposed models

(A) Cohesin complex forms a ring structure, consists of the the SMC family Smc1 and Smc3 and a kleisin subunit (Scc1 or Rec8 in meiosis). Both proteins have two coiled-coiled region with a hinge domain. It is postulated that these coiled-coiled regions fold back in an anti parallel fashion, placing the hinge domain at one end and the head domain at the other end. The head domain consists of the N-terminal Walker A motif and C-terminal Walker B motif. Scc1 (Rec8 in meiosis) binds to both head domains of Smc1 and Smc3. Scc3 interacts with the C-terminal of the SMC proteins. This ring structure is ~40 nm in diameter. Pds5 is also found loosely connected to the cohesin ring and is involved in the establishment of cohesins. Scc2 and Scc4 are involved in the association of cohesins to chromosomes. (B) Three different models proposed for cohesin attachment to chromatids. Model one is referred as the 'Embrace' model, where cohesin ring entraps both sister chromatids. Model 2 is referred to as the 'Hand cuff' model, where it was suggested that cohesins bind to DNA at one side and interact with opposite cohesins that binds to the opposite DNA and polymerize. Model 3 referred as 'Interlinking embrace' model. In this model, it was suggested that individual cohesin entrap individual sister chromatids and these cohesins are connected with each other. (C) Current proposed model for cohesin loading (the 'embrace model'). Once the cohesin ring is complete, Scc1 and Scc2 comes along with the help of ATP hydrolysis, leads to the opening of the cohesin ring. ATP hydrolysis make sure the cohesins entraps to the chromatids [adapted from (Marston, 2014)].

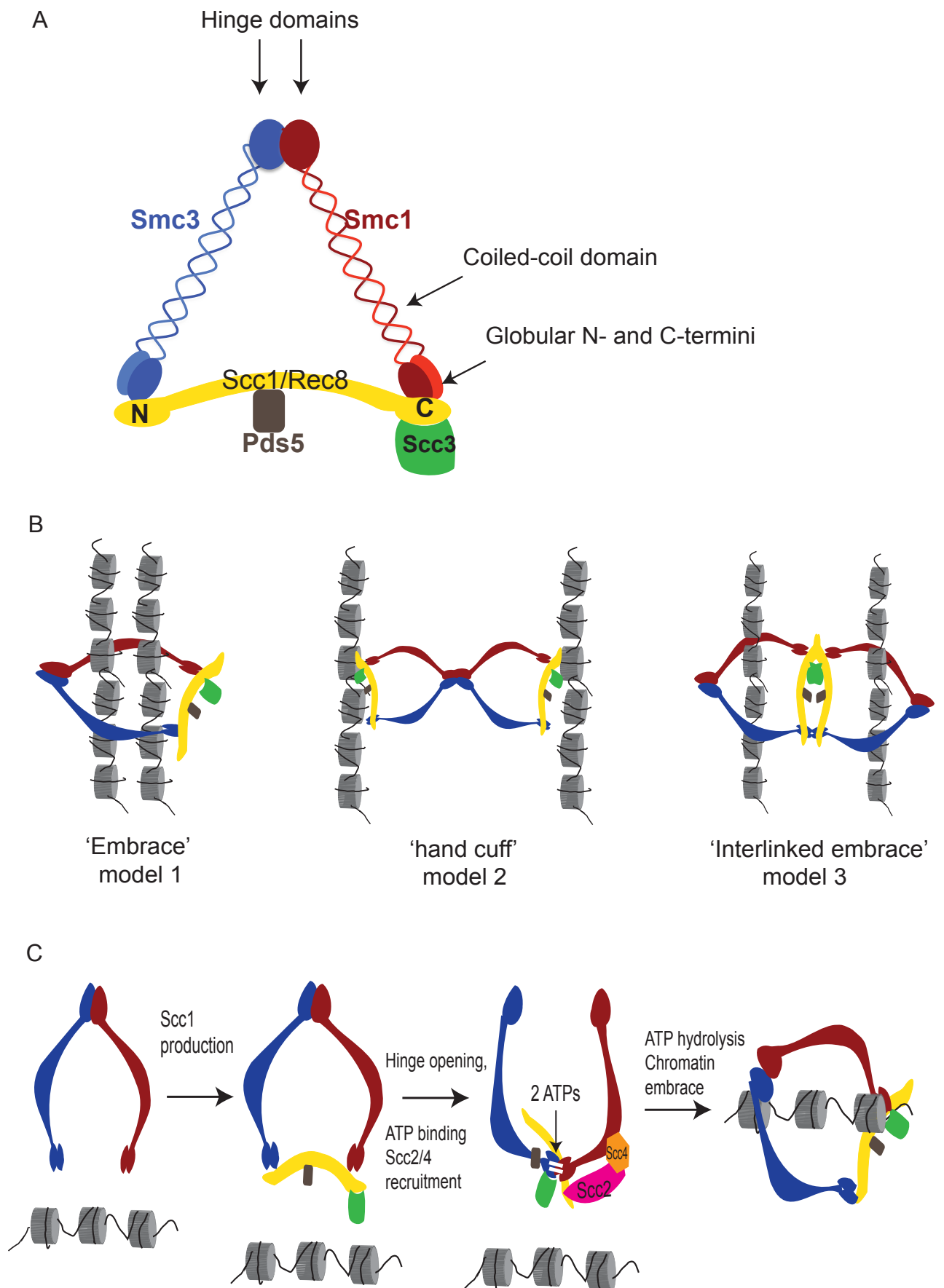


Figure 1.3 The timeline of meiotic prophase I

Four stages of prophase I is showing in this diagram, which are leptotene, zygotene, pachytene and diplotene. (A) Change of chromosomes during prophase I. During leptotene, synapsis initiation begins during this stage and punctuate foci of Zip1 can be observed under fluorescence microscopy. As SC initiates and the central element Zip1 begins to polymerize, short segment of SC observed during zygonema. Pachynema is when the SC is completely formed, this is observed with linear Zip1 staining under microscopy. Pachynema is followed by disassembly of the SC, which marks the stage of diplonema. Chiasmata are formed after SC disassembles. (B) Timeline showing changing of DNA level during meiotic prophase I. See text for detail. (C) Outline of proteins involved during each stage of prophase I. (D) Involvement of condensin and cohesin during prophase I. AE (axial element); AA (axial association); LE (lateral element DSB (double-strand breaks); SEI (single end invasion); dHJ (double Holliday Junction); SIC (synapsis initiation complex);

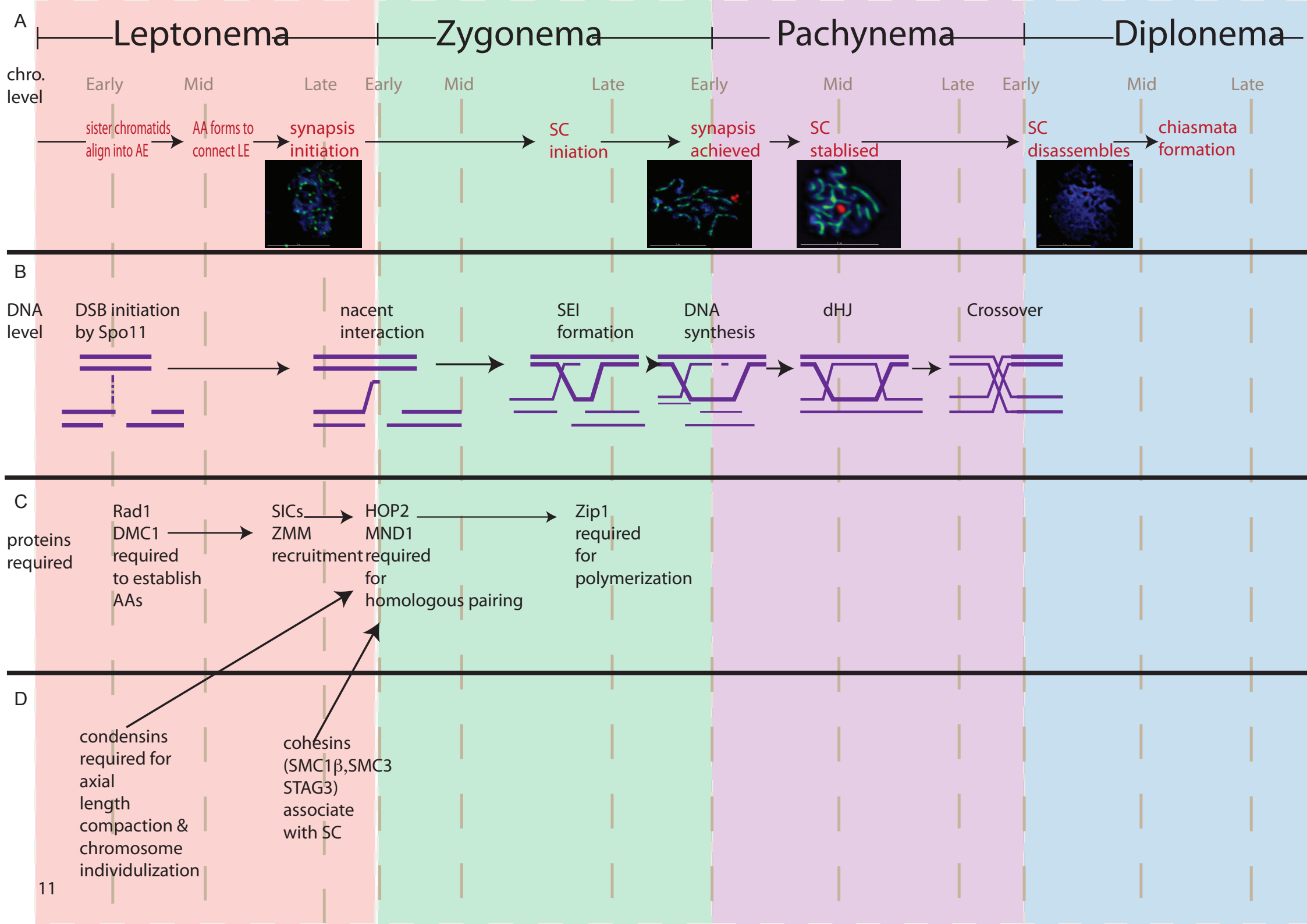


Figure 1.4 Centromere coupling in budding yeast

During pre-meiotic prophase I, non-homologous chromosomes are held together at their centromere by Zip1. As meiosis proceeds, DNA double-strand break initiation by Spo11 leads to activation of Mec1 kinase. This kinase in turn phosphorylates Zip1 on residue S75, this action leads to hyperphosphorylation of Zip1 and thus de-coupling. During prophase I, PP4 complex comes along to dephosphorylate Zip1-S75 and centromere pairing between homologous chromosomes occurs.

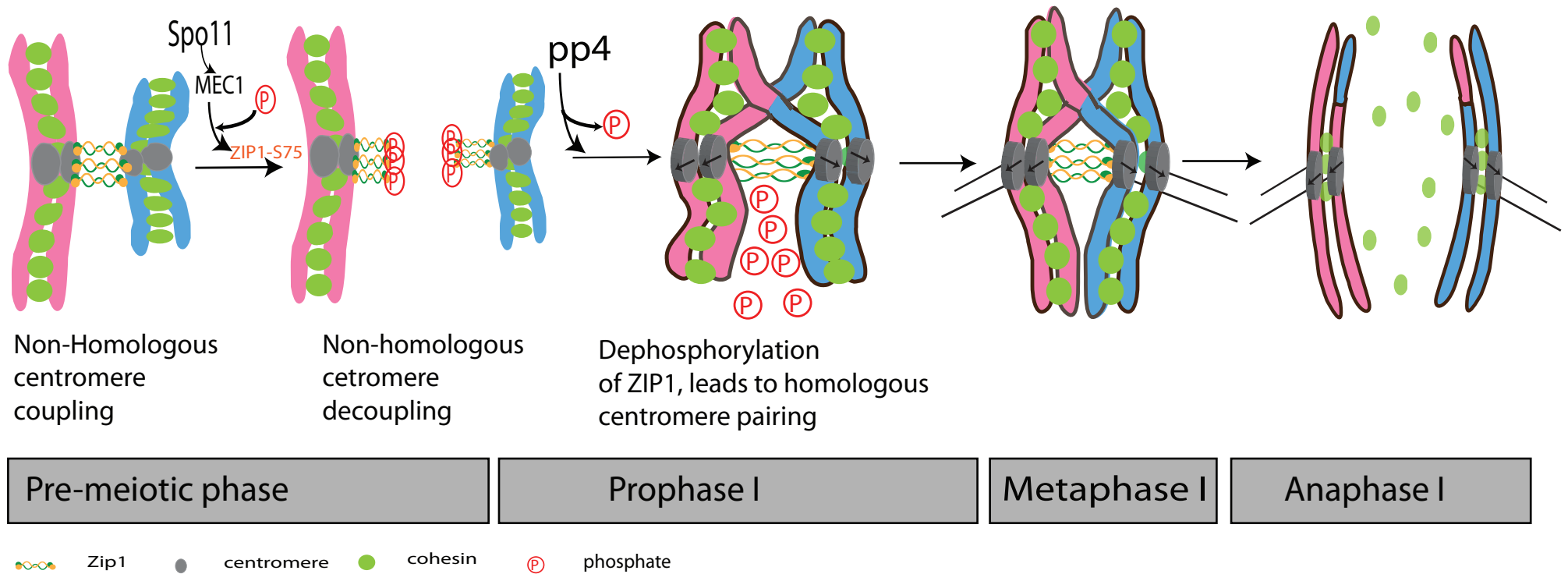


Figure 1.5 The models of meiotic DNA double strand break

(A) DNA double-strand break (DSBs) formation is catalyzed by Spo11 (orange ovals). (B) Endonuclease activity releases Spo11 covalently bound to an oligonucleotide, and 5'-to-3' exonuclease activity exposes single-stranded (ss) 3' ends. Recombinases such as Rad51 and/or Dmc1 coat the ssDNA tail and catalyze strand invasion into the intact DNA duplex of a homologous chromosome. Invasion of the Rad51/Dmc1-containing nucleoprotein filament results in an asymmetric strand-exchange intermediate. (C) The 'ZMM' pathway, in which Mer3 and Msh4-Msh5 promotes and stabilize single end invasion (SEI). Using intact DNA duplex as template, 'Displacement loop' D-loop is formed by the invading of the 3' end. This results in second end capture and repair synthesis of the other 3' end. Subsequently a double Holliday junction (dHJ) is formed through ligation of the newly synthesized strands. Cleavage of both Holliday junctions generates crossovers. (D) The synthesis-dependent strand annealing (SDSA) pathway. This pathway forms non-crossovers at the end. Second end capture is not present in this pathway compared to the 'ZMM' pathway. In fact, recapture by the second end occurs after DNA repair synthesis to yield non-crossovers. (E) The Mus81/Mms4 pathway. In this pathway, Mus81 nicks branched DNA to generate crossovers without a dHJ intermediate. Purple/pink lines represent each chromatids of a homologous chromosome. Blue/light blue lines represent the opposite chromatids of another homologous chromosome. Diagram adapted from Whitby, M. C. (2005). "Making crossovers during meiosis

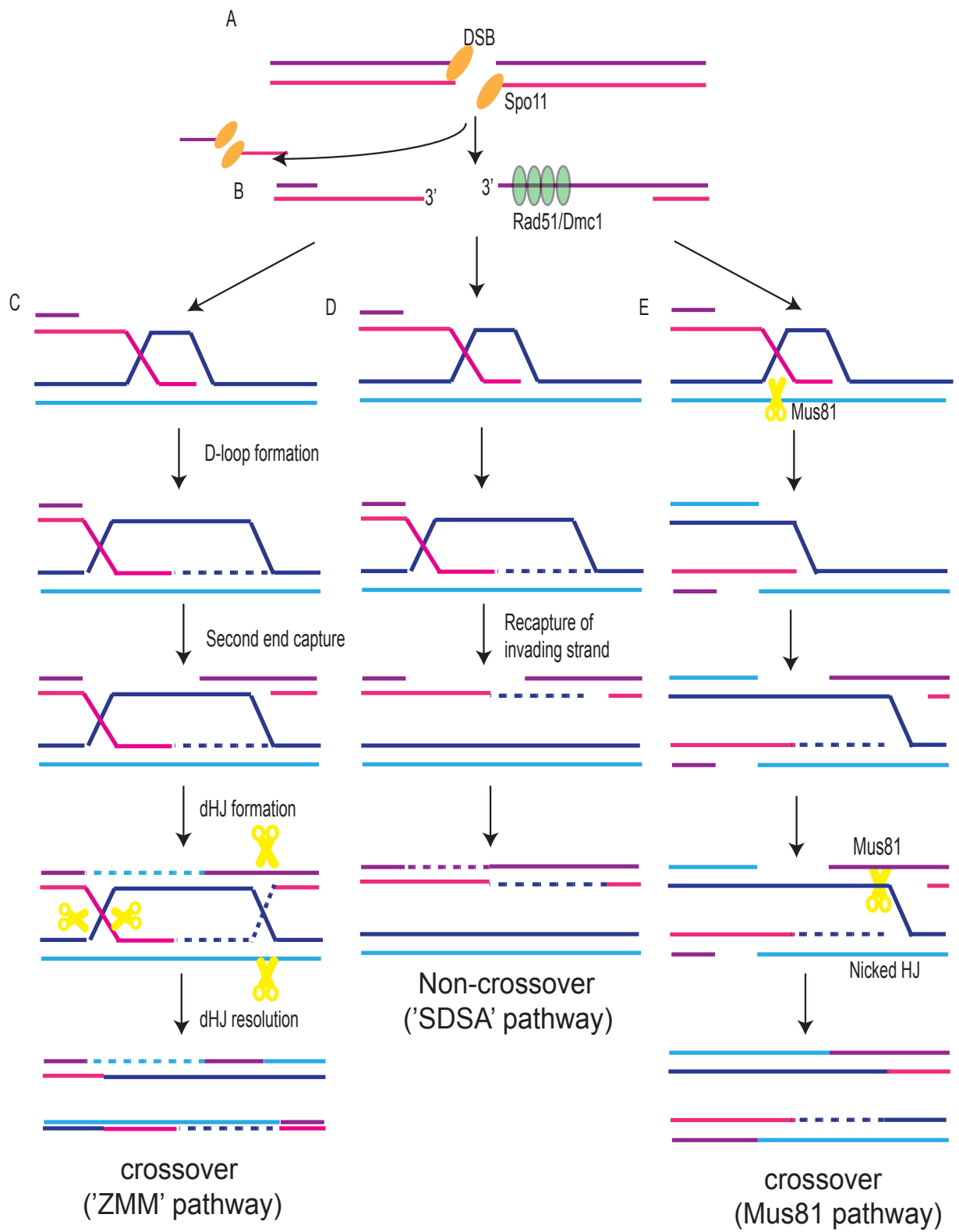
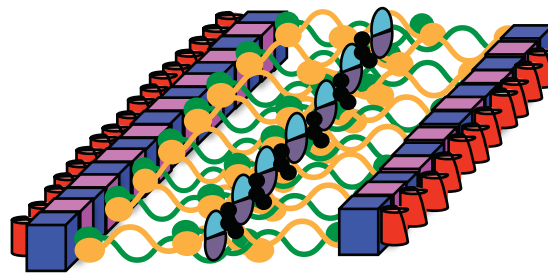








Figure 1.6 Systemic diagram present the Synaptonemal complex in different species

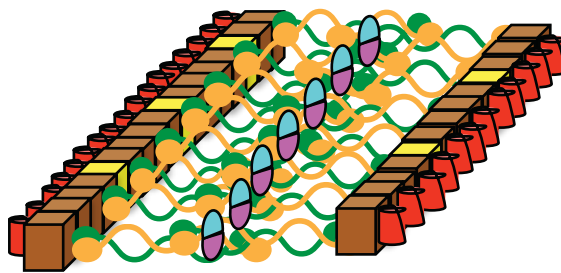
The structure of the Synaptonemal complex in different species: (A) yeast; (B) Flies (*Drosophila*); (C) Worms; (D) Mammals. See text for details.






A *Scaromyces cerevisiae*



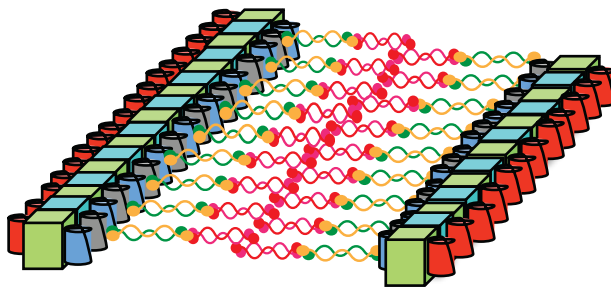
-  Cohesin
-  Red1
-  Hop1
-  Ecm11
Gmc2
-  SUMO
chain
-  Zip1








B *Drosophila*



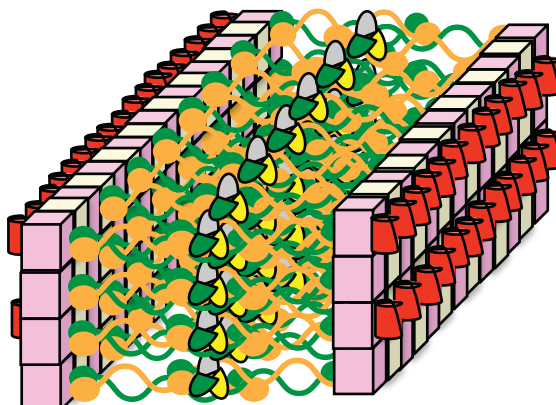
-  ORD
-  C(2)M
-  Cohesin
-  Corona
Corolla
-  C(3)G

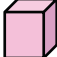




C Worms



-  SYP-1
-  SYP-2
-  HIM-3
-  HTP-3
-  HTP-1
-  HTP-2
-  Cohesin

D Mammals



-  SYCP2
-  SYCP3
-  Cohesin
-  SYCP1
-  SYCE1
SYCE2
TEX12

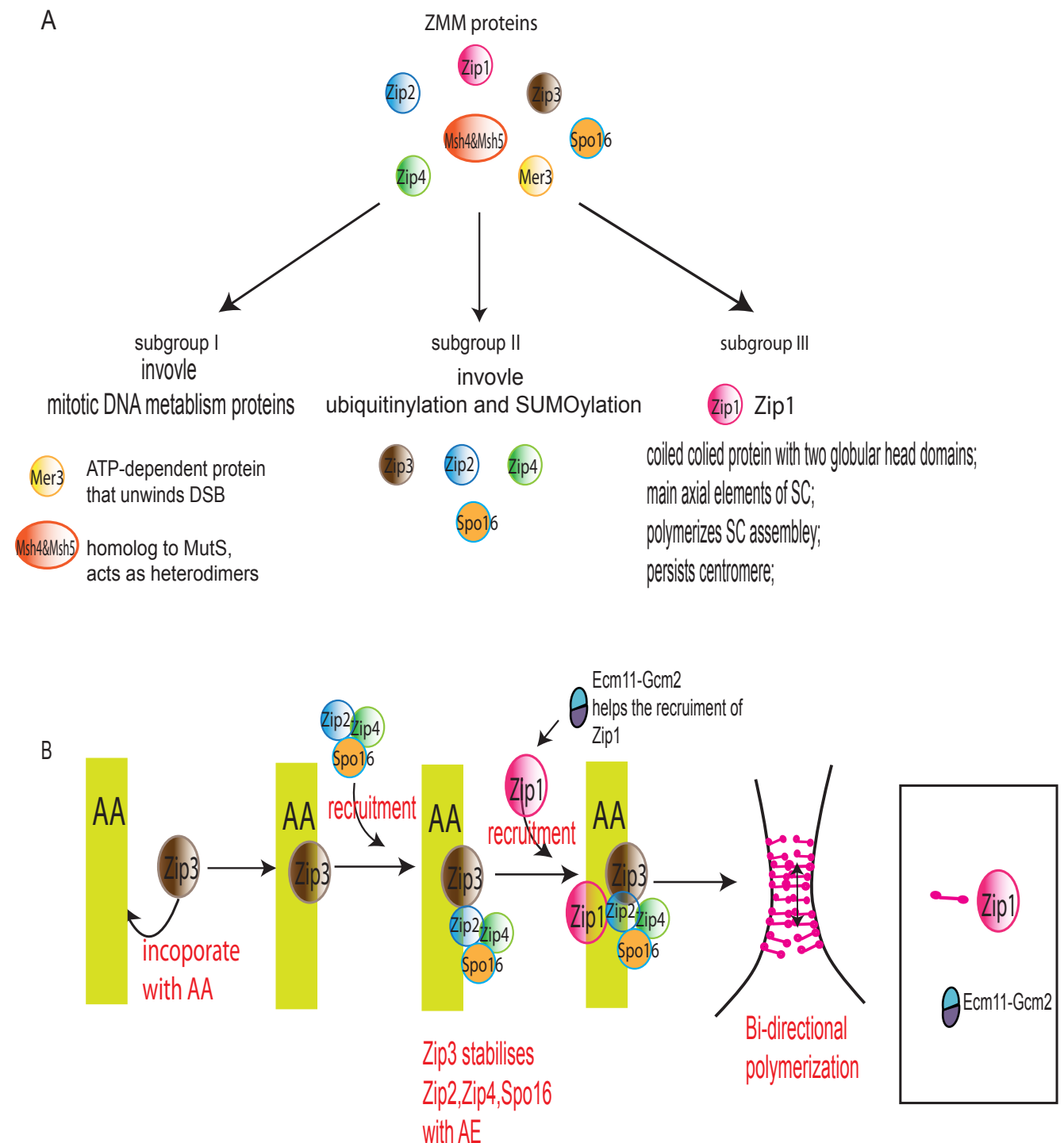


Figure 1.7. Categories of the 'ZMM' proteins and their involvements in synapsis initiation.

(A) A group of proteins involved Zip1, Zip2, Zip3, Zip4, Spo16, Msh4, Msh5 and Mer3 is termed 'ZMM' proteins. These proteins are differentiated into functional group and they share the similar phenotype in meiosis. (B) Synapsis initiation process, where Zip3 first binds to the axial association (AA) and stabilise into axial elements (AE). It then recruits Zip2, Zip4, Spo16 to the AE, which is required to help to recruit Zip1. Ecm11-Gcm2 is also required after Zip3 binding to the AA to help to polymerize Zip1. Once Zip1 is loaded onto the axis it starts to polymerize in a bi-directional manner. AA (Axial association), AE (Axial element), SC (synaptonemal complex), DSB (double-strand break)

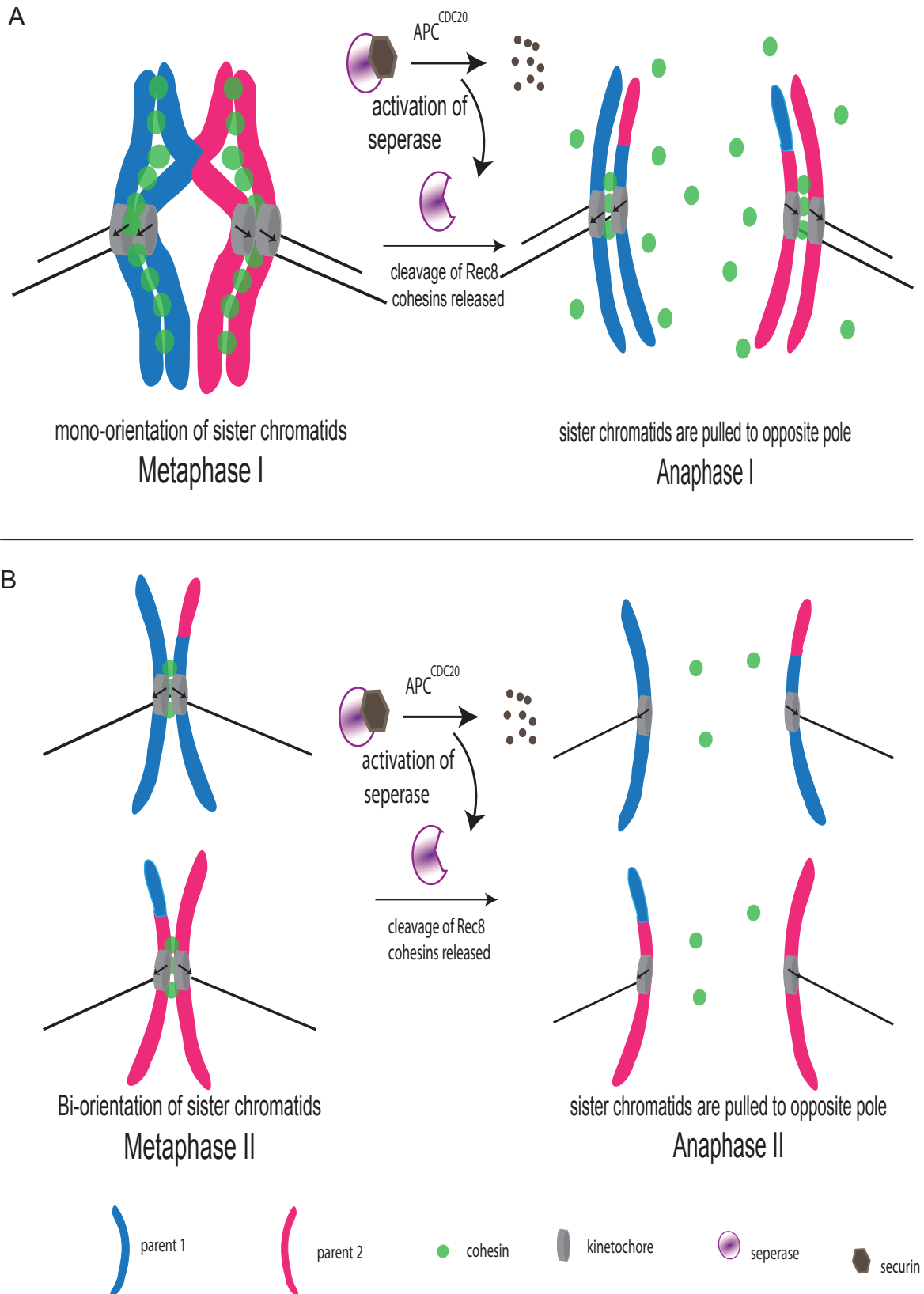


Figure 1.8: orientation of centromeres

The diagram represents the orientation of kinetochores in meiosis.

(A) The top diagram shows that sister kinetochores (grey) are mono-orientated (arrows indicate the direction). Once this is achieved, separase is activated to remove Rec8 along chromosome arms. Centromeric cohesins are preserved.

(B) The bottom diagram shows the orientation of kinetochores in meiosis II, where sister kinetochores are bi-orientated and they are pulled apart by spindle pores. Centromeric cohesins are lost at anaphase I

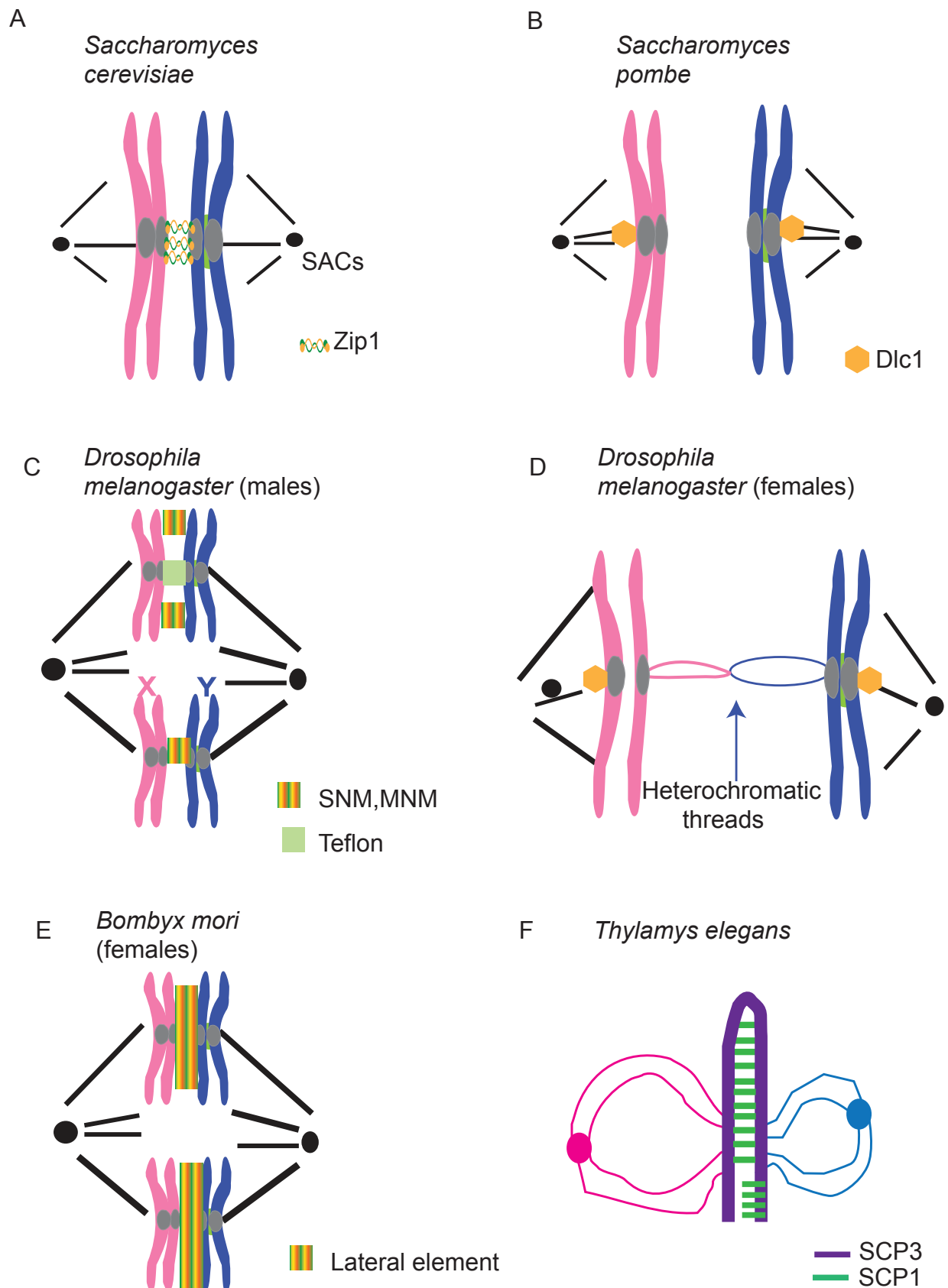


Figure 1.10: Example of few organisms in non-exchange chromosome segregation

Pink presenting one parent and blue presenting another parent. Mechanisms of few organisms are showing, see text for details.

Figure 3.1 Zip1 sites identified through Zip1 IP and Cdc5 proteomic screen

(A) Summary of Zip1-phospho serine/threonine sites identified through Zip1-IP (yellow) as well as nuclear extract method (blue). (B) Zip1-phospho sites identified from nuclear extract that were consensus for CK2 or DDK (labelled in red). The site that is only consensus for CK2 is labelled in brown (*ZIP1-S137*). (C) Systematic diagram representing mutated phosphorylation sites that were identified from Zip-IP. Three different combinations were made. One mutant contains mutation from all four sites. One mutant contains the three CDK sites and another mutant only contains T144 mutation to alanine. (D) Representative diagram showing the mutation of phosphorylation sites identified from nuclear extract, which were consensus for CK2 and DDK. (E) The *zip1-8A* mutant made by Dr. Andreas Hochwagen.

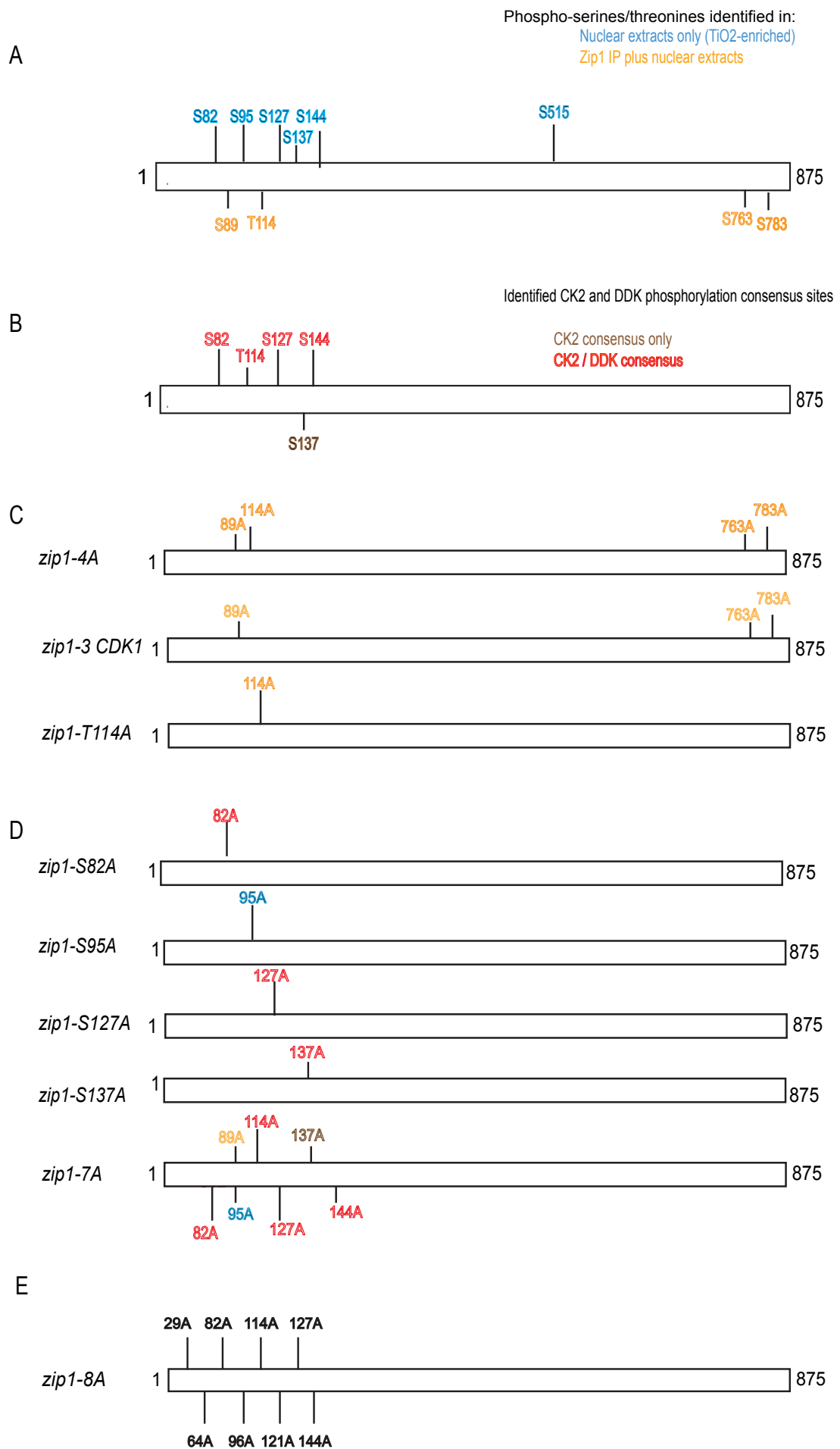


Figure 3.2 Sporulation and viability characterization for Zip1-phospho mutants

(A) A quantitative bar chart represents sporulation efficiency for all Zip1-phosphomutants. All mutants were harvested in sporulation media and samples were taken at T24. Number above shows the overall sporulation efficiency for each strain. >100 nuclei scored for each strain. Sporulation efficiency is divided into three categories. 'Tetrads' shown in blue referred to as four spores in a nucleus. 'Dyads' shown in red referred to two spores in a nucleus. 'Monads' referred to as one or none spores in a nucleus (green). Overall sporulation efficiency was calculated by dividing the total number of spores containing tetrads and dyads over the total number of spores containing tetrads, dyads and monads. (B) Spore viability for all Zip1-phospho mutants shown in a bar chart. Number above represents total number of spore viability. 100 tetrads assessed for the wild-type, *zip1Δ*, *zip1-S82A-O*, *zip1-S82A-1*, *zip1-S82A-2*, *zip1-S82A3*, *zip1-T114A*, *zip1-T114E*, *zip1-4A*, *zip1-7A*, *zip1-8A*, *zip1-8E* mutants. 20 tetrads assessed for mutants *zip1-S95A*, *zip1-S127A*, *zip1-S127E*, *zip1-S127DE* and *zip1-S137A*. Four viable spores shown in dark blue; three viable spores shown in red; two viable spores shown in green; purple represents one viable spore and light blue represents no spores growing. Asterisk indicates significant differences between the wild-type and the mutant (* $P < 0.01$; **** $P < 0.0001$, G test for homogeneity).

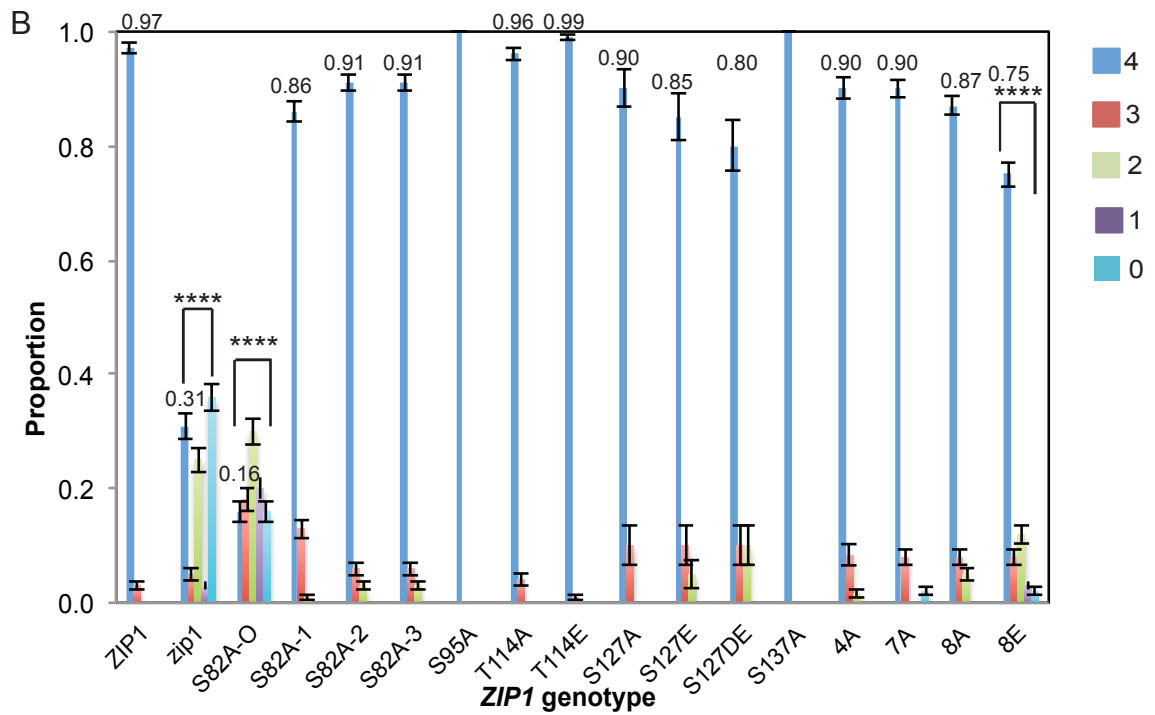
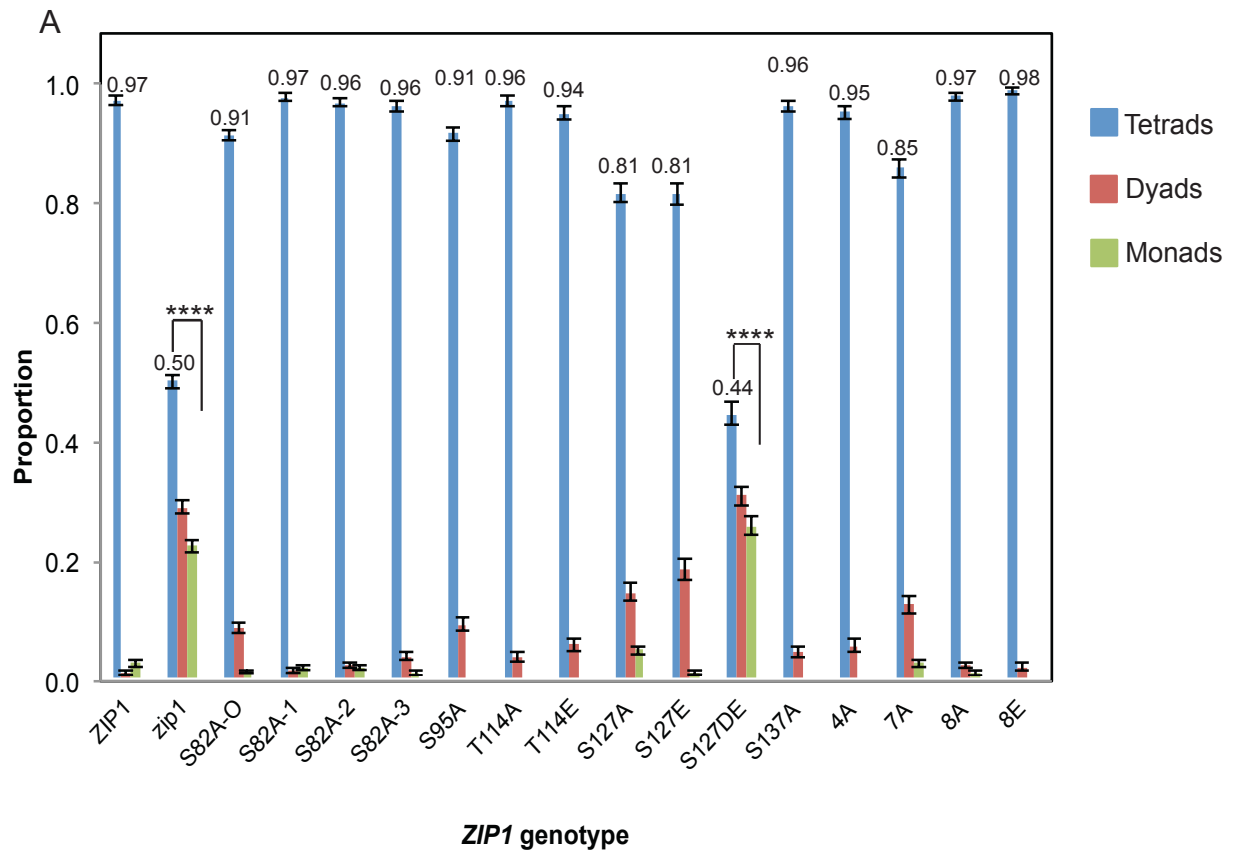


Figure 3.3 Centromeric coupling in Zip1-phospho mutants

All strains used are *spo11-Y135F* background, this is the catalytic subunit of Spo11 (see text for description). Ctf19 is a kinetochore protein and is used as a marker for the centromere, shown in green in merged images. Zip1 is shown in magenta in the merged images. (A) Representative spread images of wild-type centromere coupling and its quantification is shown in (B). Quantification of centromere coupling in the wild-type. 48 nuclei scored. (C) Representative spread images of *zip1Δ* as a control. (D) Quantification of number of Ctf19 foci in *zip1Δ*. 57 nuclei were scored (E) Representative images of centromere coupling in *zip1-T114A* with ctf19 foci quantification shown in (F). 101 nuclei were scored (G) Example of spread images for *zip1-T114E*. 50 nuclei were scored (H) Quantification of centromere coupling in *zip1-T114E*. (I) Spread images showing centromere coupling for *zip1-4A* with its quantification shown in (J). (K) A representative image shows centromere coupling for *zip1-3A*. (L) Quantification of Ctf19 foci in *zip1-3A*. (M,O,Q) Representative images for centromere coupling in *zip1-7A*; *zip1-8A* and *zip1-8E* respectively. (Q,P,R) Quantification of centromere coupling in *zip1-7A*, *8A*, *8E* respectively. Arrows indicate polycomplexes. Bars: 2μm.

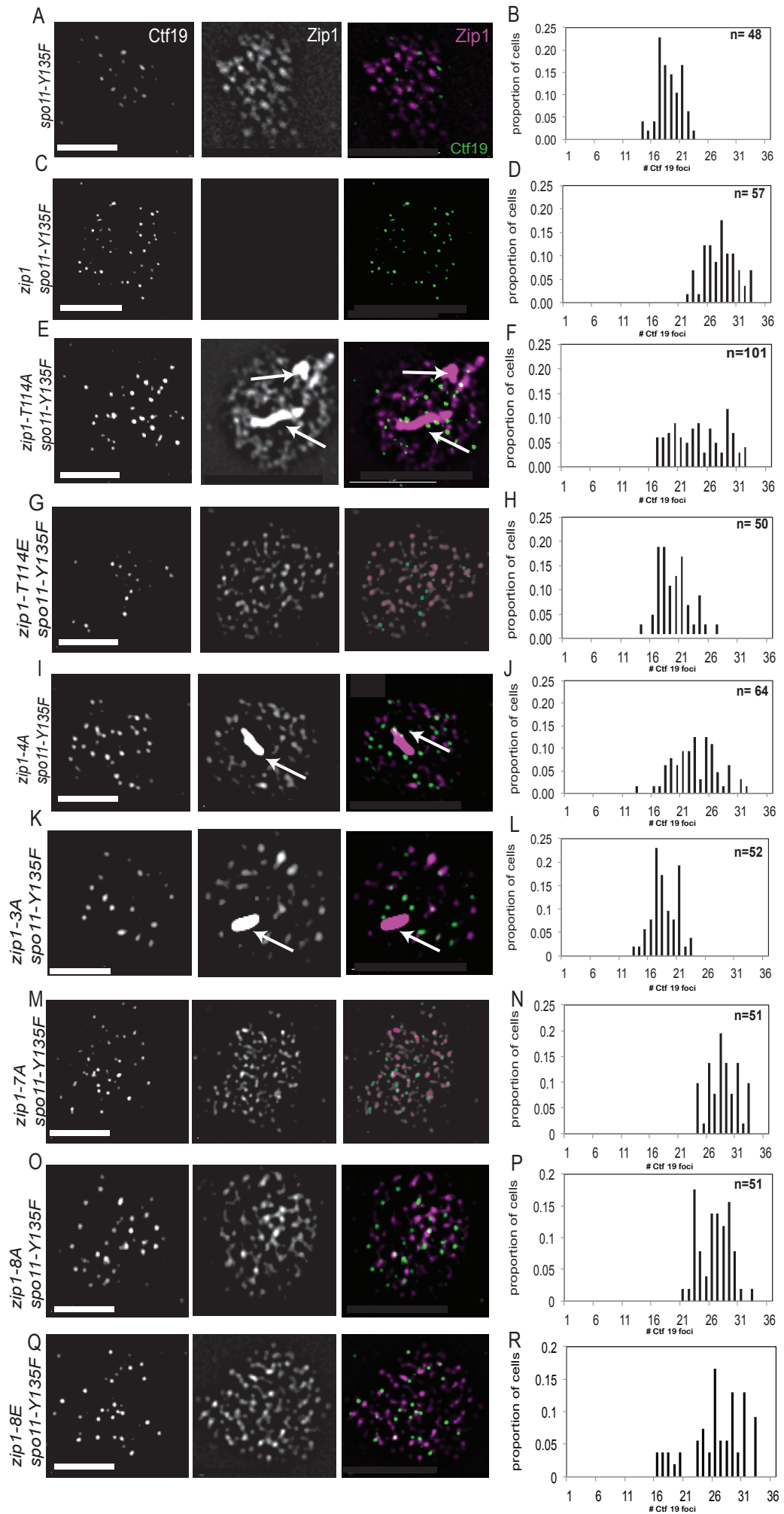
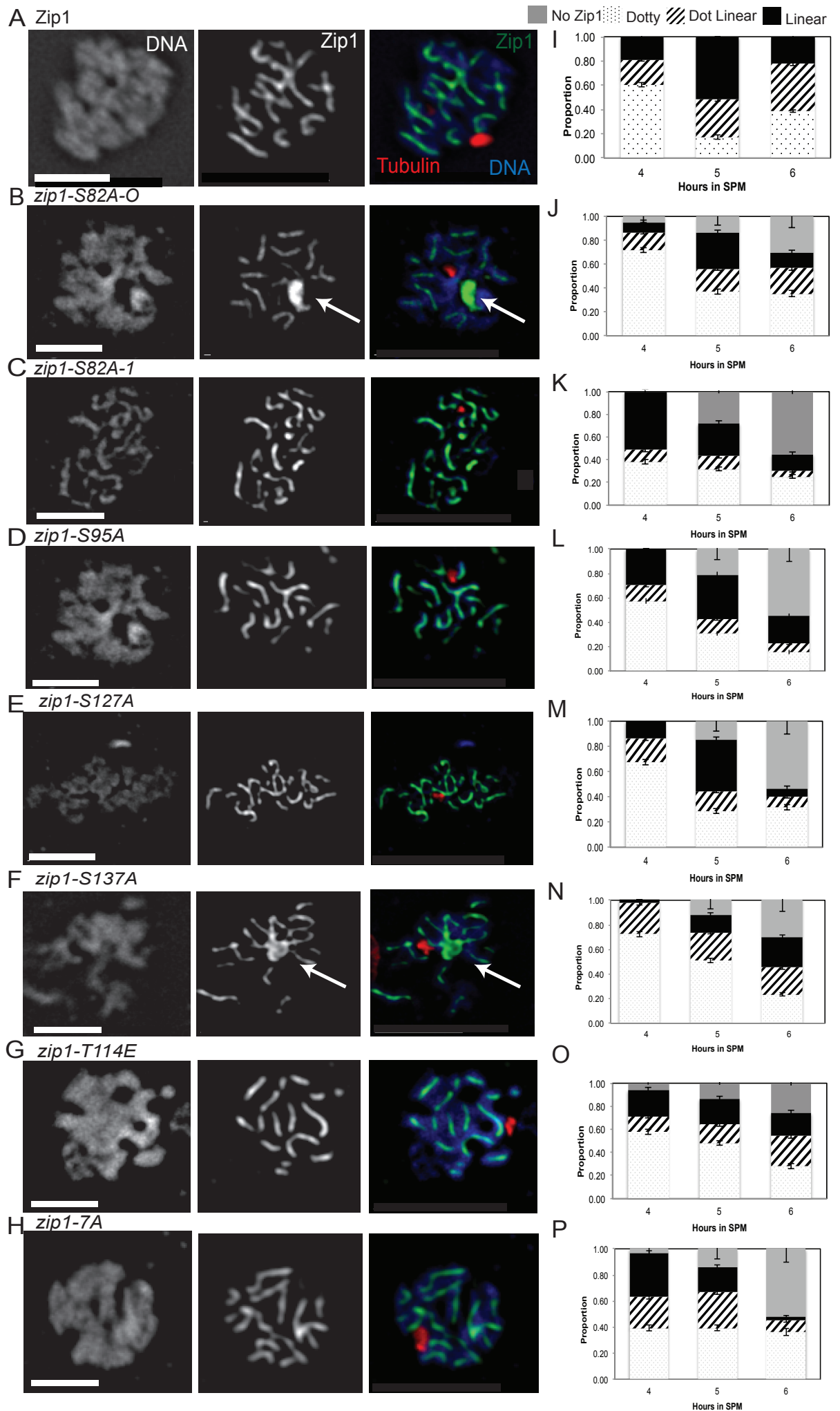


Figure 3.4 Synaptonemal complex formation analyses for Zip1-phospho mutants

(A-H) Representative pachytene spread images for the wild-type, *zip1-S82A-O*, *zip1-S82A-1*, *zip1-S95A*, *zip1-S127A*, *zip1-S137A*, *zip1-T114E* and *zip1-7A* respectively. Zip1 is stained in green, tubulin is stained in red and DNA is stained with DAPI in blue. 100> images scored for each category. (I-P) Proportion of dotty, dot linear and linear Zip1 formed in wild-type and mutants listed in A-H. Dotty is represented by a white box with black dots; dot linear is represented by black strike lines; linear represented by black box. Bars: 2 μ M. Arrows indicate polycomplexes.



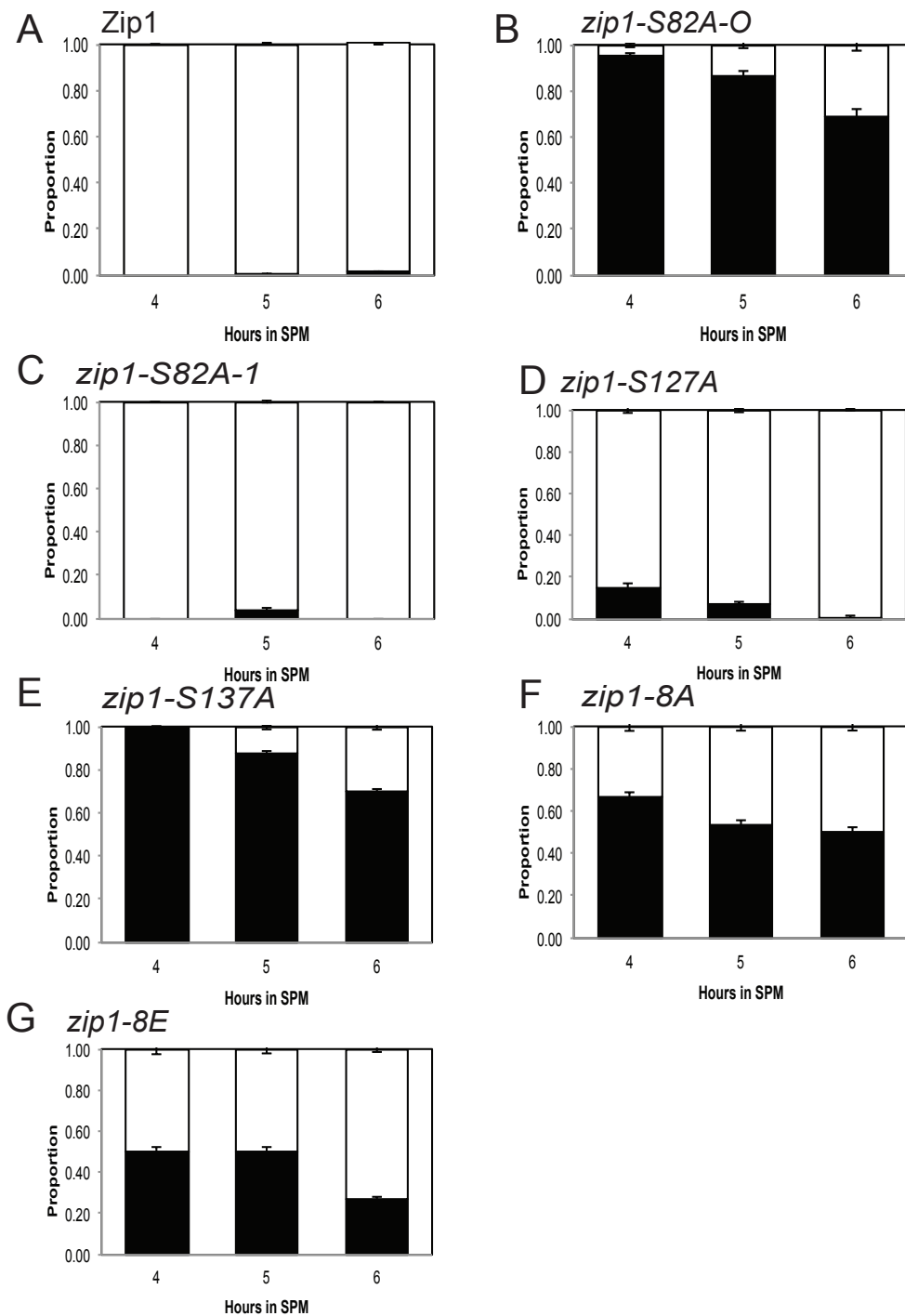


Figure 3.5 Proportions of polycomplexes in some Zip1-phospho mutants
 (A-G) Proportions of PCs observed in the wild-type, *zip1-S82A-O*, *zip1-S82A-1*, *zip1-S127A*, *zip1-S137A*, *zip1-8A* and *zip1-8E* mutants respectively.

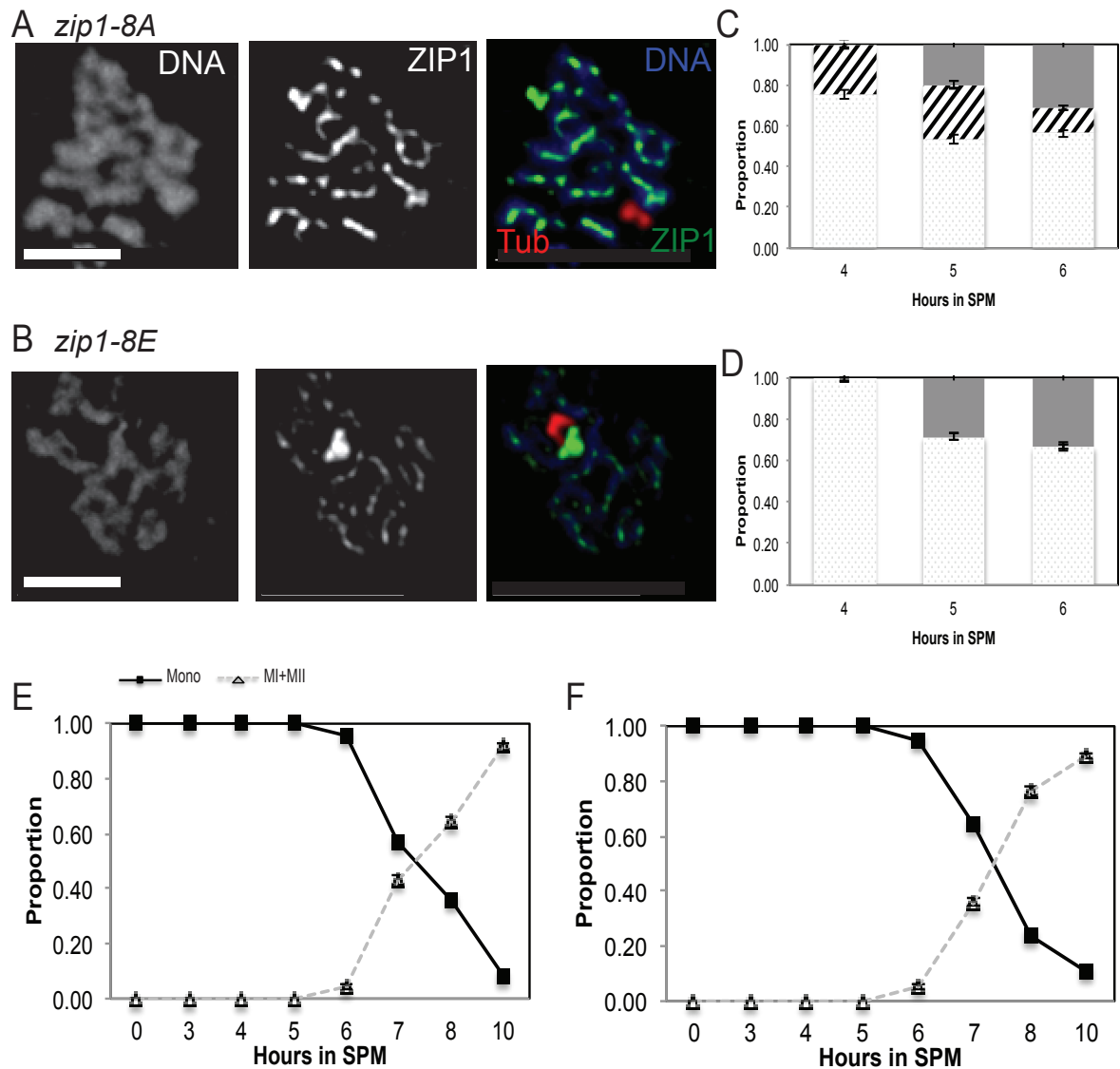


Figure 3.6 The *zip1-8A* and *zip1-8E* show defects in synaptonemal complex assembly

(A) Meiotic spread image presenting SC progression in *zip1-8A*, where dotted Zip1 and dot linear Zip1 are shown. (B) Representative imaging SC formation in *zip1-8E* where dotted Zip1 is shown. (C-D) Quantification of SC formation in *zip1-8A* and *zip1-8E*. Grey box presenting no Zip1. The White box with black dots represents dotted Zip1 staining. >50 nuclei scored for each stage. Zip1 is stained in green, tubulin is stained in red. (E-F) Meiotic nuclei division in *zip1-8A* and *zip1-8E* respectively. Bars: 2 μ m.

Figure 3.7 Synaptonemal complex formations in *zip1-4A* and *zip1-T114A*

(A) The meiotic spread represents different categories of SC formation in the wild-type. 'Dotty' refers to dots of Zip1 and diffuse DNA. 'Dot linear' refers to a mixture of dots and short stretches of Zip1 and partially condensed DNA. 'Linear' referred to full stretches of Zip1 with condensed DNA. (B) Representative images of meiotic spread for the *zip1-4A* mutant, where three categories are shown: 'Dotty'; 'Dot Linear'; 'Linear'. (C) Representative images of meiotic spread for the *zip1-T114A* mutant with different categories of SC formation. Arrows indicate polycomplexes (PCs). Scale: 2µm. (D-F) Quantification of meiotic nuclei spreads in different categories for the wild-type; *zip1-4A* and *zip1-T114A* respectively. 'Dotty' is shown with black dots; 'Dot linear' is shown with black lines; 'Linear' is shown in black. Three strains were done in the same time course. >100 nuclei were scored at each time point. (G-I) Quantification of meiotic nuclear division stained with DAPI for the wild-type; *zip1-4A* and *zip1-T114A*, are presented in two categories: Mononulceate (Mono) where only one nucleate stain was seen. Meiotic I (MI)+ Meiotic II (MII) where two or more nucleate were seen. >100 nuclei were scored for each strain. Samples were taken at the same time as meiotic spread samples. (J) Proportions of polycomplexes (PC) in the wild-type (WT); *zip1-4A*; *zip1-T114A* respectively. The black box represents PCs. (H) Spore viability for the wild-type (blue); *zip1-4A* (red); *zip1-T114A* (green). 100 tetrads were assessed.

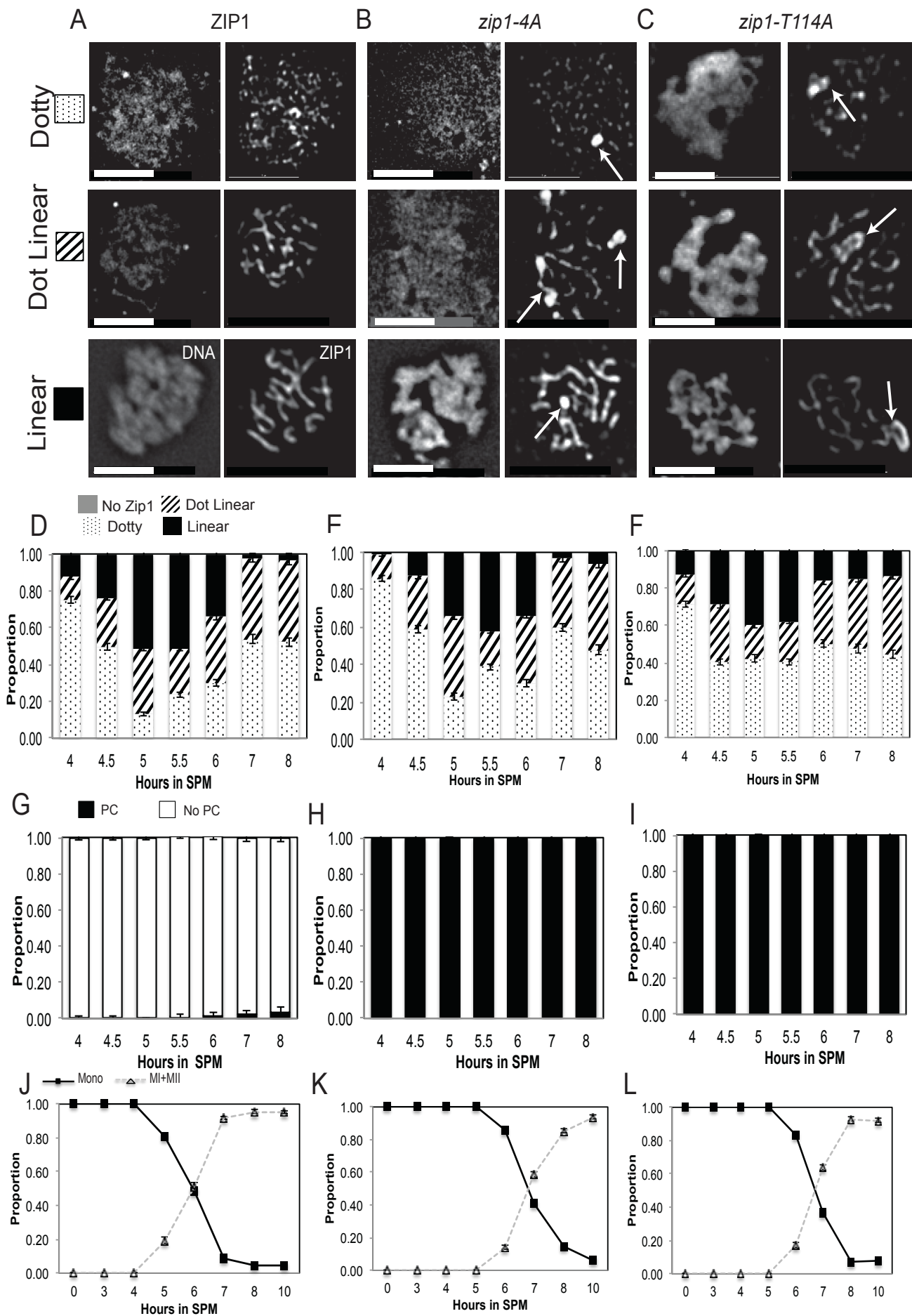


Figure 3.8 Zip1 protein levels in *zip1-4A* and *zip1-T114A* mutants

Western blots were probed with antibodies to Zip1, Hop1-T318 (DSB formation), and γ H2A to monitor induction of DSBs and their repair. Pgk1 was used as a loading control. (A) The Western blot presenting Zip1 levels in the wild-type and the *zip1-4A* mutant. (B) Zip1 expression in the *zip1-4A* mutant was measured using densitometry and normalized against the internal standard Pgk1. The gray line shows the wild type and the black line shows *zip1-4A*. (C) Western blot showing protein levels between the wild type and *zip1-T114A*. (D) Normalization of Zip1 protein level in the wild-type and the *zip1-T114A* mutant, where the wild type is shown in gray and *zip1-T114A* is shown in black. Two independent time courses were done between A and C. (E-F) SDS-PAGE gels containing 50 μ M Phos-tag™ Acrylamide were used to separate phosphorylated species in *zip1-4A* and *zip1-T114A* respectively. Gels were transferred to nitrocellulose and probed for Zip1. Time points were taken and extracted by TCA (extracted by Di Jue Sun & Dr. Copsey). Dr. Copsey ran all the protein gels in this figure.

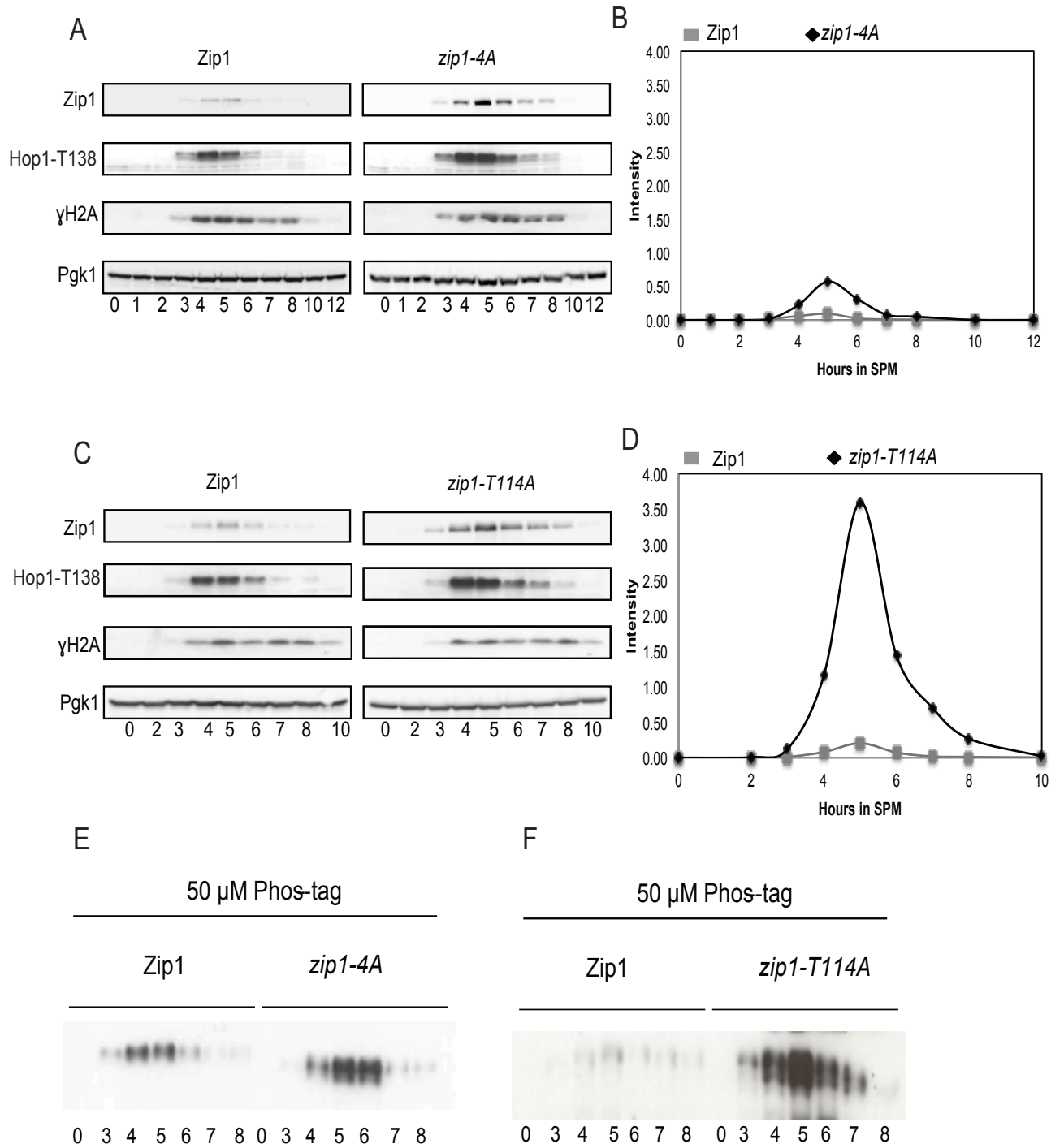


Figure 3.9 The *zip1-S137A* shown partial delay in synaptonemal complex disassembly

(A) Meiotic spread image presenting delayed disassembly at diplotene in *zip1-S137A*. (B) Representative imaging shows normal disassembled nuclei in *zip1-S137A* during diplotene. (C) Meiotic spread showing delayed SC disassembly at metaphase I in *zip1-S137A*. (D) Disassembled nuclei at metaphase I in *zip1-S137A*. (E) Quantification of SC disassembly in the wild-type. (F) Quantifications of delayed SC disassembly at diplotene and metaphase I in the *zip1-S137A* mutant. The gray box represents normal disassembled SC, hence categorized as no Zip1. The white box with black dots represents Zip1 staining in a nuclei with characteristic of dotty with PCs, during diplotene and metaphase I. >50 nuclei scored for each stage. Zip1 is stained in green, tubulin is stained in red. Bars: 2µm.

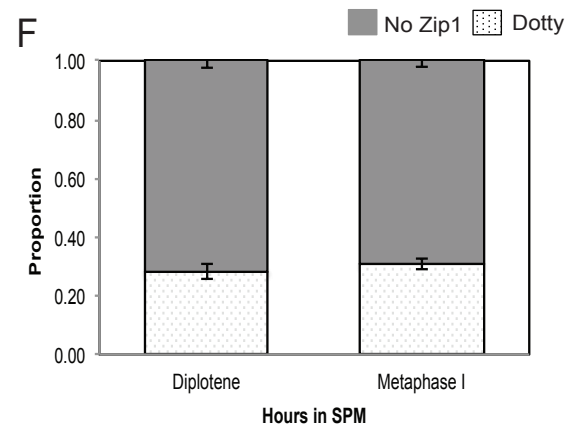
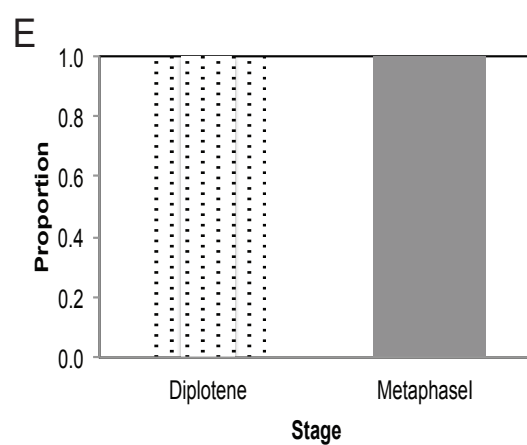
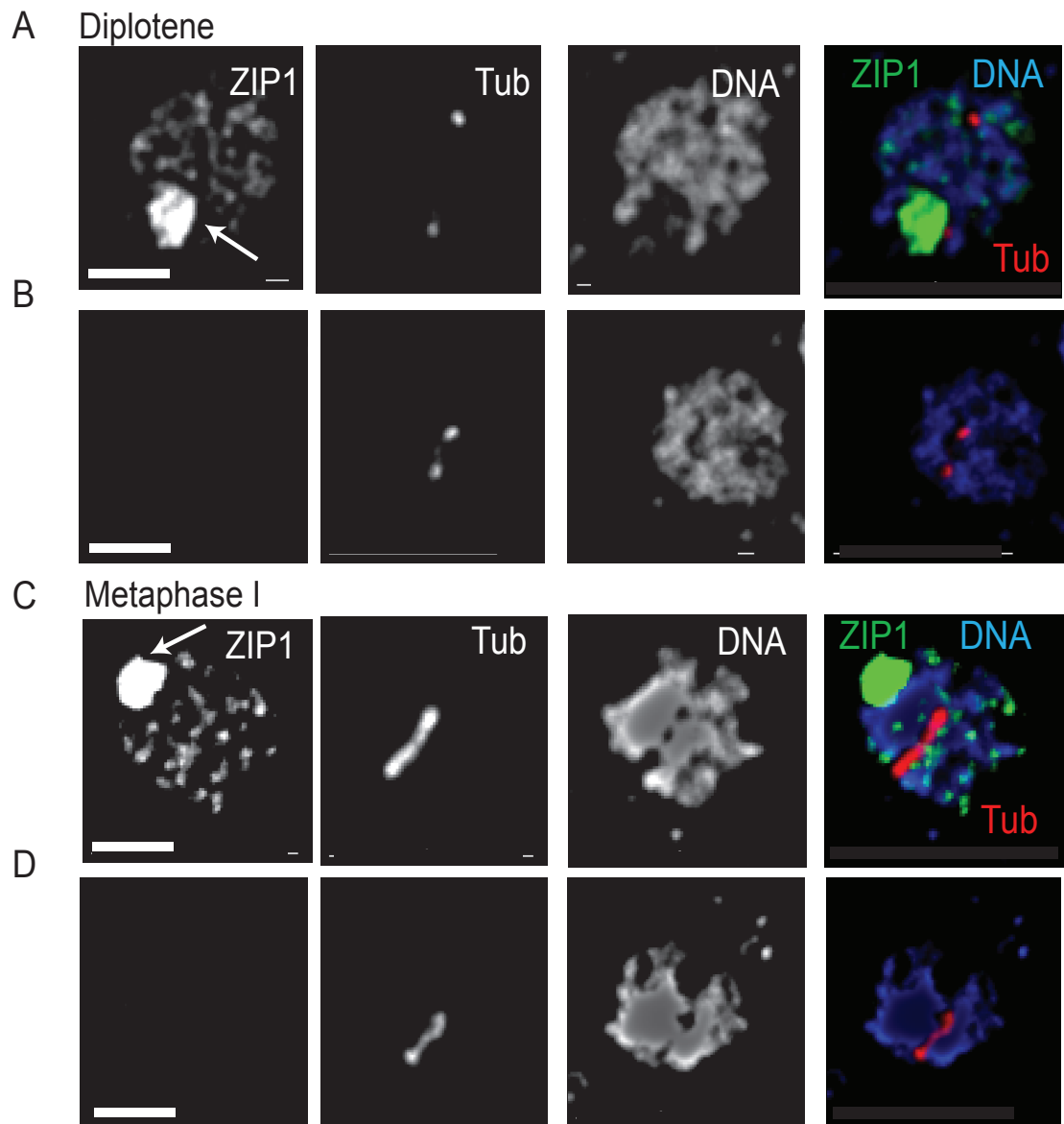
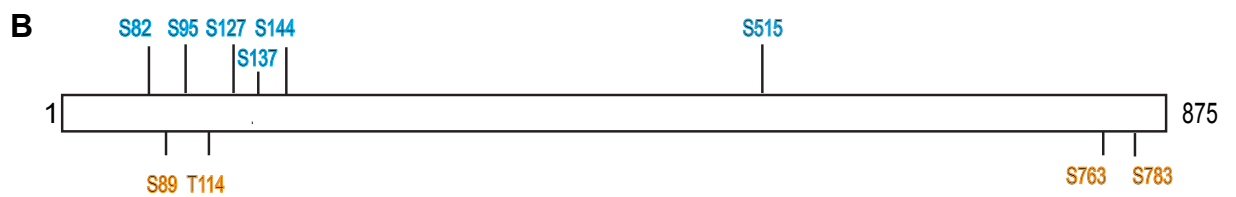
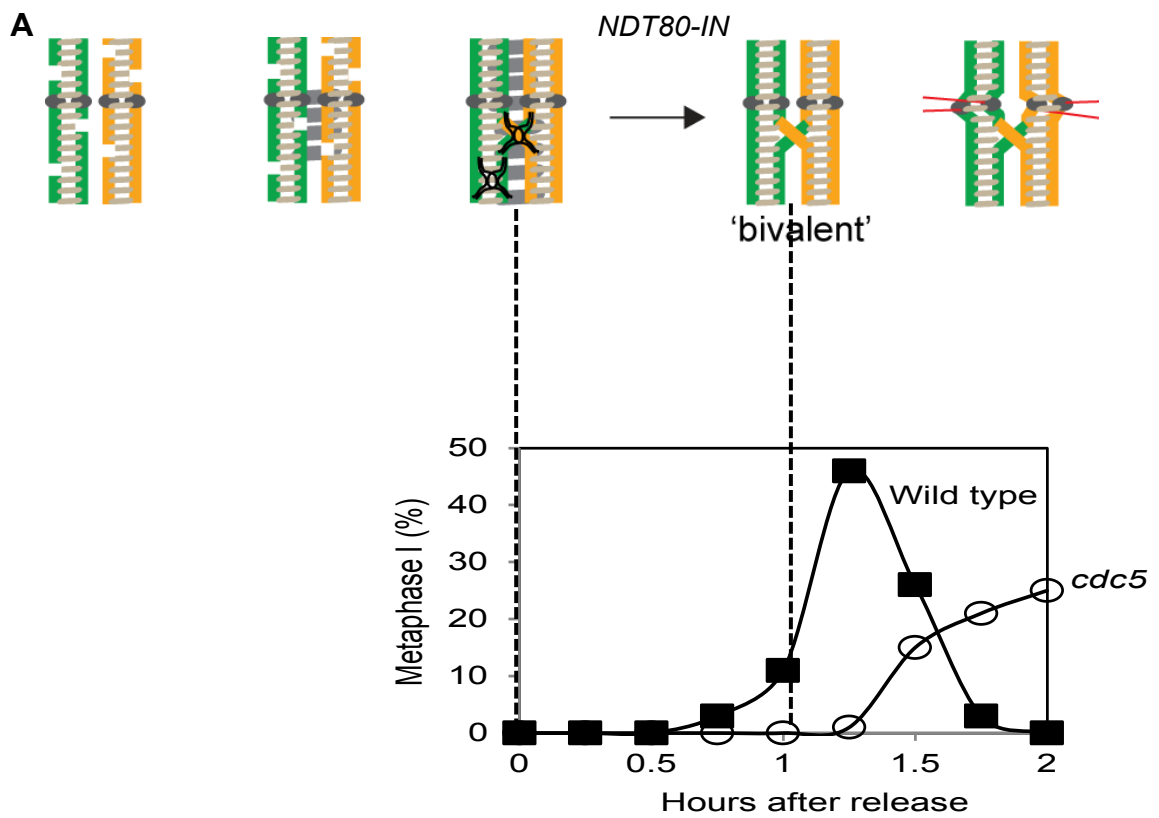


Figure 4.1 Identification of Zip1-S144 through phosphor proteomic screen

(A) The systemic diagram representing the process of meiosis. One homolog is presented in green and another one in yellow. Light gray lines presenting cohesins. Dark gray box represents Zip1. β -estradiol is added to cells reach pachytene (5 hours). This is shown with fully synapsed Zip1 and formation of COs (black crosses). Samples were taken at T=0 and T=1 (one hour after induction) and analysed by mass spectrometry. The chart below the systemic diagram represents the quantification of pachytene exit cells after induction of *NDT80* between the wild-type and *cdc5-mn* (meiotic null). (B) The simple picture shows the position of Zip1-phospho sites identified from the Cdc5 screen. Blue colour showing sites identified for the first time, yellow showing sites identified previously. (C) A table showing the changing of ratio for all sites identified in Zip1, at T=0 (pachytene arrest) and T=1 (one hour after pachytene arrest). Ratio that is greater than one is highlighted in bold. Ratio of Zip1-S144 is highlighted in red.



C

Sites	Ratio at T=0	Ratio at T=1
S82	0.5	0.8
S89	N/A	1.4
S95	0.3	N/A
T114	N/A	1.8
S127	0.03	1.6
S137	0.6	1.7
S144	0.8	0.2
S763	0.7	0.9
S783	0.8	1.2

cdc5:WT H:L <1 cdc5:WT H:L >1

Figure 4.2 Characterization of *zip1-S144A* in synaptonemal complex assembly

(A-B) Examples of surface spread nuclei: (A) The wild-type (*ZIP1-TRP1*), (B) *ZIP1-S144A-TRP*. Central element Zip1 marks the appearance of SC, stained with an α -ZIP1 antibody (left). DAPI stained DNA shown on the right. Nuclei were categorized as having 'dotty' (black dots box); 'dot linear' (black line box) and 'linear' (full black box). Arrows indicate polycomplexes. Bars: 2 μ m. (C-D) Bar plots depicting the relative proportions of each category of Zip1-positive nuclei. The wild-type is on the left (C) and the *zip1-S144A* mutant is shown on the right (D). (E-F) Bar plots indicating the percentage of nuclei containing a polycomplex, where wild-type is shown on the left (E) and the *zip1-S144A* mutant is shown on the right (F). >100 spread nuclei were counted for each time point. (G) The proportion of cells shown in cumulative curves with one (undivided), two (completions of MI) or more (completion of MII) in the wild type cells. (H) Quantification of meiotic progression for the *zip1-S144A* mutant. Nuclei stained with DAPI as a function of time (hours in sporulation medium, SPM). >100 nuclei scored for each time point. The wild type is shown on the left, *zip1-S144A* is shown on the right.

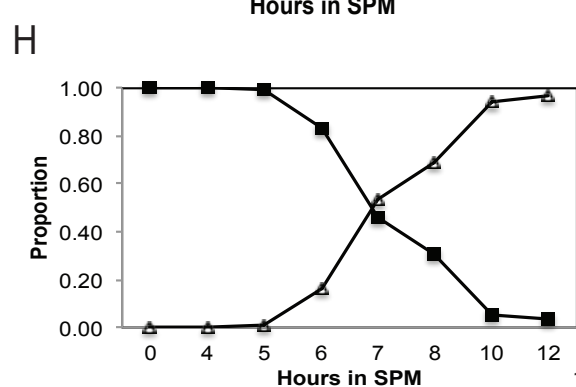
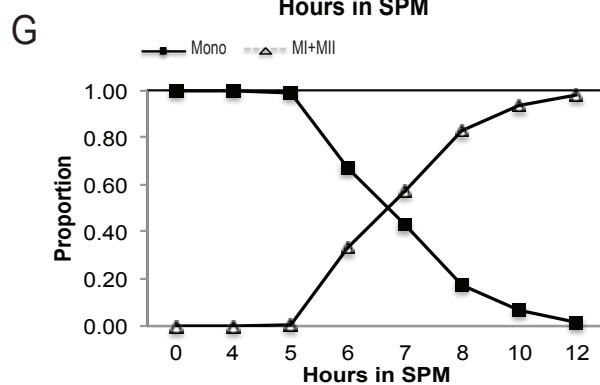
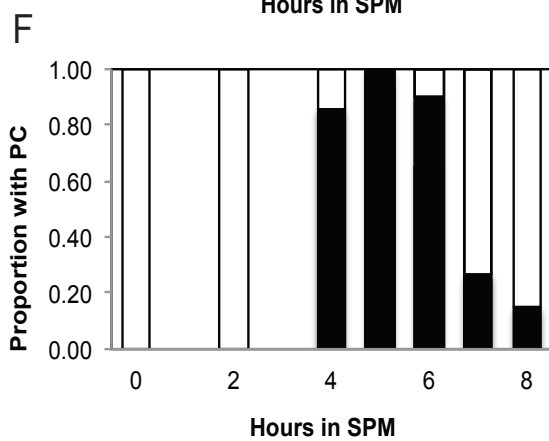
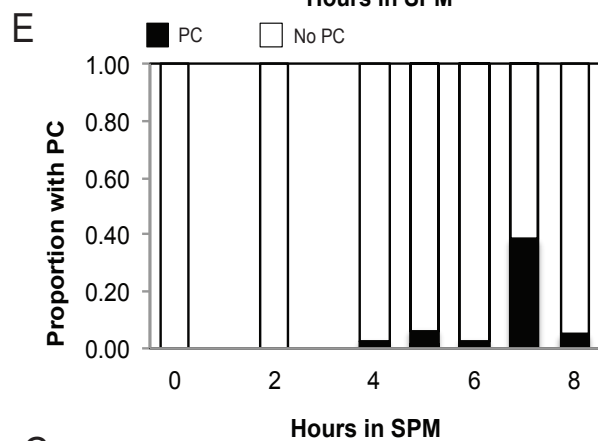
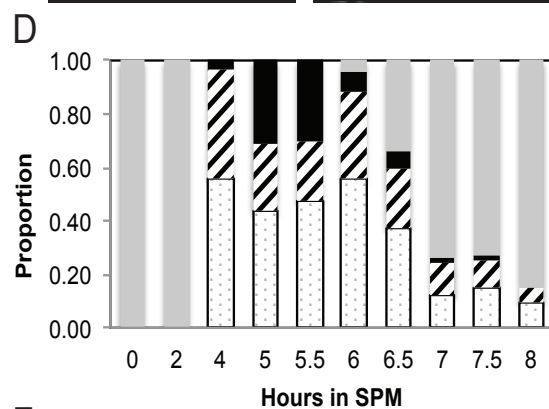
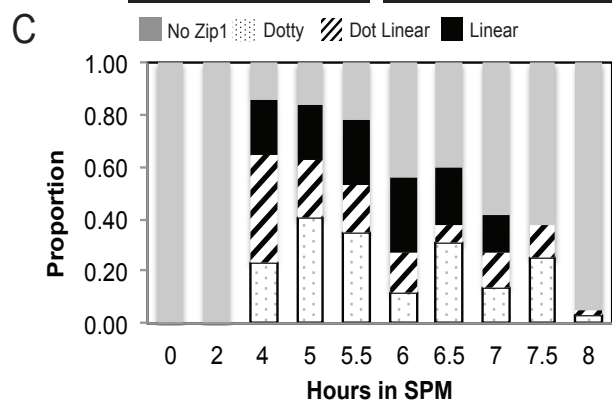
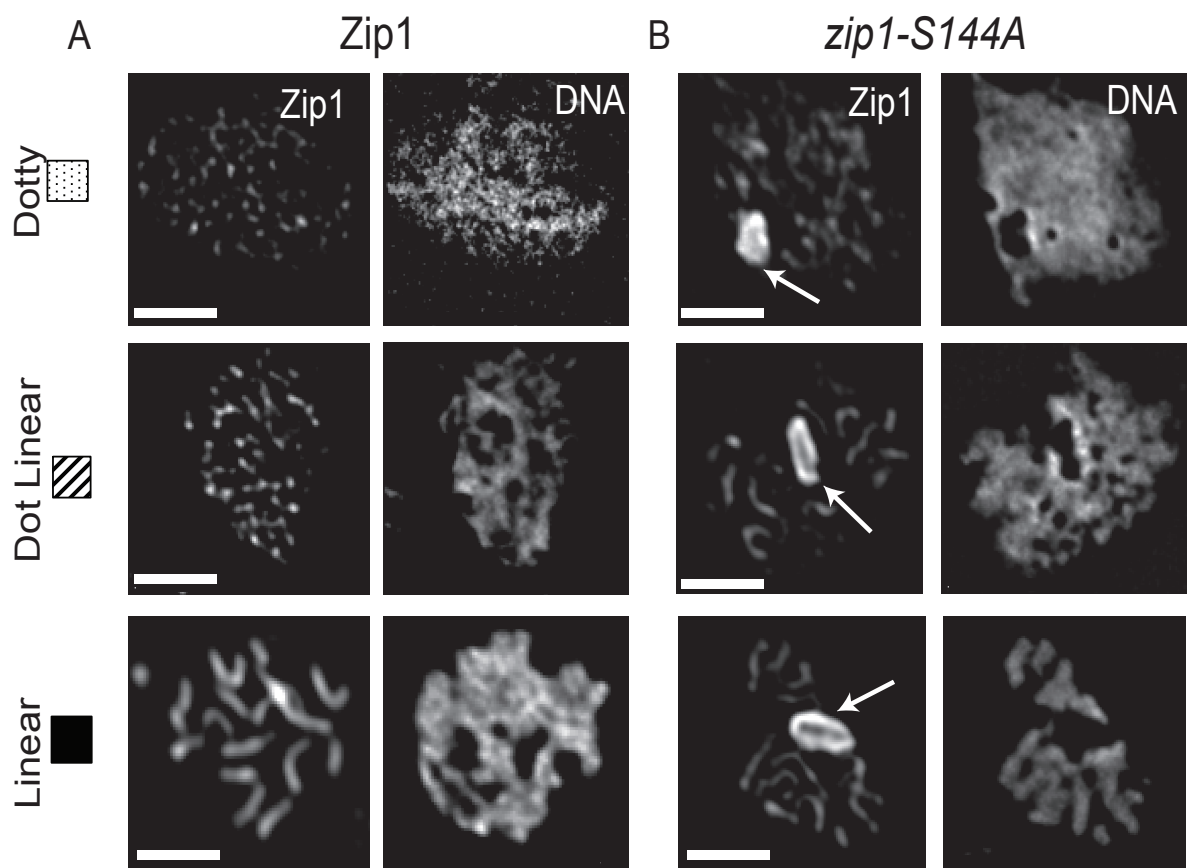
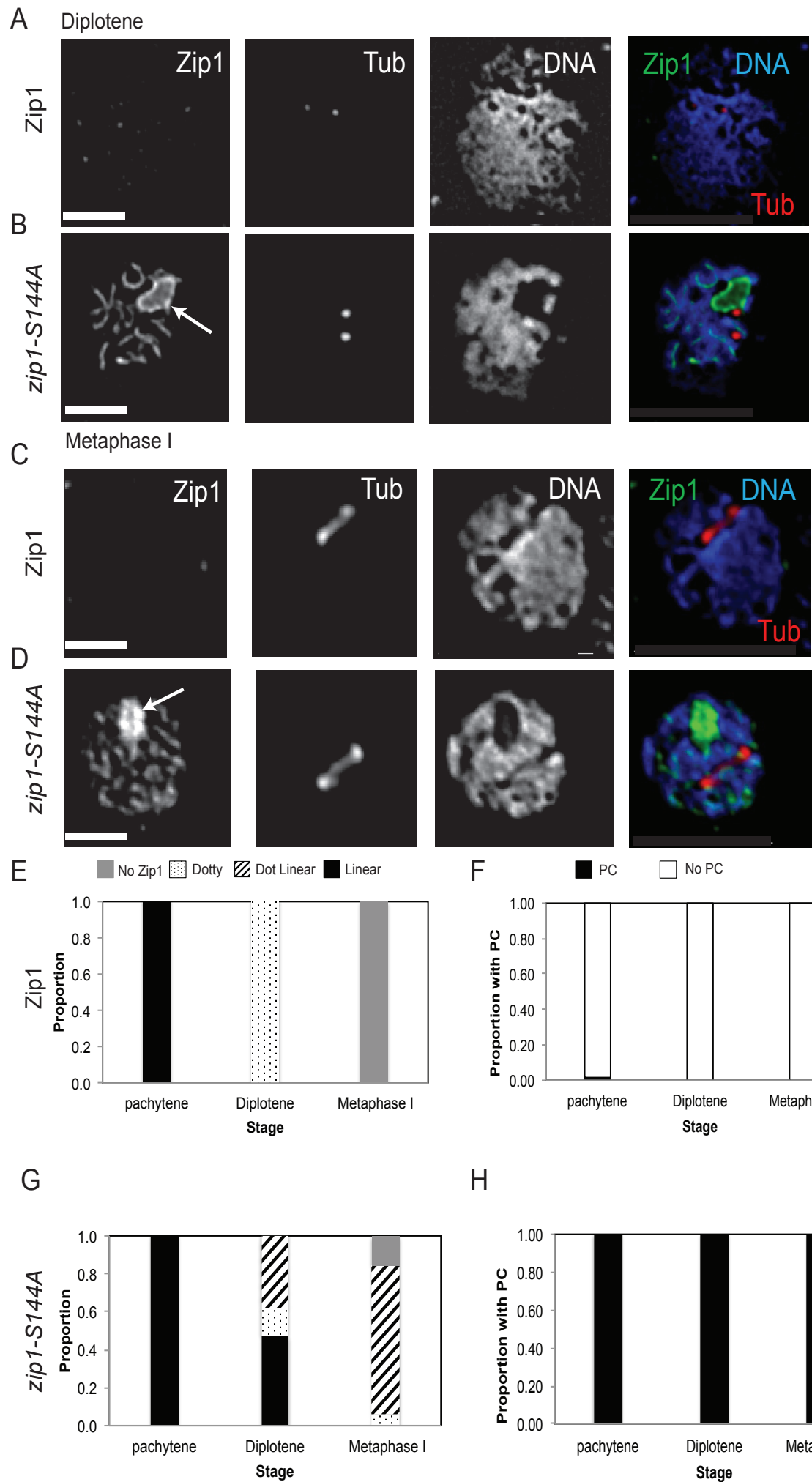
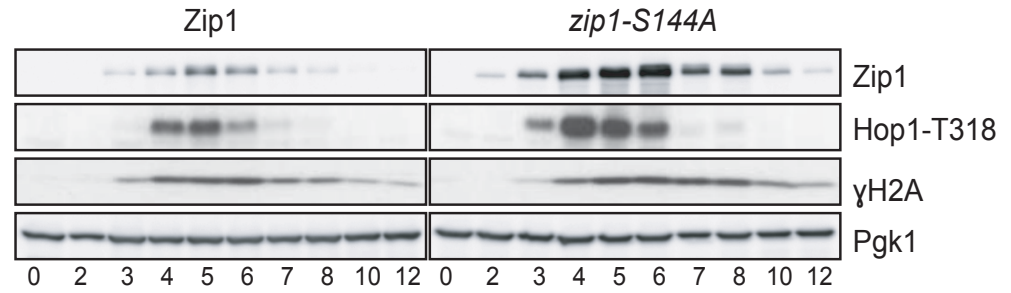


Figure 4.3 The *zip1-S144A* mutant displays delayed SC disassembly

Cells for the wild-type and the *zip1-S144A* mutant were collected from a meiotic time course between 5 to 7 hours; meiotic nuclear spreads were stained for Zip1 (Green) and tubulin (red). Zip1 was categorized as 'dotty' (white dots); 'dot linear' (black lines); 'linear' (full black); 'no Zip1' (gray). Polycomplexes (PC) are indicated with a white arrow. Bars: 2 μ m. (A-B) Representative images showing diplotene stage of (A) the wild-type (*zip1::URA3; trp1-ZIP1-TRP1*) and (B) the *zip1-S144A* mutant. (C-D) Representative images showing metaphase I stage of (C) the wild-type and (D) the *zip1-S144A* mutant. (E) The proportion of different Zip1 staining patterns in the wild type at pachytene, diplotene and metaphase I. (E) The proportion of polycomplexes (PC) in the wild type. (F) Quantification of proportion of PCs formed in the wild type at pachytene, diplotene and metaphase I. (G) The percentage of Zip1 staining patterns in the *zip1-S144A* mutant at pachytene, diplotene and metaphase I. (H) presents the portions of PCs observed in the *zip1-S144A* nuclei. >50 nuclei scored for each category



A



B

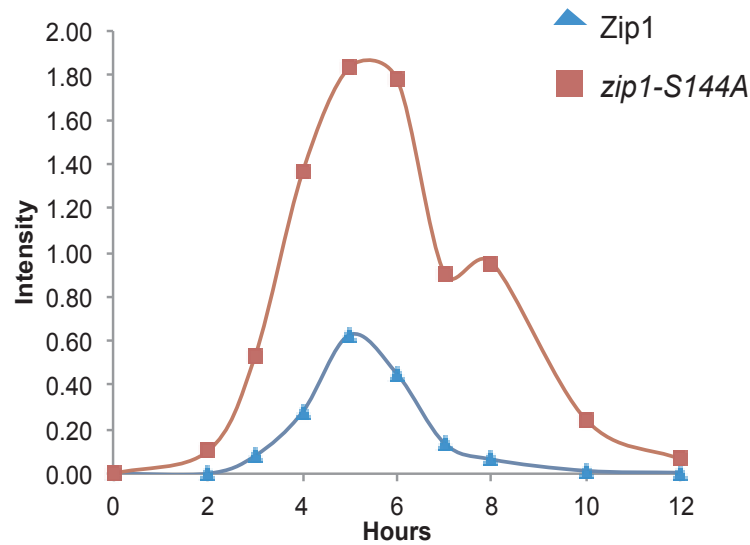


Figure 4.4 protein levels of *zip1-S144A* through meiotic progression

(A) Western blot shows Zip1 levels in the wild-type and *zip1-S144A* mutant.

The first row shows amounts of Zip1 using α -Zip1 antibody; second row shows double-strand break using α -Hop1-T318; the third row represents meiotic progression by using marker α -H2A. Pgk1 was used as a loading control. (B) Zip1 is normalized to Pgk1. Blue represents the wild-type, and red represents the *zip1-S144A* mutant.

Gel run by Dr. Alice Copsey, extraction done by Dijue Sun and Dr. Alice Copsey together

Figure 4.5 Assessing the phosphomimetic version of Zip1-S144 (*zip1-S144E*) in SC assembly

(A) Meiotic spread images show different categories of Zip1 during prophase for the wild-type (*ZIP1*) and phosphomimetic *zip1-S144E* mutant. Bar: 2 μ M (B) Quantification of SC formation in meiotic spreads for both wild-type and *zip1-S144E*. >100 nuclei were scored for each time point. (C-D) Quantification of SC assembly in the wild-type (C) and in the *zip1-S144E* mutant (D). Grey bar indicate nuclei with no Zip1, white dotted box indicate dotted staining of Zip1, black strike line indicate dot linear of the SC and black bar indicate full linear SC. (E-F) proportion of PCs formed in both the wild-type and *zip1-S144E* respectively. (G-H) DAPI stained nuclear division in the wild-type and *zip1-S144E* respectively. Samples were taken in parallel with meiotic spreads. Mononucleate shows one nucleus and MI+MII shows two or more nuclei

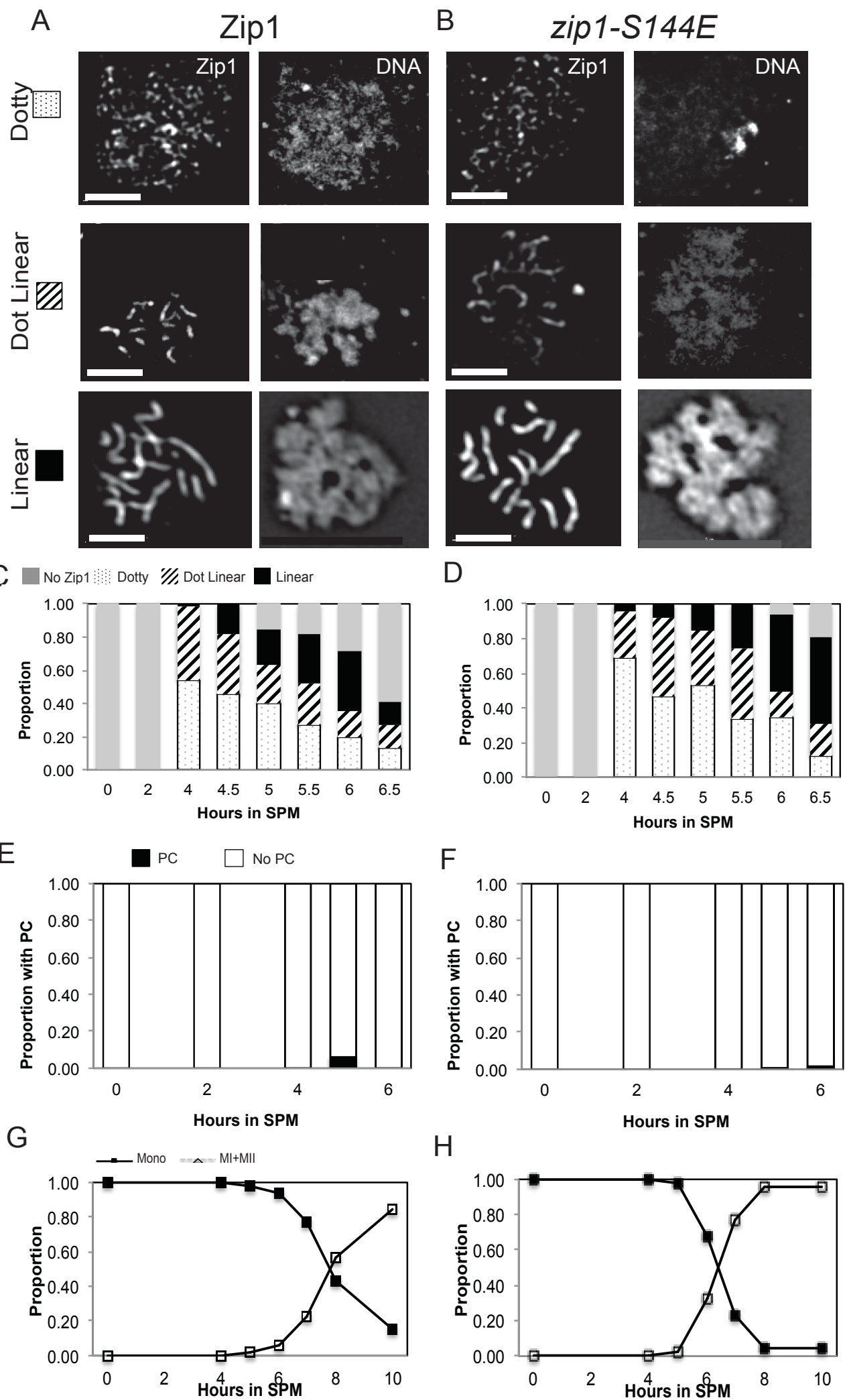
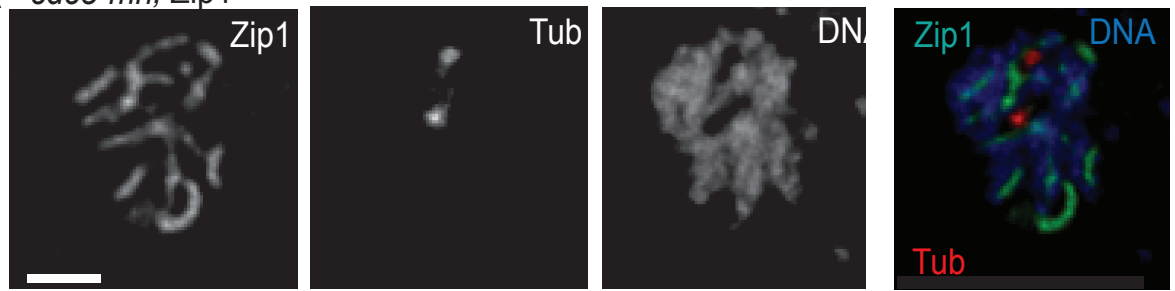


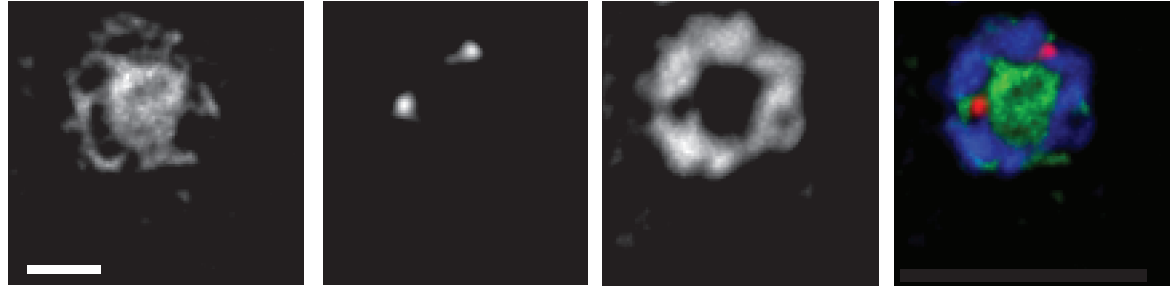
Figure 4.6 Synaptonemal complex does not disassemble in the absence of Cdc5 at diplotene in both *zip1-S144A* and *zip1-S144E*

(A-C) Diplotene meiotic spreads for the wild-type, *zip1-S144A*, *zip1-S144E* respectively. Two dots of tubulin (stained with red) marks diplotene. (D) Proportions of Zip1 staining pattern during diplotene for the wild-type, *zip1-S144A* and *zip1-S144E* respectively. White box with black dots represent dotted Zip1 staining; strike lines represent dot linear Zip1; black box represents linear Zip1. (E) Quantification of PCs in three strains at metaphase I. >100 nuclei scored for each strain; bars: 2 μ M. Two independent diploids were assessed for *zip1-S144E*.

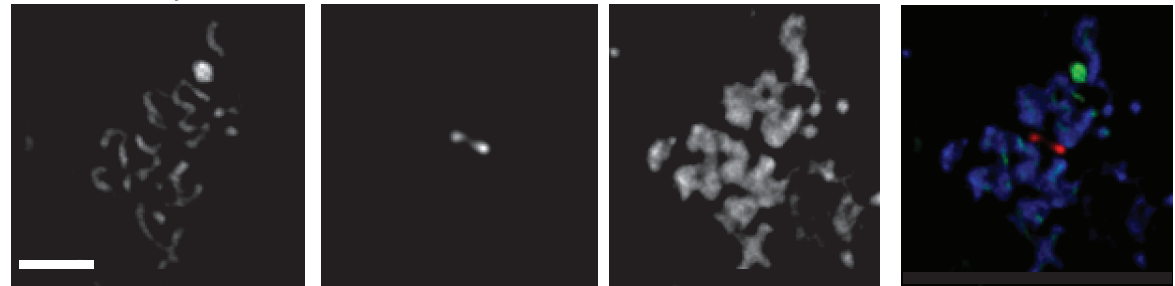
A *cdc5-mn*, Zip1



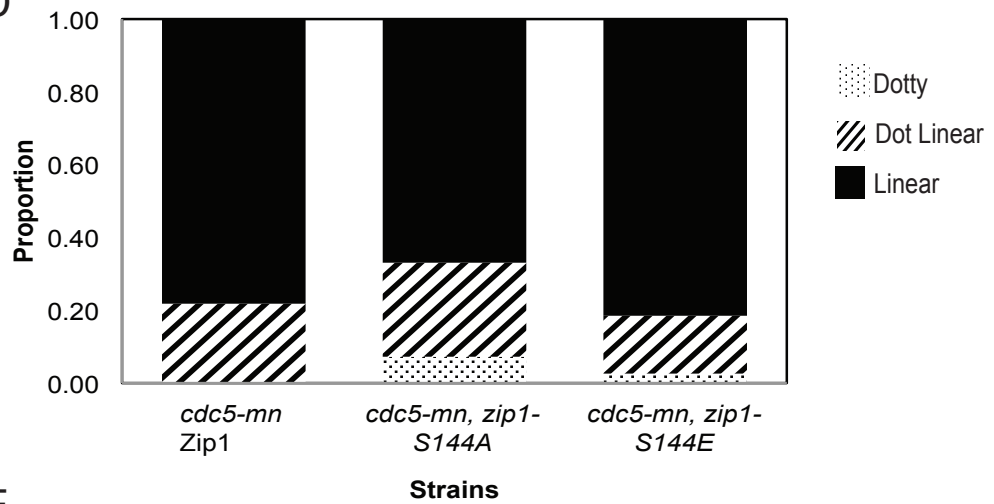
B *cdc5-mn*, zip1-S144A



C *cdc5-mn*, zip1-S144E



D



E

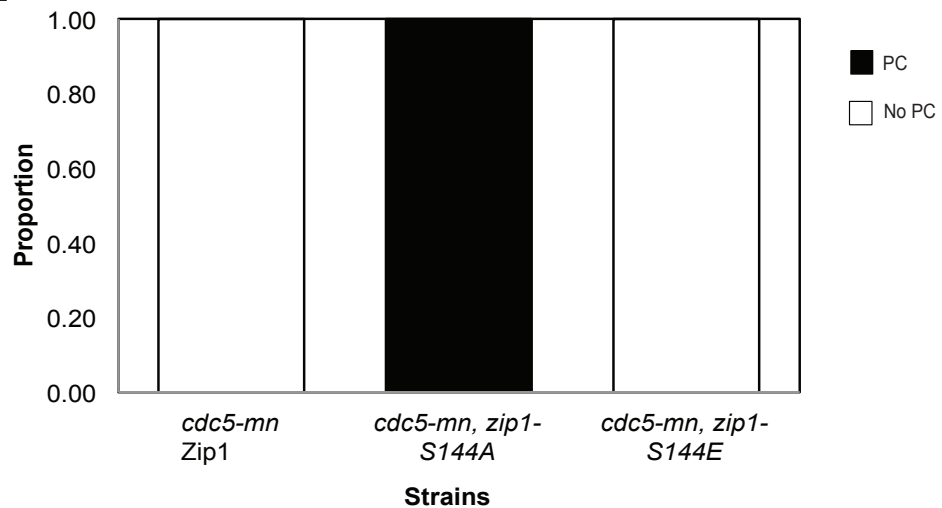
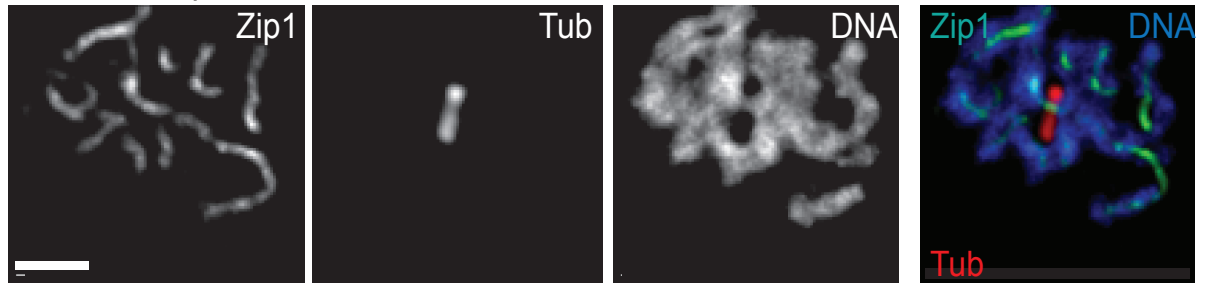


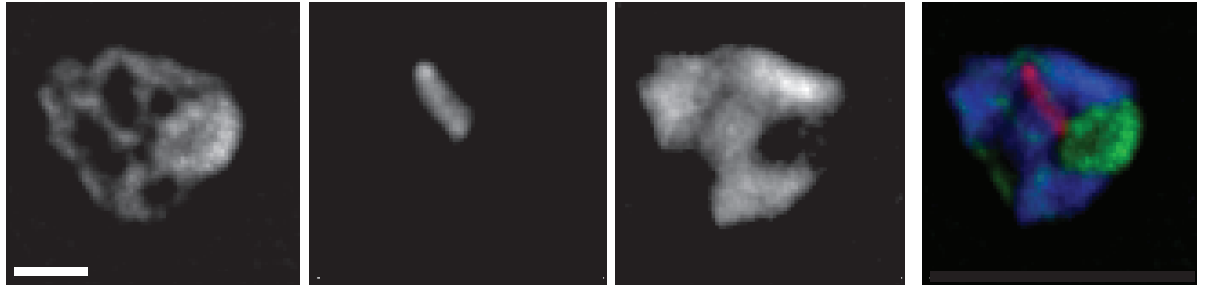
Figure 4.7 Synaptonemal complex does not disassemble in the absence of Cdc5 at metaphase I in both *zip1-S144A* & *zip1-S144E* mutants

(A-C) Diplotene meiotic spreads for the wild type (*cdc5-mn*, *ZIP1*), *zip1-S144A* (*cdc5-mn*, *zip1-S144A*), *zip1-S144E* (*cdc5-mn*, *zip1-S144A*) respectively. Two dots of tubulin (stained with red) marks diplotene. (D) Proportions of Zip1 staining pattern during diplotene for the wild type, *zip1-S144A* and *zip1-S144E* respectively. White box with black dots represent dotted Zip1 staining; strike lines represent dot linear Zip1; black box represents linear Zip1. (E) Quantification of PCs in three strains at metaphase I. >100 nuclei scored for each strain; bars: 2µM. Two independent diploids were assessed for *zip1-S144E*.

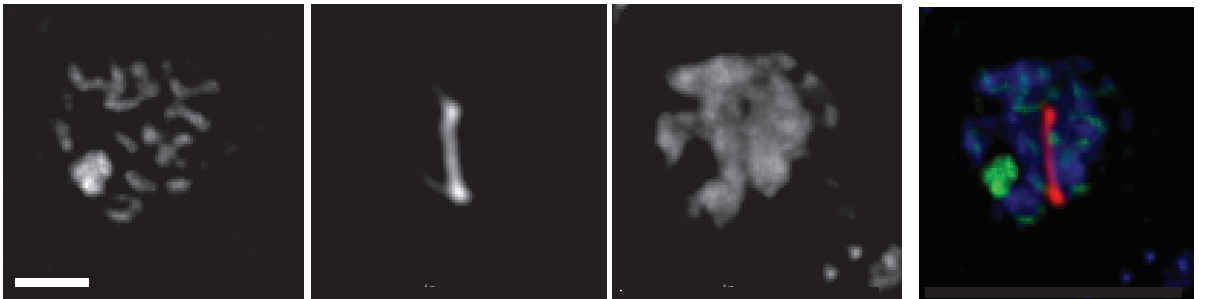
A *cdc5-mn*, Zip1



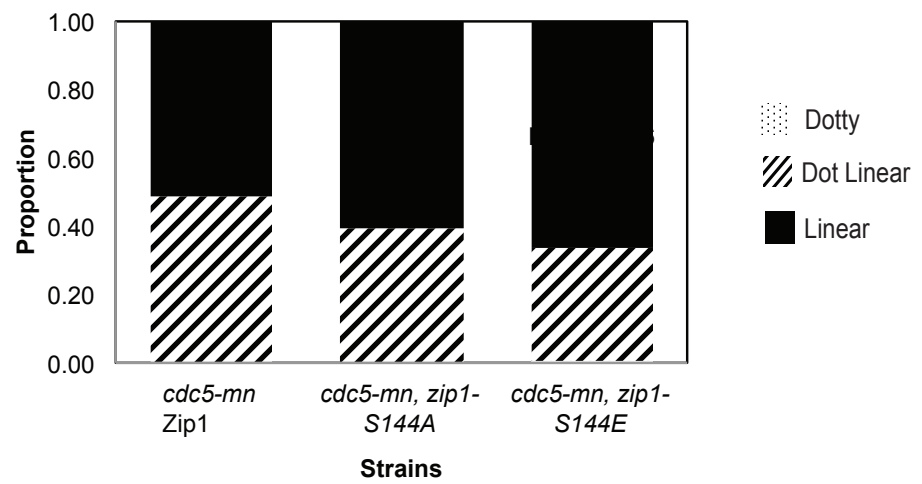
B *cdc5-mn*, zip1-S144A



C *cdc5-mn*, zip1-S144E



D



E

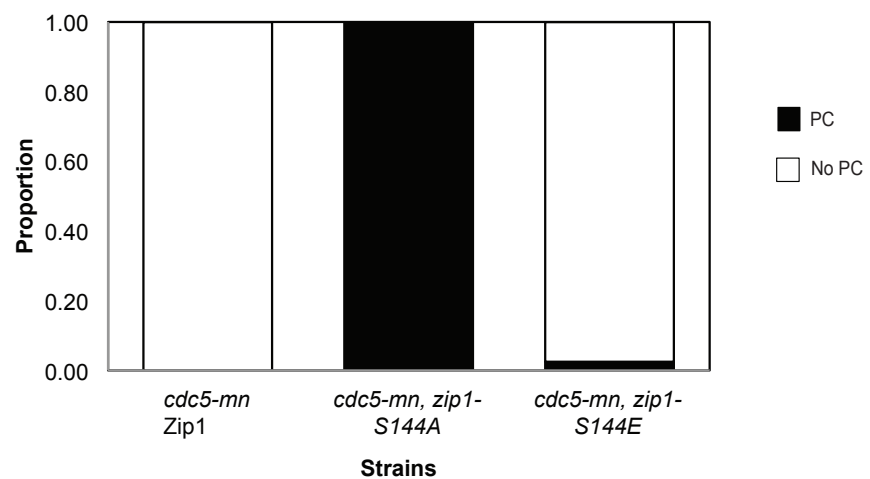


Figure 4.8 Disassembly of the synaptonemal complex still occurs when *zip1-S144A* nuclei are conditionally induced by Cdc5

(A-G) Meiotic spreads show *zip1-S144A* in a Cdc5-Inducible system. (A-C) Show three categories of SC in mock-treated (-ED) cells and (D-G) Show four types of SC in induced (+ED) cells. Bars: 2 μ M. (H) A simple diagram indicating the timing of induction in this experiment, and the time points taken after induction (I) Quantification of mock-treated cells in the wild-type where Cdc5 was un-induced. >100 nuclei examined at each time point. (J) Quantification of wild-type cells that were induced with Cdc5. >100 nuclei scored. (K) Quantification of Zip1 status in the *zip1-S144A* mutant when un-induced with β -estradiol and its induced version is shown in (L). >100 nuclei scored for each time point. Three independent diploids were repeated in this experiment.

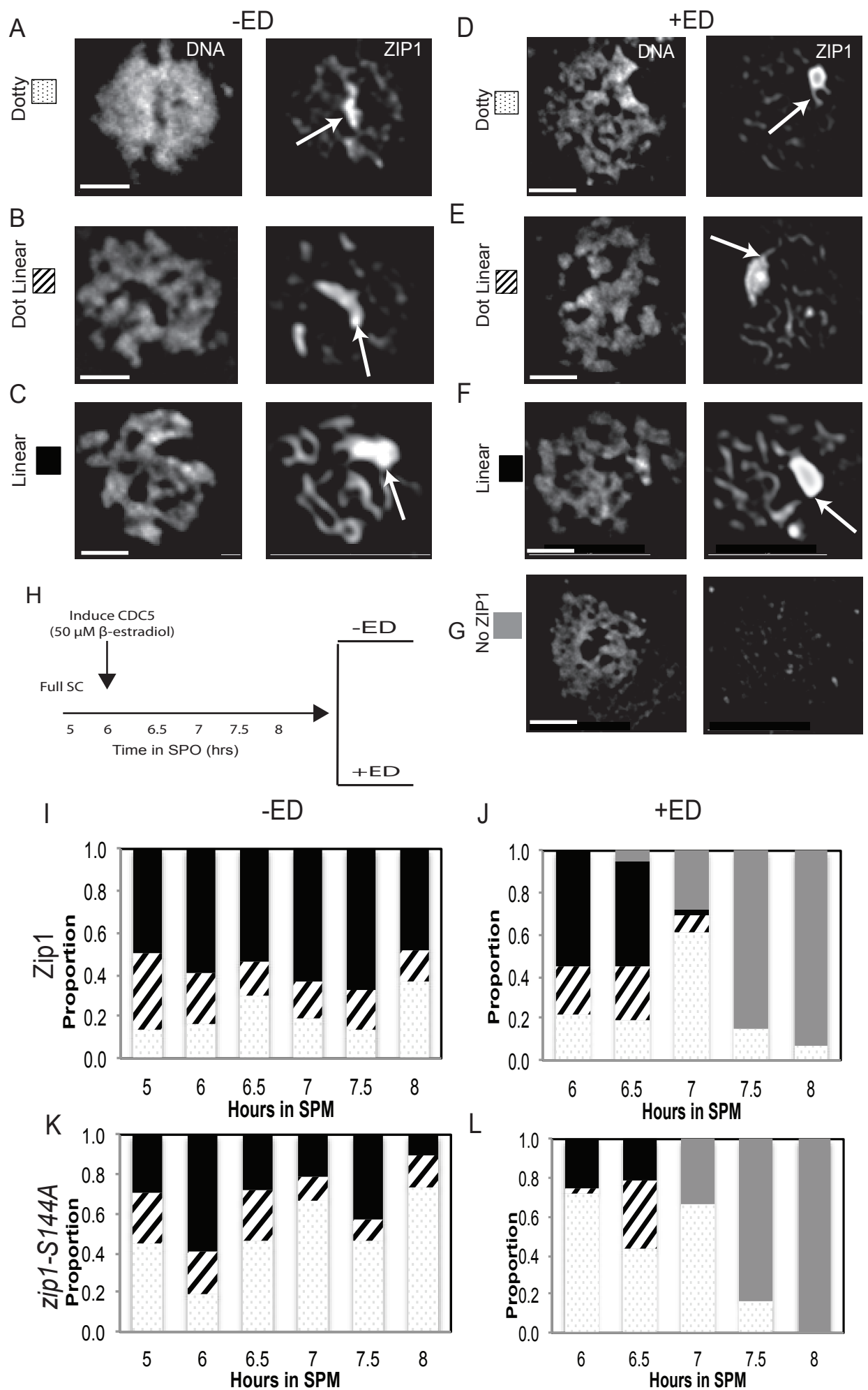


Figure 4.9 The *zip1-S144A* mutant displays normal sporulation and spore viability

Sporulation and spore viability were assessed from the same meiotic time course after 24 hours. The wild type is shown in blue, *zip1-S144A* mutant is shown in red. (A) Tetrads refer to four spores in an ascus; dyad refers to two spores in an ascus; monads refer to one or no spores in an ascus. >200. (B) Shows the spore viabilities between the wild type and *zip1-S144A*, where a different number of spores per each tetrad grown after two days were counted. N=100.

Figure 4.10 Confirmation that *ZIP1-TRP1* strain behaves the same as standard Hunter wild type

(A) Genetic and physical maps of the *HIS4LEU2* locus, strain obtained from (Hunter and Kleckner, 2001). 33c is the open reading frame (ORF) for *YCR033C*. The locus was created by the insertion of 2.8 KB adjacent to *HIS4* containing *LEU2* (red box), as well as a part of the *NSF1* gene plus 77 bp of bacterial DNA that includes the DSB site (Xu et al., 1995). Each homolog is labelled with “mum” and “dad” respectively. *XhoI* restriction site polymorphisms distinguish parent strains (white circled Xs). DNA species are detected with a specialized probe4 (black box) (Zakharyevich et al., 2012). CO: crossovers; DSB: double strand breaks. The size of each expected product is shown underneath. (B) A Southern blot from wild-type time courses shows DNA of interest. Jacob Kirk performed Hunter_WT (this strain has the same genetic information as shown in A) (Hunter and Kleckner, 2001). *Zip1; trp1::ZIP1-TRP1* (from now on referred as *ZIP1-TRP1*) strain contains Hunter genetic information and also has a knockout of its endogenous locus *ZIP1* (*zip1::HYG*). The wild-type copy of *ZIP1* is inserted into the *TRP* locus (see methods). (C) Quantification of DSB comparison in both wild-types. (D) Quantification of COs in both wild types. DNA samples quantified via Ayida. The gray line represents the Hunter_wild-type. The blackline is shows the *ZIP1-TRP1* wild-type.

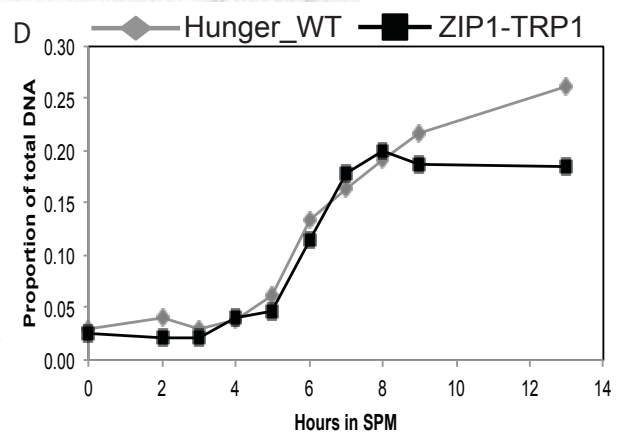
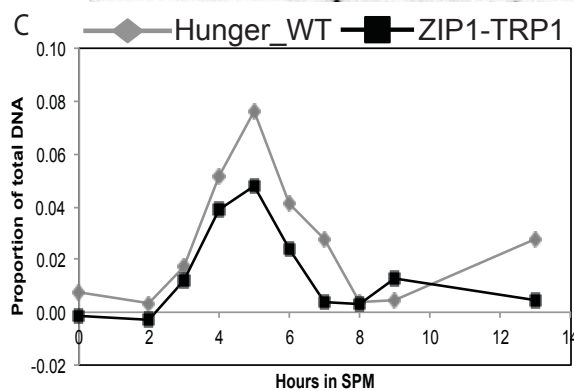
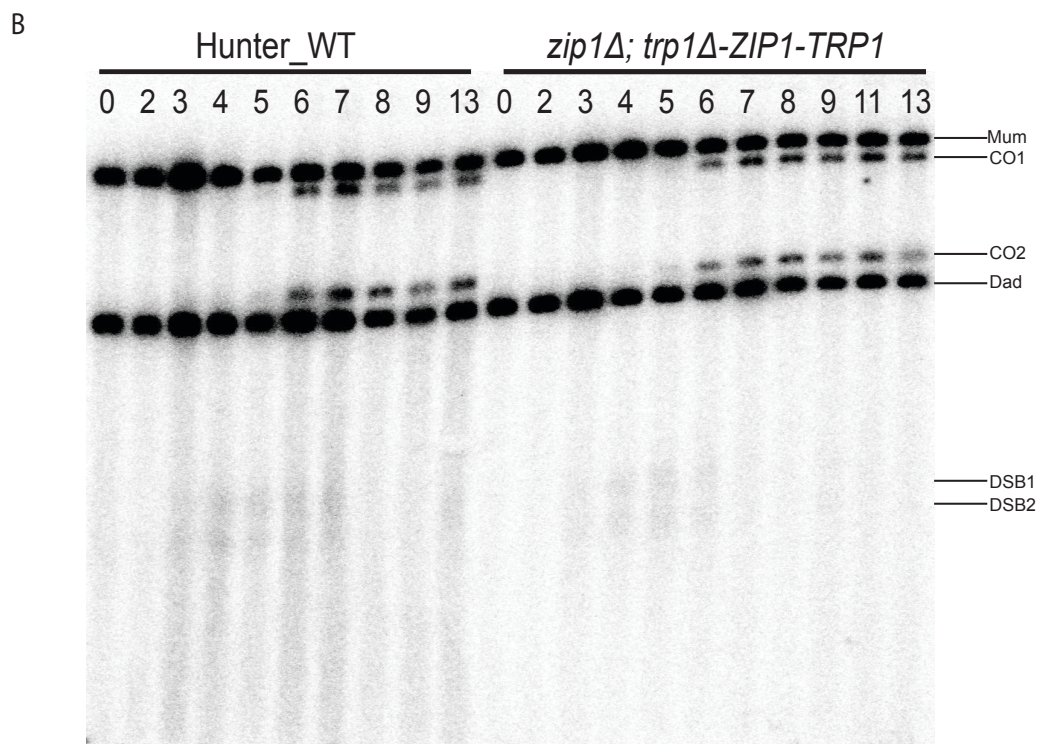
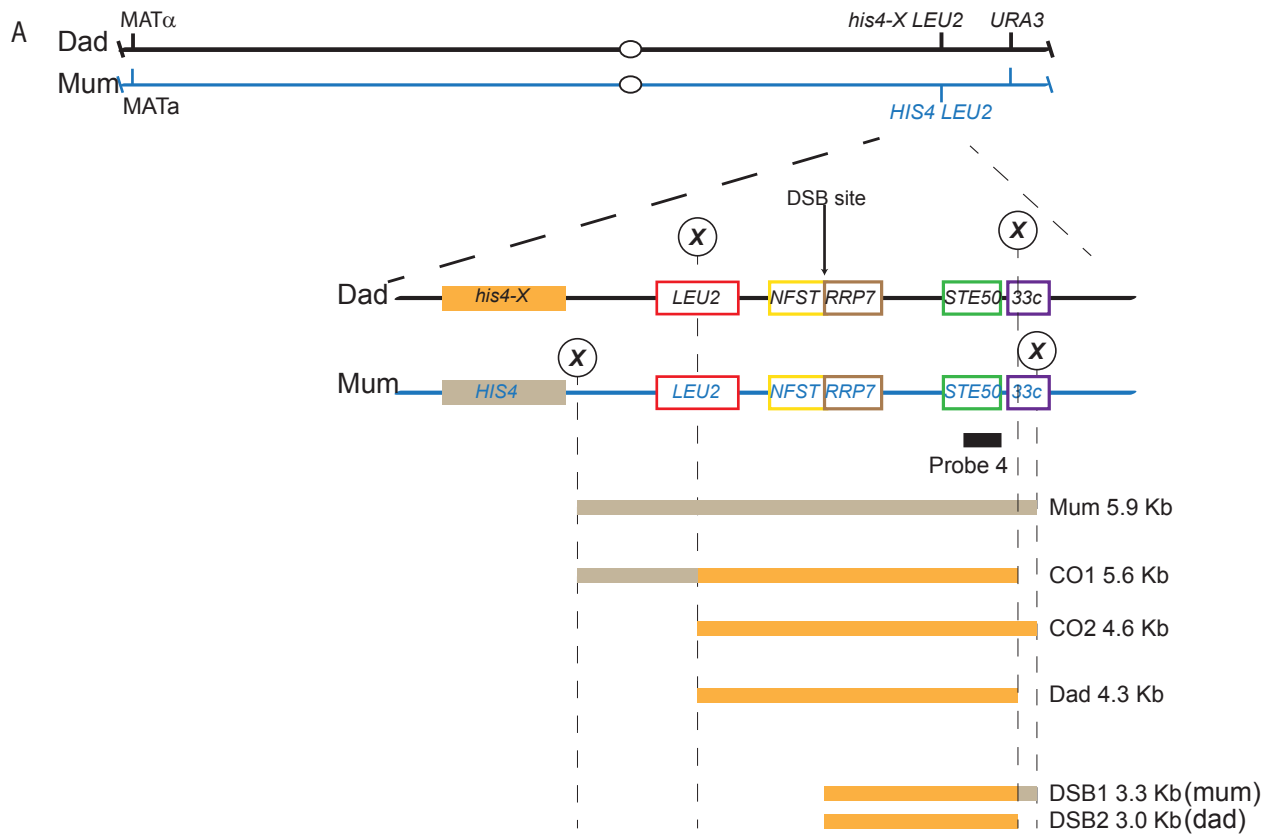
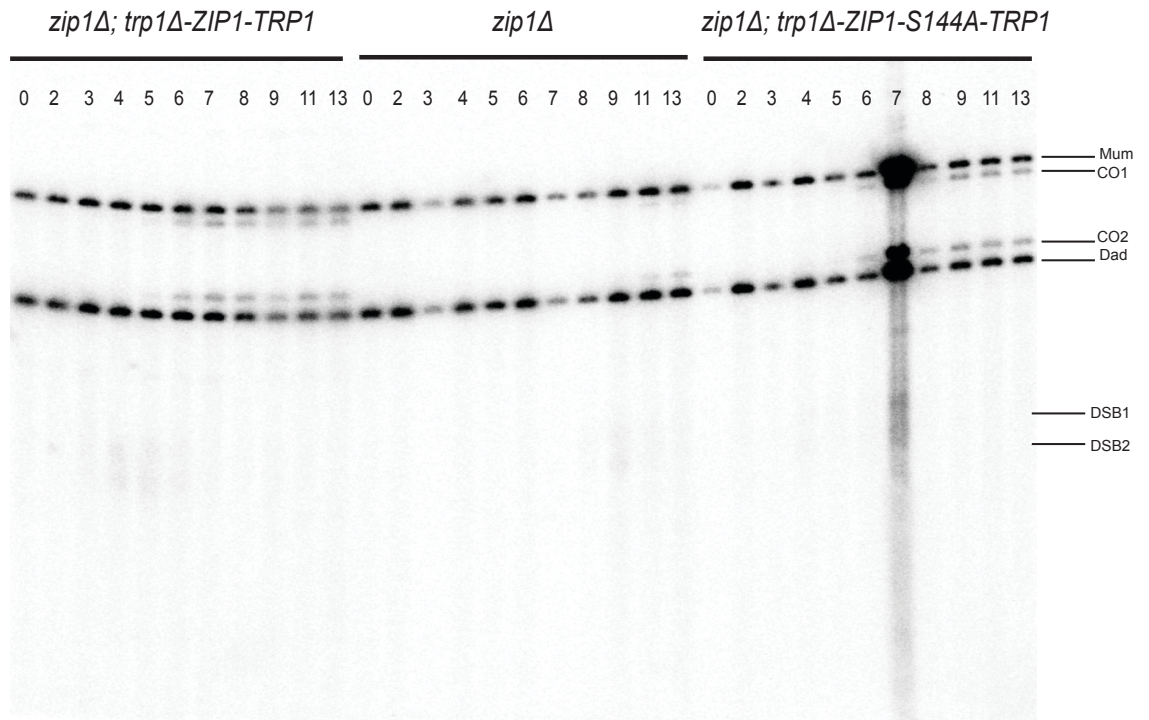


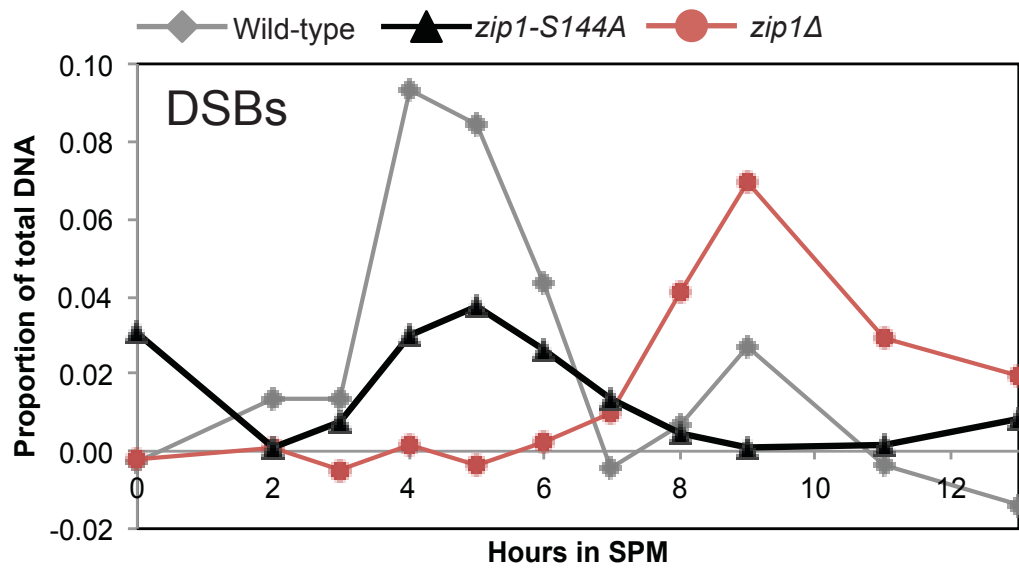
Figure 4.11 Recombination analysis of the wild type, *zip1*, and *zip1-S144A*

A) One-dimensional gel analysis of crossovers and DSBs. Samples obtained from a single meiotic time course. DNA was extracted and digested with *Xho*I (see Figure 4.10). (B) DSBs quantification for the wild type; *zip1* Δ ; *zip1-S144A*. (C) COs quantification for the wild type; *zip1* Δ ; *zip1-S144A*. The wild type is represented by the gray line; *zip1* Δ is shown by the red line; *zip1-S144A* is shown by the black line.

A



B



C

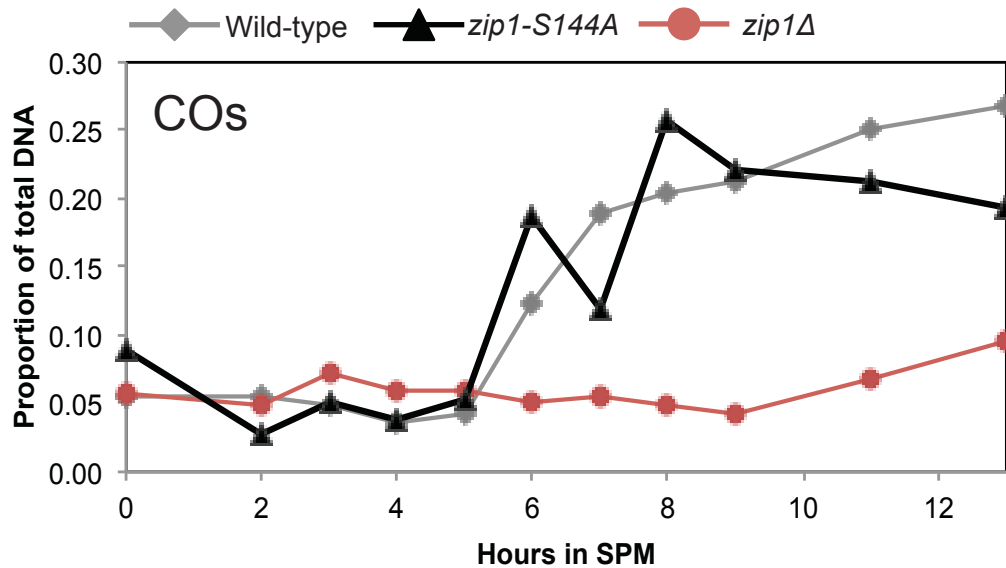


Figure 4.12 meiotic recombination is not affected in *zip1-S144A*

A) One-dimensional gel analysis of crossovers and DSBs between the wild type (left) and *zip1-S144A* (right). Samples were obtained from a single meiotic time course. DNA was extracted and digested with *Xho*I (see Figure 4.10). (B-C) Meiotic progression for the wild-type and *zip1-S144A* mutant respectively. DNA stained with DAPI. ~200 cells counted for each time point. Mononucleate refers to one nucleus; Binucleate refers to two or more nuclei. (D) Quantification of DSBs in both the wild type and *zip1-S144A* mutant. (E) Quantification of COs in the wild type and *zip1-S144A* mutant. CO (crossovers); DSB (double strand breaks). The wild type is represented by a gray line, *zip1-S144A* mutant is represented by a black line. All samples were quantified via Ayida.

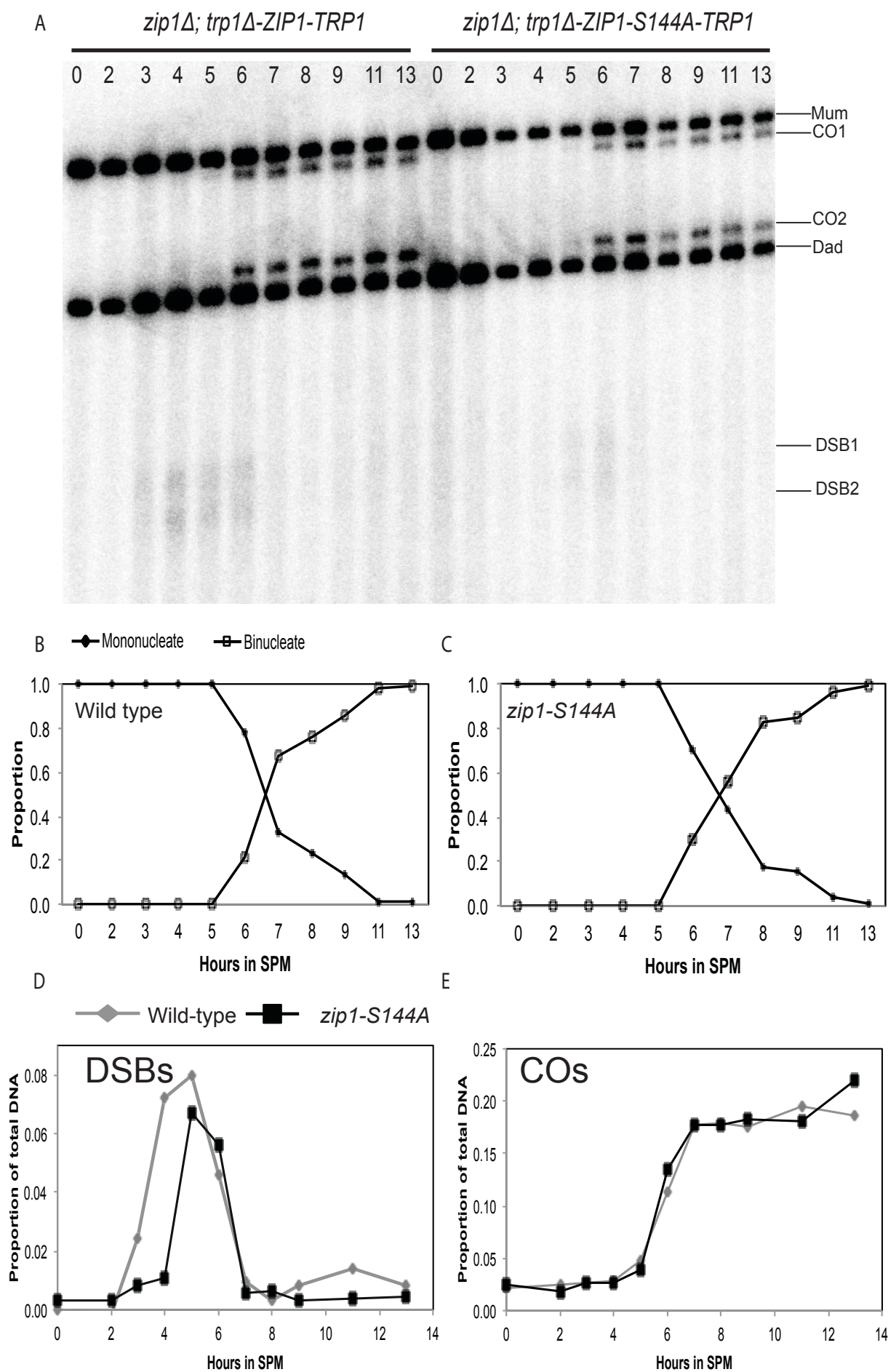
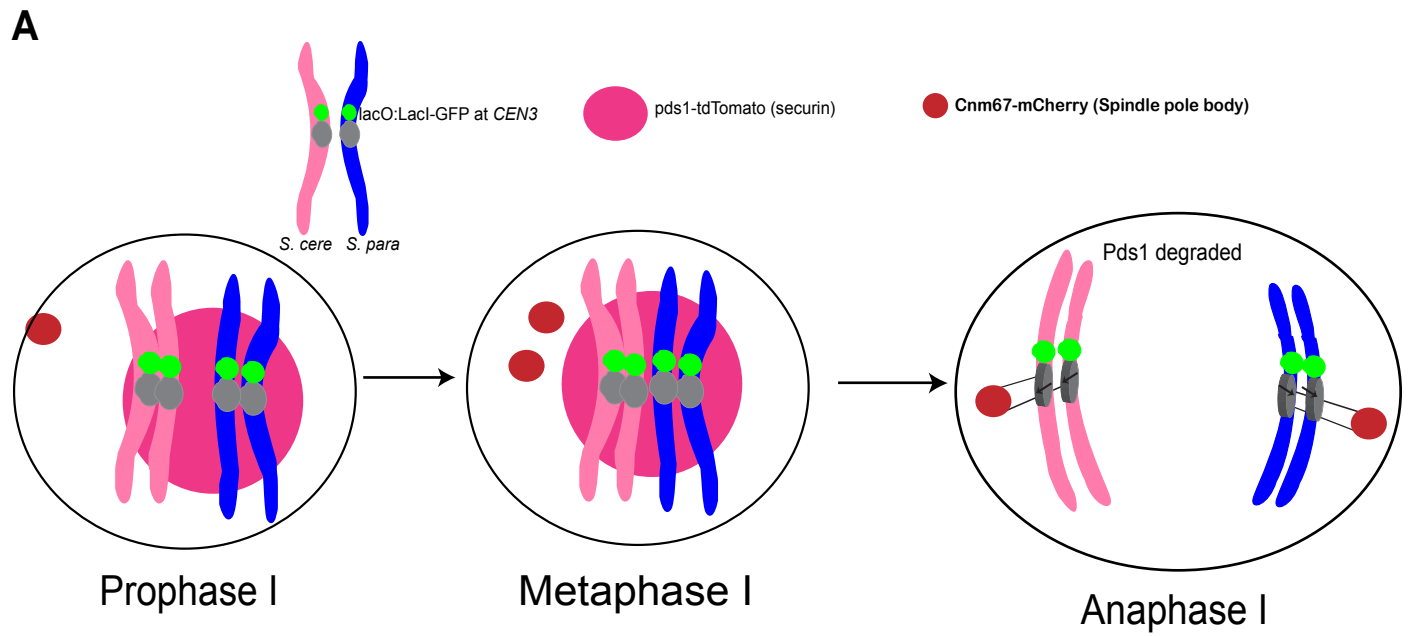
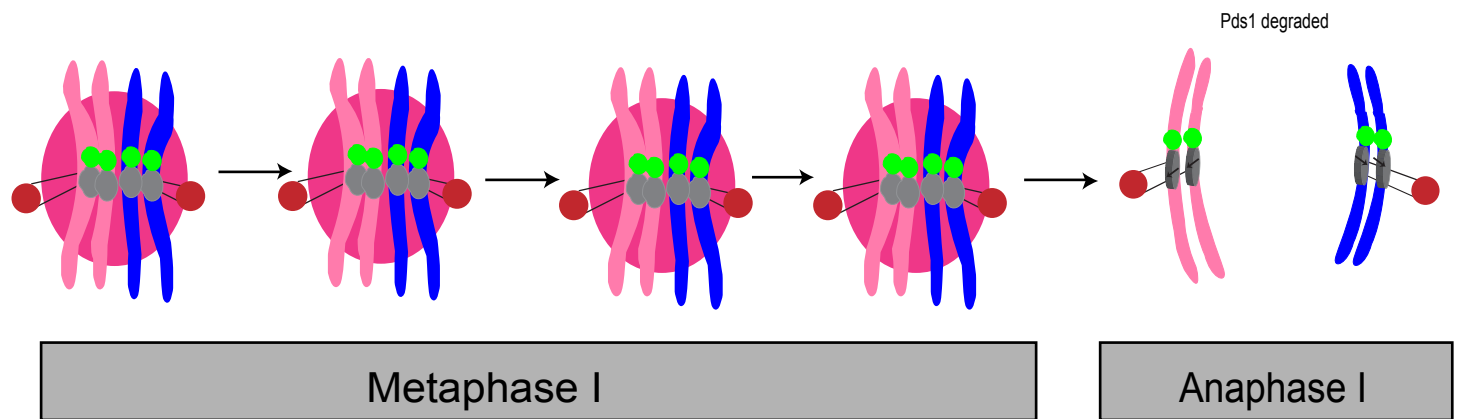


Figure 5.1 The hypothesis of centromere behaviour in non-exchange chromosome pathways

(A) The systemic diagram represents the live cell imaging system. Centromeres on chromosome III were tagged with lacO/LacI GFP (green dots). Cnm67 is a spindle pole body protein (SPB), which was tagged with mCherry (dark red dot), marking metaphase I entry. Pds1 is a securin and is degraded by Esp1 upon entry into anaphase I, and this is marked with tdTomato (pink circle). At prophase I in the exchange segregation, a nucleus contains paired centromeres (green) and one SPB (Red), Pds1 is expected as a red emission. During metaphase I, two dots of Cnm67 (Red) are formed and homologous centromeres are still paired (one green dot). Pds1 remains in the nucleus. The disappearance of Pds1 in the nucleolus indicates entry of anaphase I. SPB starts to move to opposite poles with each attached to a centromere (green). (B) One of the hypothesis of centromere pairing scenarios in NEC is termed gradual movement, which is where centromeres were held together all the way till anaphase I. (C) The hypothesis of another centromere behaviour in NEC. This is named dynamic movement and it is where centromeres were moving together and apart all the time until entry into anaphase I.



B Gradual movement



C Dynamic movement

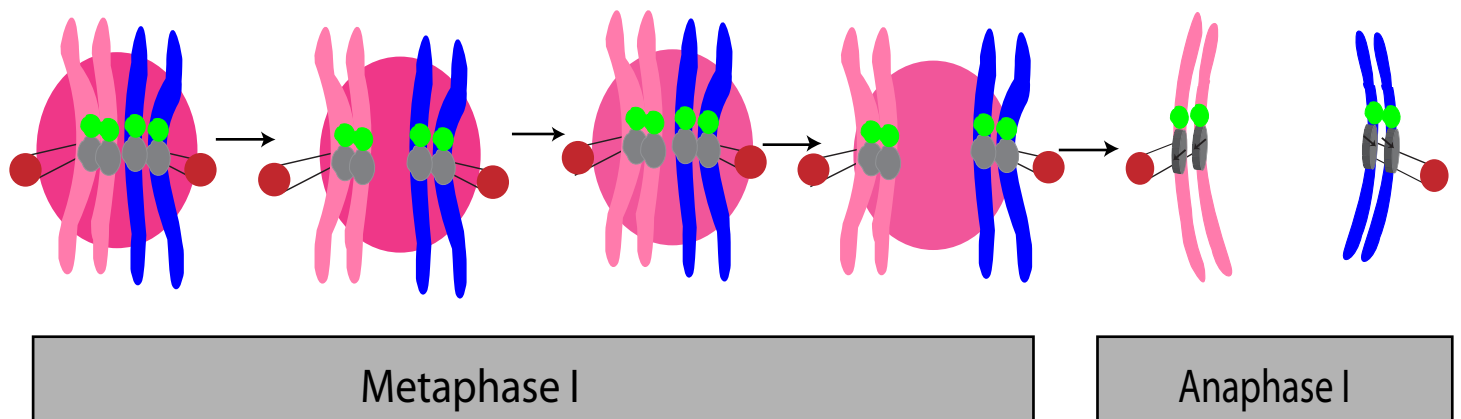


Figure 5.2 Systemic diagram showing the steps of transferring the homeologous chromosome

The *S. cerevisiae* haploid contains a genotype of Cycloheximide resistance (CycR); Canavanine resistance (CanR) and ura negative, which is mated with the *S. paradoxus* haploid that contains both CyhR and CanR, but *URA*⁺. This *URA* is the marker for YFC (Your favourite chromosome), hence the chromosome that wants to transfer. *S. paradoxus* haploid also has a *kar1* mutated. Mating of both *KAR1* parents results in nuclear fusion with a genotype of CanS; CyhS; *URA*⁺ diploids (Left). CanS and CyhS are dominant genes. Mating of a *kar1/KAR1* (heterokaryons) results in two types of diploids produced, which is due to chance. The first type is termed as a 'Cytoductants', which inherits cytoplasms from both parents and a nucleus only from one parent. Another type that rarely happens is termed a chromoductant, and in this case is named YACductant. This haploid contains the chromosome tagged with *URA* from one species but everything else remains the same from other species. Figure adapted from (Spencer et al., 1994).

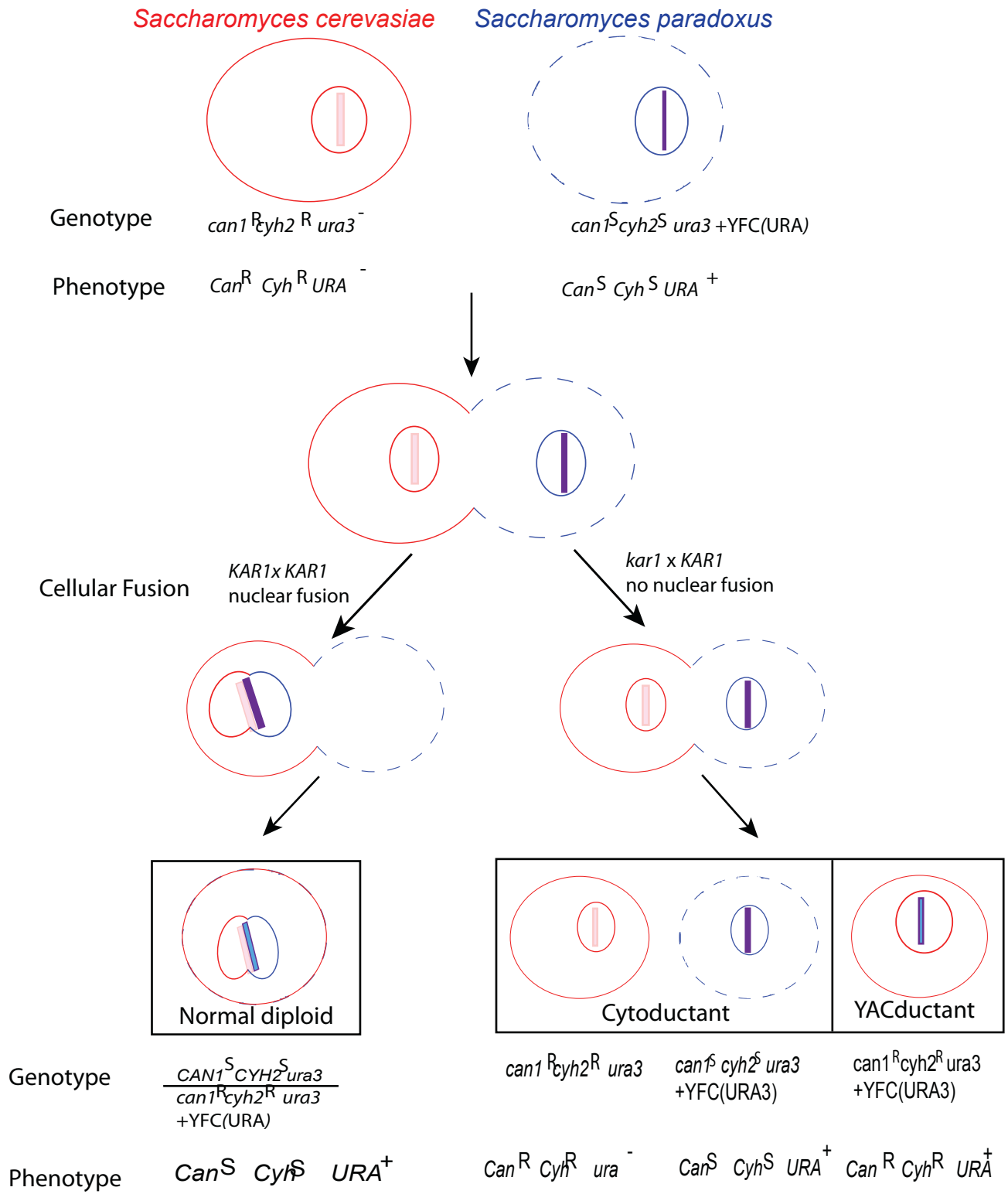


Figure 5.3 Verification of successfully transferred chromosome III

The bar chart shows individual chromosome size for both *S. cerevisiae* and *S. paradoxus*. *S. cerevisiae* is shown in black and *S. paradoxus* is shown in gray. *S. cerevisiae* SK1 genome size is obtained from (http://cbio.mskcc.org/public/SK1_Mv0/), *S. paradoxus* N17 genome size is obtained from: (<http://www.sanger.ac.uk/research/projects/genomeinformatics/browser.html>).

(B) Pulsed-field gel electrophoresis (PFG) represents the successful transfer of *S. paradoxus* (S.p) chromosome III into *S. cerevisiae* (S.c) genome. From left to right, column 1 represents a Yeast chromosome PFG ladder from NEB, and the estimate of individual chromosome is indicated on the left. Column 2 is the *S. cerevisiae* recipient strain (chromosome III is indicated by a white arrow). Column 3 is the *S. paradoxus* donor strain (chromosome III is indicated by a red arrow). Column 4 is the control strain (III_{con}) where *S. paradoxus* chromosome III has transferred into *S. cerevisiae* S288c background (the strain is adapted from (Greig, 2007)). Column 5 is the disomes of chromosome III where both *S. cerevisiae* and *S. paradoxus* chromosomes were contained in the genome (disome). Column 6 shows the replacement of *S. paradoxus* chromosome III into the *S. cerevisiae* genome (III_{rep}).

(C) Viability verification of successfully transferred homeologous chromosome from *S. paradoxus*. Wild-type S.c diploids in SK1 background are shown in gray with 100 tetrads examined; the already published wild-type *S. cerevisiae* homeologous chromosome in S288c (Newnham et al., 2010) is shown in black (100 tetrads) and the partial hybrid containing one *S. paradoxus* chromosome III and 15 *S. cerevisiae* chromosomes is shown with strike lines (140 tetrads are examined).

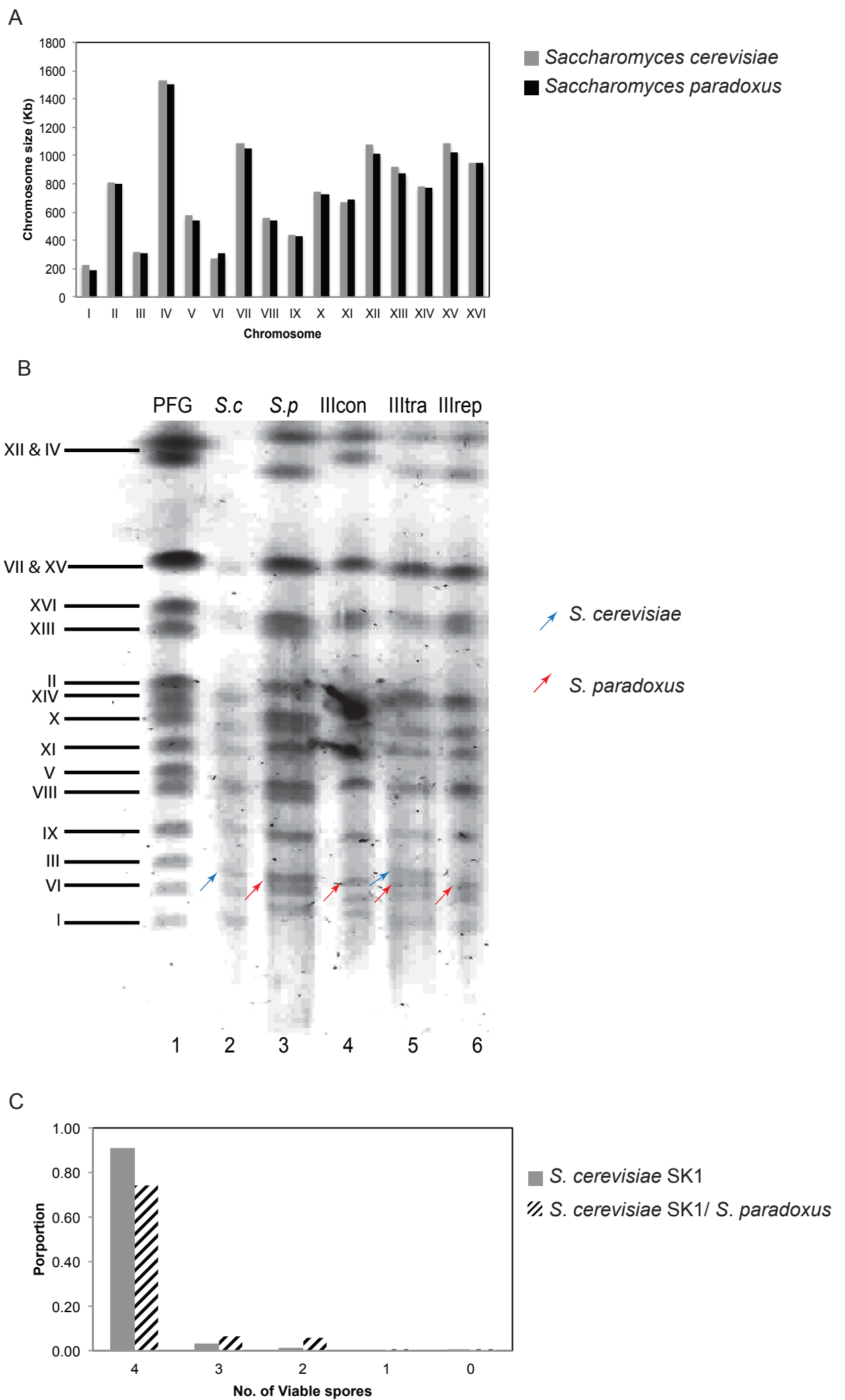


Figure 5.4 Centromere pairing of the homeologous *S. paradoxus* x *S. cerevisiae* non-exchange chromosome pair is decreased compared to homologous centromere pairing in SK1 strain

(A) Representative images of meiosis segregation pattern in SK1 homeologous chromosome. Normal meiosis yields a tetrad containing a single GFP (*CEN3*) focus in each spore (A left), and Meiosis I non-disjunction (NDJ) yields two spores each containing two GFP foci and two containing none (A right). (B) Quantification of meiosis I non-disjunction in SK1 homeologous chromosomes. (C-E) representative spread images of pachytene containing 'paired' *CEN3* in SK1 homeologous chromosomes, S288c Homeologous chromosomes, *zip1Δ* in SK1 homeologous chromosomes respectively. (F-H) presents spread images of pachytene containing 'unpaired' *CEN3* in different yeast homeologous chromosomes (SK1, S288c and *zip1Δ* in SK1 respectively). (I) Quantification of *CEN3* pairing between SK1 wild type (black), S288c wild type (grey), SK1 *zip1Δ* (black line) homeologous chromosomes. 0.5 μm distance between two GFP dots were measured as paired; > 50 nuclei for each strain were scored. Arrow indicates Cen3. Image scale: 2 μm

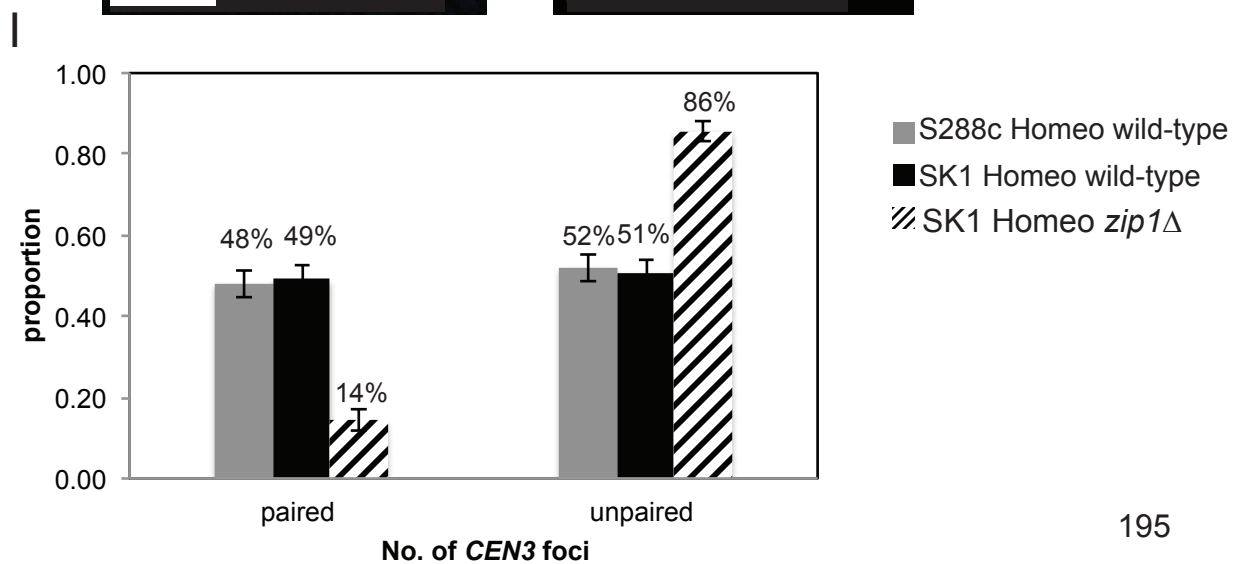
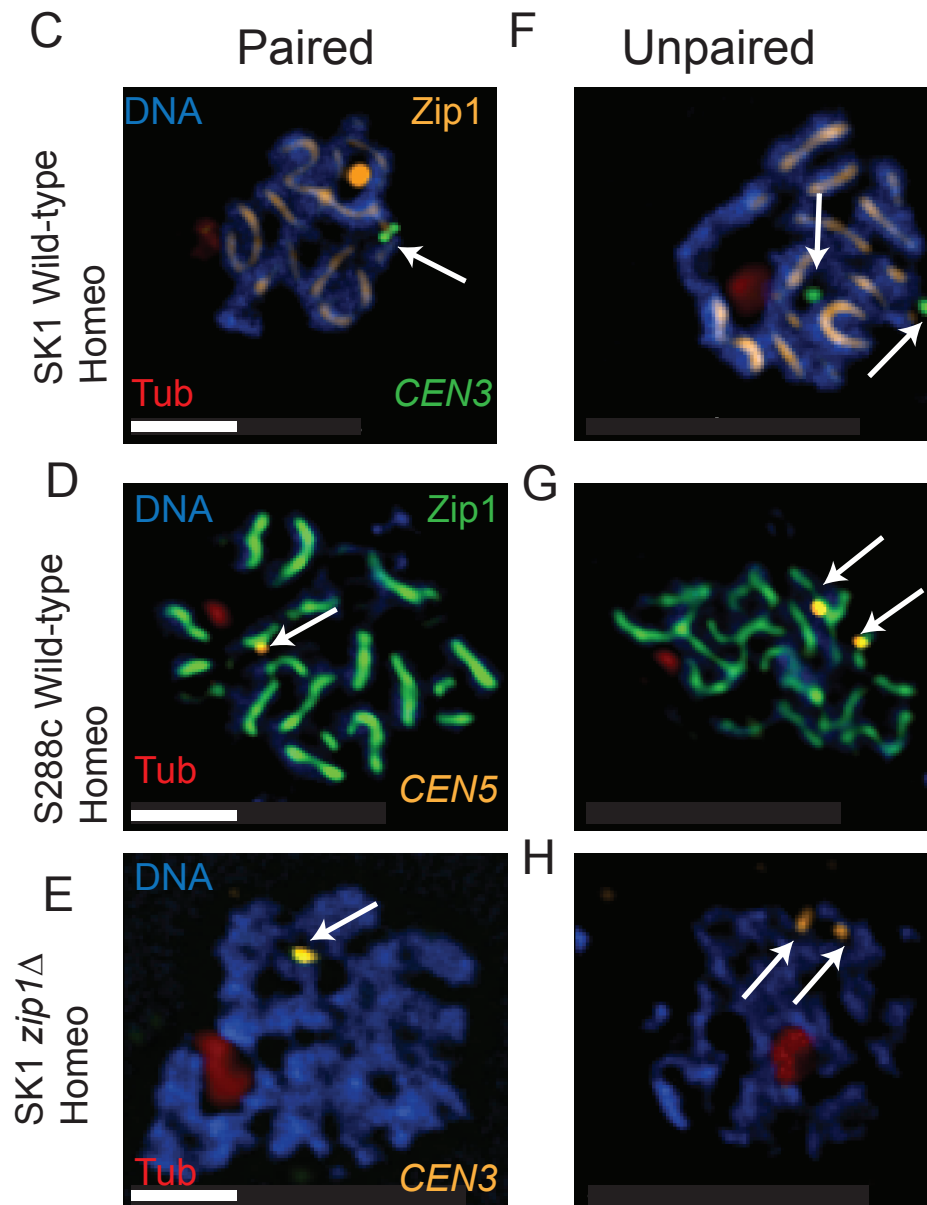
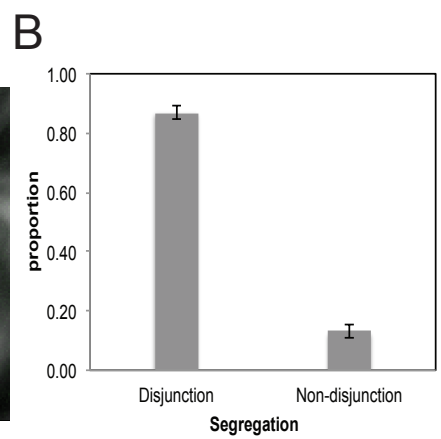
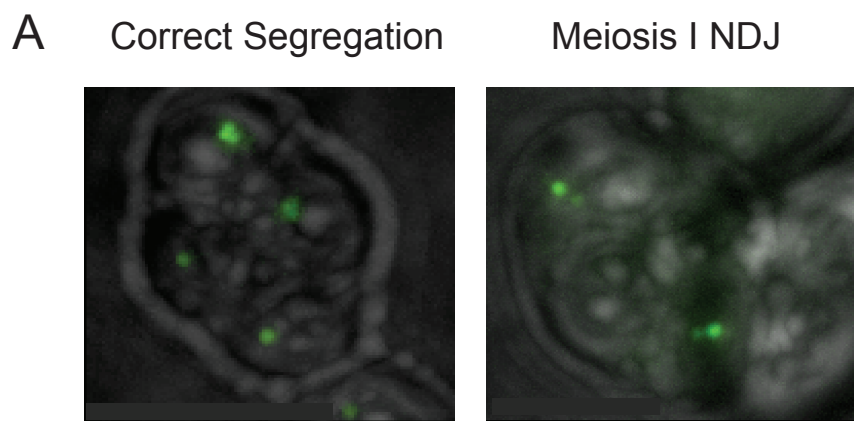
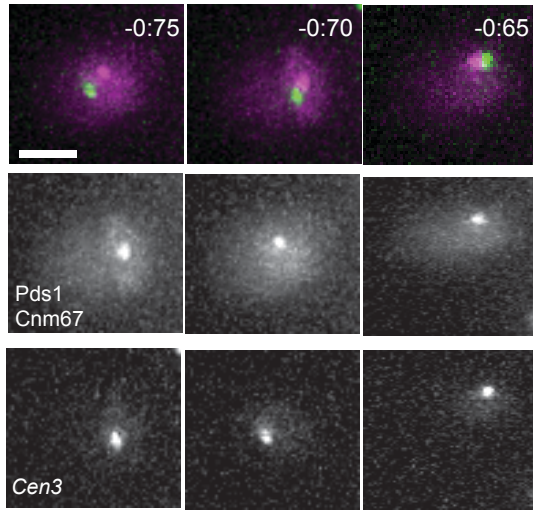


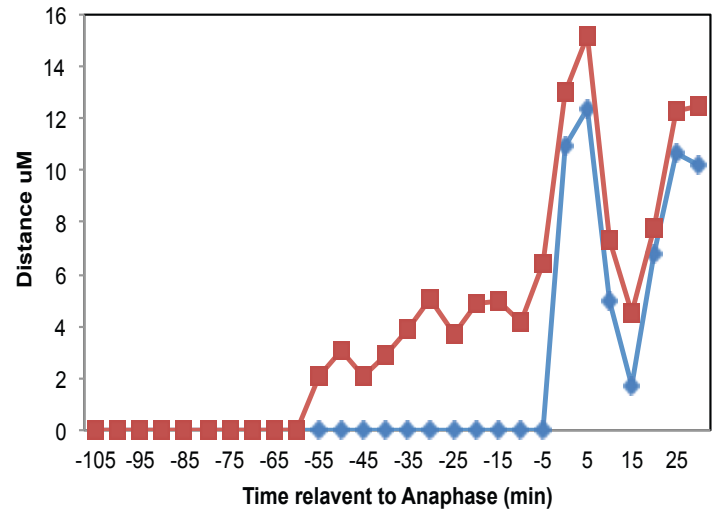
Figure 5.5 Live centromere movements in the homologous wild type

(A) Example of centromere movements in prophase I. (B) Centromere movements continued to metaphase I. (C) Centromere movements in anaphase I. Centromere three was tagged with green GFP; spindle pole body Cnm67 was tagged with mCherry and anaphase I marker Pds1 was tagged with tdTomato. Bars: 2 μm . (D) Quantification of *CEN3* movements in 21 cells was examined. Time at 0 indicates anaphase I entry. (E) Quantification of spindle pole body (Cnm67) movements in 21 cells were studied. (F) Example of centromere and spindle movements in a particular homologous chromosome. This cell is the same one used for images in A-C. Red showing Cnm67; Blue representing *CEN3*.

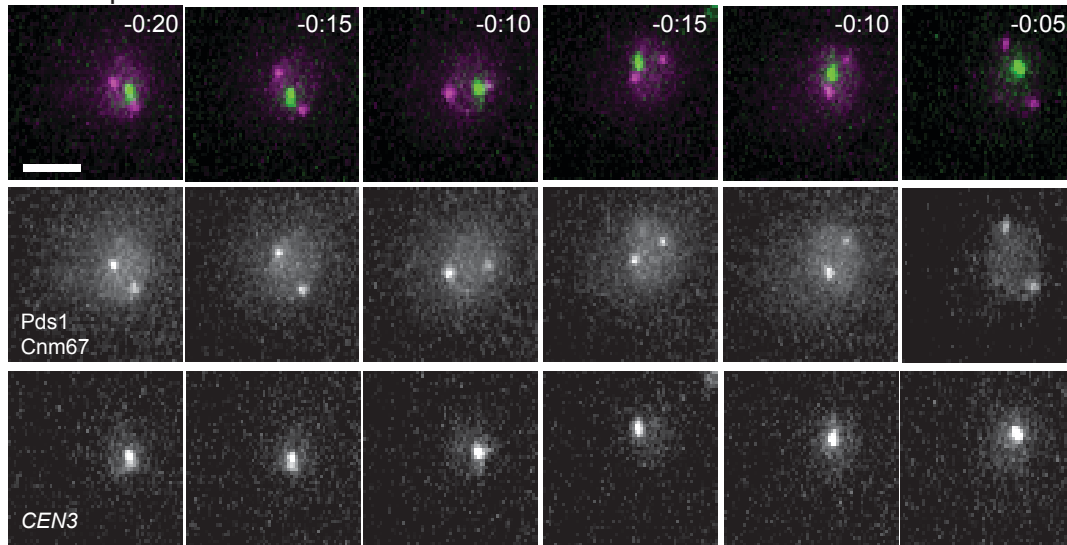
A Prophase I



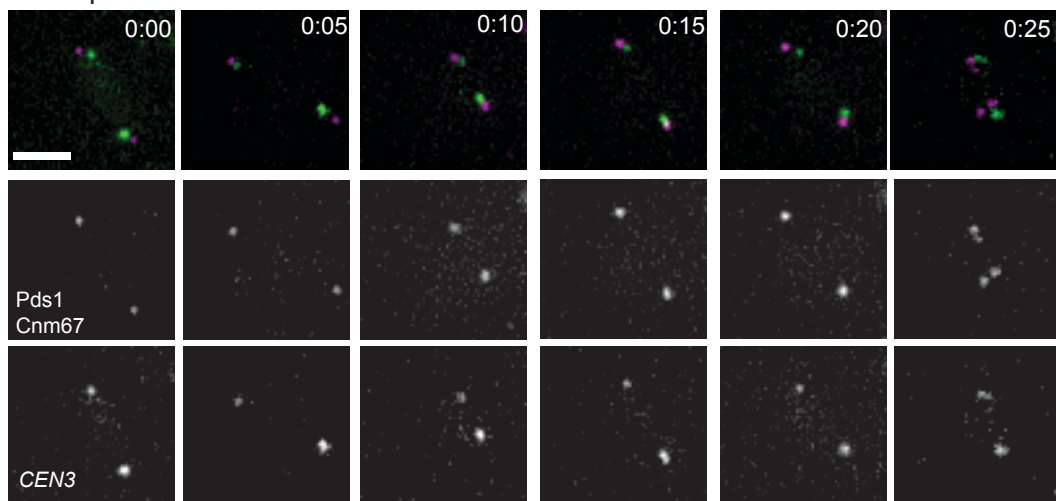
F



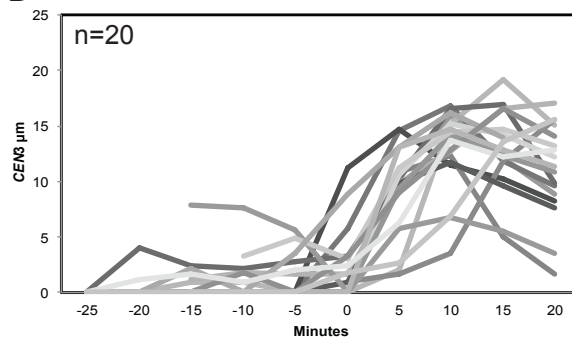
B Metaphase I



C Anaphase I



D



E

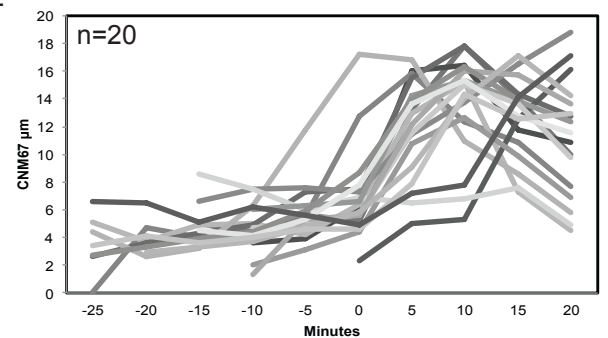
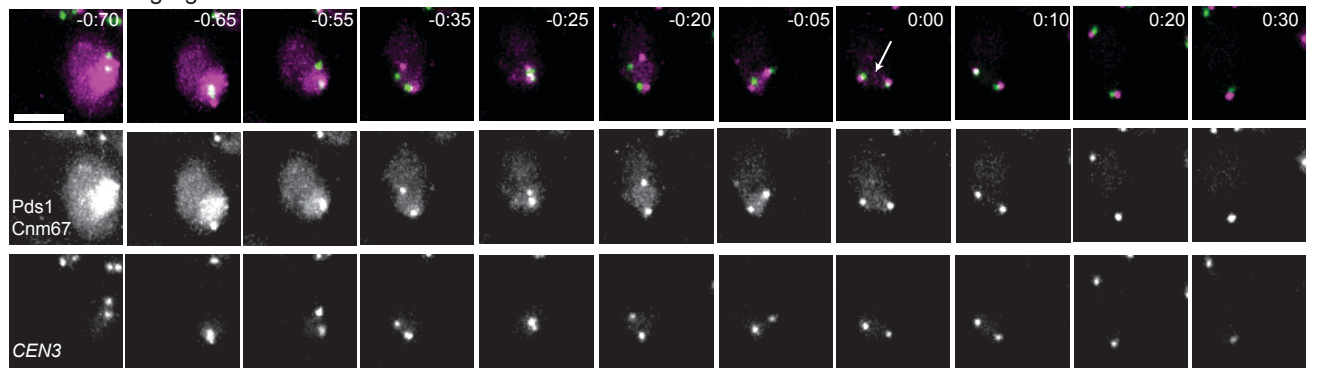


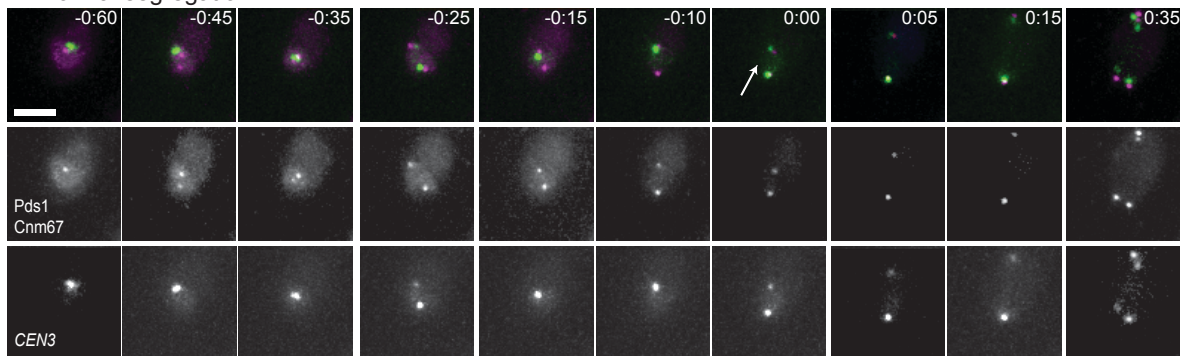
Figure 5.6 Live centromere movements in homeologous wild-type

(A) Normal segregation in NEC wild-type cells that are shown from prophase to anaphase I. (B) Quantification of *CEN3* movements in another normal segregated cells. 28 cells were examined. Time at 0 indicates anaphase I entry. (C) Example of centromere movements in meiosis I non-disjunction (MI NDJ) in the homeologous wild-type. Bars: 2 μ m. (D) Quantification of *CEN3* movements in normal cell segregation. (E) Quantification of Cnm67 movement in normal segregated cells. (F) Quantification of centromere movements in MI NDJ cells. 4 out of 32 cells observed were MI NDJ. (G) Quantification of Cnm67 movement in MI NDJ cells. (H) The bar chart represents the proportion of disjunction and non-disjunction in homeologous chromosomes. N=32. Centromere 3 was tagged with lacO/LacI GFP; Cnm67 was tagged with mCherry, seen as red dots. Pds1 is a marker used for entry into anaphase I, as it was degraded just before onset of anaphase I and II by Anaphase-promoting complex (APC) (Ciosk et al., 1998; Nasmyth et al., 2000; Uhlmann et al., 1999), and was tagged with tdTomato, appearing as a confluent of red emission from prophase I until metaphase I, and suddenly disappearing just before anaphase I.

A Normal segregation 1



B Normal segregation 2



C Meiosis I non-disjunction

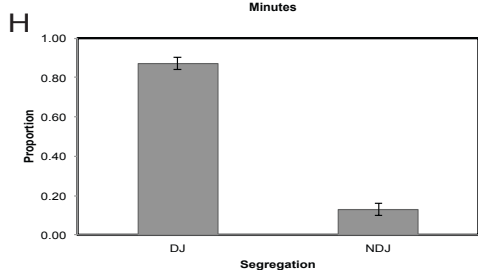
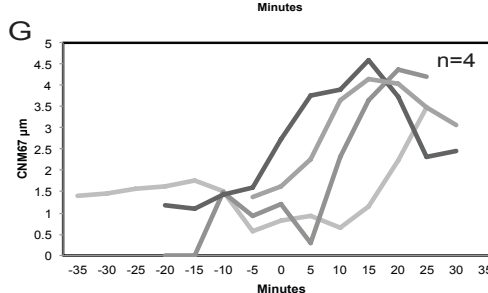
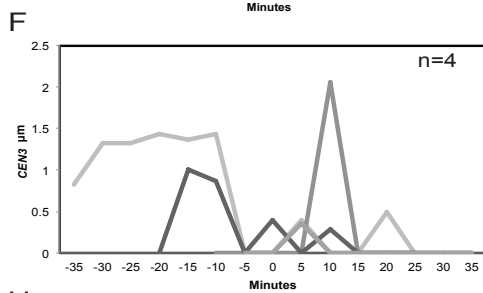
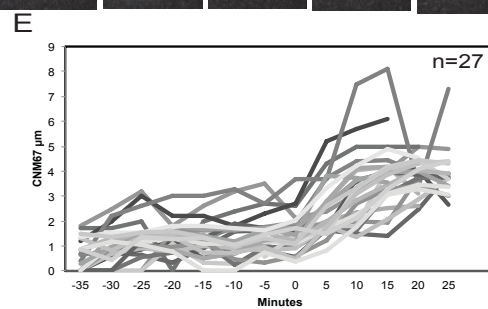
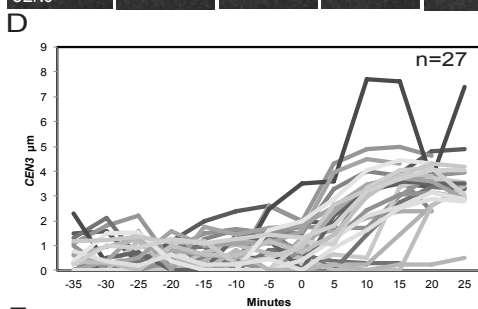
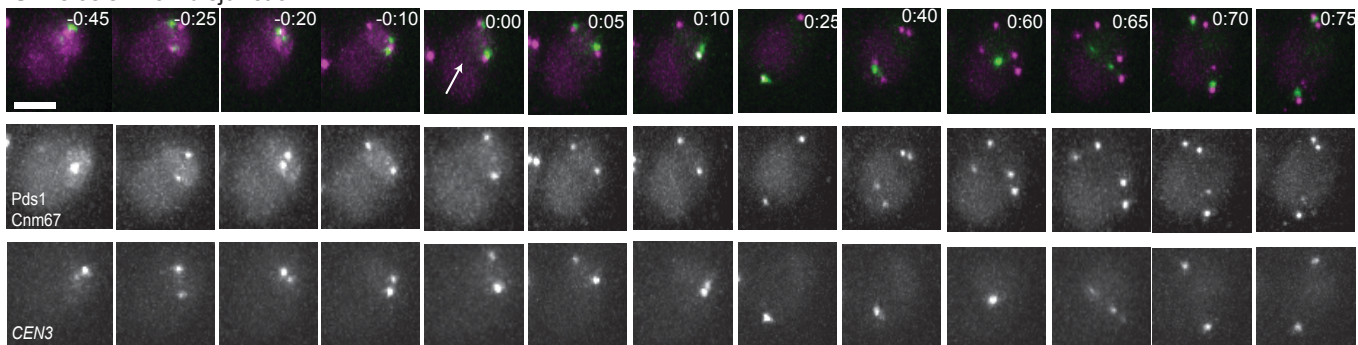


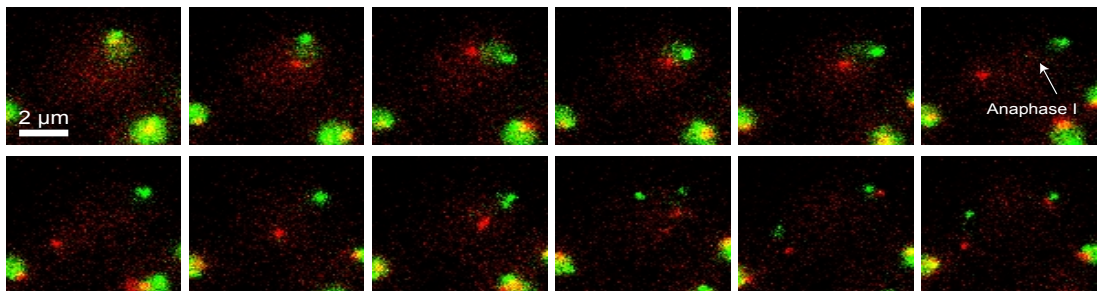
Figure 5.7 Non-exchange chromosome segregation in *zip1-T114A*

(A) Meiotic spreads showing paired centromeres in a *zip1-T114A* mutant at pachytene. (B) Representative spread images of unpaired centromeres in a *zip1-T114A* mutant at pachytene. (C) Representative spread image showing separation of sister chromatids (SSC) pairing in a *zip1-T114A* mutant. Bars: 2 μ m. N=46. Zip1 is stained in orange; Tubulin stained in Red; DNA stained in Blue; centromere stained in green. (D) Proportions of centromere pairing at pachytene in a *zip1-T114A* mutant. (E) Example of live cell imaging of normal segregation in a *zip1-T114A* mutant. (F) Meiosis I non-disjunction live cell in a *zip1-T114A* mutant. (G) Representative images showing SSC in a *zip1-T114A* mutant using live cell imaging. Centromere is tagged with GFP, Cnm67 represents spindle pole body tagged with mCherry and anaphase I marker Pds1 is marked with tdTomato. (H) Quantification of *CEN3* and Cnm67 movements respectively in a *zip1-T114A* mutant with normal segregation. (I) Distance of non-disjunction cells analysis of *CEN3* and Cnm67 movements respectively in a *zip1-T114A* mutant. (H) Proportion of disjunction and non-disjunction in a *zip1-T114A* mutant. N=30. (J) bar chart representing the segregation pattern in a *zip1-T114A* mutant.

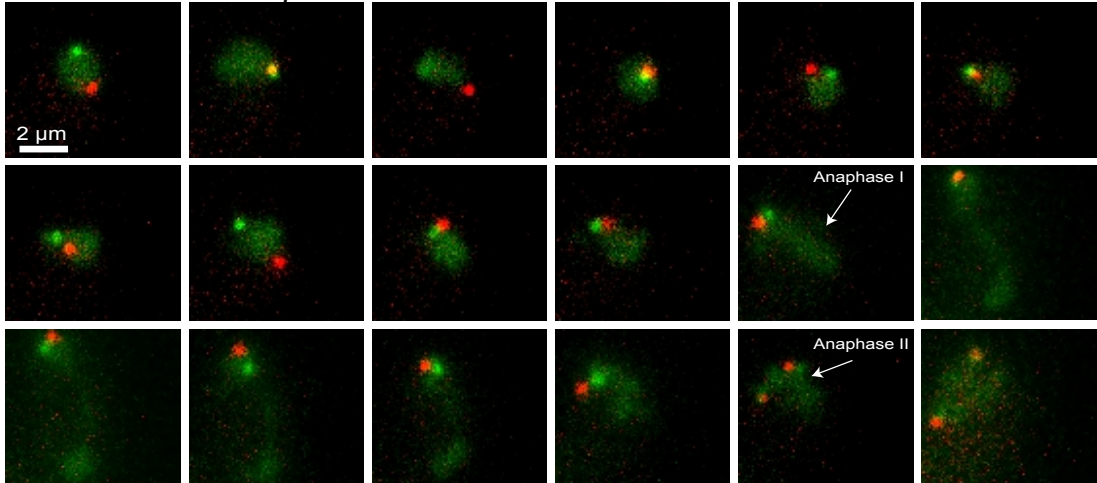
Figure 5.8 chromosome segregation by tagging *S. cerevisiae* with mCherry and *S. paradoxus* *CEN3* with lacO/LacI GFP

(A) Representative live cell images showing normal segregation in wild-type homeologous chromosomes. Three cells presented on these images. Arrows indicate the time when anaphase I occurs in each cell. (B) Example of meiosis I non-disjunction (MI NDJ) in NEC wild type. Anaphase I and anaphase II entry is labeled with arrows. (C) Example of precocious sister chromatid separation (PSCS) in wild-type NEC. Arrow indicates three centromeres. *S. paradoxus* centromere 3 is labeled with lacO/LacI; *S. cerevisiae* centromere 3 is labeled with mCherry. Tagging of *S. cerevisiae* with mCherry was done by Dr Louise Newnham. Bars: 2 μ m (D) Proportion of segregation patterns in NEC wild-type cells. DJ: Disjunction; NDJ: Non-disjunction; PSSC: Precocious separation of sister chromatids. N=111

A Correct segregation



B Meiosis I Non-disjunction



C Precocious separation of sister chromatids

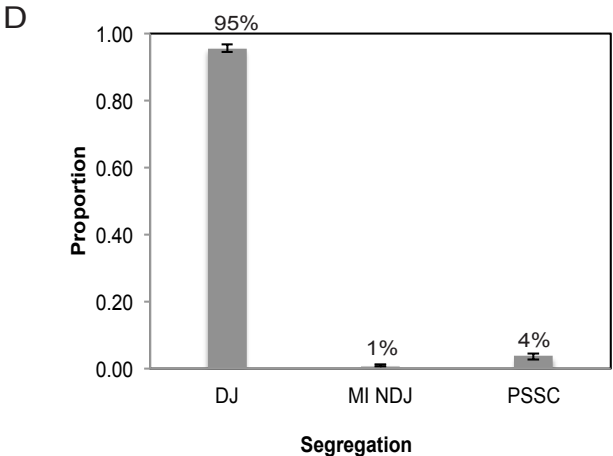
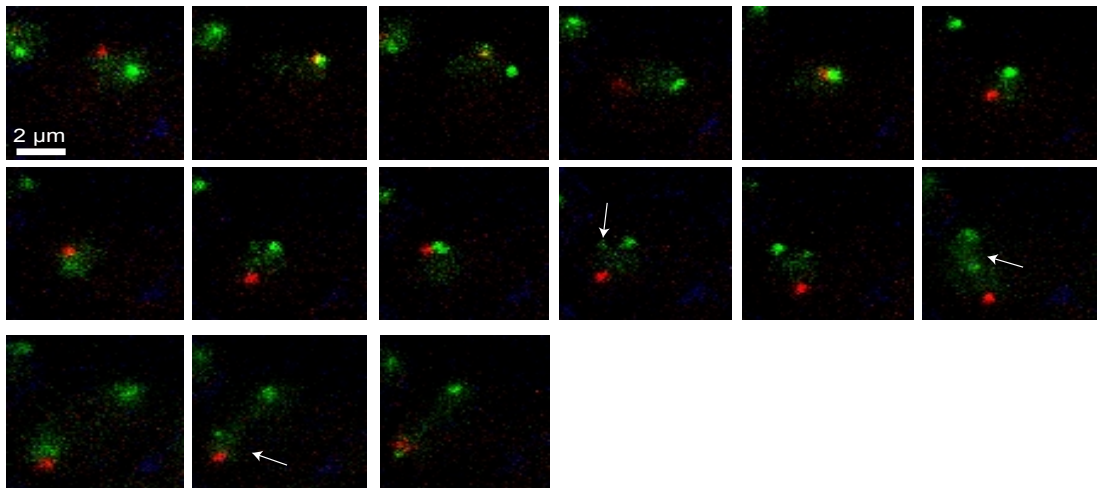
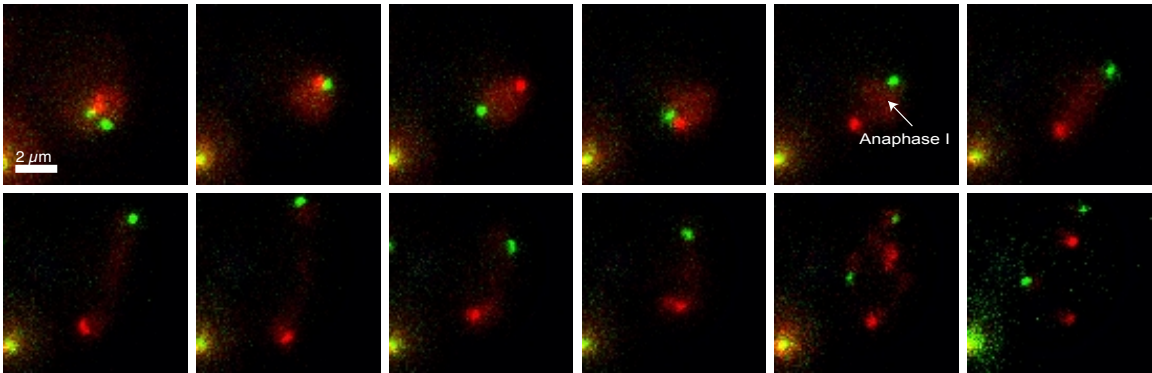


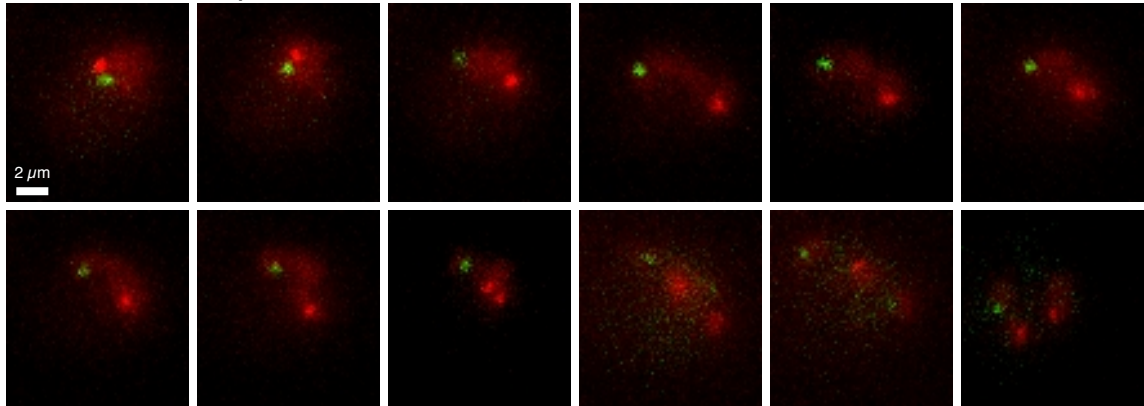
Figure 5.9 Live cell of non-exchange chromosome centromere in *zip1-T114A* using mCherry and lacO/LacI GFP

(A) Representative images showing correct segregation (DJ) of non-exchange chromosome in a *zip1-T114A* mutant. (B) Live cell images showing meiosis I non-disjunction (MI NDJ) in a *zip1-T114A* mutant. (C) Precocious separation of sister chromatids (PSSC) in a *zip1-T114A* NEC. *S. cerevisiae* *CEN3* is tagged in red and *S. paradoxus* *CEN3* is tagged in green. Bars: 2 μ m. (D) Sporulation images corresponding to (A) DJ (B) MI NDJ (C) PSSC respectively. (E) Quantification of segregation patterns in a *zip1-T114A* NEC. N=48

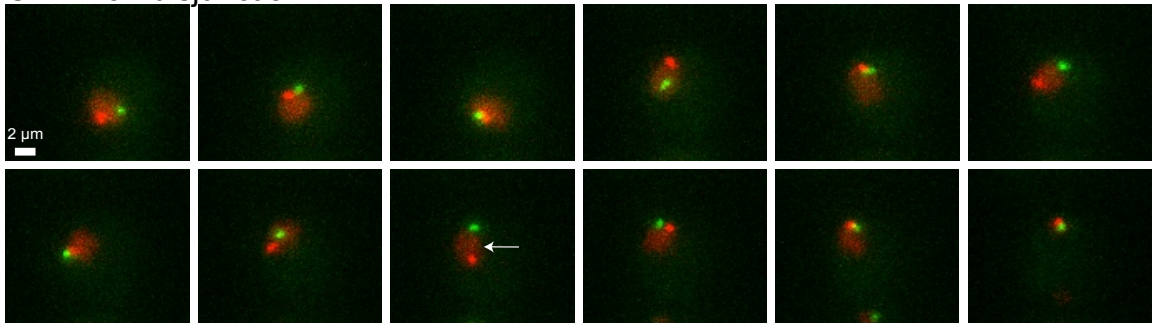
A Correct segregation



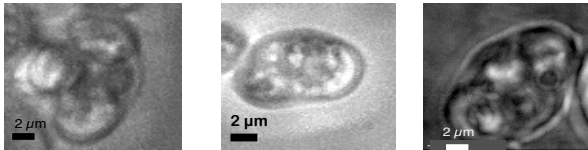
B Precocious separation of sister chromatids



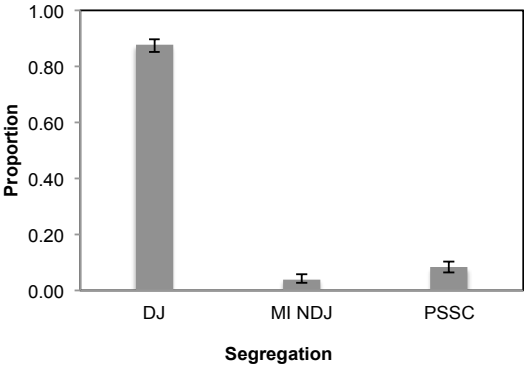
C MI Non-disjunction



D



E



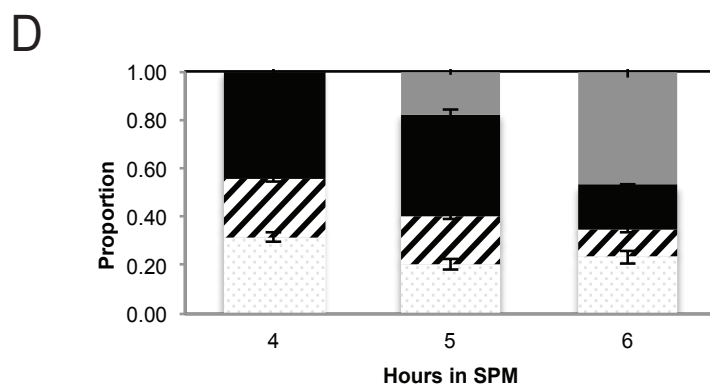
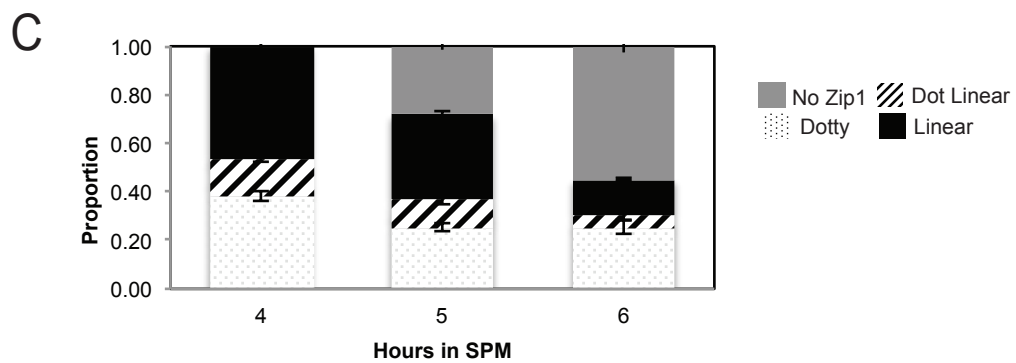
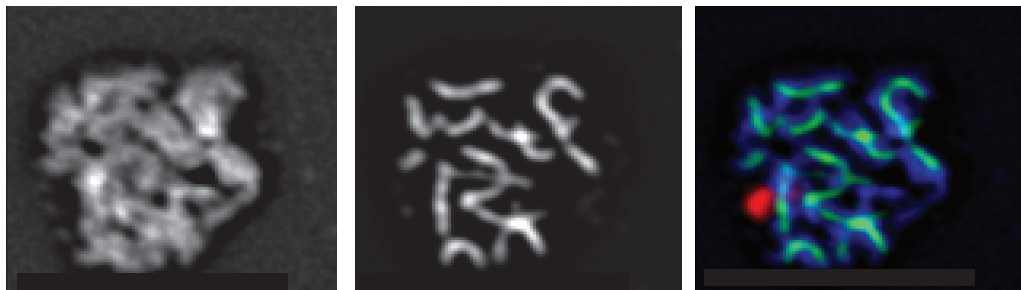
Appendix 1. Synaptonemal complex formation in another two independent *zip1-S82A* transformants

(A-B) Representative images showing linear SC in *zip1-S82A-2* and *zip1-S82A-3* mutants respectively. (C-D) Proportion of different stages of Zip1 in *zip1-S82A-2* and *zip1-S82A-3* mutants respectively. Bars: 2 μ m

A *zip1-82A-2*

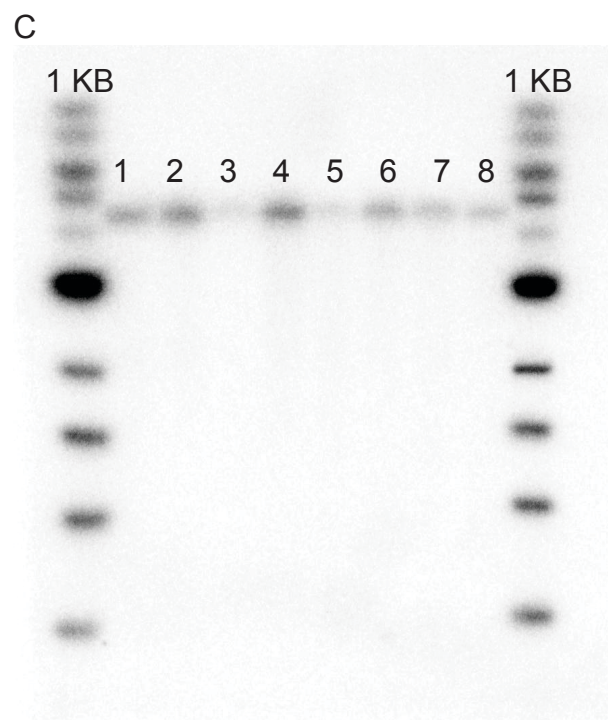
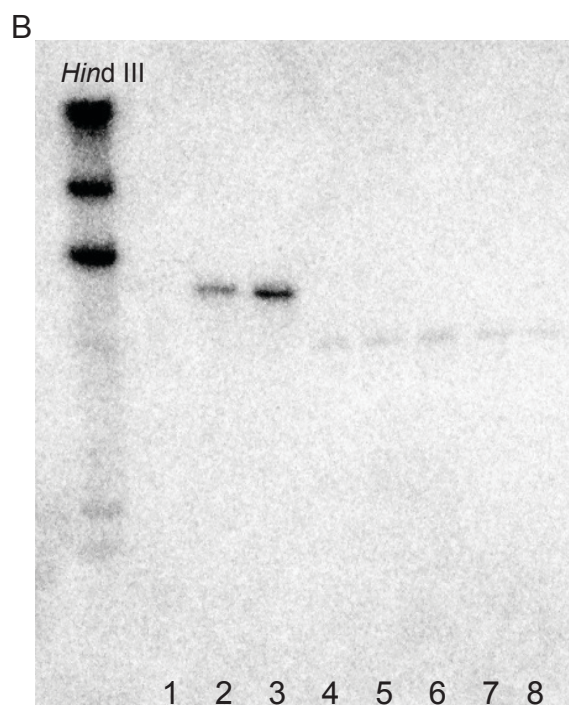
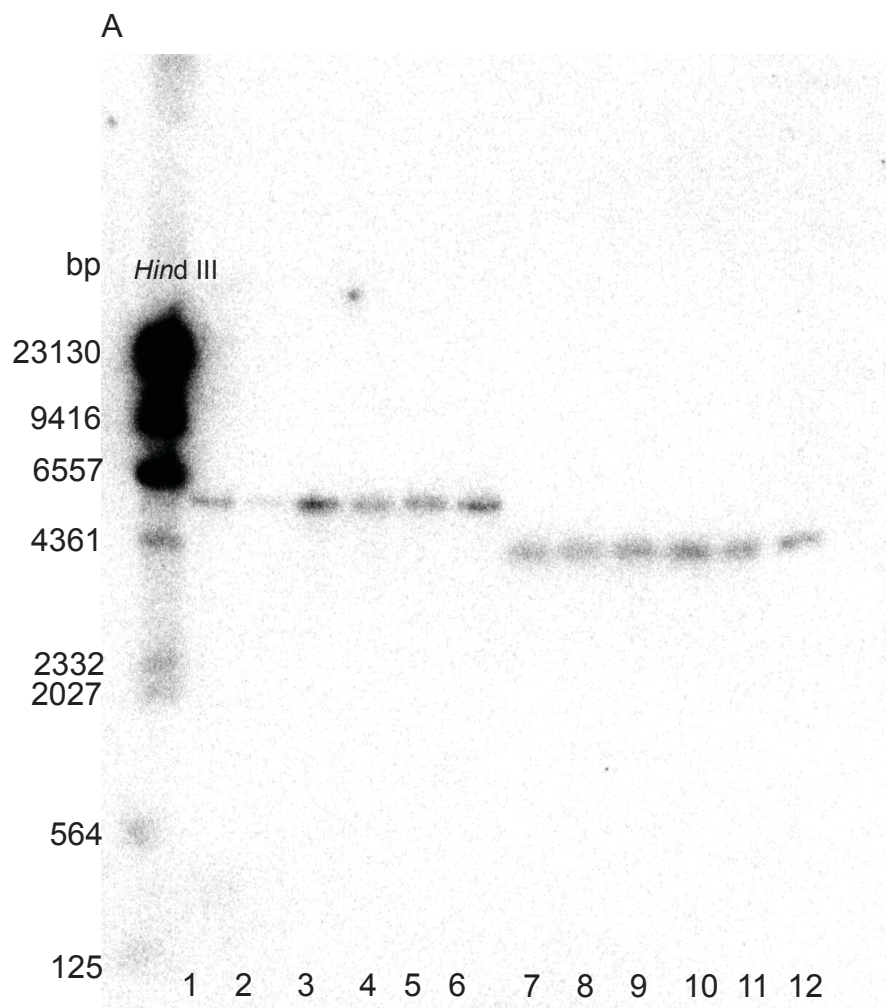


B *zip1-82A-3*

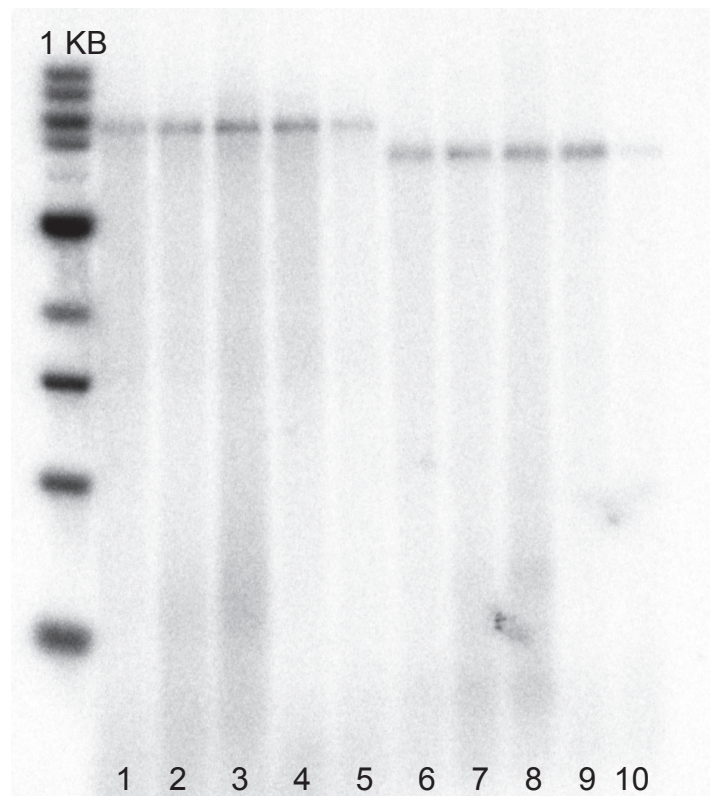


Appendix 2 Transformation of Hunter base strain and the *zip1-S144A* Hunter transformation

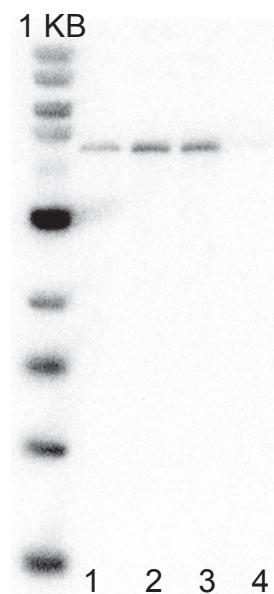
(A) Southern gel representing the modified Hunter parent strains (Y1176 and Y1177 respectively). *HindIII* digested λ -DNA (Biolab) used as the ladder. Corresponding size is showing on the left. Lanes 1 to 6 representing dissected 6 haploids that have the same genotype as Y1176 (expected size of 5.86 Kb). Lane 1 to 3 showed three dissected haploid that are *Mata*; lane 4 to 6 representing *Mata* α . Lanes 7 to 12 representing another 6 haploids derived from Y1177 (expected size of 4.27 Kb). Lanes 7 to 9 representing *Mata* and Lane 10 to 12 representing *Mata* α . Lane 1 and 4 has saved as Y5019 and Y5020 respectively. Lane 7 and 9 has saved as Y5021 and Y5022 respectively (see table 2.9 for strain information). (B) Southern blot showing the transformation of the *zip1-S144A* plasmid into the modified Hunter strain (Y5019 to Y5022). Lane 1 to 3 showing Y5020_*zip1-S144A*_1; Y5020_*zip1-S144A*_2; Y5020_*zip1-S144A*_3 transformants. Lane 4 and 5 showing two independent transformants derived from Y5021; Lane 6 to 8 showing three independent transformants derived from Y5022. (C) Southern integration gel to check strains identified in B contain only one copy of the plasmid. 1 Kb ladder has used as a marker. DNA is digested with *BsgI*. Lane 1 and 2 used two wild-type strains as control; Lane 3 correspond to the B1 lane; Lane 4 correspond to the B2 lane; lane 5 correspond to strain showing in B4 lane; Lane 6 correspond to the B6 lane; Lane 7 corresponds to the B7 lane and Lane 8 corresponds to the B8 Lane.



A



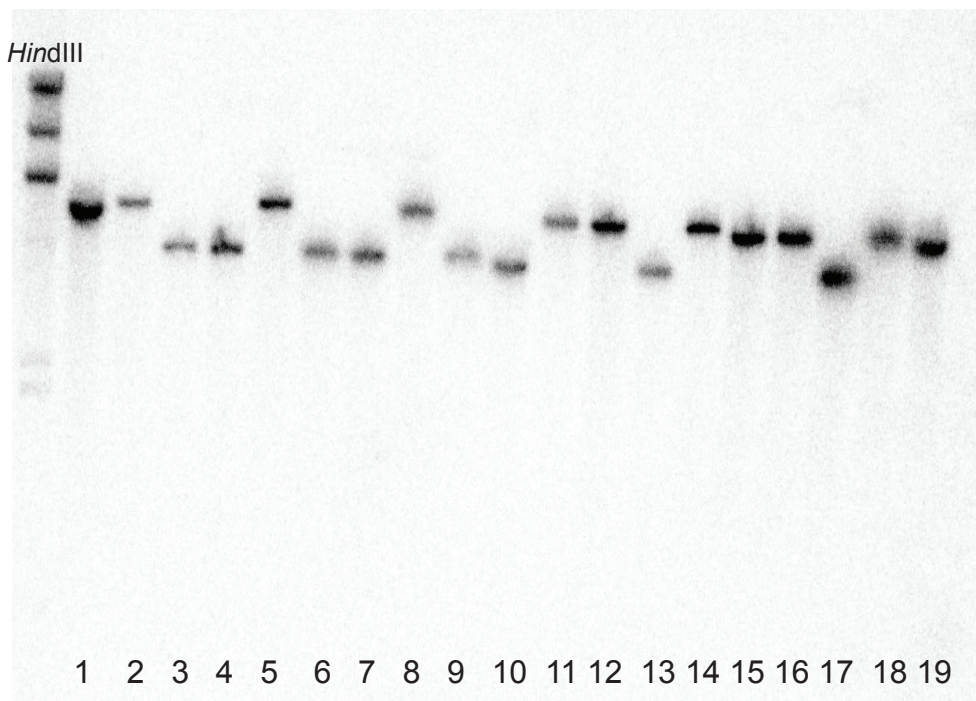
B



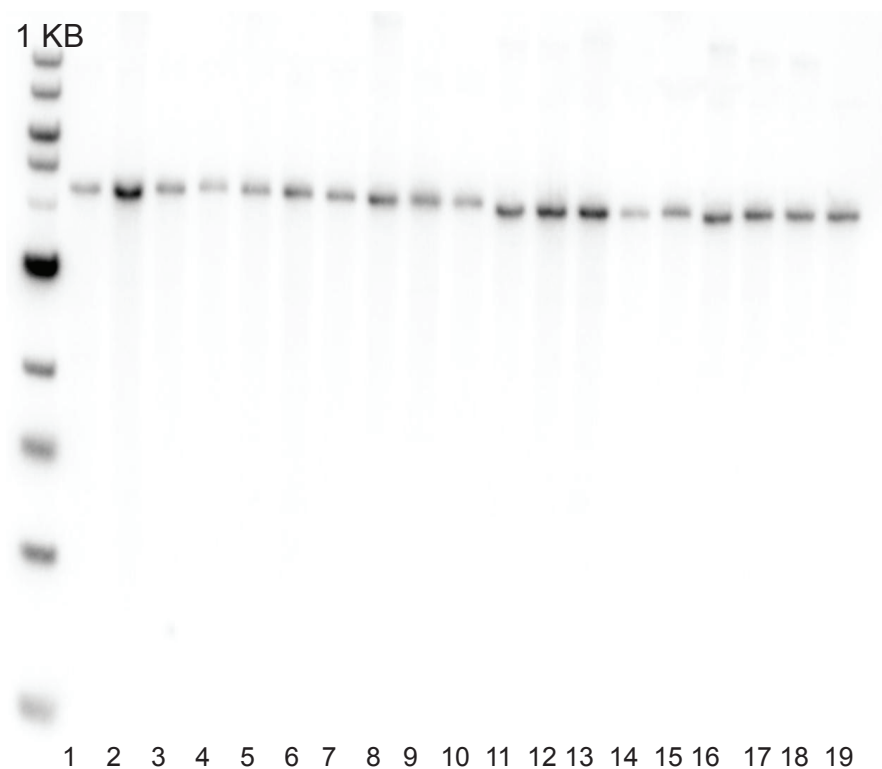
Appendix 3 Southern Blot to check *zip1-4A* and *zip1-T114A* integration

(A) Intergration gel representing the *zip1-4A* mutant. Lane 1 to 5 showing DNA restriction digest using *NcoI*, expect size of 5.9 Kb. Lane 6 to 10 showing DNA restriction digest using *BsgI*, expect size of 4.6 Kb. Lane 1 used the wild-type strain Dr. Andrea Hochwagen made as a control. Lane 2 to 4 showing four candidates after transformation. Lane 6 used the wild-type control. Lane 7 to 10 are four independent colonies after transformation. Candidate 4 (lane 5 and lane 10) is picked as the haploid for the *zip1-4A* mutant. (B) Intergration Southern Blot showing three independent transformants from the *zip1-T114A* mutant. Lane 1 is the wild-type control and Lane 2 to 4 is the three individual colony. Lane 2 is picked as the *zip1-T114A* mutant

A



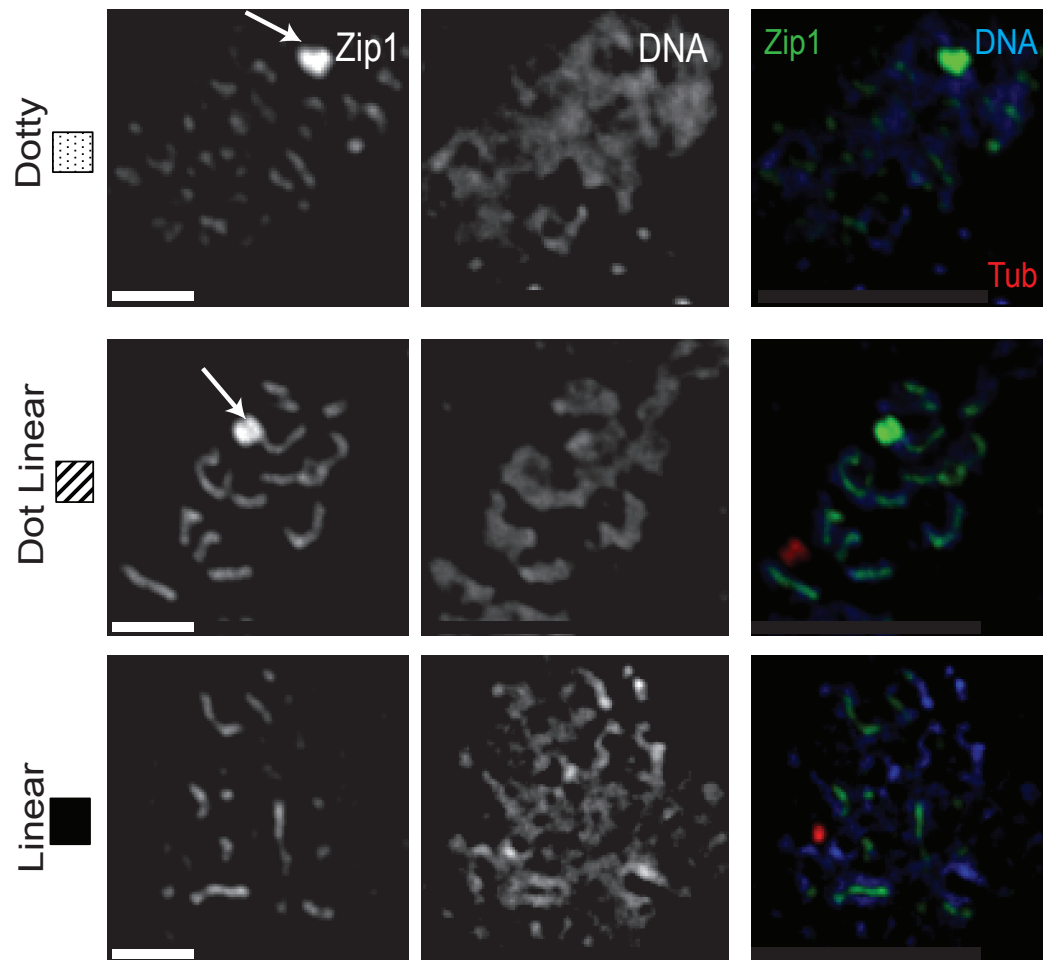
B



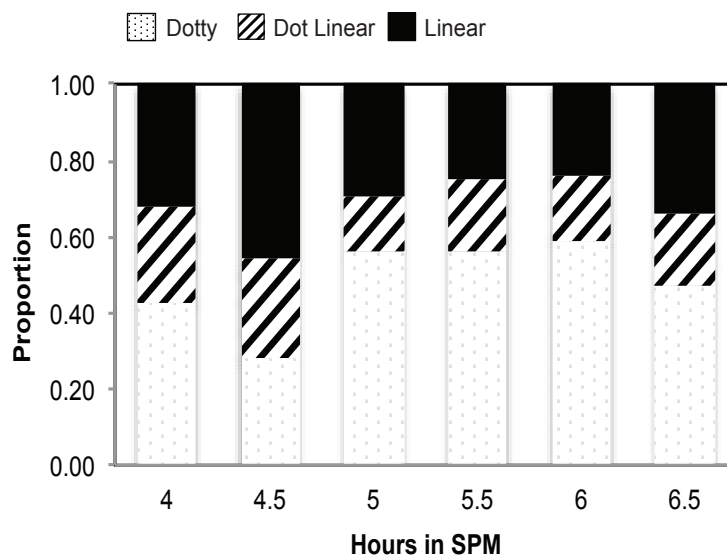
Appendix 4 Southern Blot verifications on other Zip1-phospho mutants

(A) Southern Blot to check individual Zip1-phospho mutants contain the correct genotype of Hunter strains. Lane 1 and 2 showing the *zip1-S82A* mutant derived from Y5020. Lane 3 and 4 showing the *zip1-S82A* mutant derivative of Y5021. Lane 5 showing *zip1-S75A*; *zip1-S127A* mutants derived from Y5020. Lane 6 and 7 showing *zip1-S75A*, *zip1-S127A* mutants derived from Y5021. Lane 9 showing *zip1-S127A* mutant derived from Y5020 and lane 10 to 11 showing derivative of Y5021. Lane 11 and 12 showing derivative of Y5020 (*zip1-S127DE*); lane 13 showing Y5021_ *zip1-S127DE*. Lane 14 to 16 showing the *ZIP1-TRP1* wild type derived from Y5020. Lane 17 showing the wild type from Y5021. Lane 18 to 19 showing two other *zip1-S144A* derived from Y5020. (B) Integration showing in the same order as in A.

A



B



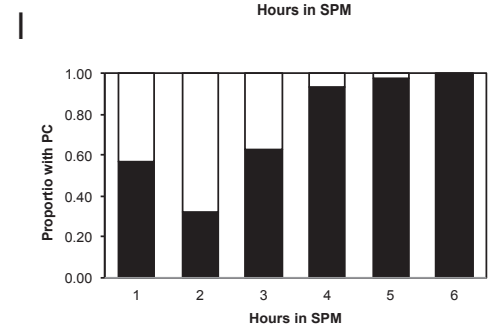
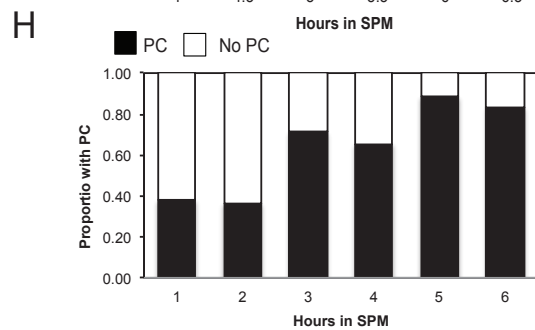
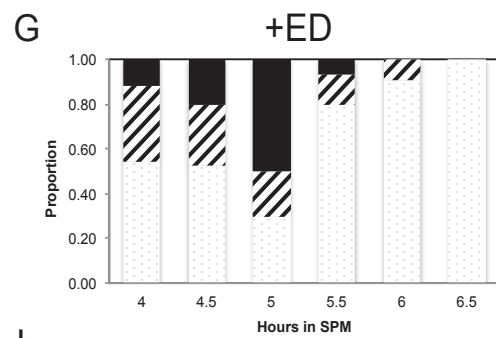
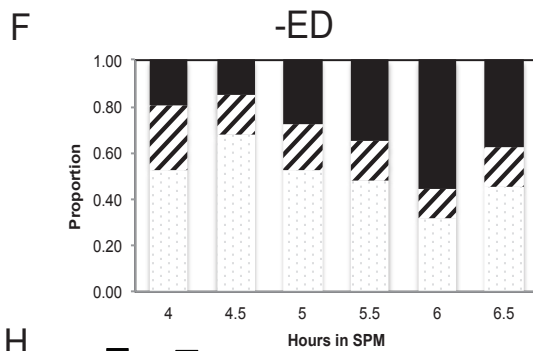
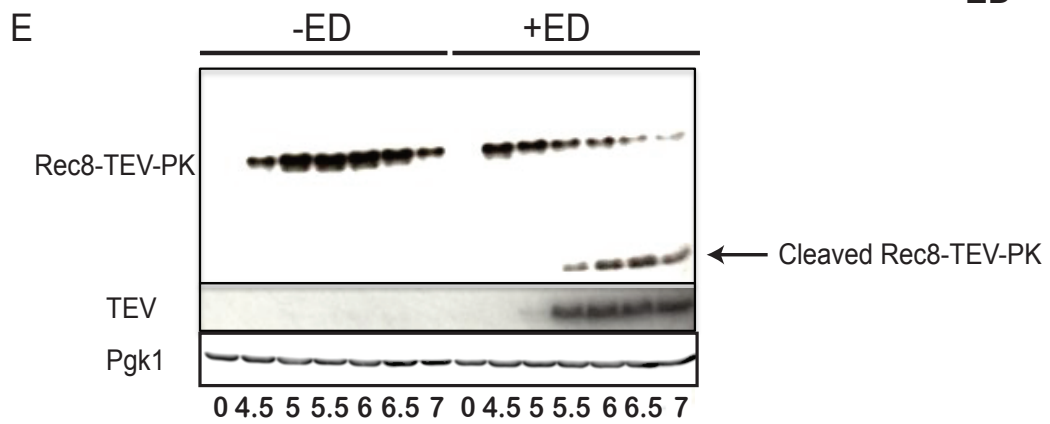
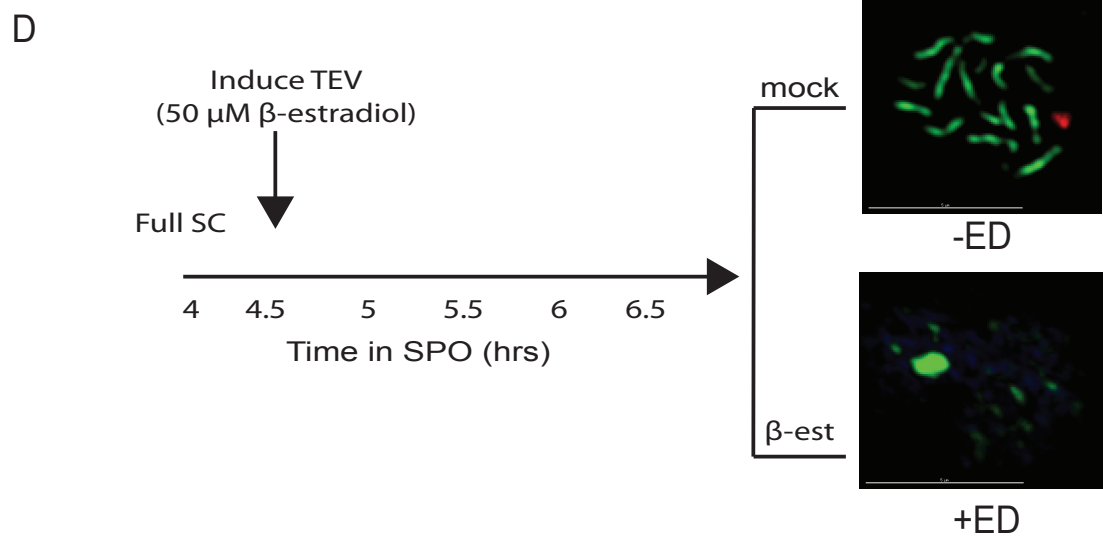
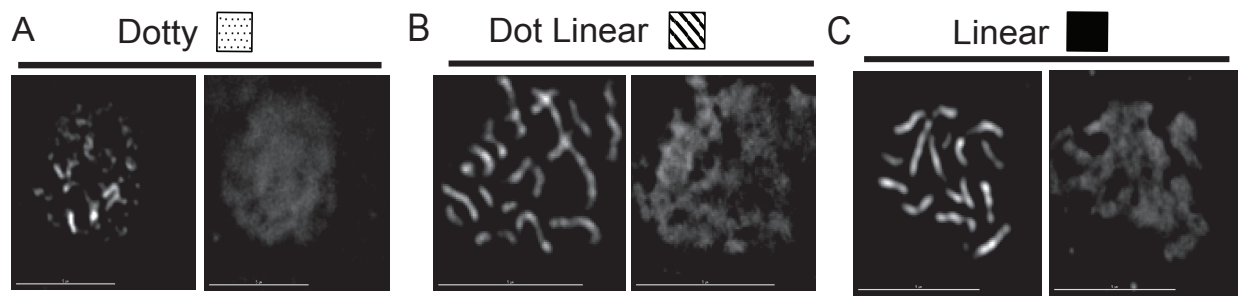
Appendix 5 Optimisation of Rec8-Tev, Ndt80-Inducible system

(A) Representing different stages of Zip1

(B) Proportions of different stages of Zip1 during different time point.
four and half hour have the most linear Zip1

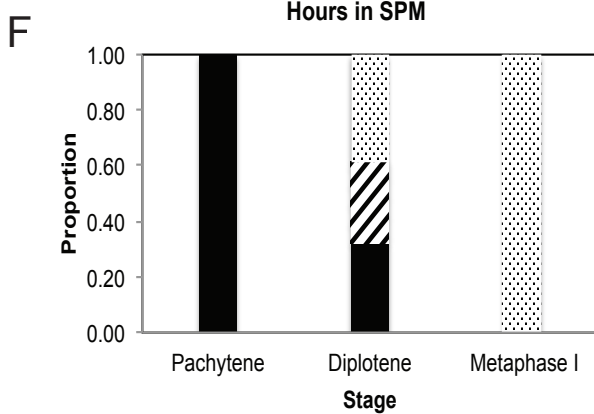
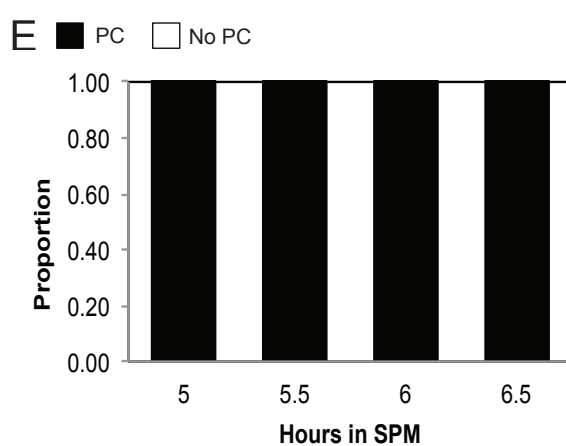
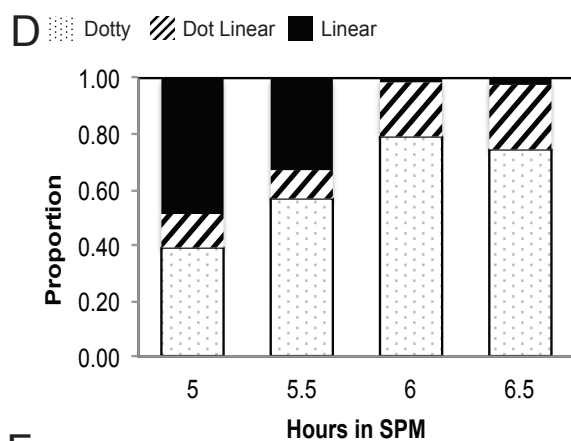
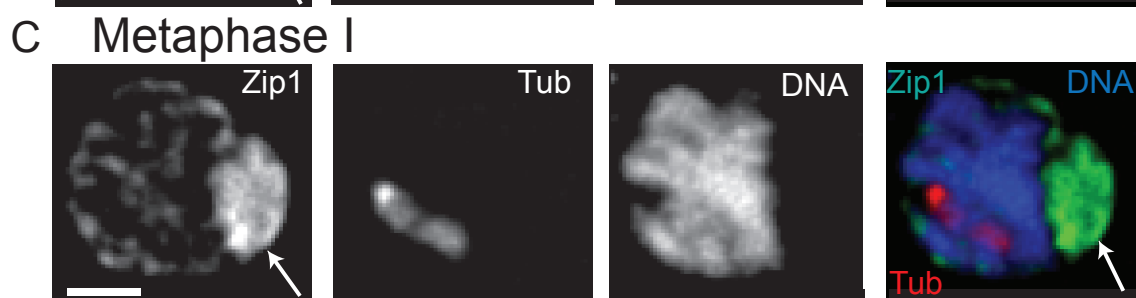
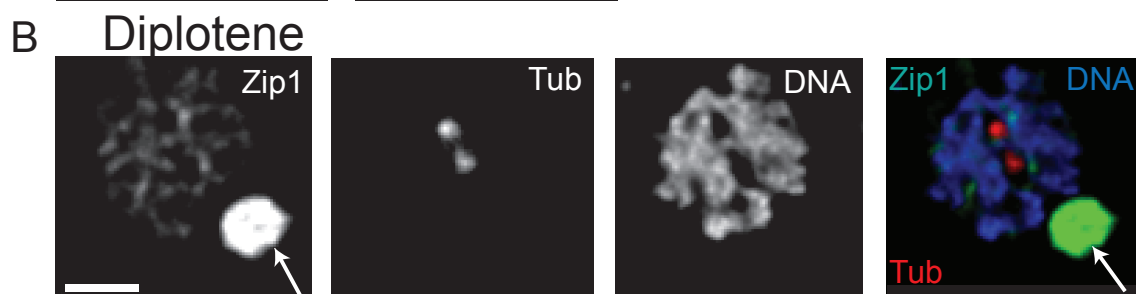
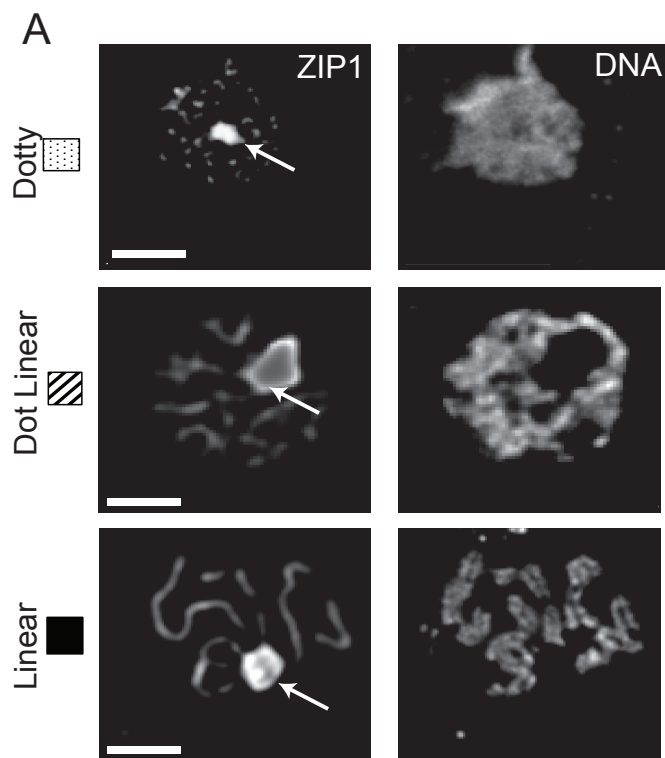
Appendix 6 Cleavage of Rec8-Tev leads to instability of Zip1

(A-C) Representative images showing diplotonema, zygonema and pachynema respectively when Rec8 was not cleaved in *ndt80Δ*. (D) Showing the timing when β -estradiol is conditionally induced during the time course, two representative images showing when Rec8 was cleaved and Rec8 un-cleaved on the right. (E) Western presenting Rec8 protein in the uninduced samples and induced samples. Cleaved Rec8-Tev-PK products are showing in the right panel. (F) Proportion of different Zip1 stages in uninduced samples. > 100 nuclei scored for each time point. (G) Proportions of different Zip1 in induced samples. >100 nuclei scored. (H-I) corresponding of polycomplexes formation in both uninduced and induced samples respectively.

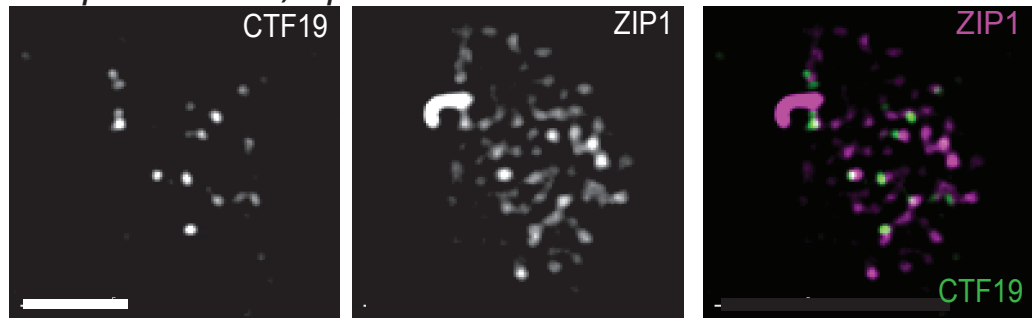


Appendix 7 Repeat of the *zip1-S144A* mutant with a different transformant

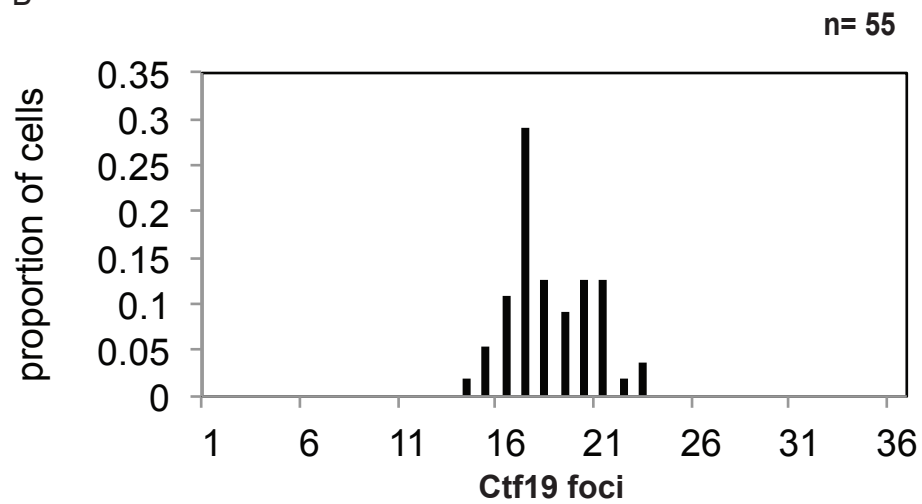
(A) Representative images showing the prophase I stage of the *zip1-S144A* mutant. Arrows indicate polycomplexes. (B) Representing images of the *zip1-S144A* mutant during diplotene. (C) Representative images showing the *zip1-S144A* mutant during metaphase I. (D) Quantification of different categories of Zip1 in the *zip1-S144A* mutant during prophase I. (E) Quantification of proportions of polycomplexes formed in the *zip1-S144A* mutant. N=50. (F) Proportion of different categories of Zip1 in the *zip1-S144A* mutant during pachytene, diplotene and metaphase I



A *spo11-Y135F, zip1-7A*



B



Appendix 8 Centromere coupling is not affected in *zip1-S144A*

(A) Representative images showing centromere coupling in *zip1-S144A*

(B) Proportion of Ctf19 foci in *zip1-S144A*